Fire Resistance Tests on Wood and Composite Wood Beams

Venkatesh Kodur, PhD-PE, James Stein, and Rustin Fike, PhD
Department of Civil and Environmental Engineering, Michigan State University

Mahmood Tabaddor, PhD
Predictive Modeling and Risk Analysis Group, Corporate Research, UL

DECEMBER 2011

Underwriters Laboratories Inc.
333 Pfingsten Road, Northbrook, IL 60062-2096 USA
T: 847.272.8800/W: UL.com

DOCUMENT INFORMATION

Release Type	☐ Internal ☐ External (Confidential) ☒ External (Public)
UL Distribution	Corporate Research
External Distribution	National Institute of Standards and Technology, www.ul.com
Date: December 2011	**Keywords:** Fire, Wood, Engineered Wood
Title: : Fire Resistance Tests on Wood and Composite Wood Beams	

Author(s)	Department	Email
V. Kodur, J. Stein, R. Fick	MSU	kodur@egr.msu.edu

Reviewer(s)	Department	Email
Mahmood Tabaddor	Corporate Research - UL	Mahmood.tabaddor@ul.com

ACKNOWLEDGEMENTS

The authors of this report wish to acknowledge the following sources of financial support:

- The National Institute of Standards and Technology (NIST)
- Underwriters Laboratories (UL)
- Michigan State University (MSU)
- Additional office support and contract accounting at Michigan State University/College of Engineering/ Department of Civil & Environmental Engineering.

EXECUTIVE SUMMARY

There has been much research conducted on the structural stability of wood based flooring systems in the past few years with a focus on the relative fire performance of traditional lumber with engineered wood based supports. Results have shown that there is a dramatic drop in the performance of flooring systems supported by engineered wood when unprotected. To help build upon this research and advance the use of computer modeling of structures in fire, specifically wood-based, fire testing was carried out on a variety of wood and wood composite beams.

With single beam tests, the failure mode can be carefully studied through video and detailed measurements throughout the beam test specimen. For this study, beams were tested at MSU's structural fire test facility subjected both to mechanical loadings and thermal loadings following the ASTM E-119 fire exposure profile. The beam only tests confirm the significant performance difference observed for full flooring systems. Traditional lumber beam with rectangular cross section did outperform the engineered wood I-joist in these fire tests. These results show the potential for assessing the fire performance of new wood-based constructions using simple single beam fire tests.

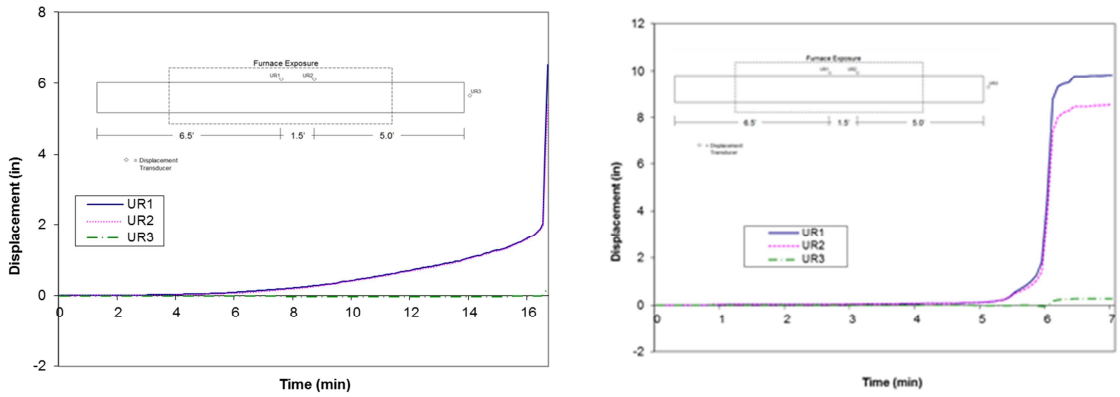

Deflections for traditional lumber beam (left) and engineered wood I-joist (right)

In addition, the availability of video of the burning process for the beams provided insight into the failure path. For the engineered wood I-joists, the failure sequence involves the burnout of the thin web, thereby creating a sudden drop in stiffness as the lower chord, though mostly un-burnt is no longer available for loading sharing.

Image from video of flaming of web for I-joist fire test

The design of these beam only tests gave consideration to the use of the test data for validation of computer models. In such cases, the test must be designed to provide measurements throughout the specimen especially at key locations where high gradients in variables such as temperature or deflection are expected. In addition, the boundary conditions must be constructed in a manner that allows for quantification within the model. Now with the test data and detailed information available on these beam fire tests, a valuable database has now been created to help advance the use of computer modeling tools in understanding the fire performance of structures.

Some other results coming out of this research are:

- The application of an intumescent coating to an engineered I-joist shows promise in improving its fire resistance.
- The connections in the steel/wood hybrid joists are the weak link during fire exposure and influence the resulting fire resistance.
- The presence of plywood sheathing on the top of a joist enhances fire resistance and better simulates being part of a floor system.
- The presence of axial restraint conditions does not significantly influence the fire resistance of wood joists.
- The load level has an influence on the fire resistance of wood joists. The higher the load level, the lower the fire resistance will be.

TABLE OF CONTENTS

INTRODUCTION

Engineered wooden I-beams (joists) are very efficient in resisting floor loads over short spans, and therefore are attractive for use in residential construction. These joists capitalize on the strength of wood and the efficiency of the I-shaped section to enhance flexural load bearing capacity, while at the same time reducing the mass and cost of the structural member. Additionally, with such material mass reductions, these products are more environmentally sustainable building materials. However, due to numerous events in which fire fighters entering a building fall through engineered joist floor systems and are unable to escape from the building, fire resistance of these members has come into question [1,2,3]. Research relating to this topic has been conducted by organizations such as Underwriters Laboratories (UL) [4], National Institute of Standards and Technology's [5], National Fire Protection Research Foundation [6], and National Research Council Canada [7], but the participants in this study feel that further element testing is necessary. These results have shown that there is a dramatic drop in the performance of flooring systems supported by engineered wood when unprotected when compared to traditional lumber supported flooring systems. To help build upon this research and advance the use of computer modeling of structures in fire, specifically wood-based, fire testing was carried out on a variety of wood and wood composite beams.

To further investigate the fire resistance of engineered lumber, in a combined effort with UL, Michigan State University (MSU) conducted a series of fourteen fire tests on both dimensional lumber and three types of modern engineered lumber. This report details the test specimens, test setup, test procedure, and the measured response parameters.

DESCRIPTION OF TEST SPECIMENS

Test specimens

The test program consisted of fire resistance tests on fourteen floor joists. All specimens were tested under ASTM E-119 fire exposure and under loaded conditions. Four types of wood joists, namely dimensional lumber, engineered I-joists, castellated I-joists, and steel/wood hybrid joists, were selected for the experimental studies. Five of the joists tested were 2x10 dimensional lumber designated as T1, T2, T3, T4, and T5, three were engineered I-joists with a constant cross-section designated as E1, E2, and E3, two were castellated I-joists designated as C1 and C2, and four were steel/wood hybrid joists designated as H1, H2, H3, and H4. Table 1 provides details on the test specimens together with test parameters. Detailed dimensions of each beam are presented in Table 2, and typical pictures of the four types of joists tested as part of this study are shown in Figure 1.

All dimensional lumber was purchased from a local lumber yard while the engineered lumber was delivered directly to MSU's Civil Infrastructure Laboratory (CIL) from UL. After acquisition of the specimens, they were stored at 75 ˚F in MSU's CIL.

The beams supplied by UL and those purchased from the lumber yard were 14 to 16 feet in length. For the fire resistance tests, the distance between the supports was 12 feet. All axially unrestrained beams were trimmed to a length of 13 feet for testing. In order to achieve axially restrained conditions, the axially restrained beams were shimmed to a length of 16 feet such that they fit snuggly against the furnace test frame. Restraint conditions are illustrated in Figure 2.

Both the castellated and hybrid joists contained cut-outs in their web regions. The castellated beams comprised of an engineered I-joist with sections of the web removed. The hybrid beams comprised of an engineered I-joist with a web only at the ends. Light gauge steel fixed to both the top and bottom chords replaced the web for the open midsection. Figure 3 displays the orientation of these cut-outs and illustrates their positioning in the furnace.

The moisture content in the joists was measured following ASTM D-4442 procedure [8]. It was found that the moisture content of the dimensional lumber was consistently around 10.5%, while the

moisture content of the three different types of engineered lumber was consistently around 9.2%. Though stored in the same environment, the different composition of the beams accounts for the variation in initial moisture content.

For enhancing the fire resistance of wood joist systems, special features were applied to some of the joists. The first feature was the application of an intumescent coating to engineered I-joist E3 over the fire exposed region. The intumescent coating used was previously evaluated under ASTM E-119 fire exposure for structural steel applications. This coating was applied to a thickness of 65 mils as specified by UL and following the manufacturer's specifications. The second improvement was the insertion of screws into the steel/wood connections in hybrid joists H3 and H4. This was done to improve the fire resistance of these connections and thereby delay structural failure under fire conditions. The screws used for joist H3 were coarse thread #6 x 1 inch drywall screws, selected because of their wide availability. The screws used for joist H4 were zinc plated #6 x 1-1/4 inch wood screws, selected because of their higher quality consistency when compared to the previously used drywall screws.

Pursuant to the discussion following the tests on traditional joists T1 and T2, typical sheathing used in residential construction was attached to the top of the test specimens. To avoid fire exposure being from four sides, the top of the sheathing was provided with ceramic blankets as shown in Figure 2 to simulate, as closely as possible, the fire exposure conditions present in residential fires.

Instrumentation

The instrumentation on the specimens consisted of thermocouples, strain gauges, and deflection gauges. To measure cross-sectional temperatures in joists, twenty four thermocouples were mounted on each engineered joist, while twenty were mounted on each of the traditional joists. The thermocouples were welded Type K chromel alumel thermocouples with a thickness of 0.0358 inches (0.91 mm). These thermocouples were applied at various locations shown in Figure 4. Internal thermocouples were inserted into 0.1875 inch diameter holes drilled from the top surface of the beam. Surface mounted thermocouples were attached to the surface of the wooden beam via small metal staples. Care was taken to ensure that the staples were sufficiently far from the thermocouple as to not influence the time-temperature profile experienced by the thermocouple. Thermocouple

wires on the beam were routed through the sheathing and adjacent to the joists to minimize any interference with mechanical deflections and fire exposure experienced by the beam.

Due to the problems inherent to attaching strain gauges to wood at elevated temperatures, strain gauges were only placed at locations outside the fire exposed zone as depicted in Figure 4. These locations being very close to the supports generated very little data from unrestrained beams as determined from fire tests on traditional joists T1 and T2. As such, strain gauges were only applied to the restrained beams for the remainder of the fire tests. For each restrained beam, two strain gauges were applied, one on the top flange and one on the bottom flange of the beam, 16 inches from the outer edge of the furnace wall. The strain gauges were manufactured by Texas Instruments and were 120 Ω with an overall length of 1.18 inches (30 mm). In all instances, except for the bottom gauge of joist T4, the strain gauges maintained their integrity for the full duration of the fire exposure allowing strains to be captured throughout the fire test.

Deflections in the joists were measured by linearly varying displacement transducers attached to each test specimen. For each joist, vertical deflections were measured at the center of the joists and also at one loading point. On unrestrained joists, axial deflection was also measured at the neutral axis. Figure 5 illustrates the location of the displacement transducers.

Upon structural failure of the beams, the displacement transducers were disconnected from the beams being tested to protect the instrumentation. The axial displacement transducers were manually disconnected upon beam failure, and the vertical displacement transducers disconnected automatically using a break-away system designed specifically for these tests. This system consisted of a wire that connected the instrumentation to a screw attached to the top surface of the sheathing. As the beam deflected down and eventually failed, a stopper prevented overextension of the displacement transducer. The screw then pulled out of the sheathing, allowing the beam to continue deflecting or attain free-fall within the furnace without hindrance.

The furnace and joist cross-sectional temperatures, strains, and deflections were recorded at 5 second intervals using DAQ 32 data acquisition software. Photographs and video recordings were also taken at frequent intervals or when major events occurred during each test.

Test conditions and procedures

The fire resistance tests were conducted at MSU's structural fire test facility, the combustion chamber of which is 8 feet by 10 feet by 5 feet high. This furnace facilitates testing of two joists simultaneously in each fire test. The test furnace is pictured in Figure 6. The maximum heat output that can be generated by the six natural gas burners which power the furnace is 2.5 MW. The beams were placed in the furnace such that no support was offered to the beams as they deflected down due to loss of strength and stiffness resulting from high temperatures. Additionally, the top of the beams were placed against the furnace lid to limit fire exposure to the beams such that no additional load was applied to them. This produced three sided fire exposure to the joists. Voids between the joists and the furnace wall were sealed with ceramic fiber insulation such that there was minimal gas exchange with the outside environment, and no hindrance to joist deflection was provided.

The furnace temperature was measured by six Type K chromel alumel thermocouples specifically designed for quick response. The thermocouples were spatially distributed within the combustion chamber, and the average of the six thermocouple temperatures was used to control the furnace temperature. A comparison was performed between the furnace thermocouples and ASTM E-119 thermocouples as provided by UL. The recorded temperatures from this comparison are displayed in Figure 7.

As displayed in Figure 2, two point loads were applied to each joist during fire exposure. For each joist, the point loads were 3 feet apart straddling mid-span along the axis of the joist. Mechanical loads were incrementally applied 30 minutes prior to fire exposure. Specially designed loading apparatuses were installed to apply loads to the top of the joists. Loading remained unchanged throughout fire exposure duration until structural failure occurred in the beams. Throughout testing, the loading system was monitored to ensure no obstructions altered the loading level. For traditional joists T1 and T2, the applied load represented 70% of the design load (250 pounds per point load). For the remaining joists, the applied load represented 50% of the design load (ranging from 180 to 480 pounds per point load). Appendix C contains load calculations.

At the loading points, lateral bracing was provided to prevent lateral displacement of the joist during fire exposure. To accomplish this, lateral bracing systems, consisting of vertical hollow structural section (HSS) members, were placed next to the joist as shown in Figure 2. Care was taken, when placing the lateral supports around the joist, to minimize the effect of the supports on the fire

exposure experienced by the joist. To ensure that the lateral bracing system was able to be used in multiple tests, the temperature rise within the section was minimized through the placement of water within the HSS sections. This ensured that the steel sections maintained their structural integrity and did not induce instability or out of straightness in any of the tests.

The end supports for all joists were spaced 12 feet apart. At one end, the joist rested on round bar stock that acted as a roller support since there was no axial or rotational restraint. The support at the other end consisted of the joist resting on square bar stock that acted as a pin support. This pin support simulated no rotational restraint condition, but there was axial resistance since the square bar stock could not roll upon axial loading. The support locations and configuration are illustrated in Figure 2.

All tests were carried out by exposing the beams to ASTM E-119 fire, as shown in Figure 8. During fire tests, the temperatures in the furnace were controlled to follow as closely as possible those specified in ASTM E-119 standard [9]. Control of the furnace temperature was achieved through a manual control valve which the operator adjusts based on the real time average of six thermocouples spatially distributed in the combustion chamber. All beams experienced temperatures of approximately 200°F for 2 minutes prior to recording the data and initiation of the fire exposure because the furnace required pre-heating prior to initiation of a fire exposure.

During fire exposure, failure of the specimen was assessed based on stability of the member. The result is that the beam was permitted to reach runaway conditions prior to the end of the test. After the failure was observed, the gas to the furnace was shut off, but the joists continued to burn due to the inability to extinguish a fire within the furnace. As such, there was no opportunity to conduct post fire assessment immediately after fire exposure was completed as the entire beam was consumed by the fire.

RESULTS AND DISCUSSION

Data generated from the above fire tests include surface and cross-sectional temperatures, deflections, and strains in the joists, and visual observations throughout the fire tests. The results of the fourteen wood joist fire resistance tests are summarized in Table 1 in which the failure times and mode of failure are given for each joist. The exact location of the thermocouples and strain gauges can be found in Figure 4, while the location of the deflection gauges can be found in Figure 5. Comparisons of average temperatures in the different joist types are plotted in Figures 9-14, each plot corresponding to a thermocouple location on a typical engineered lumber cross-section. Examples of strain and displacement measurements are plotted in Figures 15 and 16 respectively. Appendix A contains detailed plots of cross-sectional temperatures, strains, and deflections for each joist. Temperature and deflection plots contain diagrams indicating the exact measurement locations. Appendix B contains photographs of the test setup, instrumentation, and joists after failure.

A general observation made throughout testing was that the joists (lumber) ignite at about 4 minutes after initial fire exposure under ASTM E-119 fire [9]. This observation was consistent in all joists tested except for joist E3, which had the intumescent coating, and joist H3, which ignited after only 3 minutes. A potential reason for joist H3 igniting prior to the other unprotected wood joists is that it was tested simultaneously with joist E3.

The fire performance of traditional joists can be gauged by examining the average temperature profiles plotted in Figures 9, 10, 12 and 13. Figure 9 shows a comparison of the cross-sectional temperatures within (inside) the different types of joists. Temperatures displayed for traditional lumber are the averages of temperatures recorded internally at mid-depth and quarter-depth of all three cross-sections exposed to fire loading. Temperatures displayed for engineered lumber are the averages of temperatures recorded at the center of the top chord of all three cross-sections exposed to fire loading. This figure shows that the temperatures within traditional joists reach 600˚F during the fire resistance tests. The temperatures within unprotected engineered joists remain much cooler, reaching temperatures of only 100 to 200˚F. This suggests that the high temperatures within traditional joists contributed to their failure, while temperatures within the top chord of engineered lumber did not play a significant role in failure.

The temperature profile for joists T1 and T2 stand out in Figure 10, which shows a comparison of temperatures at the top surface of the different types of joists. At 7 minutes they experience temperatures of 1400˚F while the other joists experience temperatures around 150˚F. Further examination reveals that the temperature profile for joists T1 and T2 in Figure 10 closely resembles the surface temperature profiles for joists T1 and T2 shown in Figures 12 and 13. The elevated temperatures experienced by joists T1 and T2 can be largely attributed to their lack of plywood sheathing. All other joists had plywood sheathing mounted to their top surface, protecting the top surface of the joists.

Unprotected joists T3, T4, T5, E1, E2, C1, C2, H1, H2, H3, and H4 had similar temperature profiles as shown in Figures 9-14. In each figure, the temperatures for each type of joist followed the same general trends at similar temperatures. This is illustrated by the grouping of the temperature profiles on each figure. These trends were experienced for the first 6 to 7 minutes until the engineered joists (E1, E2, C1, C2, H1, H2, H3, and H4) failed.

Figures 9-14 can be used to determine the protective capabilities of the intumescent coating applied to joist E3. In these figures, joist E3 experienced lower temperatures than the other joists.

The measured strains during the fire resistance test for joist C2 are displayed in Figure 15 as an example of the strains recorded throughout the fire resistance tests. The strain values obtained were sporadic with little consistency resulting in no correlation with deflections or any other data. This can be attributed to strain gauges not working properly under high temperatures. As such, no conclusions can be drawn regarding stains in the joists.

The measured vertical displacements during the fire resistance tests on joists T4, H2, and E3 are displayed in Figure 16 as a representation of typical vertical displacement values recorded through the fourteen fire resistance tests. The displacements recorded for joist T4 were typical of those recorded for the traditional joists (T1 to T4). Negligible displacements were recorded until 6 minutes into testing, at which point the displacements increased gradually to 1.5 inches by about 20 minutes. At this point, the joist failed and attained free-fall corresponding to the recorded displacements of 7 to 9 inches. The displacement plots for joist H2 characterize those recorded for the engineered lumber (E1, E2, C1, C2, H1, H2, and H3). From 4 to 6 minutes, the displacements increased gradually from 0 to 1.5 inches. At this point, the joist failed, achieving free-fall and displacements ranging from

7.5 to 11 inches. Joist E3, which had an intumescent coating, is also represented in Figure 16. At about 4 minutes, the displacements began to increase gradually, and by 24 minutes they reached about 2 inches. At this point, the joist failed, reaching free-fall and displacements as high as 9.5 inches were recorded. Based on UL's Report on Structural Stability of Engineered Lumber in Fire Conditions [4], deflection and deflection rate limits from ISO 834:1 were consulted to define structural failure. It was found that these criteria did not apply to these tests because these limits described failure times after the joists had already clearly ruptured.

From observations made during the fire resistance tests and the generated test data discussed above, the failure modes of the different joist types can be determined. It was observed that the failure times for joists T1 and T2 ranged from 13 to 15 minutes, while the failure times for joists T3, T4, and T5 ranged from 16 to 20 minutes. Because of the high internal temperatures recorded within these joists, it was determined that the failure mode for the traditional joists (T1 to T5) was cross-sectional reduction. Joists E1 and E2 failed at around 6 minutes. During the fire resistance tests, it was observed that the web burned through before the chords did. Therefore, it was determined that the failure mode for engineered I-joists (E1 and E2) was the burn-out of the web. The failure time for joist E3 was 24 minutes. The intumescent coating applied to joist E3 made observations difficult, but it was determined that its failure mode was burn-out of the web as well. Joists C1 and C2 failed at around 7 minutes. Observations similar to those for joists E1 and E2 were made; therefore the failure mode for castellated joists (C1 and C2) was determined to be web burn-out. Joists H1, H2, H3, and H4 all failed at around 6 minutes. It was determined through visual observations during testing that the failure mode for the hybrid joists (H1, H2, H3, and H4) was the failure of the steel/wood connection.

CRITICAL FACTORS INFLUENCING FIRE RESISTANCE

Results generated from the above fire tests can be utilized to gauge the effects of various factors on the fire resistance of different types of wood joists.

Effect of joist type

The effect of joist type on fire resistance can be gauged by comparing the failure times in different joists. Traditional joists T1 to T5 failed between 13 and 20 minutes, providing the highest fire resistance. Engineered joists E1, E2, H1, and H2 all failed at around 6 minutes while joists C1 and C2 failed at around 7 minutes. In general, engineered joists had only 30 to 50% the fire resistance of traditional joists.

The failure mode of traditional joists was evaluated by analyzing test data and recorded observations during tests on joists T1 to T4. It was determined that the failure of these joists was caused by reduction in cross-section. In this process, the exposed surfaces of a traditional joist ignited and burned. As the joist burned, the cross-section gradually burned away corresponding to a gradual loss of stiffness and strength of the joist. Eventually, the cross-section, stiffness, and strength were reduced to the point that the joist could no longer support the applied load, leading to rupture of the joist. Also, the average internal temperatures in joists T3 and T4 were elevated at the time of failure when compared to other joist types. This may be due to the reduction in cross-section. It could also be attributed to the joist experiencing fire conditions (elevated temperatures) for an extended time period, when compared to other joist types, due to the higher failure time of traditional joists. For repeatability purposes, joist T5 was tested under 70% of its design load (similar to joists T1 and T2) with sheathing attached to its top surface (similar to joists T3 and T4). As expected, the data obtained was very similar to data collected from joists T3 and T4.

The test data and observations from tests on joists E1, E2, C1, and C2 can be used to determine the failure mode of engineered I-joists and castellated I-joists. They indicate that the cause of failure was the burning through of the web. As one of these beams ignited and burned, voids in the web appeared and the cut-outs enlarged as depicted in Figure 18 for joist C2. Eventually, the integrity of

the web was reduced enough for the joist to fail. This failure process occurred quickly and suddenly relative to the traditional joists.

Observations made when testing the hybrid joists H1 and H2 were used to determine the failure mode of these joists. It was concluded that the failure mode for the hybrid joists was the failure of the steel/wood connections on the bottom cord. It was observed that these connections failed, and because they were no longer connected to the bottom cord, the steel members' capacity was reduced to zero. Without support from the steel members, the top cord failed under the applied load. Coinciding with these failures, the ends of some steel members hung freely below the joist, identifying the steel/wood connection on the bottom cord as the source of failure. The photograph in Figure 17 depicts this type of failure on joist H2. Similar to the other types of engineered joists, this failure process occurred quickly and suddenly relative to the traditional joists. Further testing and analysis is required to determine the mechanism and progression of failure in these connections. It should also be noted that in these tests, much of the plywood web at the ends of the joists were not exposed to fire conditions.

Effect of sheathing

The effect of sheathing on fire resistance can be gauged by comparing the results from fire tests on joists T1 and T2 with other joists. At first, joists T1 and T2 experienced three sided fire exposure since their top surfaces were tight against the furnace lids and the remaining surfaces were exposed to fire conditions. However, because they did not have any sheathing attached to their top surfaces, upon vertical deflection the top surface was also exposed to fire conditions resulting in four sided exposure. The other joists had sheathing attached to their top surfaces, maintaining top-surface protection even under vertical deflection. This three sided exposure is more realistic for a floor joist in a floor joist system which would have plywood sheathing attached to it. The result of four sided exposure (joists T1 and T2) can be seen in Figures 9 and 10. In these figures the temperatures for joists T1 and T2 are much higher than the other joists, namely joist T5 which was tested in the same manner as joists T1 and T2 except T5 had sheathing attached to its top surface. The results confirm that the presence of sheathing increases fire resistance.

Effect of axial restraint conditions

Results from the fire tests can be utilized to gauge the effect of axial restraint on fire resistance. For each type of joist, one of the beams was tested under axially restrained conditions. Joists T1, T3, E1, C1, and H1 were axially unrestrained while joists T2, T4, E2, C2, and H2 were axially restrained. As tabulated in Table 1, T2 failed before T1 and C2 failed before C1 providing two cases where the axially restrained joist failed first. T3 failed before T4 and E1 failed before E2 providing two cases where the axially unrestrained joist failed first. H1 and H2 failed at similar times. These results indicate that the axial restraint conditions do not significantly influence the fire resistance of wood joists.

Effect of load level

The effect of load level on the fire resistance of wood floor joists can be gauged by examining the results of fire tests on joists T1 through T4. Joists T1 and T2 were loaded to 70% of their design capacity, and they failed at around 15 minutes and 13 minutes respectively. Joists T3 and T4 were loaded to 50% of their design capacity, and they failed at around 16 minutes and 20 minutes respectively. The increase in fire resistance correlating to the decrease in load level suggests that lower load levels increase fire resistance. However, joists T1 and T2 were exposed to four sided fire exposure while joists T3 and T4 were exposed to three sided fire exposure. This difference in fire exposure also contributed to the early failure of joists T1 and T2 while somewhat negating the validity of the above conclusion that lower load levels increase fire resistance. As a follow up, joist T5 was tested with sheathing attached to its top surface and was loaded to 70% of its design capacity. It failed at around 16 minutes. Comparing this failure time with joist T4 (20 minutes) which was tested in the same manner except for load level, the data supports the idea that lower load levels increase fire resistance.

Effect of intumescent coating

Data from fire tests on joists E2 and E3 can be used to gauge the effect of intumescent coating on the fire resistance of wood joists. Both of these joists were tested under similar specimen and test configurations except that an intumescent coating was applied to joist E3 (while joist E2 was

unprotected). In these tests, joist E2 failed at an earlier time than joist E3 indicating that the application of intumescent coatings increases the fire resistance of wood joists.

Effect of reinforcing steel/wood connections in hybrid joists

Data from fire tests on joists H2, H3, and H4 can be used to gauge the effect of screws used to reinforce steel/wood connections on fire resistance of hybrid joists. These joists were tested under similar specimen and test configurations except that the connections in joists H3 and H4 were reinforced with screws. Joist H3 was reinforced with common drywall screws while joist H4 was reinforced with wood screws. Joist H2 failed at 6 min while joist H3 failed at 6 min 20 seconds and joist H4 failed at 6 minutes 50 seconds. With under a minute increase in fire resistance, the results indicate that reinforcing the steel/wood connections with screws does not influence the fire resistance of wood joists.

SUMMARY

Based on the fire resistance test results on wood joists presented in this report, the following points can be summarized:

- Wood joists made with dimensional lumber provide higher fire resistance as compared to engineered floor joists. In this test program, traditional lumber joists failed at about 16 minutes, while engineered floor joists failed at about 6 minutes under ASTM E-119 fire exposure.
- The webs of engineered I-joists and castellated I-joists are the weakest parts in these joists, and failure occurred through the burn-out of the web.
- The application of an intumescent coating to an engineered I-joist can enhance its fire resistance.
- The connections in the steel/wood hybrid joists are the weak link during fire exposure and influence the resulting fire resistance.
- Reinforcing the steel/wood connection of the hybrid joists with screws does not enhance fire resistance.
- The presence of plywood sheathing on a joist enhances fire resistance and better simulates being part of a floor system.
- The presence of axial restraint conditions does not significantly influence the fire resistance of wood joists.
- The load level has an influence on the fire resistance of wood joists. The higher the load level, the lower the fire resistance will be.

REFERENCES

1. Preventing Injuries and Deaths of Fire Fighters Due to Truss System Failures, NIOSH Publication No. 2005-132, 2005.

2. NIOSH [2006]. Career engineer dies after falling through floor while conducting a primary search at a residential structure fire – Wisconsin. Morgantown, WV: U.S. Department of Health and Human Services, Centers for Disease Control and Prevention, National Institute for Occupational Safety and Health, Fatality Assessment and Control Evaluation (FACE) Report F2006-26.

3. NIOSH [2007]. Volunteer Fire Fighter Dies After Falling Through Floor Supported by Engineered Wooden-I Beams at Residential Structure Fire – Tennessee. Morgantown, WV: U.S. Department of Health and Human Services, Centers for Disease Control and Prevention, National Institute for Occupational Safety and Health, Fatality Assessment and Control Evaluation (FACE) Report F2007-07.

4. Report on Structural Stability of Engineered Lumber in Fire Conditions, Project 07CA42520, Underwriters Laboratories, Inc., 2008.

5. NISTIR 7393, A Study of Metal Truss Plate Connectors When Exposed to Fire, Harman, K. A., Lawson, J. R. *Fire Research Division Building and Fire Research Laboratory.*

6. National Engineered Light Weight Construction Fire Research Project Technical Report, National Fire Protection Research Foundation, October 1992.

7. IRC-IR-764, Results of Fire Resistance Tests on Full-Scale Floor Assemblies, Sultan M. A.; Séguin, Y.P.; Leroux, P. National Research Council Canada.

8. ASTM D-4442-07, *Standard Test Methods for Direct Moisture Content Measurement of Wood and Wood-Base Materials*, American Society for Testing and Materials, Philadelphia, PA., 2007.

9. ASTM E-119-09c, *Standard Methods of Fire Tests of Building Construction and Materials*, American Society for Testing and Materials, Philadelphia, PA., 2009.

10. Kodur V. K. R., Sultan M. A. Performance of Wood Stud Shear Walls Exposed to Fire. *Fire and Materials.* 2000;**24**:9-16.

11. Kodur V. K. R., Sultan M. A., Denham E. M. A. *Temperature Measurements in Full-Scale Wood Stud Shear Walls*, Internal Report No. 729, Institute for Research in Construction, national Research Council, Ottawa, Canada, 1996.

12. National Design Specification for Wood Construction, AF&PA American Wood Council, Washington D.C., 2005.

Table 1: Summary of test parameters and results from fire resistance tests on wood joists

Joist #	Joist Type	Joist Depth (in)	Axially Restrained	Sheathing	Joist Insulation	% of Design Load	Special Features	Failure Time (min:sec)	Failure Mode
T1	Dimensional lumber	9 1/4	No	No	-	~70	-	15:35	Cross-section reduction
T2	Dimensional lumber	9 1/4	Yes	No	-	~70	-	13:05	Cross-section reduction
T3	Dimensional lumber	9 1/4	No	Yes	-	~50	-	16:40	Cross-section reduction
T4	Dimensional lumber	9 1/4	Yes	Yes	-	~50	-	20:40	Cross-section reduction
T5	Dimensional lumber	9 1/4	Yes	Yes	-	~70	-	16:50	Cross-section reduction
E1	Engineered I-joist	11 7/8	No	Yes	-	~50	-	6:15	Web burn through
E2	Engineered I-joist	11 7/8	Yes	Yes	-	~50	-	6:25	Web burn through
E3	Engineered I-joist	11 7/8	Yes	Yes	Intumescent coating	~50	-	24:05	Web burn through
C1	Castellated I-joist	16	No	Yes	-	~50	-	7:10	Web burn through
C2	Castellated I-joist	16	Yes	Yes	-	~50	-	6:50	Web burn through
H1	Hybrid joist	14	No	Yes	-	~50	-	6:00	Connection failure
H2	Hybrid joist	14	Yes	Yes	-	~50	-	6:00	Connection failure
H3	Hybrid joist	14	Yes	Yes	-	~50	Reinforced connection	6:20	Connection failure
H4	Hybrid joist	14	Yes	Yes	-	~50	Reinforced connection	6:50	Connection failure

Table 2: Cross-sectional dimensions of different joist types

Joist Type	Depth (in)	Width (in)	Flange Thickness (in)	Flange Width (in)	Web Depth (in)	Web Thickness (in)
Traditional (T)	9-1/4	1-1/2	-	-	-	-
Engineered I-joist (E)	11-7/8	-	1-1/2	2-1/2	8-7/8	3/8
Castellated I-joist (C)	16	-	1-1/2	3-1/2	13	3/4
Hybrid (H)	14	-	1-1/2	2-1/2	11	15/32

(a) Traditional joist (T)

(b) Engineered I-joist (E)

(c) Castellated I-joist (C)

(d) Hybrid joist (H)

Figure 1: Different types of wood joists used in fire resistance tests

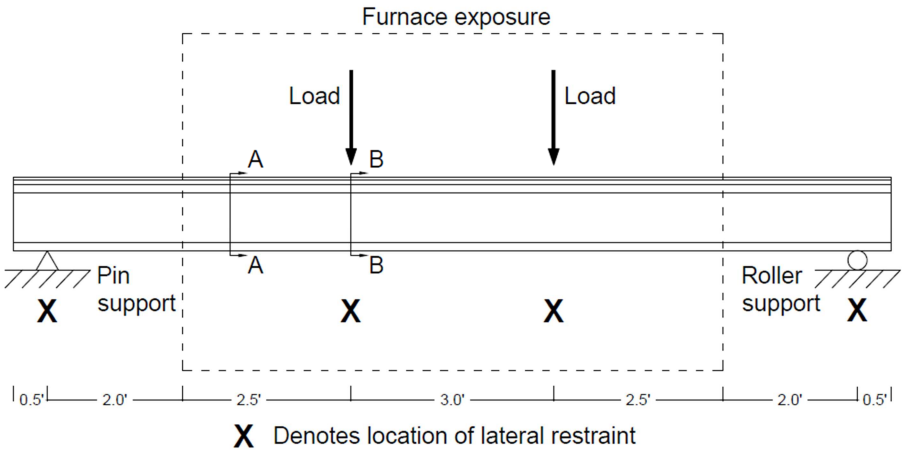

(a) Loading and restraining network used for axially unrestrained joists

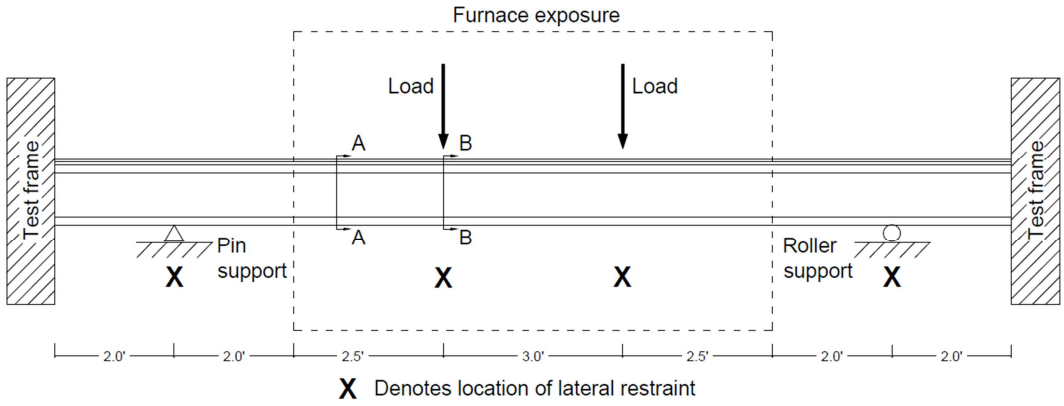

(b) Loading and restraining network used for axially restrained joists

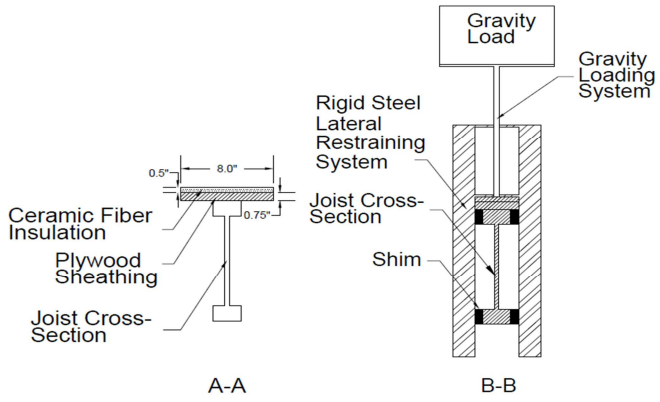

(c) Joist cross-sections with no lateral restraint (A-A) and with lateral restraint (B-B)

Figure 2: Loading and restraining networks used in fire resistance tests

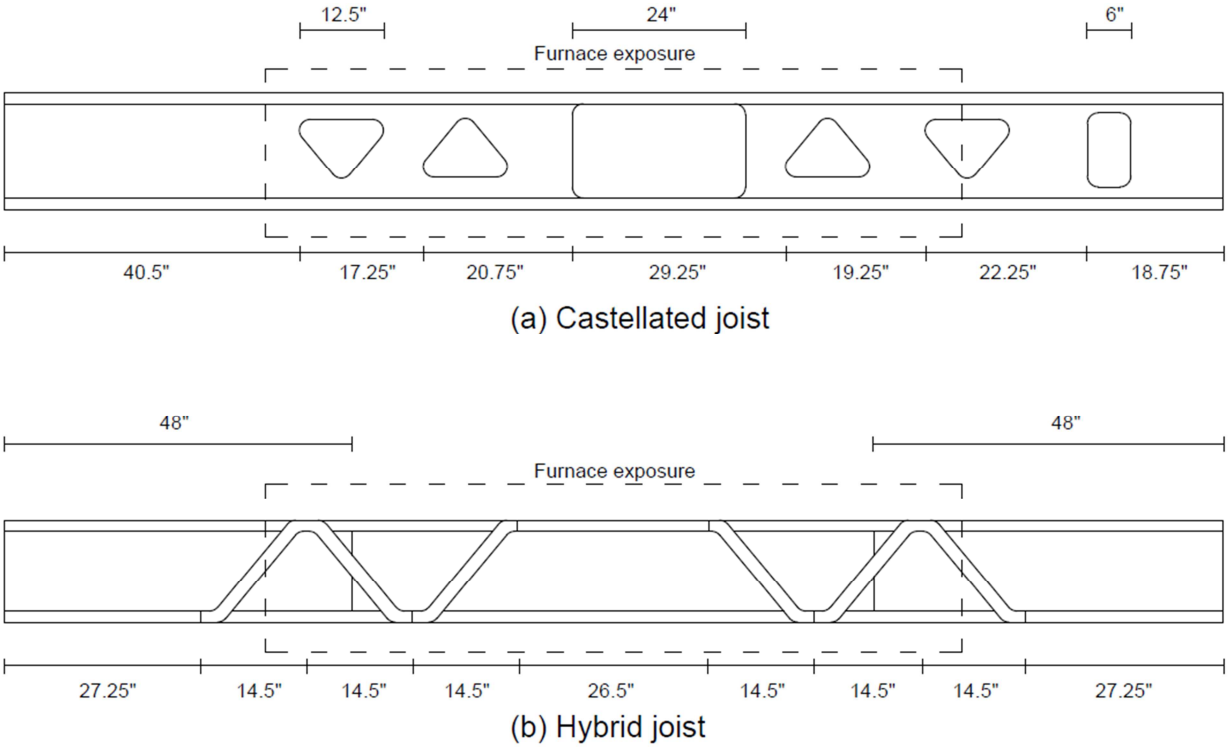

Figure 3: Engineered lumber cut-out orientation

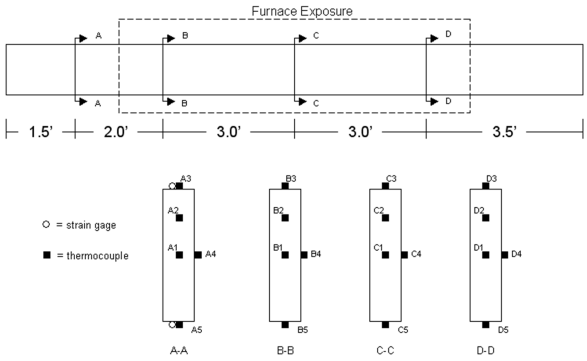

(a) Traditional joist (T1 to T4)

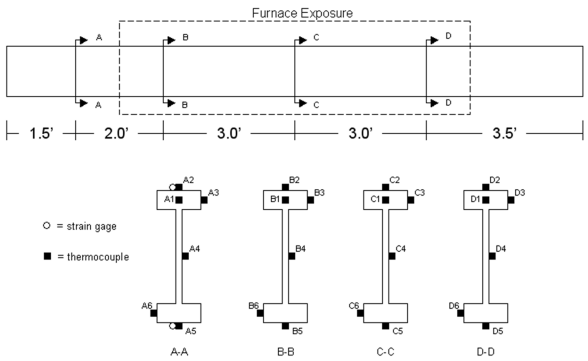

(b) Engineered I-joist (E1 to E3)

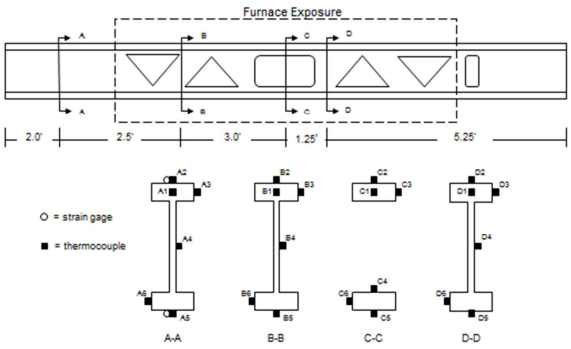

(c) Castellated I-joist (C1 and C2)

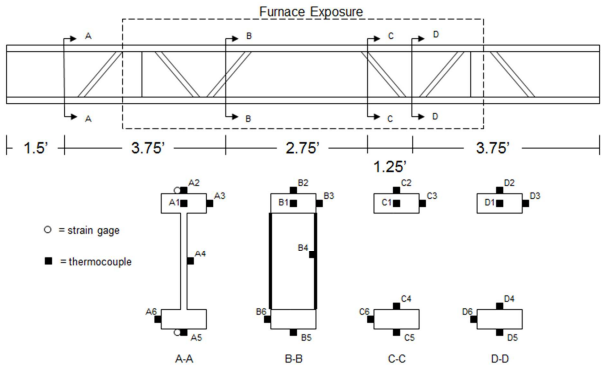

(d) Hybrid joist (H1 to H3)

Figure 4: Thermocouple and strain gauge network in different wood joists

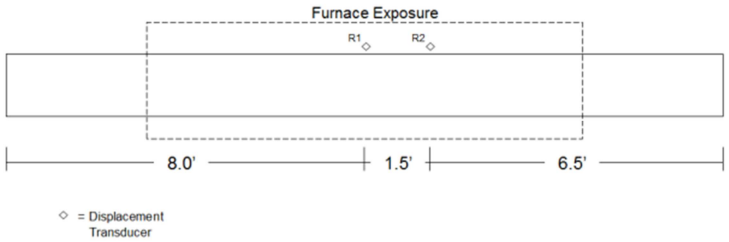

(a) Axially restrained joist

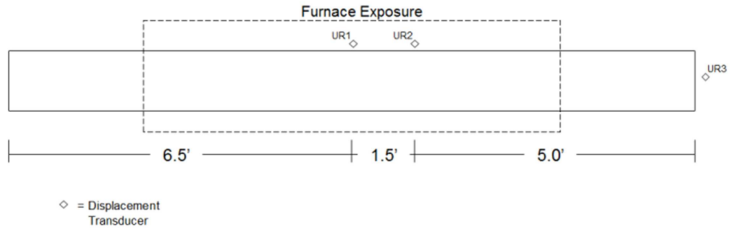

(b) Axially unrestrained joist

Figure 5: Displacement transducer network used in fire resistance tests on wood joists

Figure 6: MSU's structural fire test facility

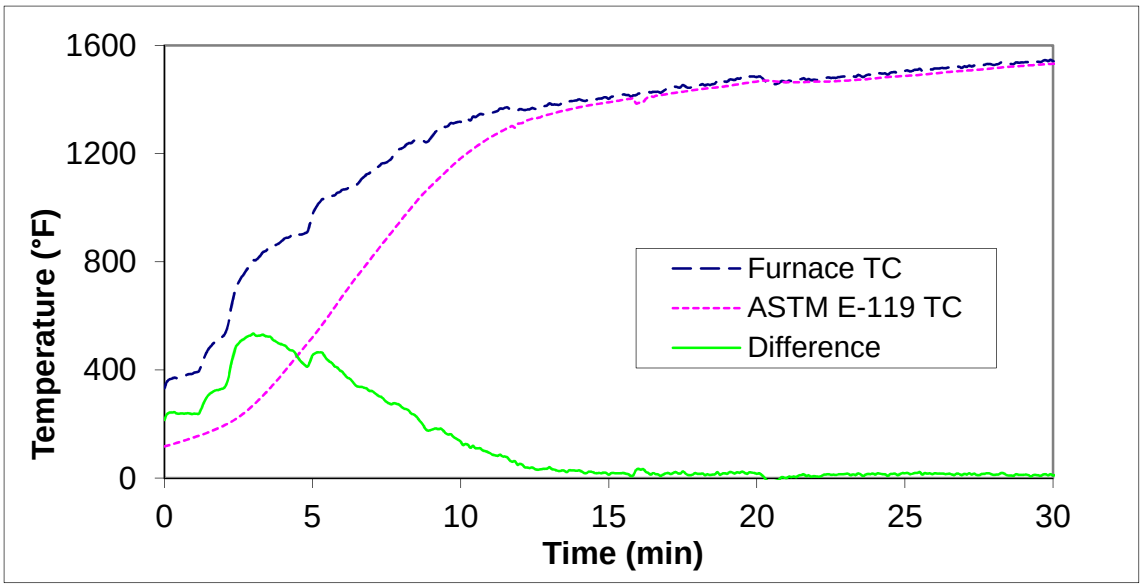

Figure 7: Comparison between the response of furnace and ASTM E-119 Thermocouples

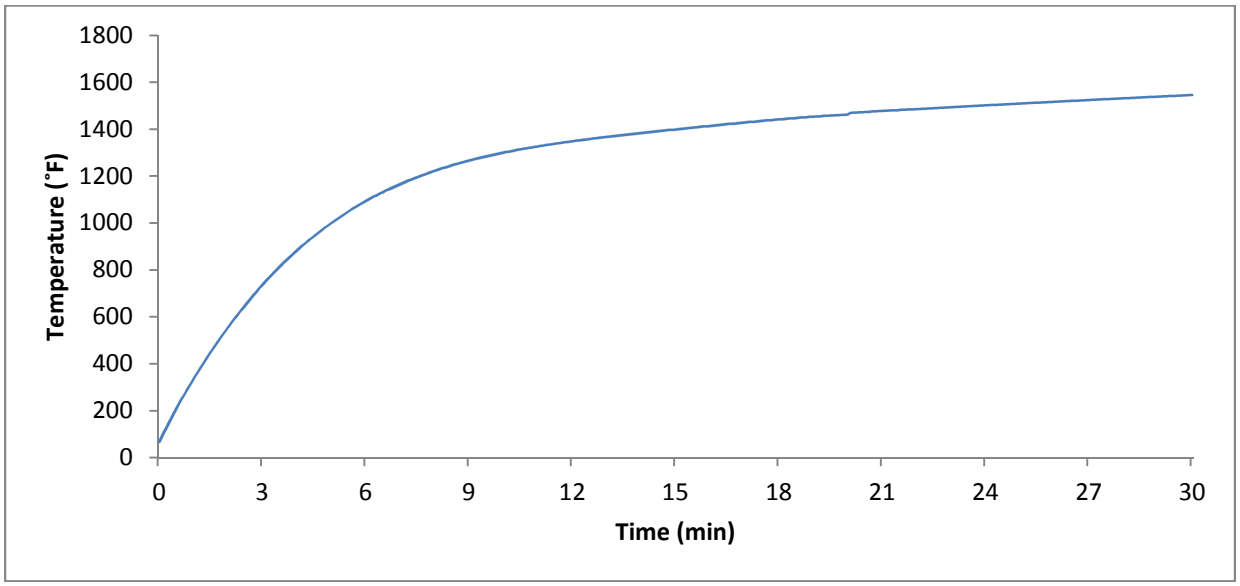

Figure 8: ASTM E-119 time-temperature curve used in fire tests

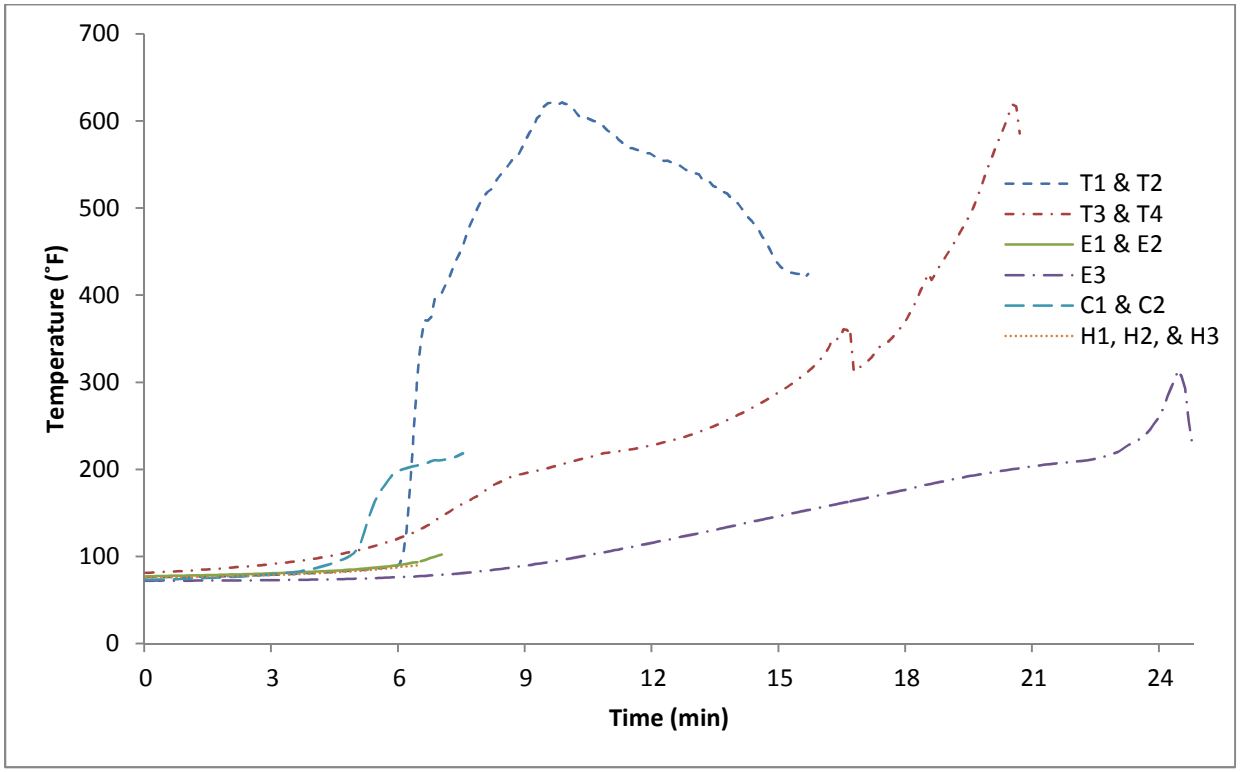

Figure 9: Comparison of averaged temperatures in different joist types at thermocouple location 1

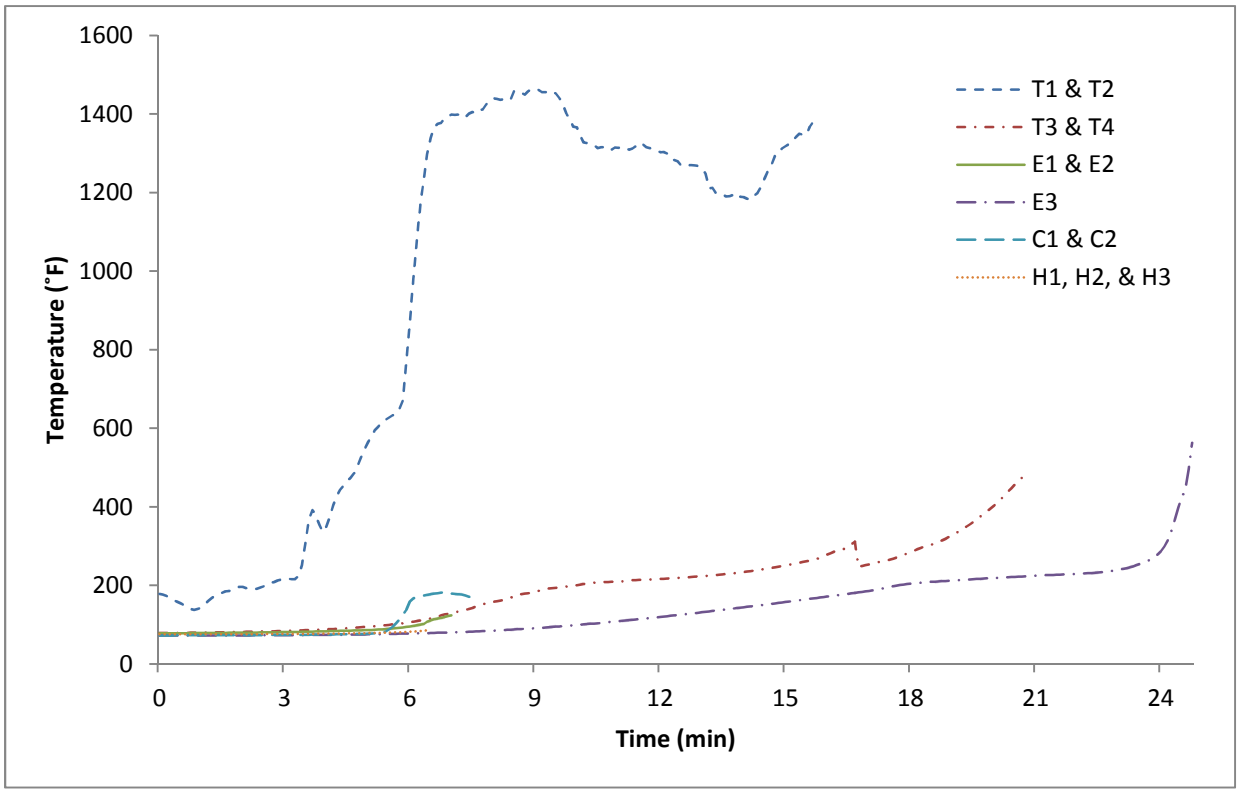

Figure 10: Comparison of averaged temperatures in different joist types at thermocouple location 2

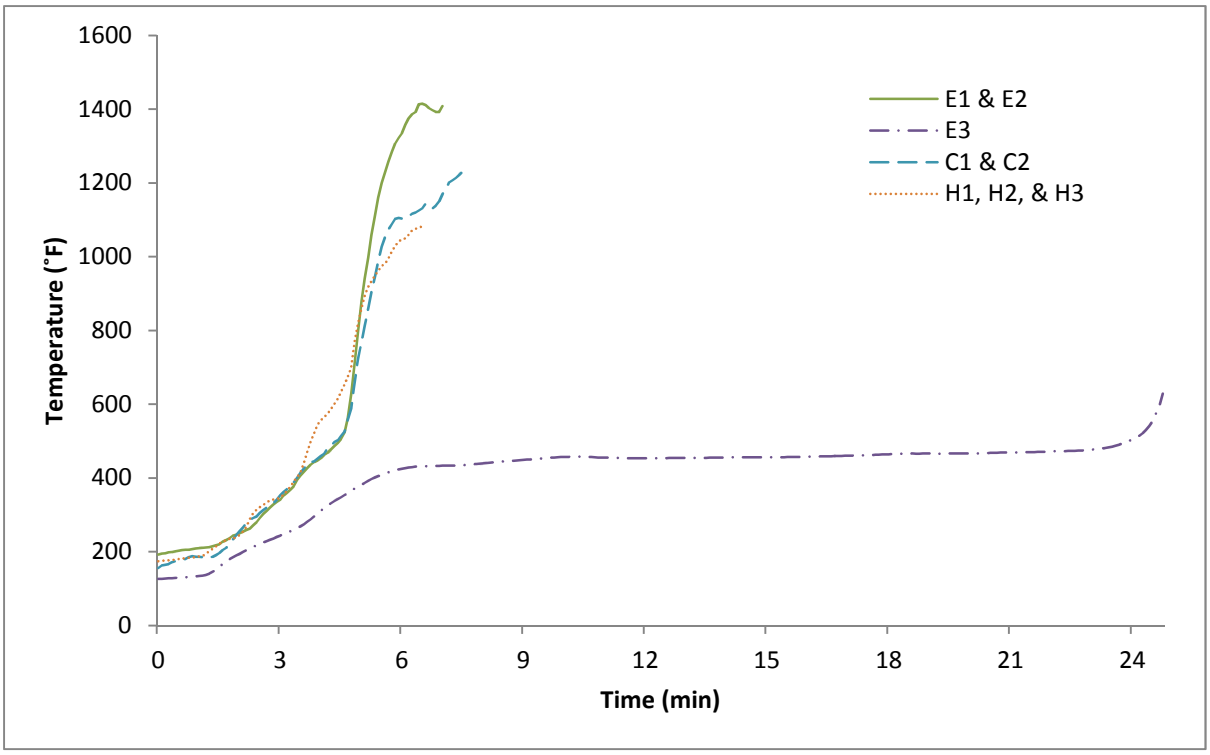

Figure 11: Comparison of averaged temperatures in different joist types at thermocouple location 3

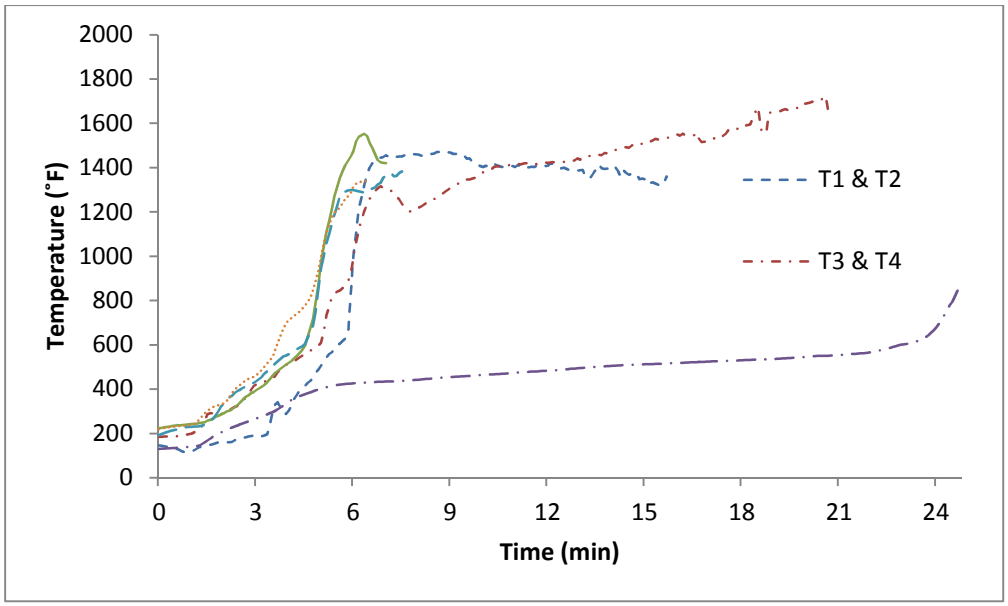

Figure 12: Comparison of averaged temperatures in different joist types at thermocouple location 4

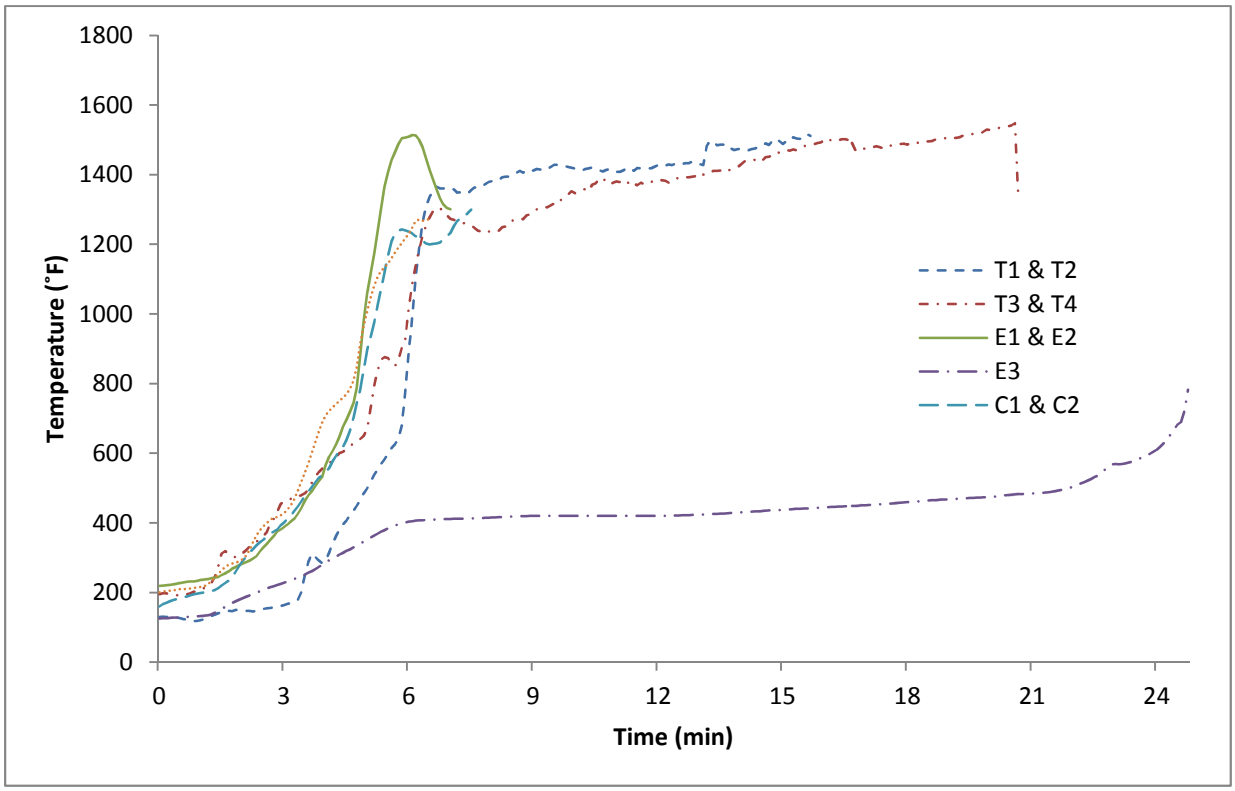

Figure 13: Comparison of averaged temperatures in different joist types at thermocouple location 5

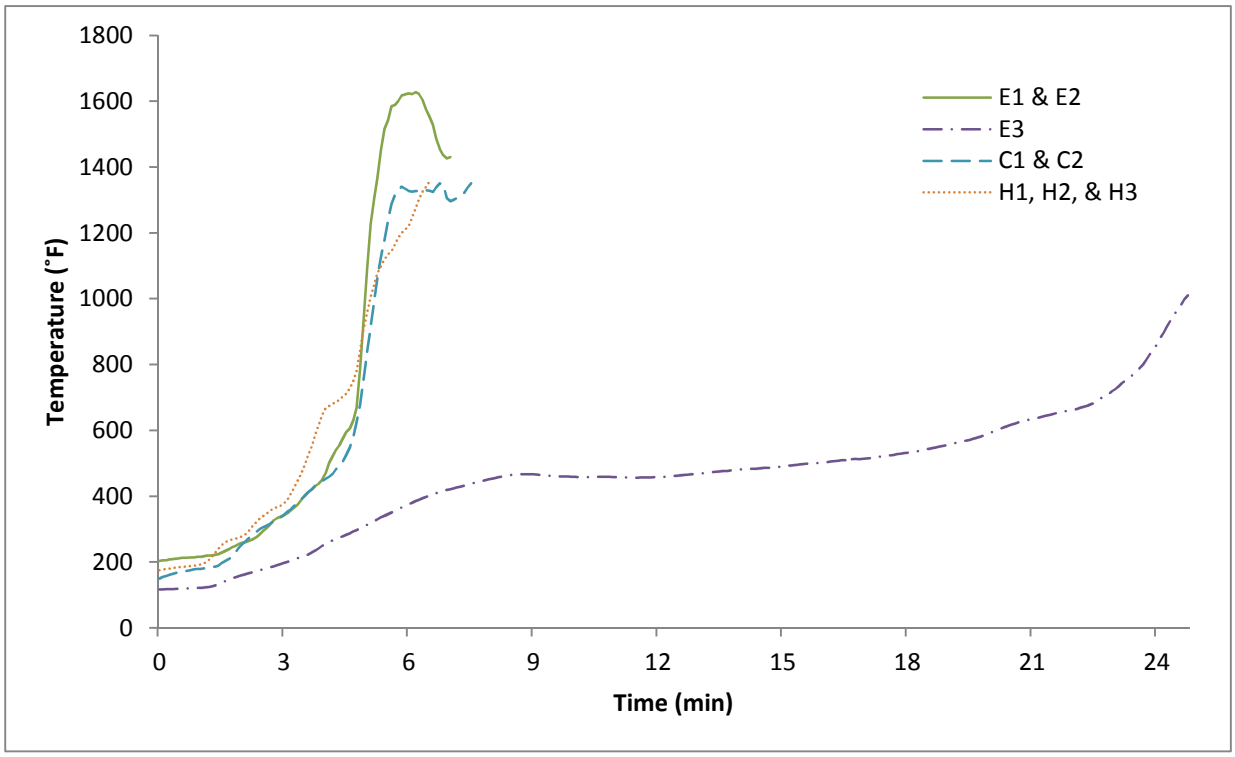

Figure 14: Comparison of averaged temperatures in different joist types at thermocouple location 6

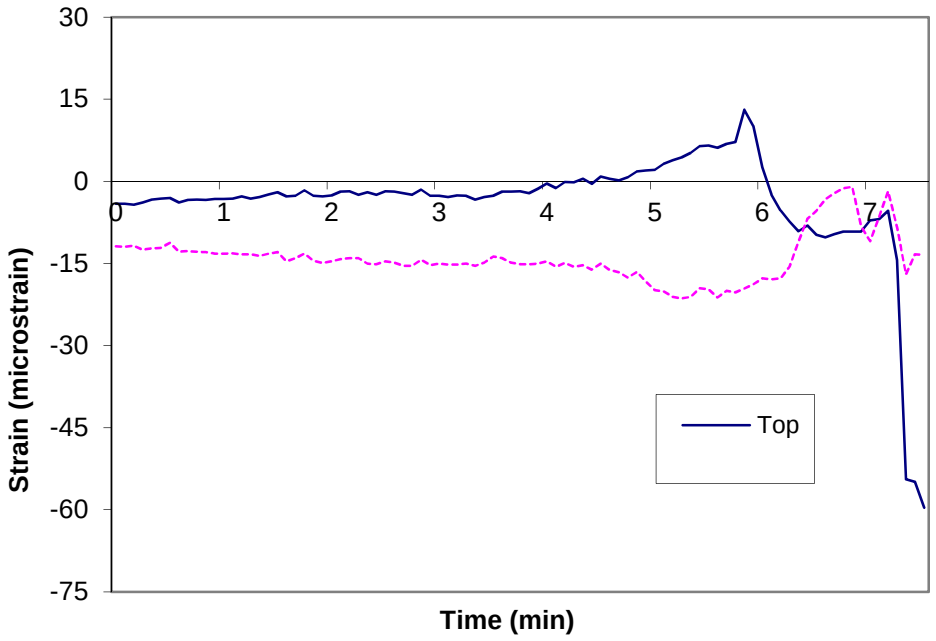

Figure 15: Measured representative strains during fire resistance test of joist C2

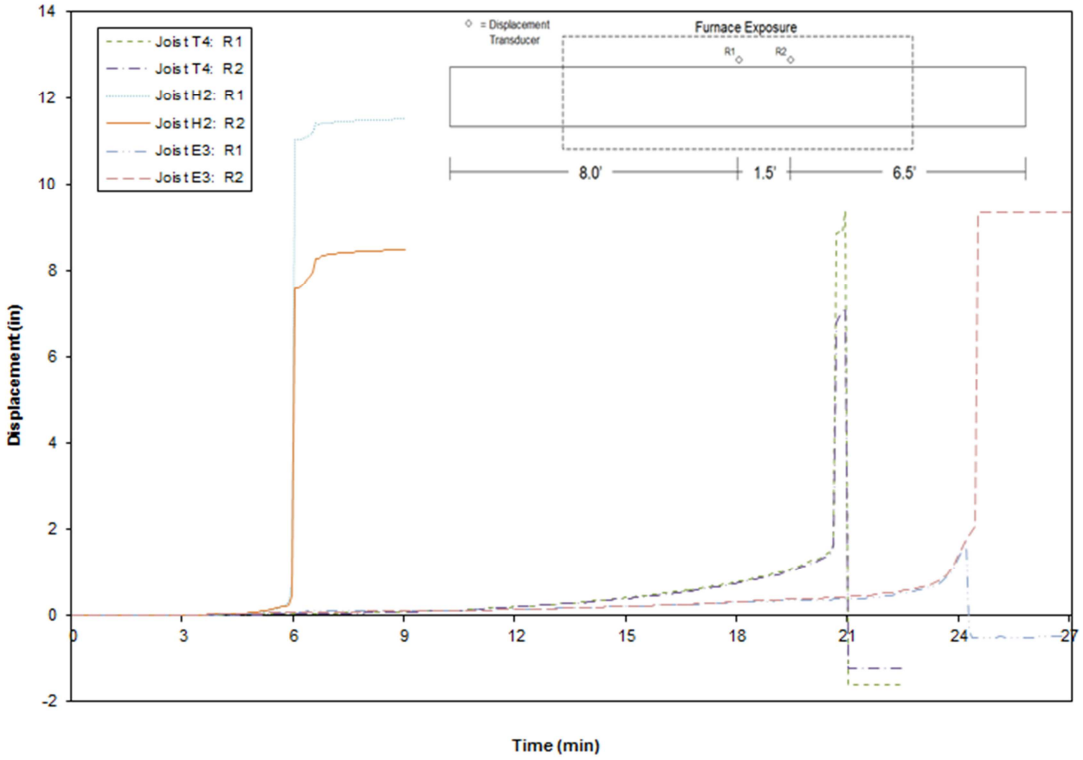

Figure 16: Measured representative vertical displacements during fire resistance tests on joists T4, H2, and E3

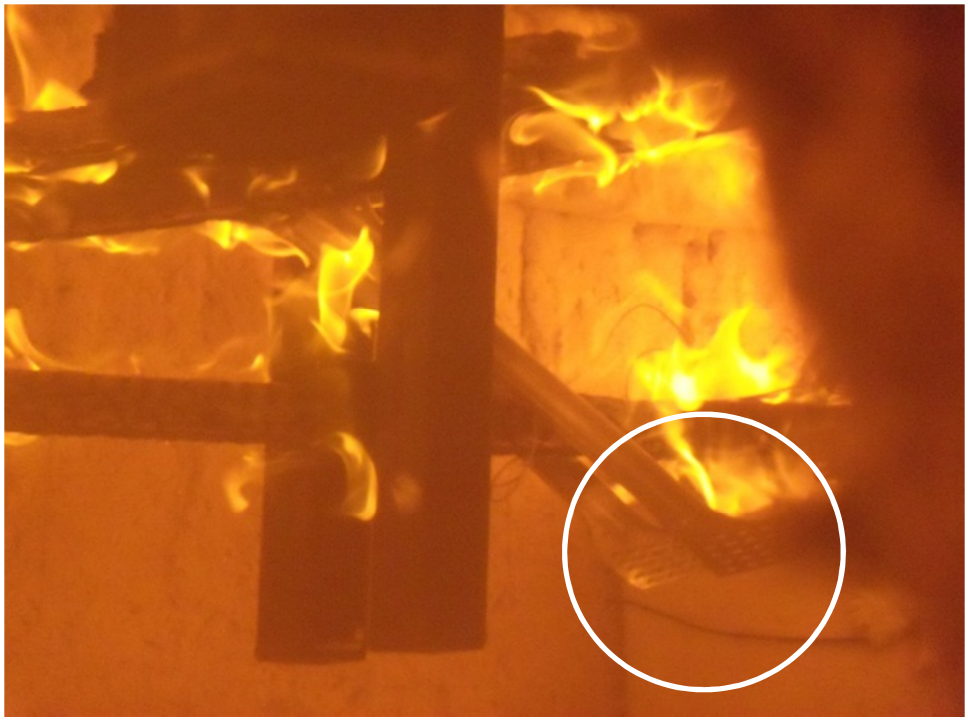

Figure 17: Connection failure of hybrid joist H2

Figure 18: Formation and enlargement of voids in web of joist C2

APPENDIX A

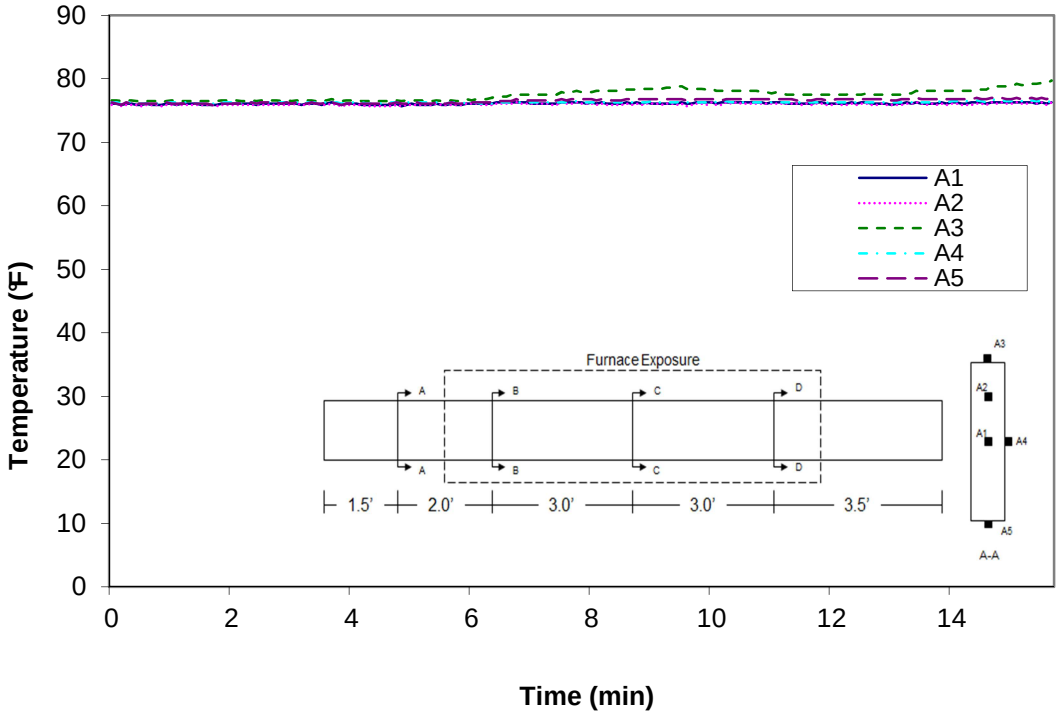

Figure A-1: Temperature distribution in wood joist T1 at cross-section A

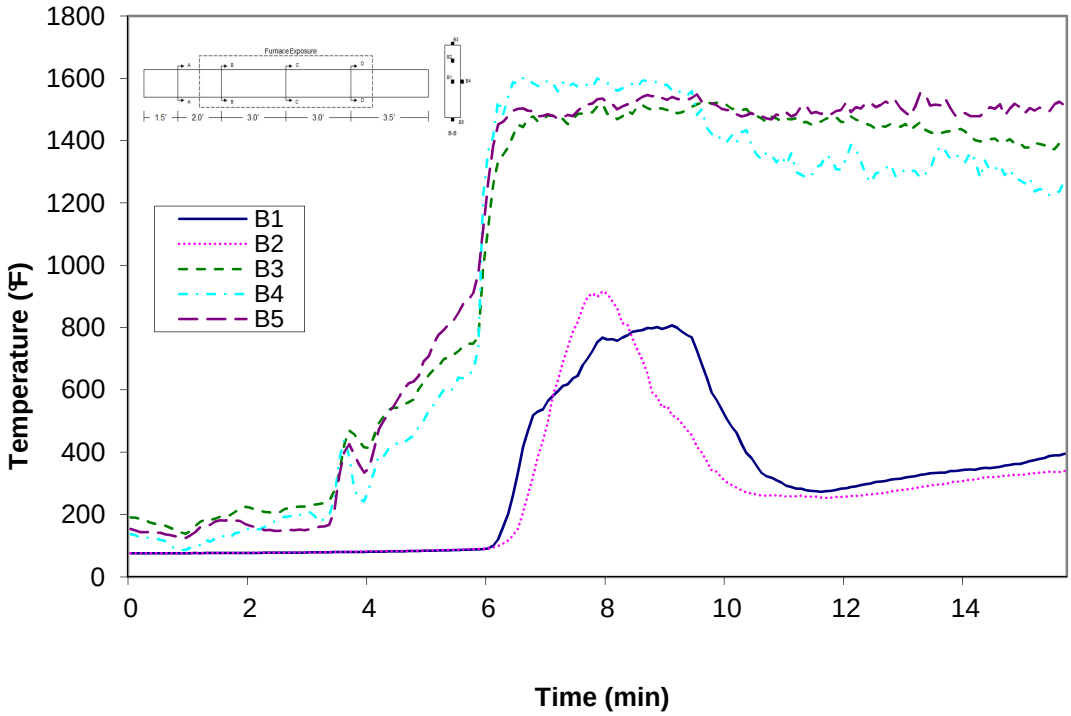

Figure A-2: Temperature distribution in wood joist T1 at cross-section B

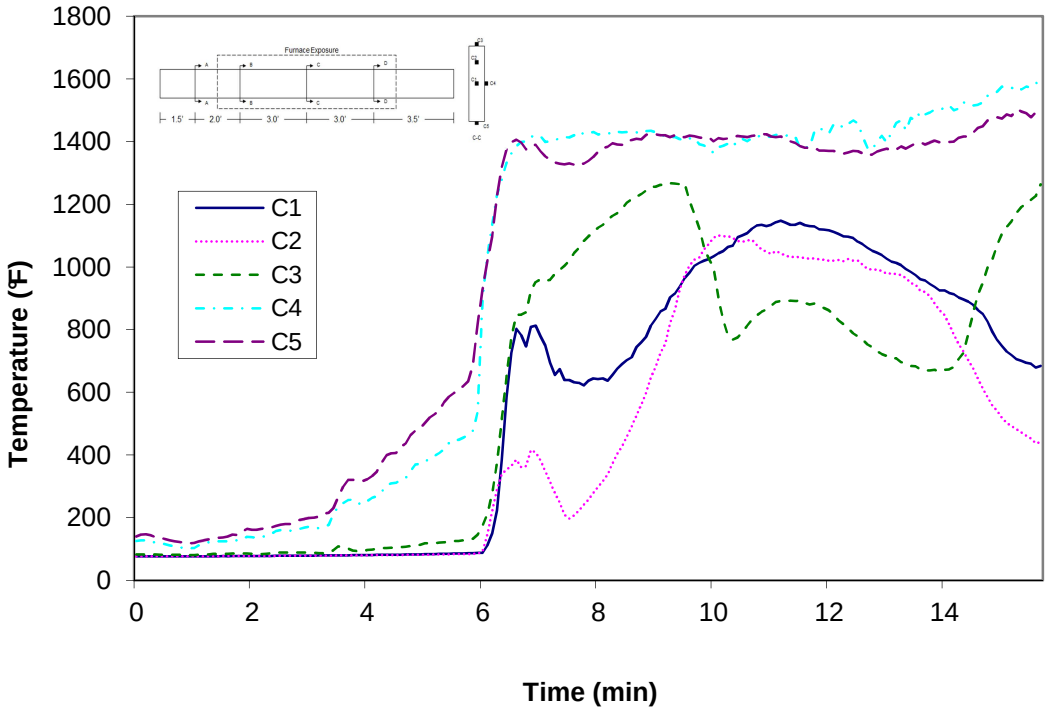

Figure A-3: Temperature distribution in wood joist T1 at cross-section C

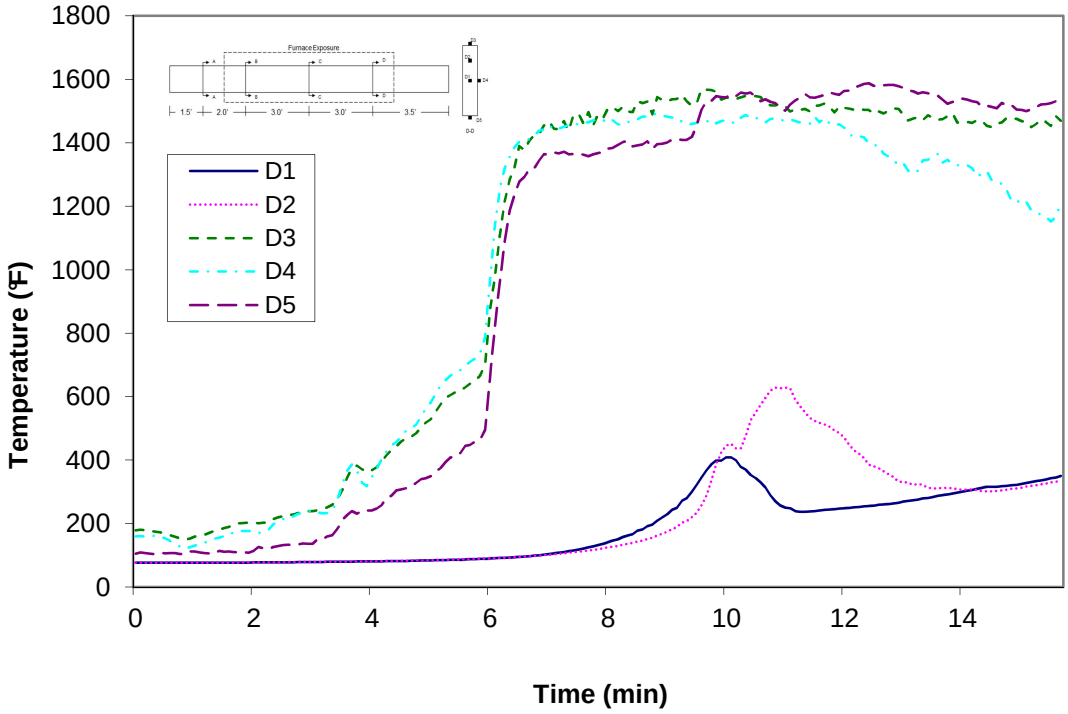

Figure A-4: Temperature distribution in wood joist T1 at cross-section D

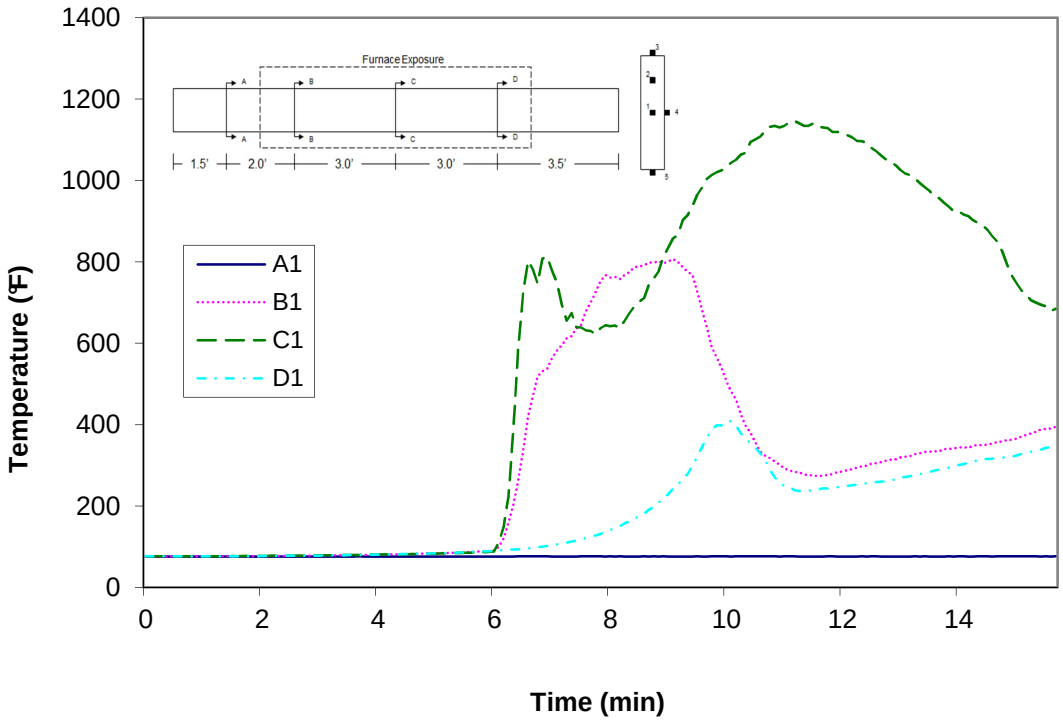

Figure A-5: Temperature distribution in wood joist T1 at thermocouple location 1

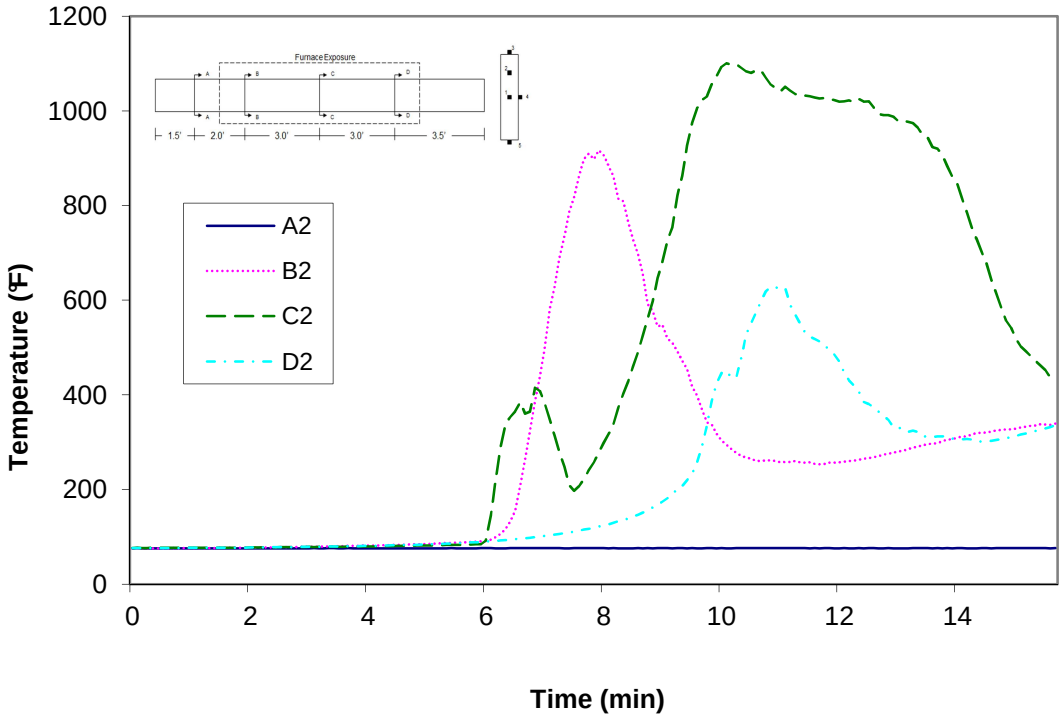

Figure A-6: Temperature distribution in wood joist T1 at thermocouple location 2

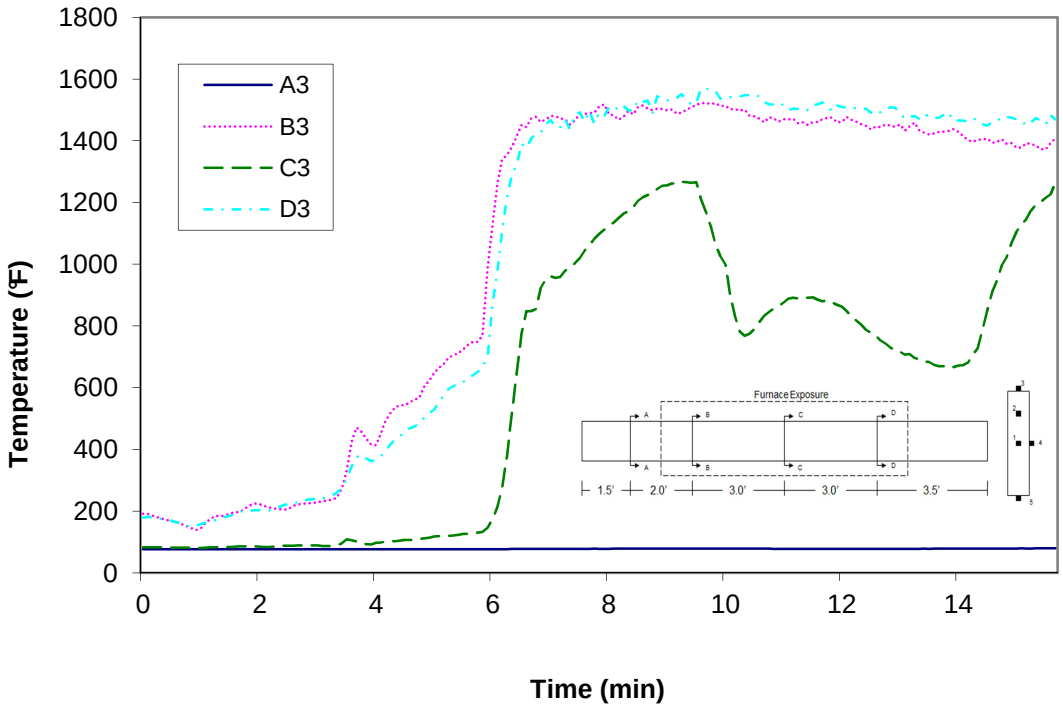

Figure A-7: Temperature distribution in wood joist T1 at thermocouple location 3

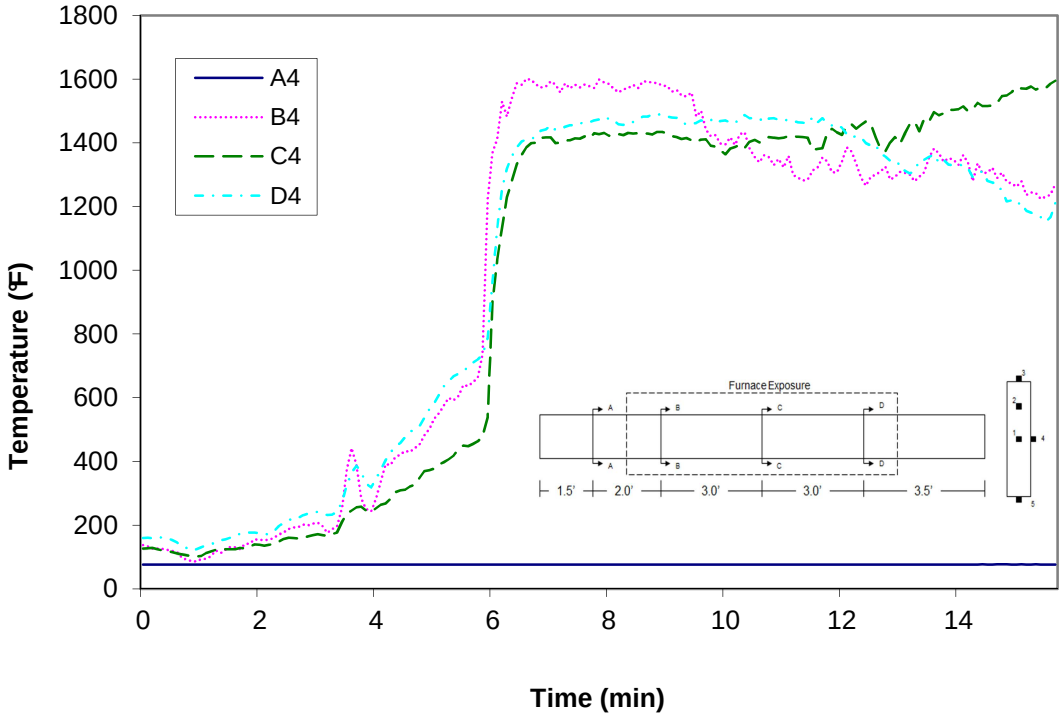

Figure A-8: Temperature distribution in wood joist T1 at thermocouple location 4

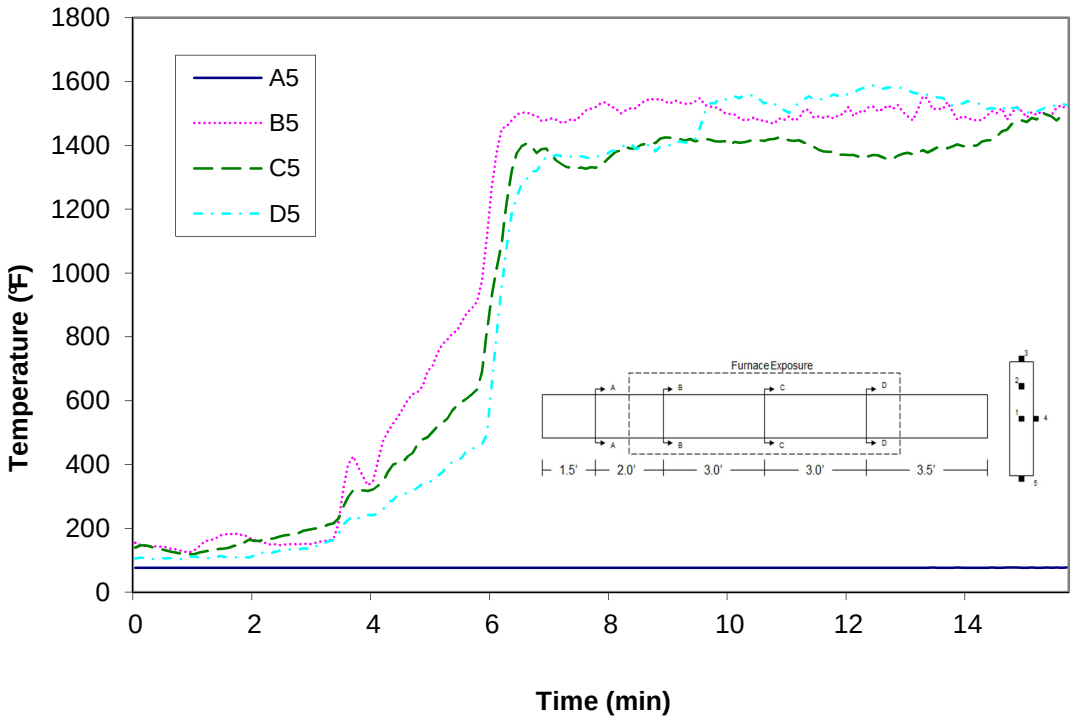

Figure A-9: Temperature distribution in wood joist T1 at thermocouple location 5

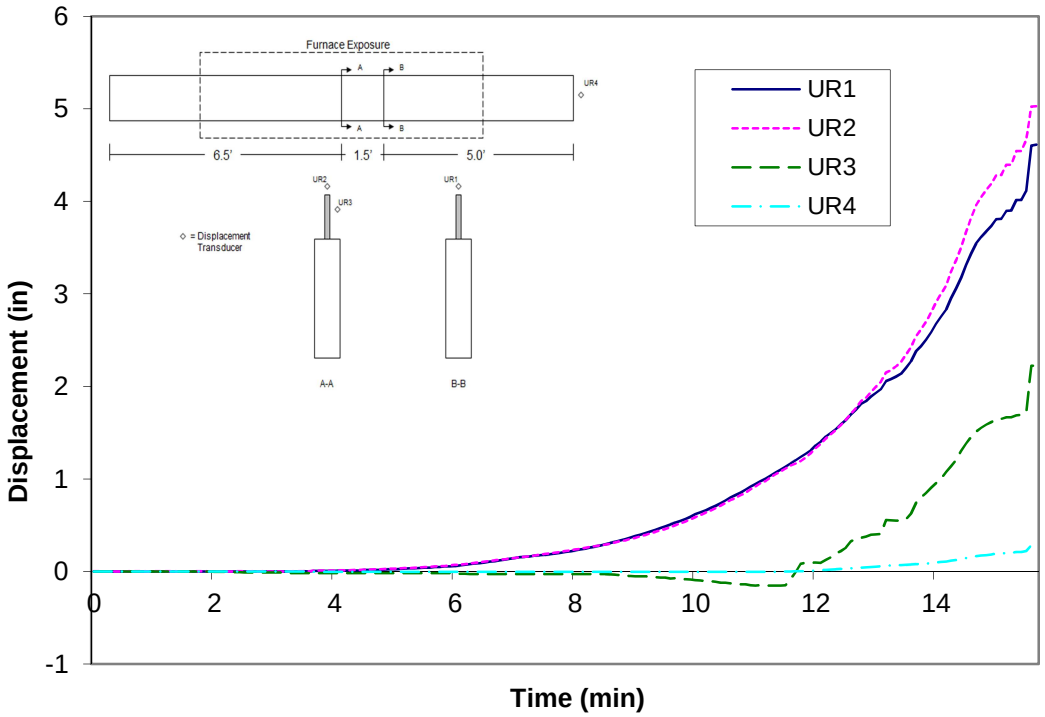

Figure A-10: Measured displacements recorded during fire resistance tests of wood joist T1

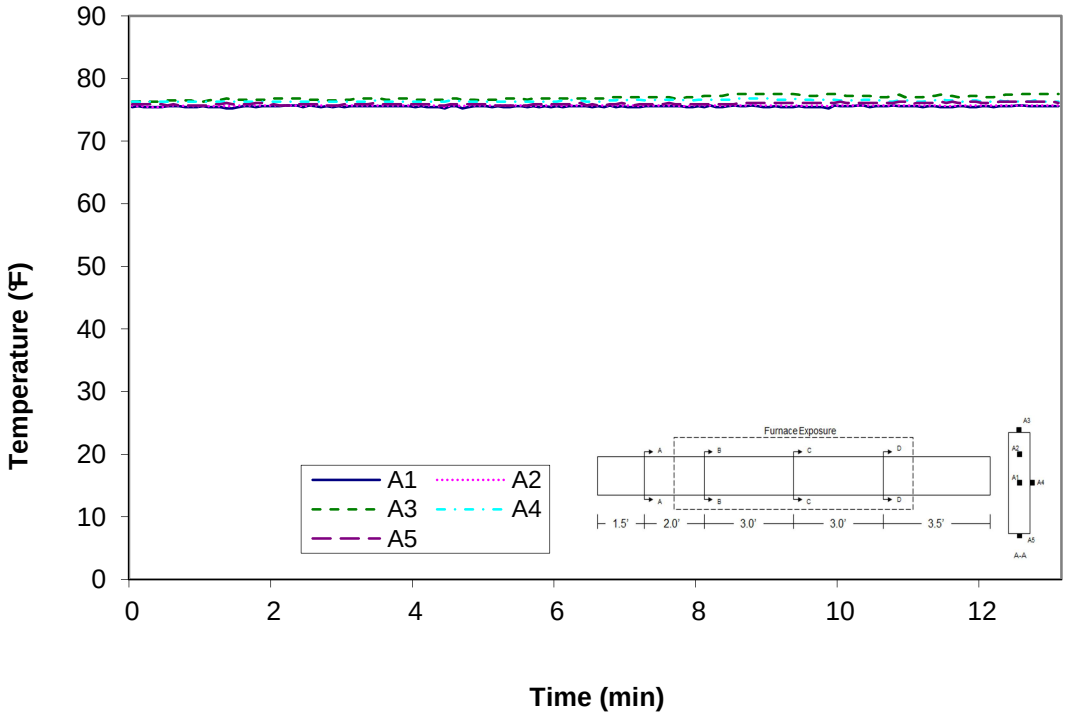

Figure A-11: Temperature distribution in wood joist T2 at cross-section A

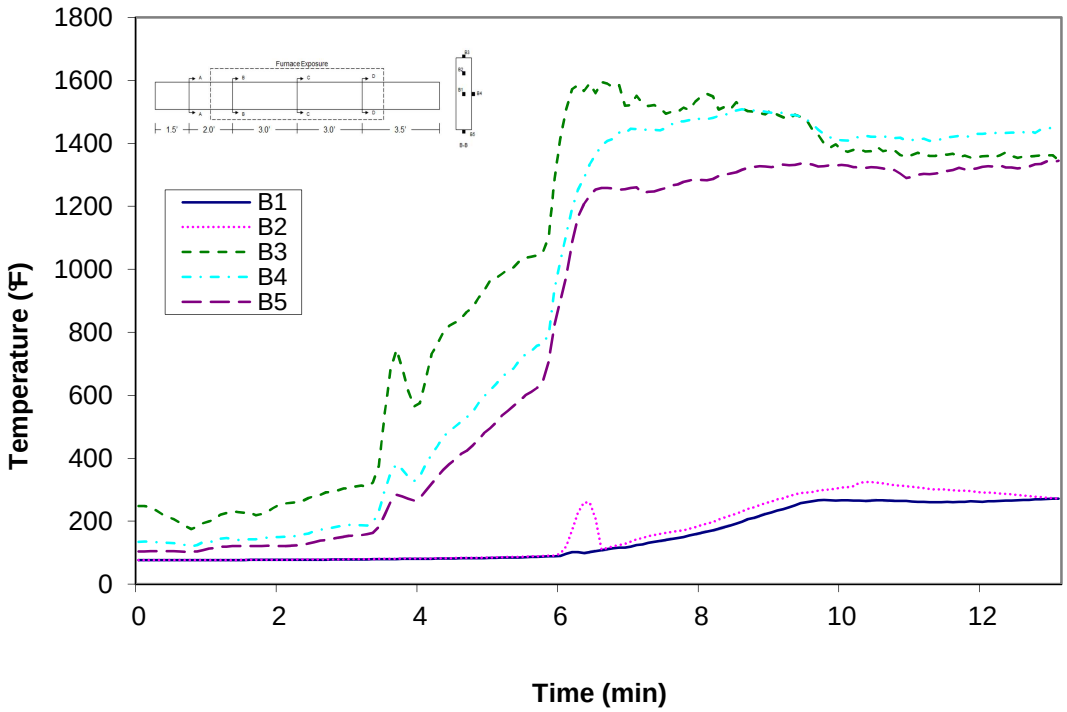

Figure A-12: Temperature distribution in wood joist T2 at cross-section B

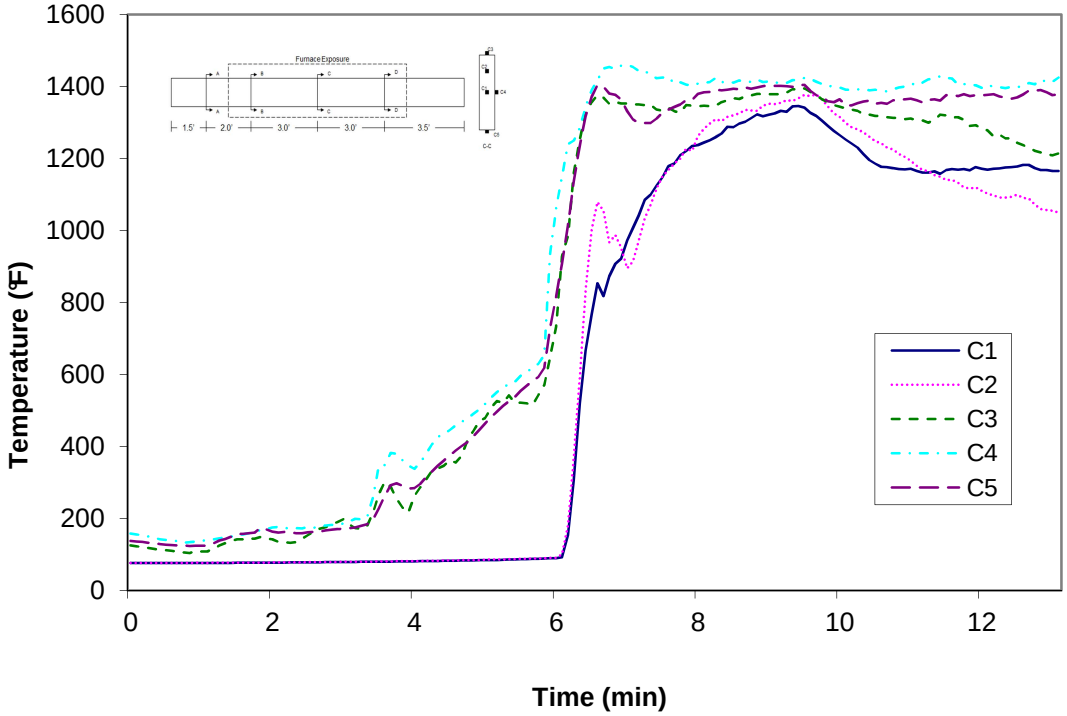

Figure A-13: Temperature distribution in wood joist T2 at cross-section C

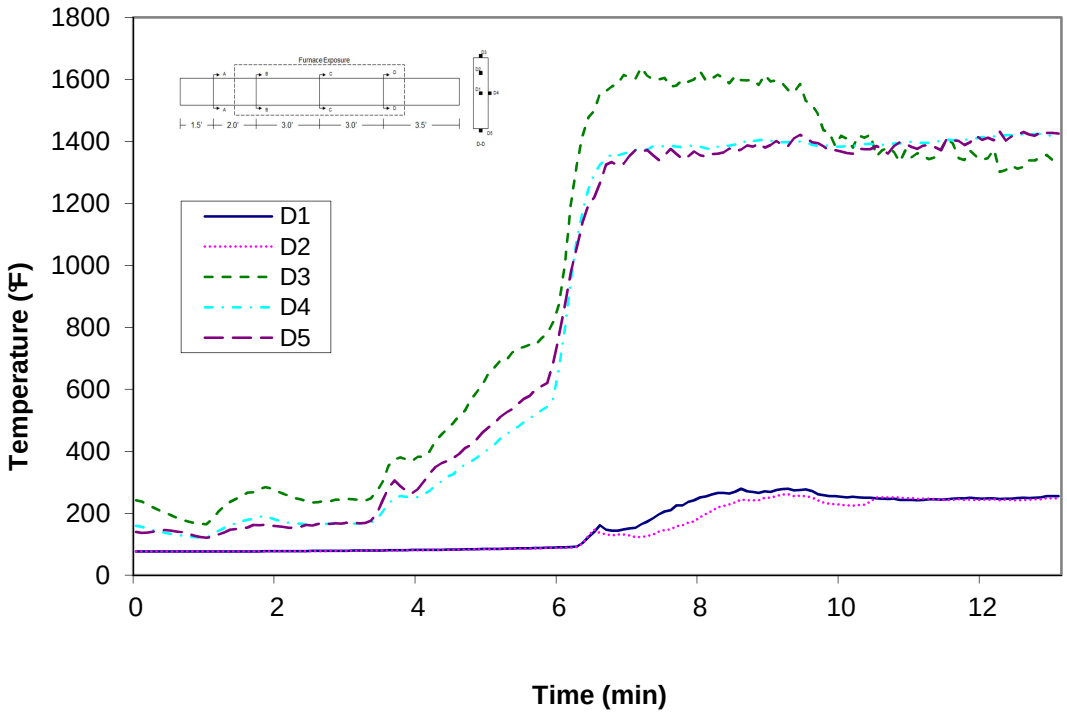

Figure A-14: Temperature distribution in wood joist T2 at cross-section D

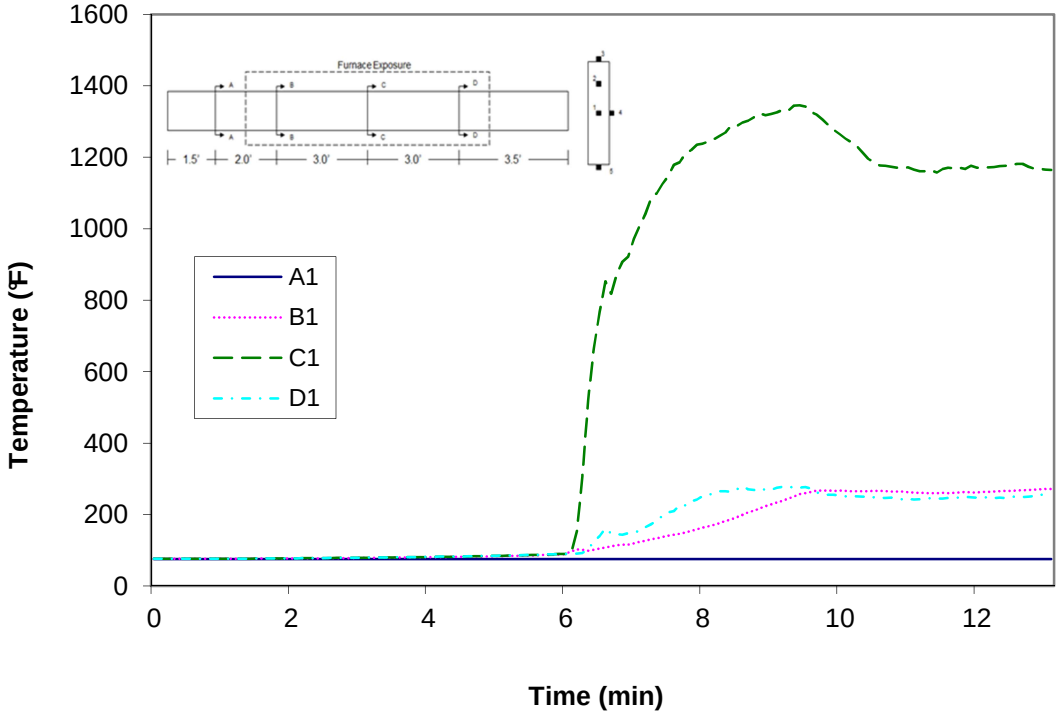

Figure A-15: Temperature distribution in wood joist T2 at thermocouple location 1

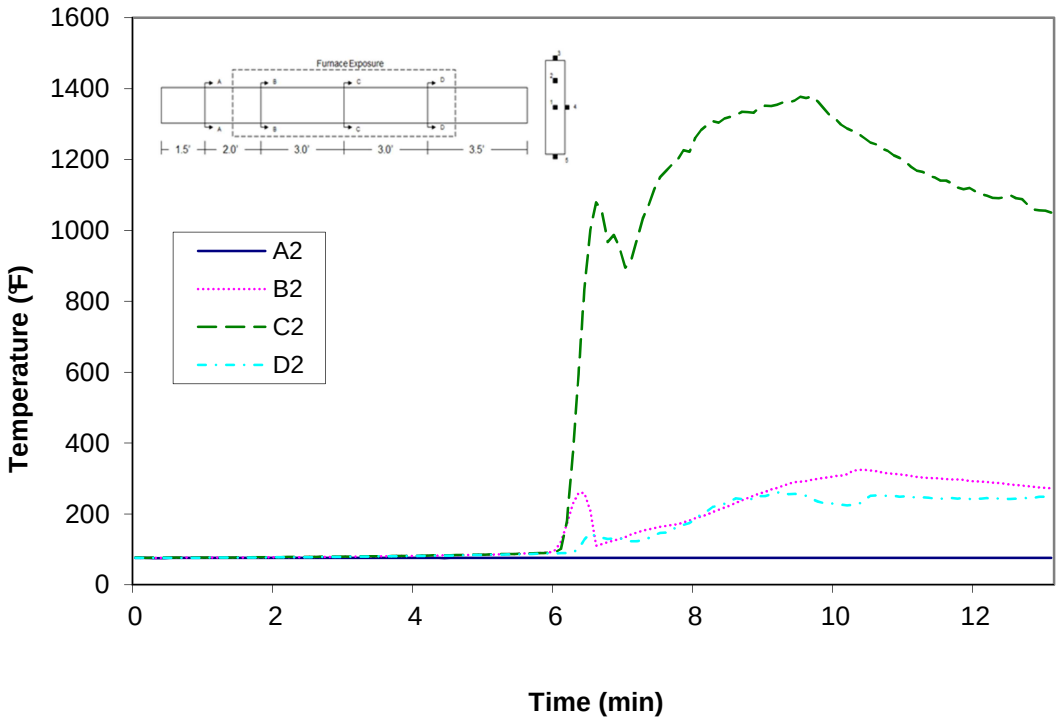

Figure A-16: Temperature distribution in wood joist T2 at thermocouple location 2

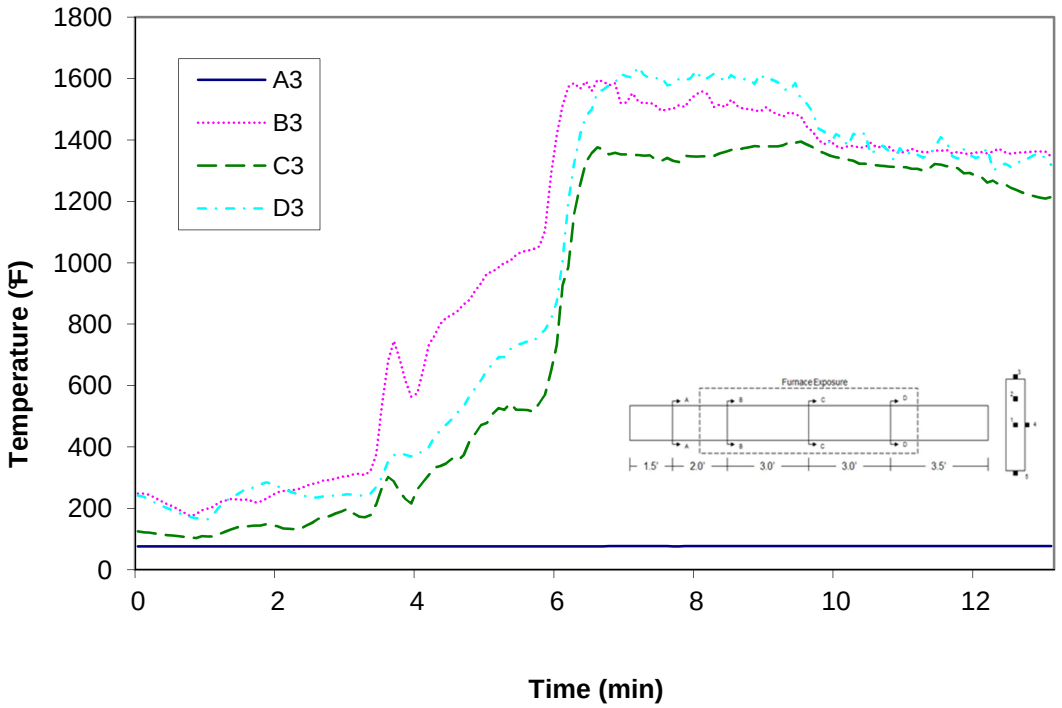

Figure A-17: Temperature distribution in wood joist T2 at thermocouple location 3

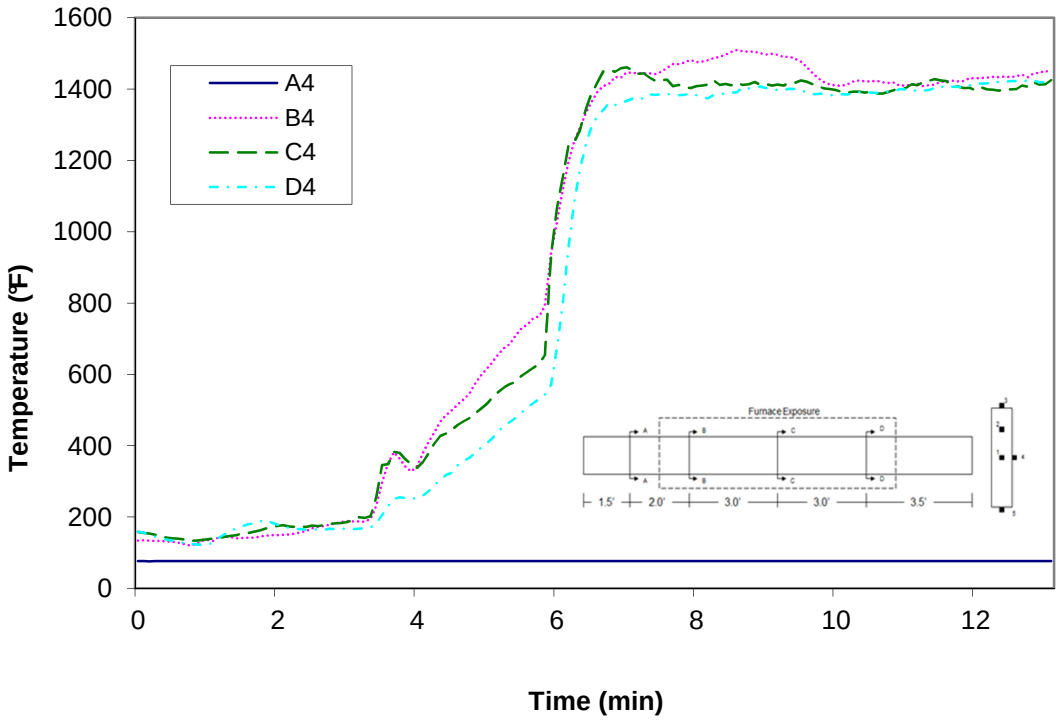

Figure A-18: Temperature distribution in wood joist T2 at thermocouple location 4

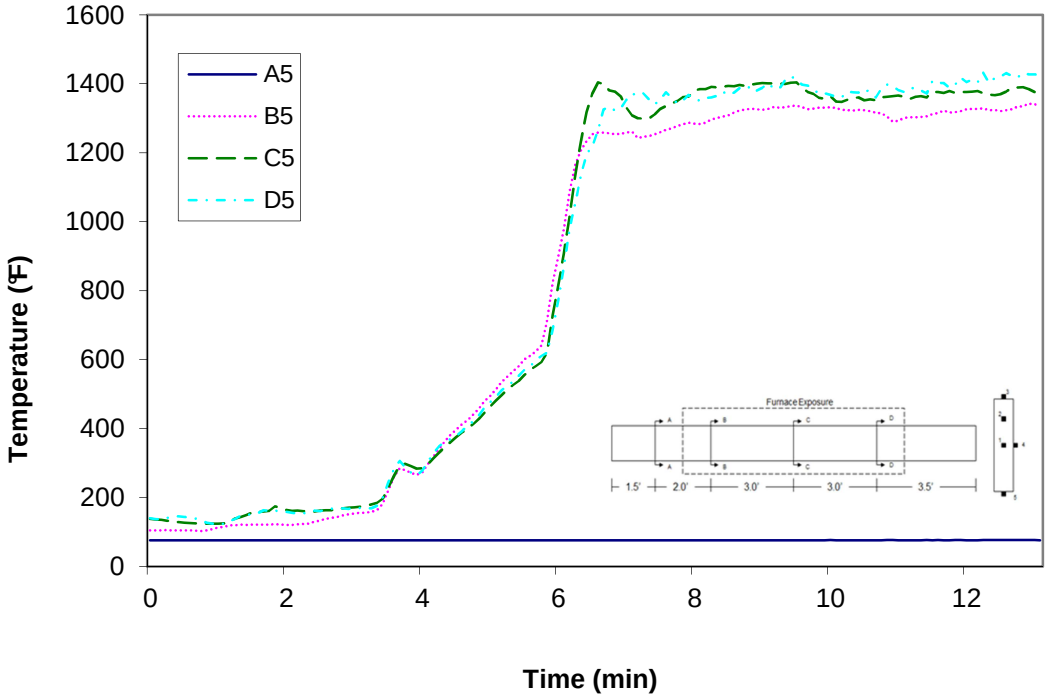

Figure A-19: Temperature distribution in wood joist T2 at thermocouple location 5

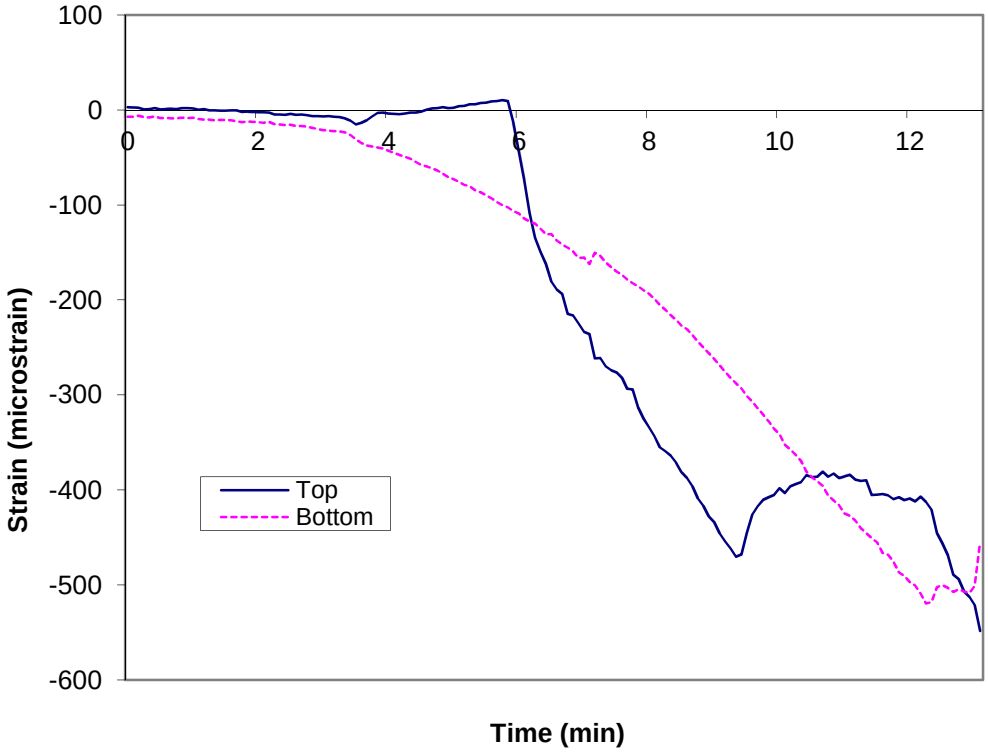

Figure A-20: Measured strains recorded during fire resistance tests of wood joist T2

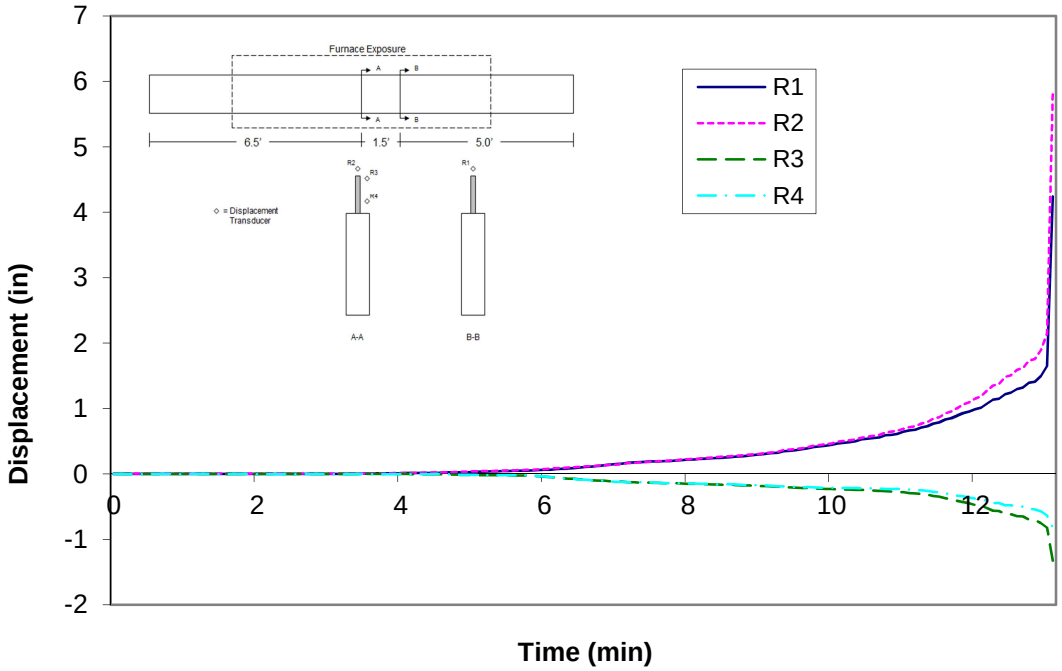

Figure A-21: Measured displacements recorded during fire resistance tests of wood joist T2

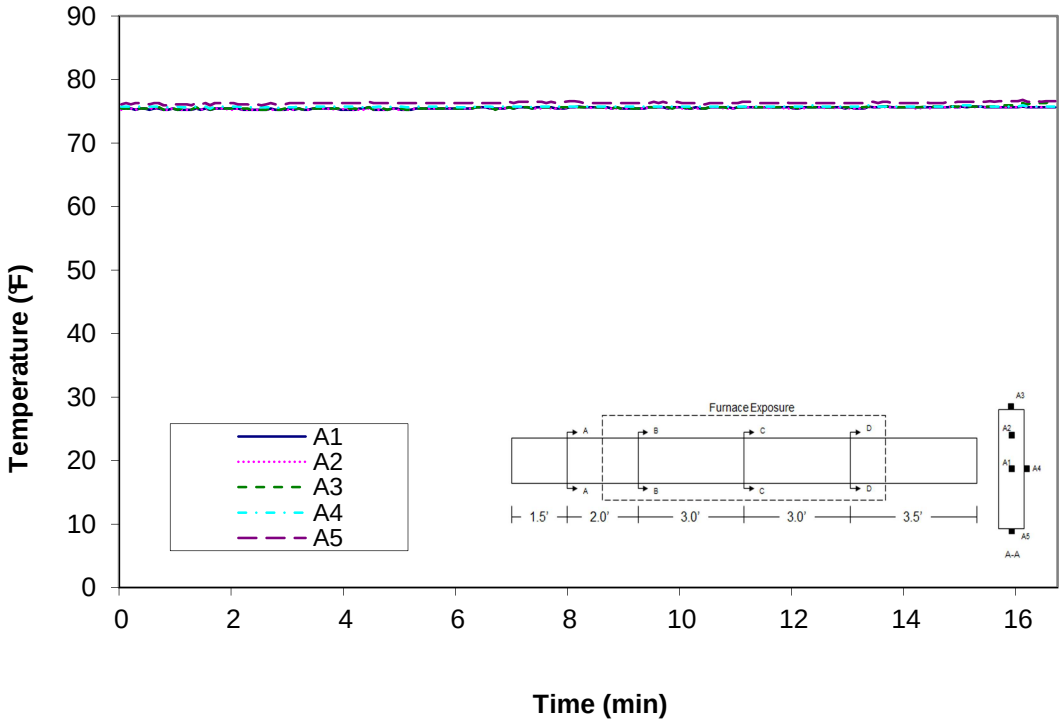

Figure A-22: Temperature distribution in wood joist T3 at cross-section A

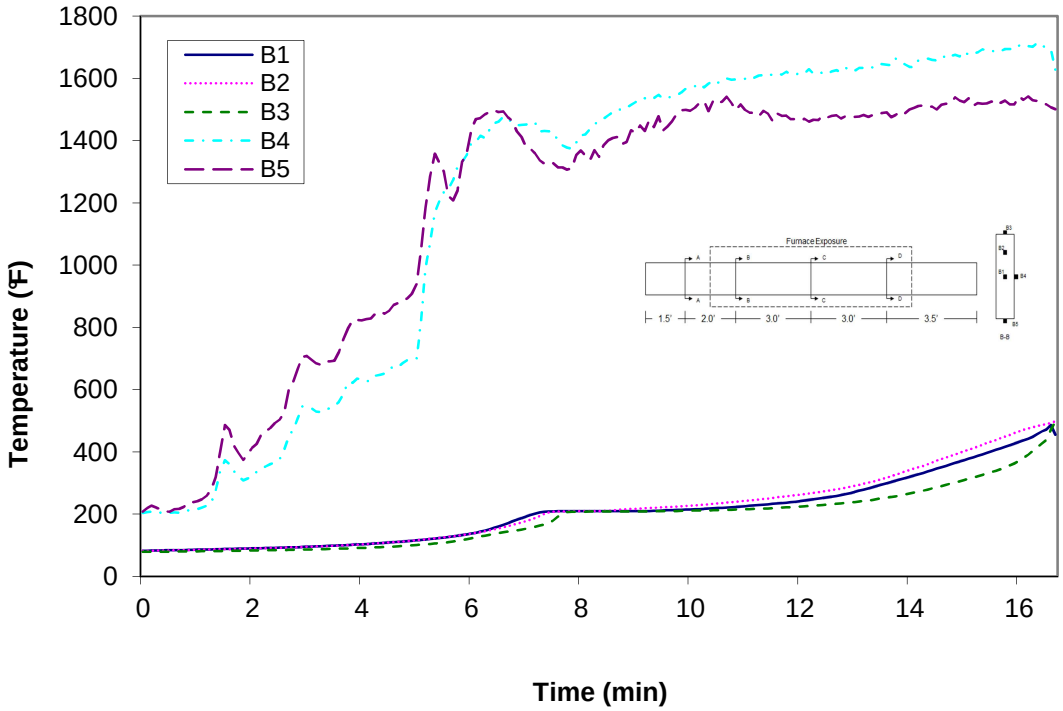

Figure A-23: Temperature distribution in wood joist T3 at cross-section B

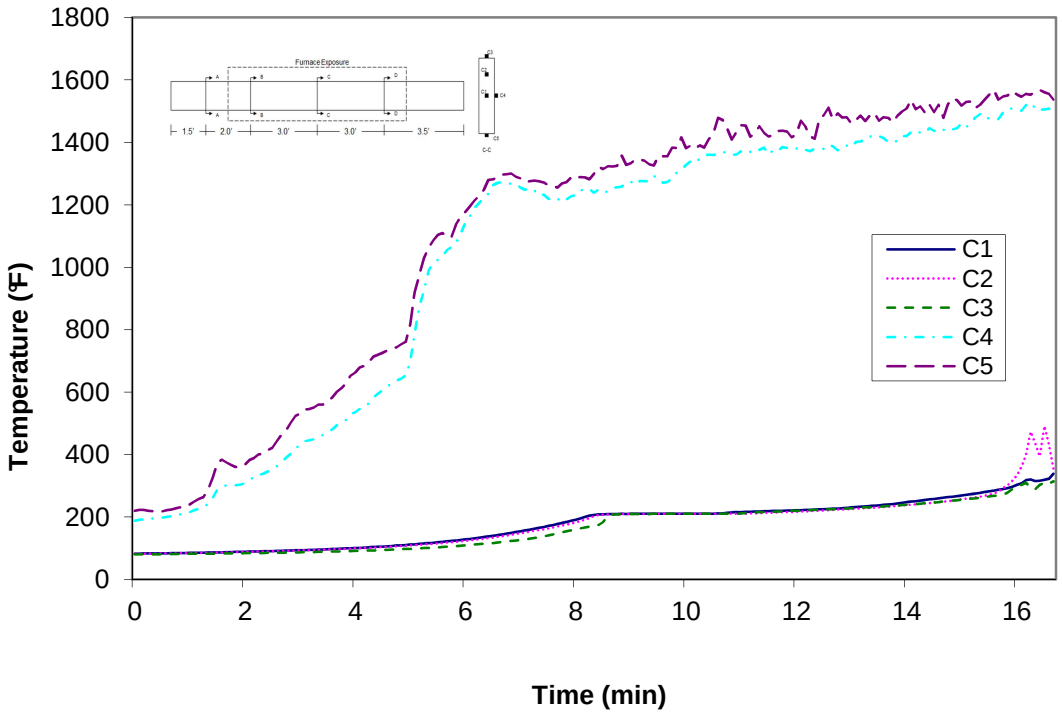

Figure A-24: Temperature distribution in wood joist T3 at cross-section C

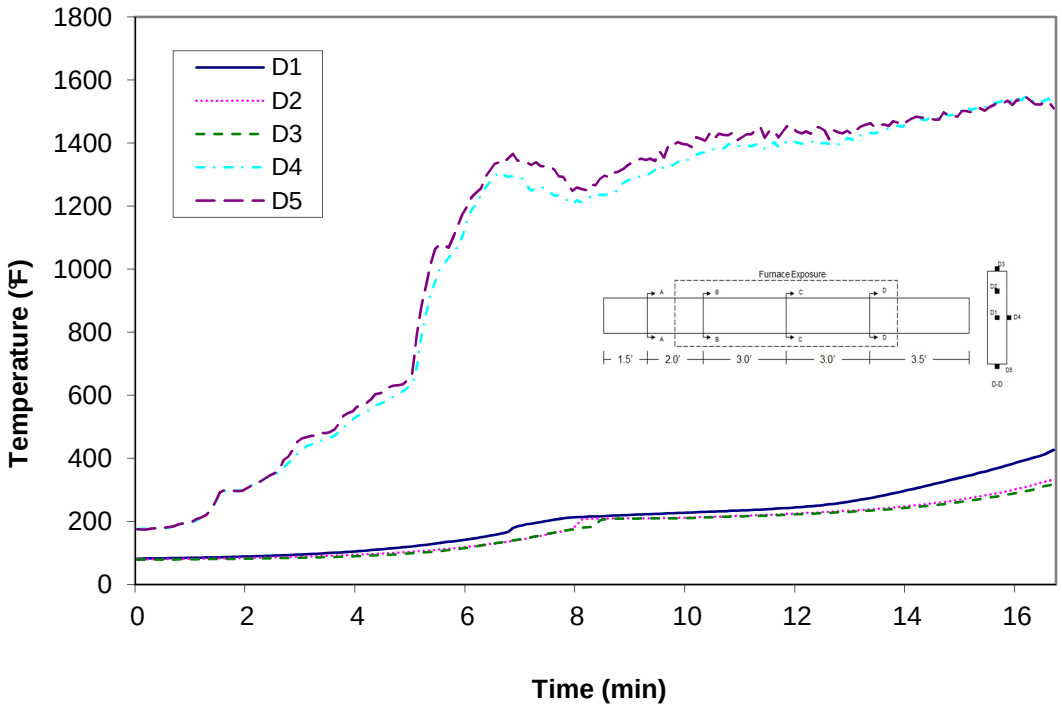

Figure A-25: Temperature distribution in wood joist T3 at cross-section D

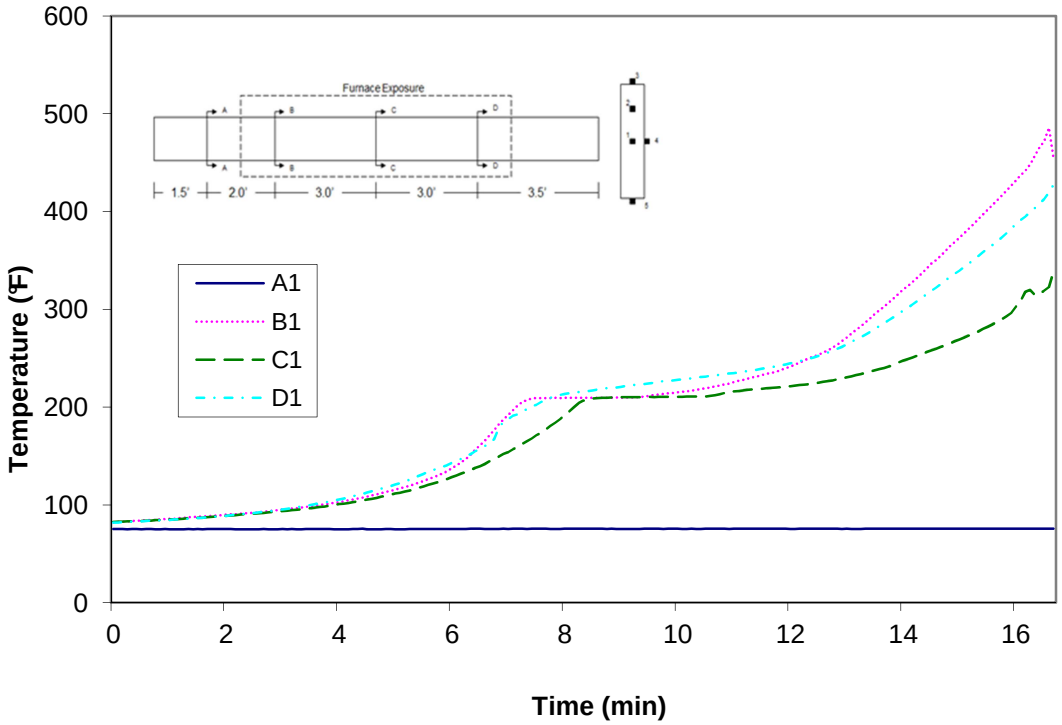

Figure A-26: Temperature distribution in wood joist T3 at thermocouple location 1

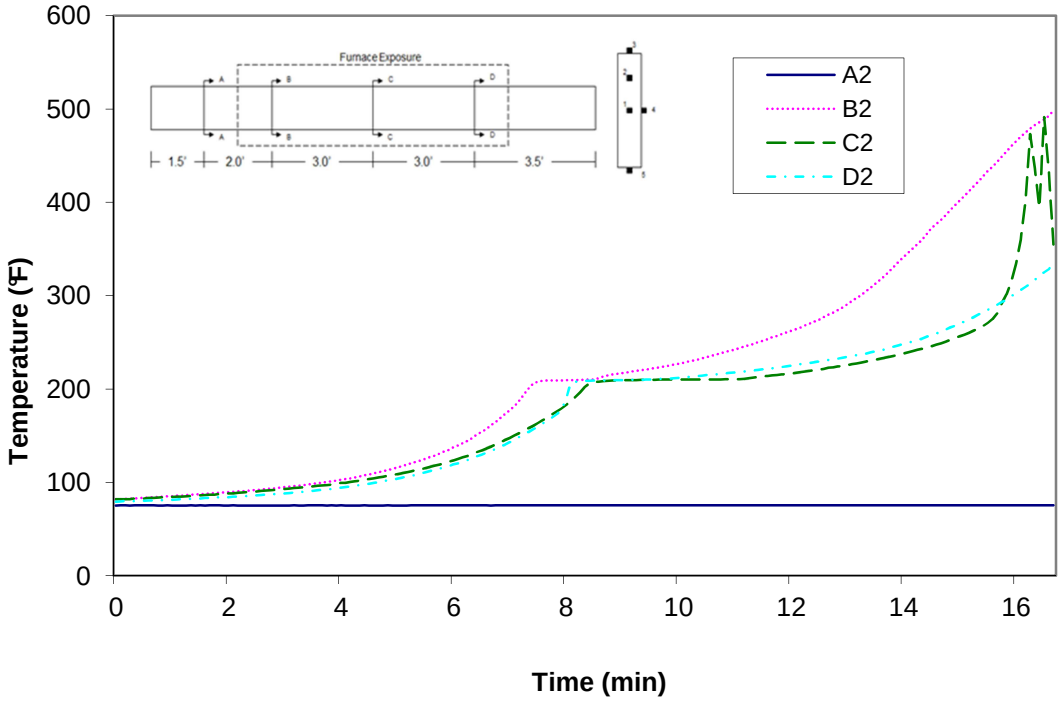

Figure A-27: Temperature distribution in wood joist T3 at thermocouple location 2

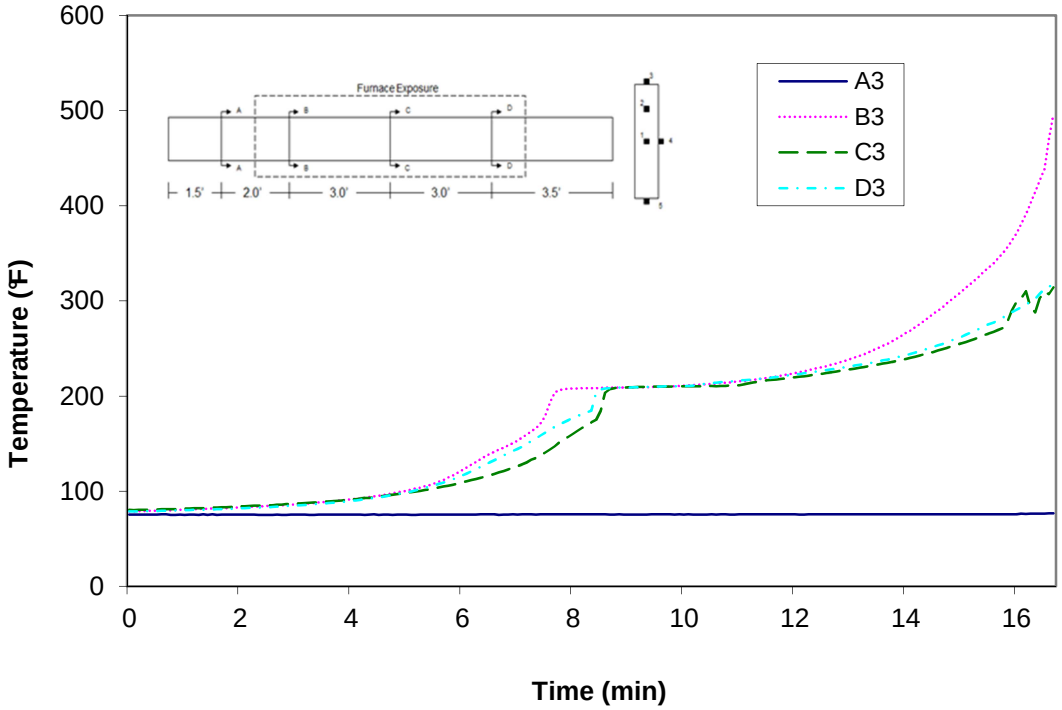

Figure A-28: Temperature distribution in wood joist T3 at thermocouple location 3

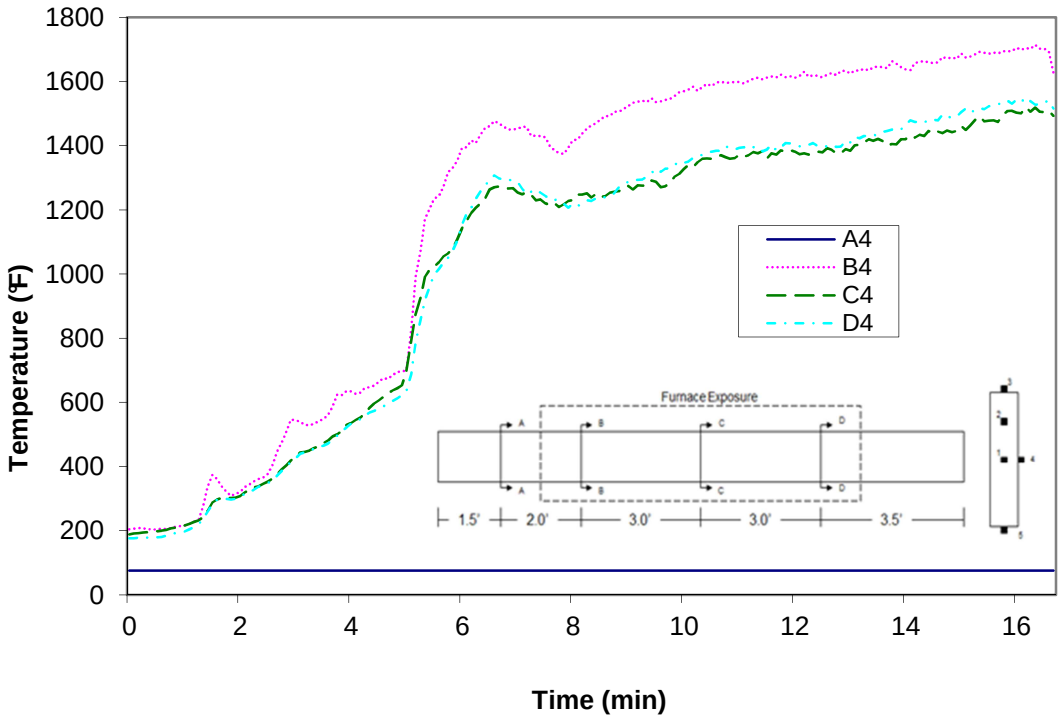

Figure A-29: Temperature distribution in wood joist T3 at thermocouple location 4

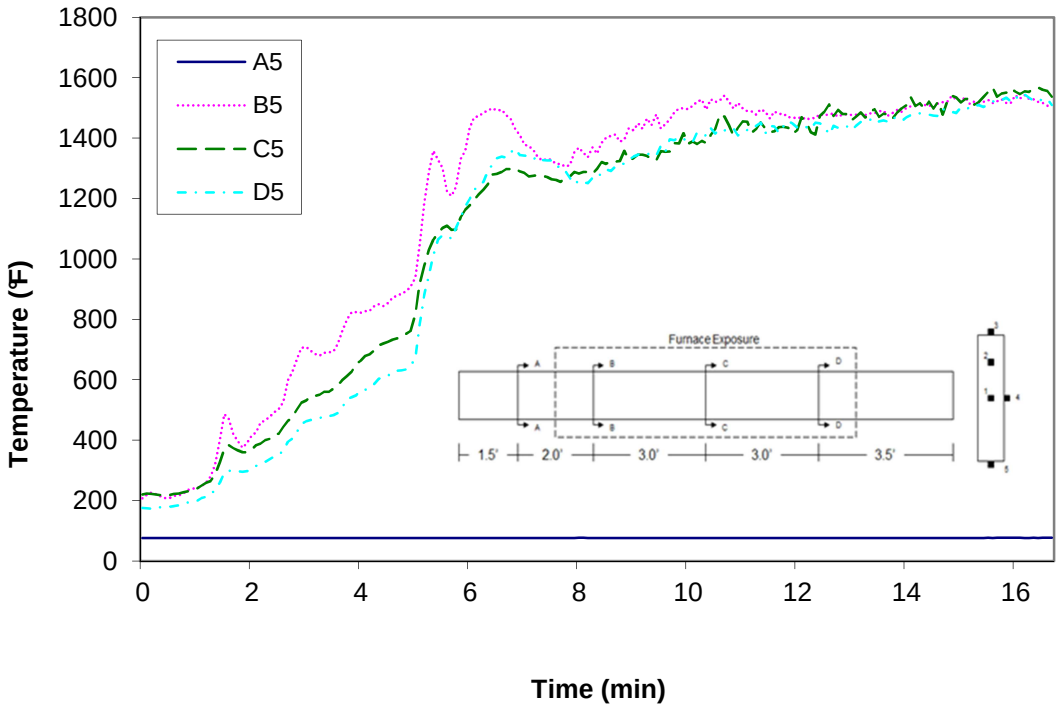

Figure A-30: Temperature distribution in wood joist T3 at thermocouple location 5

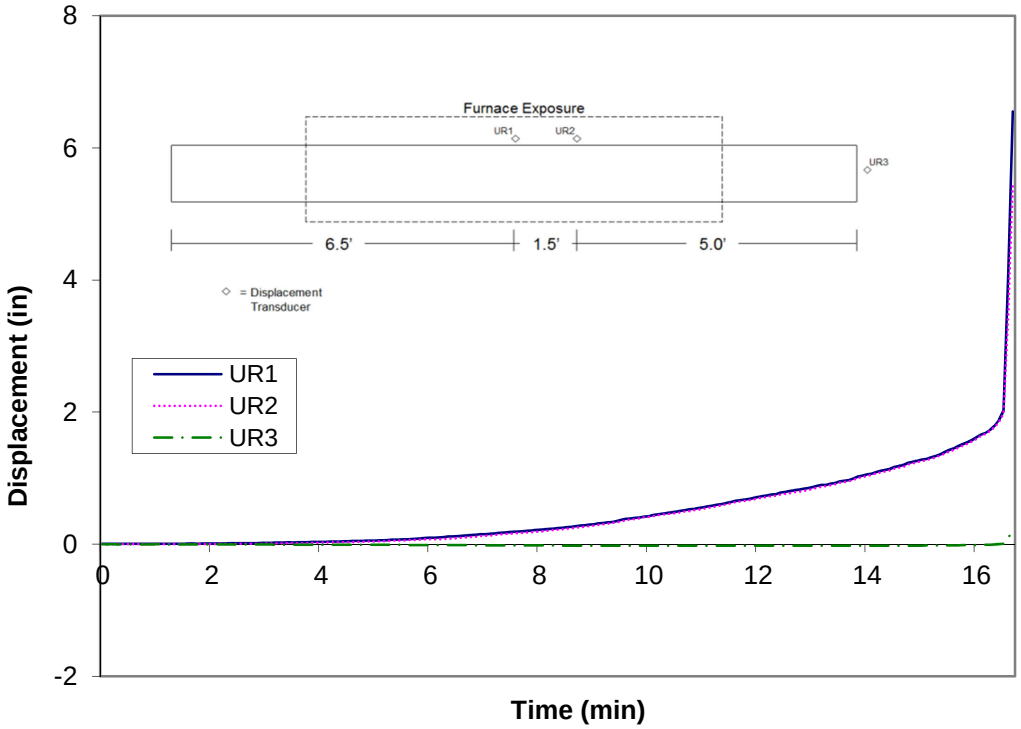

Figure A-31: Measured displacements recorded during fire resistance tests of wood joist T3

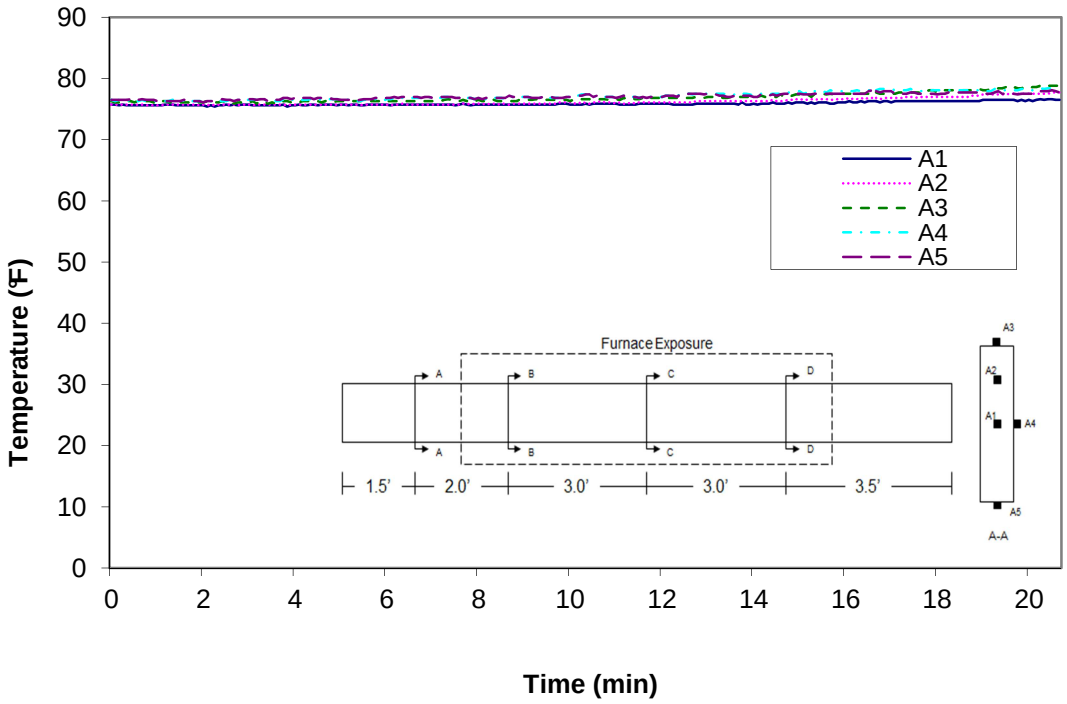

Figure A-32: Temperature distribution in wood joist T4 at cross-section A

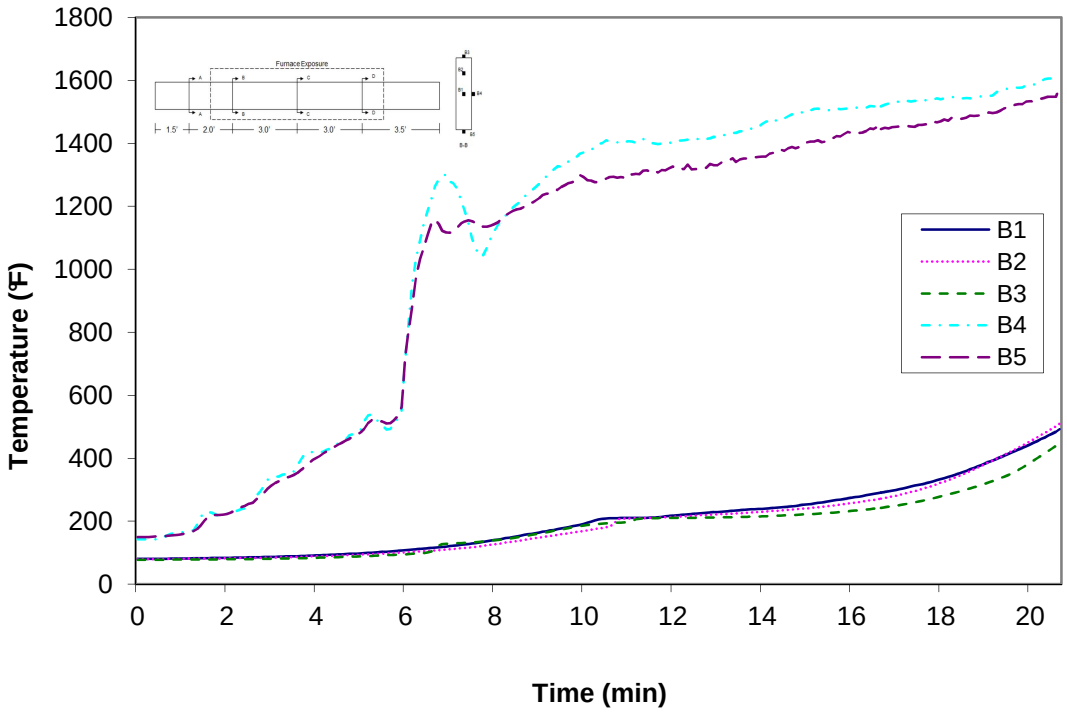

Figure A-33: Temperature distribution in wood joist T4 at cross-section B

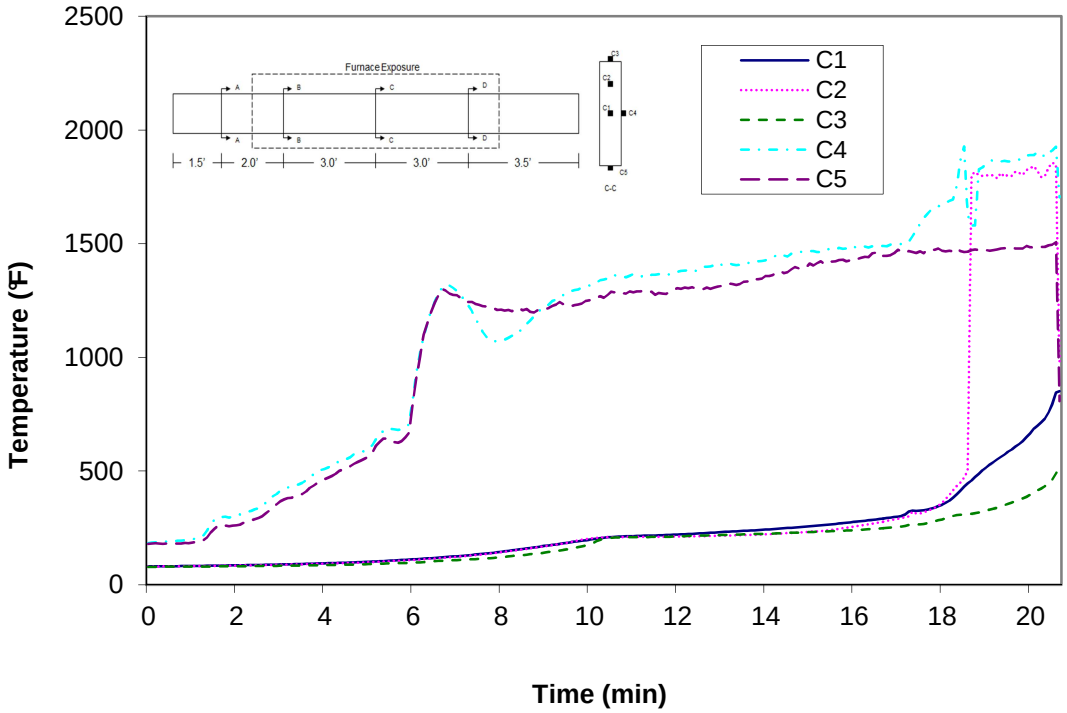

Figure A-34: Temperature distribution in wood joist T4 at cross-section C

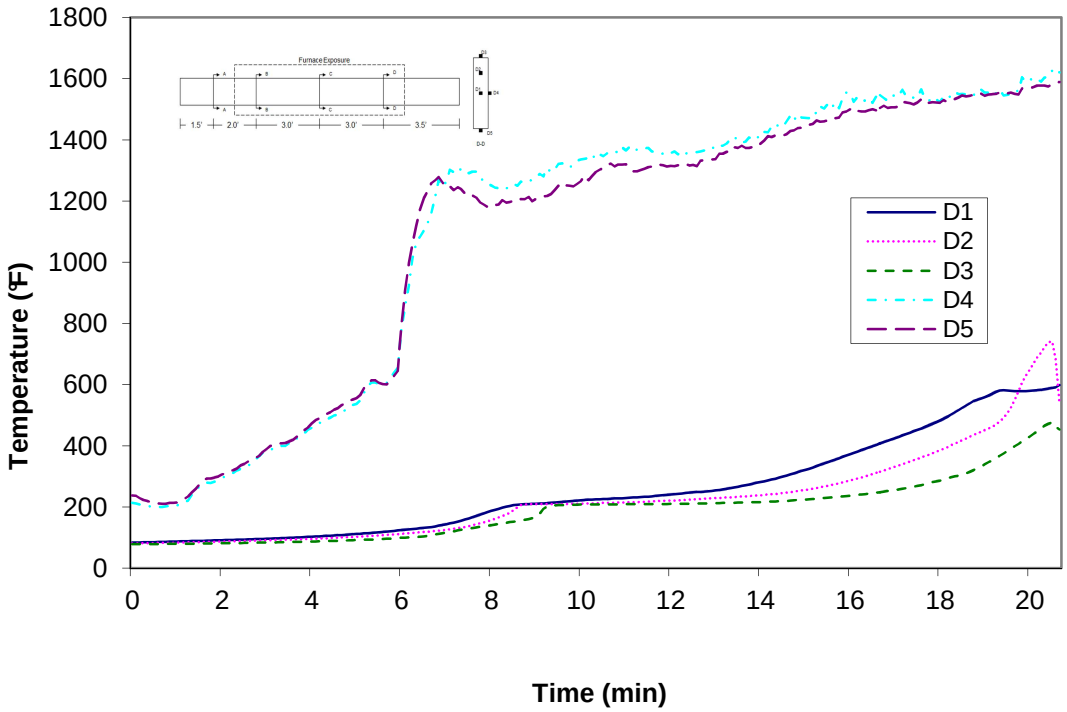

Figure A-35: Temperature distribution in wood joist T4 at cross-section D

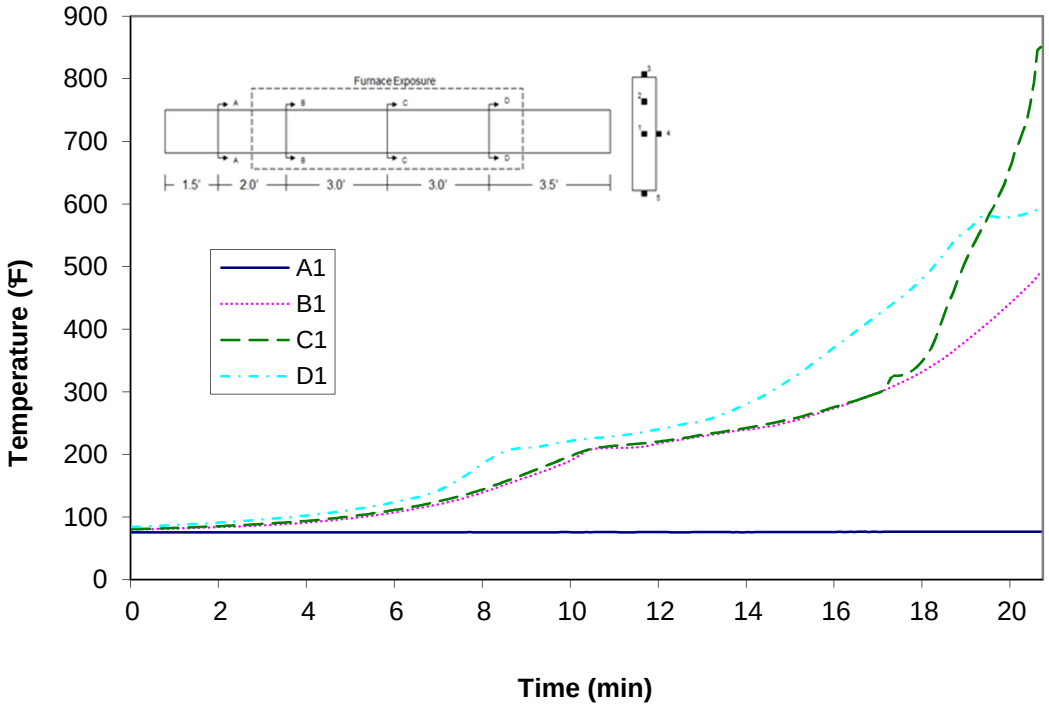

Figure A-36: Temperature distribution in wood joist T4 at thermocouple location 1

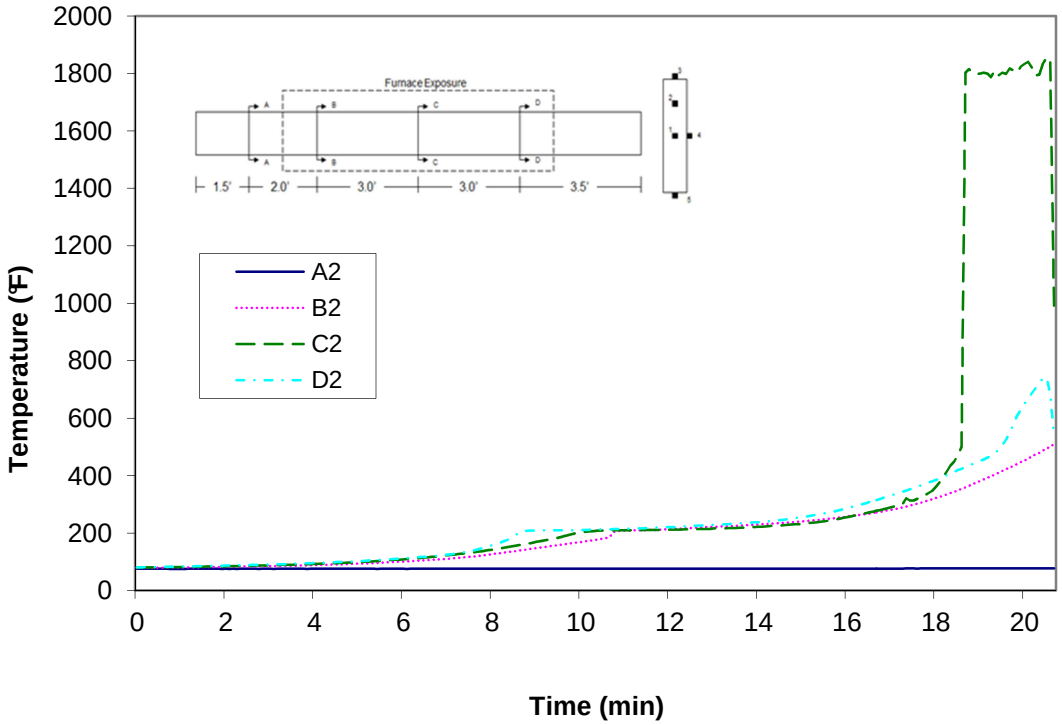

Figure A-37: Temperature distribution in wood joist T4 at thermocouple location 2

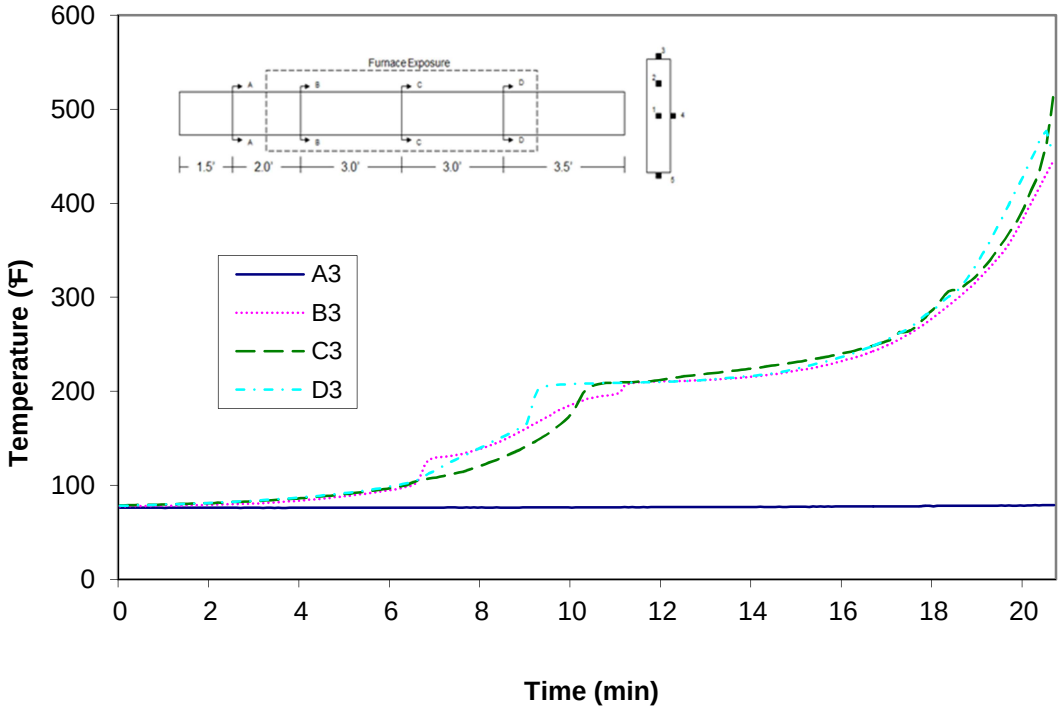

Figure A-38: Temperature distribution in wood joist T4 at thermocouple location 3

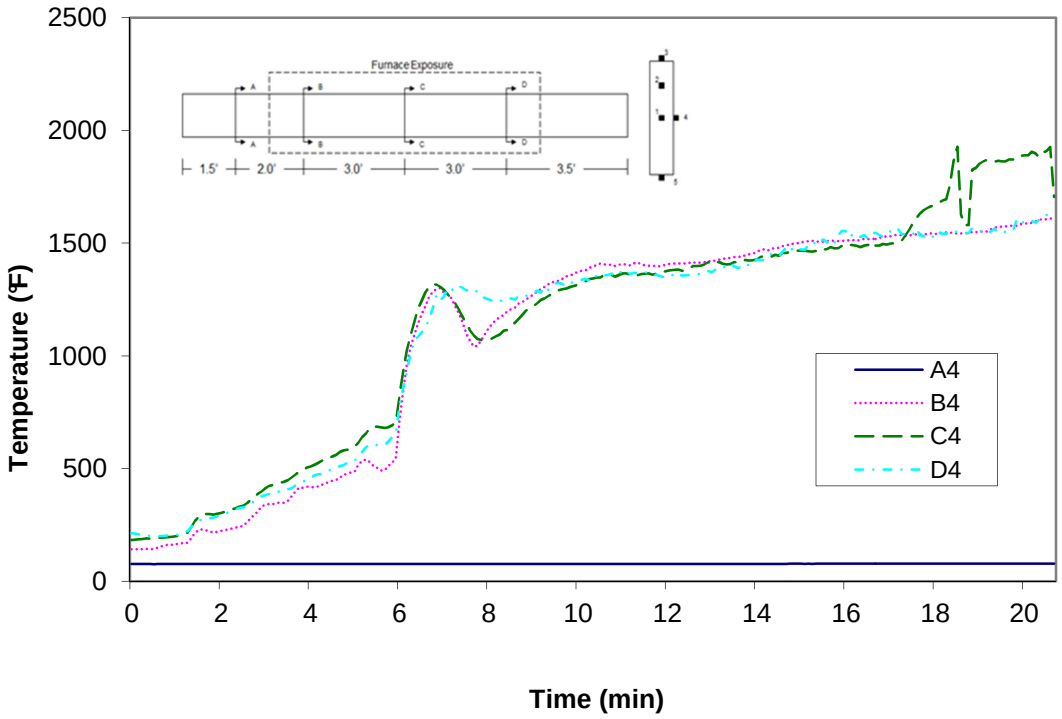

Figure A-39: Temperature distribution in wood joist T4 at thermocouple location 4

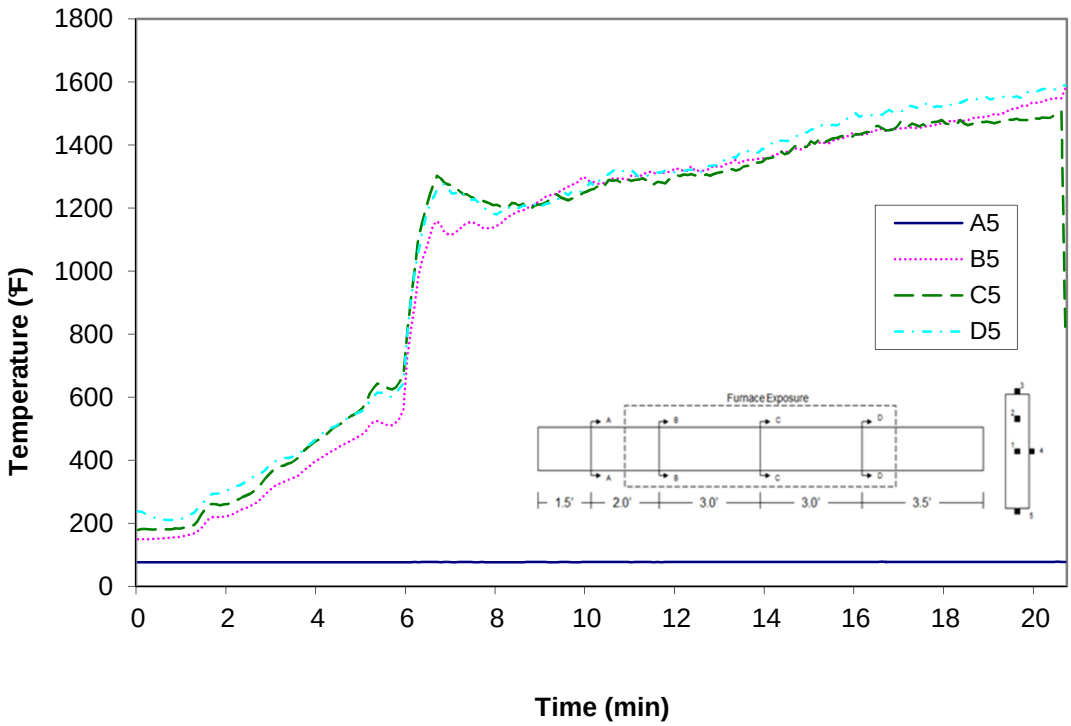

Figure A-40: Temperature distribution in wood joist T4 at thermocouple location 5

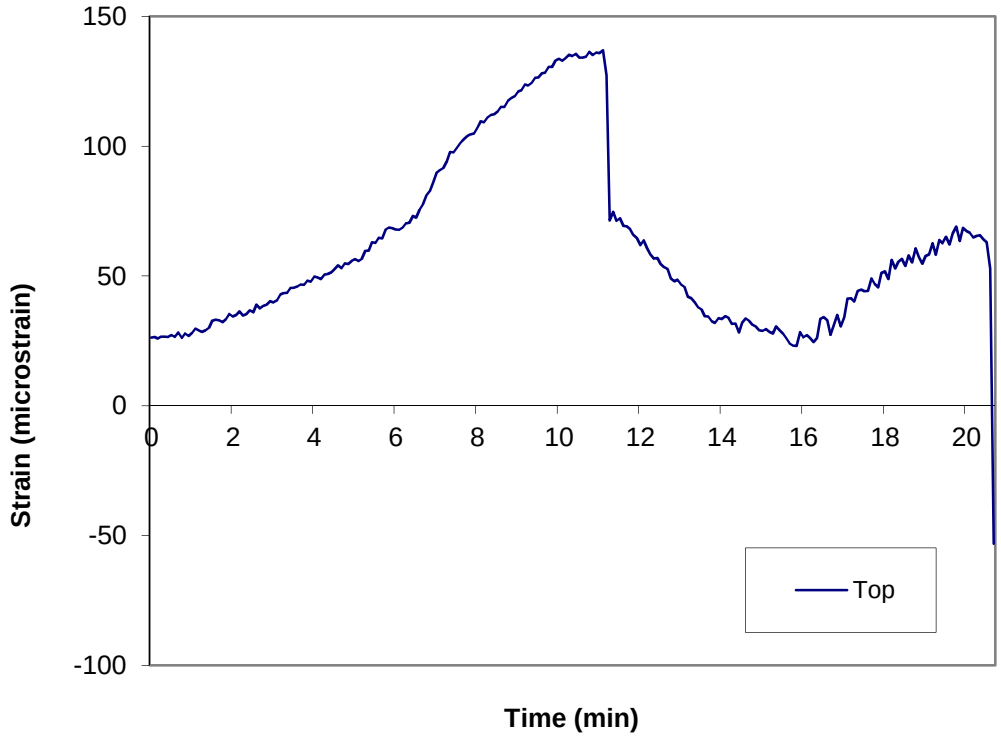

Figure A-41: Measured strains recorded during fire resistance tests of wood joist T4

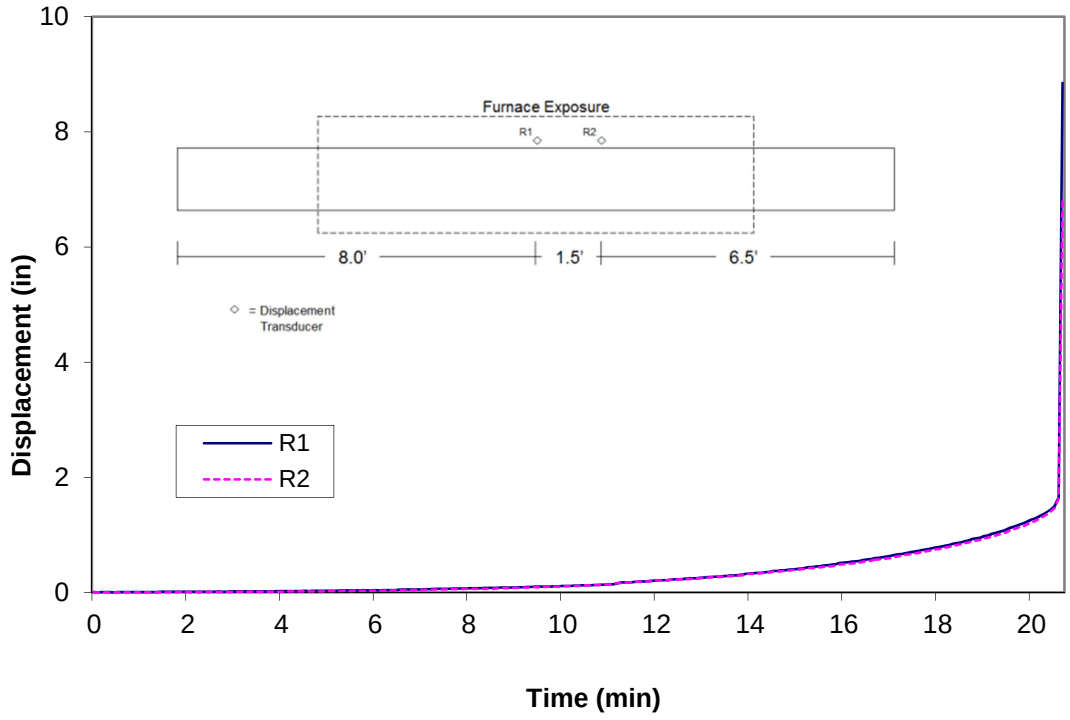

Figure A-42: Measured displacements recorded during fire resistance tests of wood joist T4

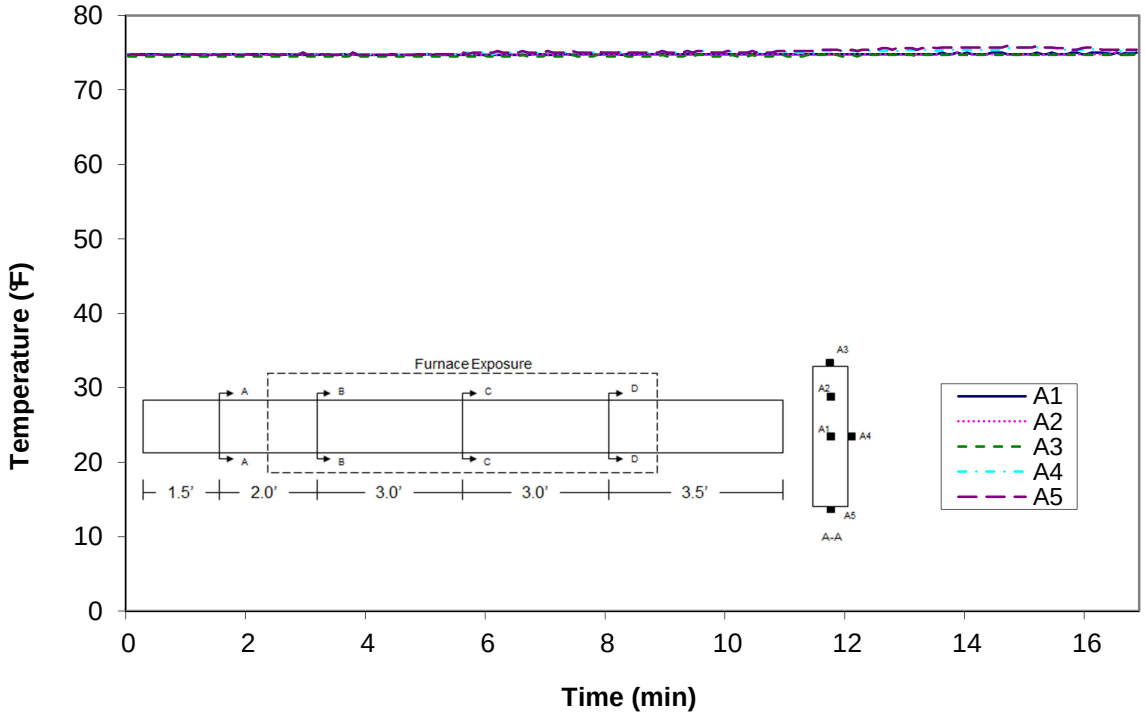

Figure A-43: Temperature distribution in wood joist T5 at cross-section A

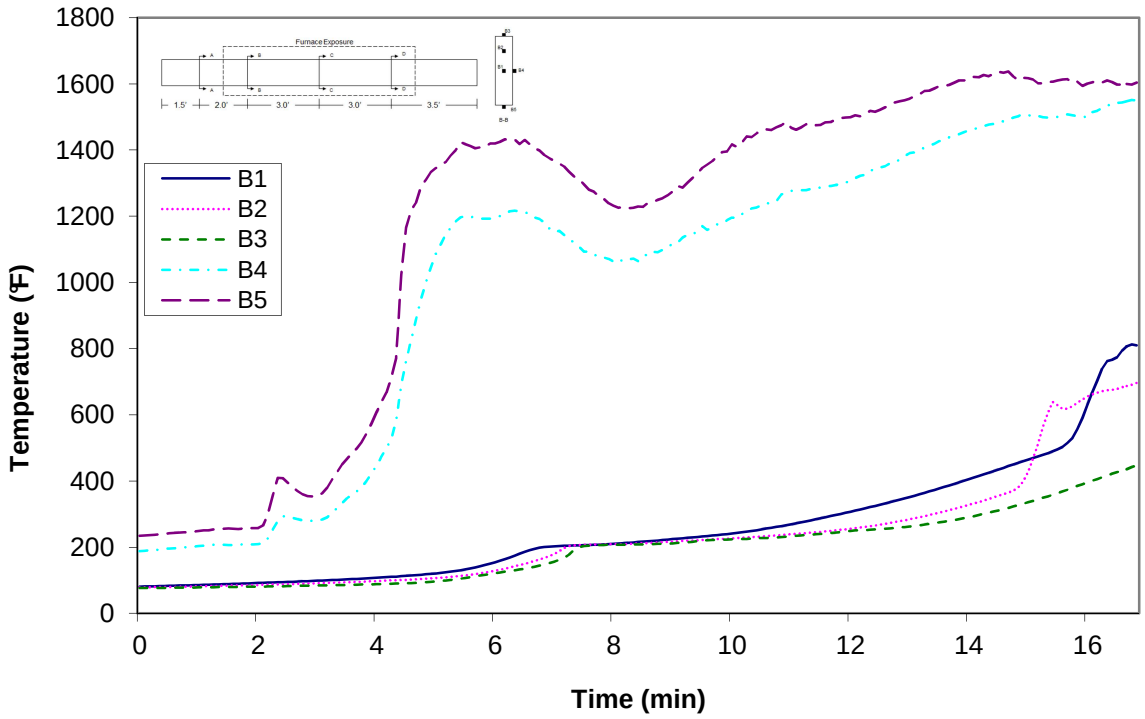

Figure A-44: Temperature distribution in wood joist T5 at cross-section B

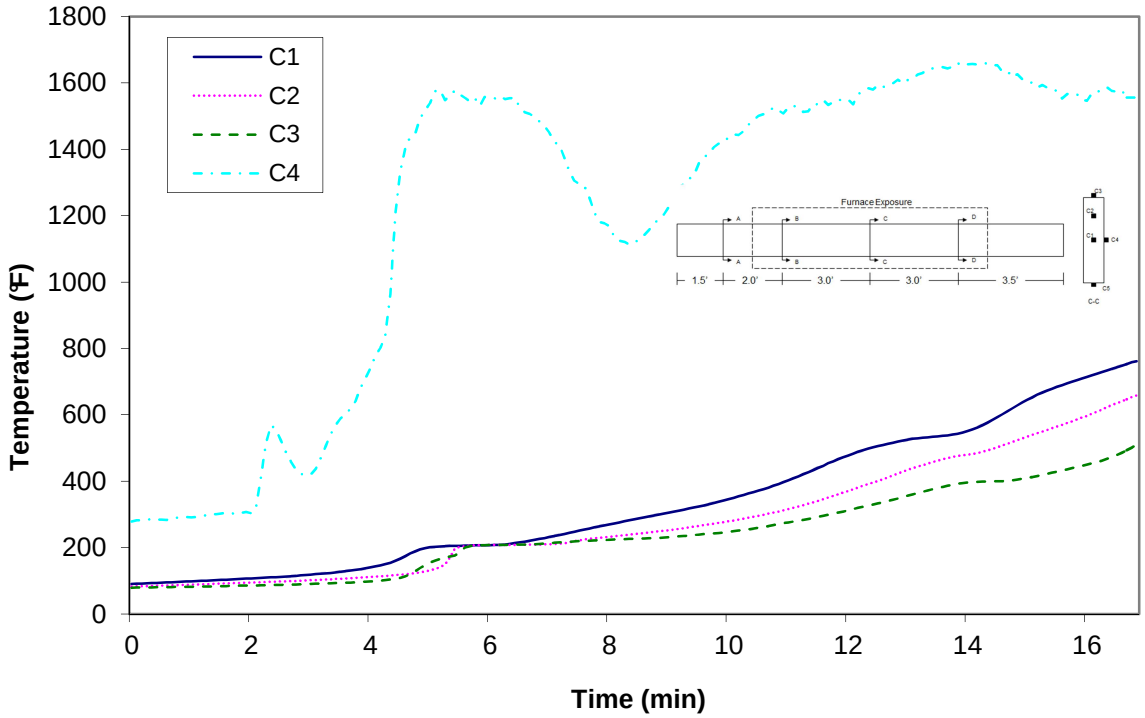

Figure A-45: Temperature distribution in wood joist T5 at cross-section C

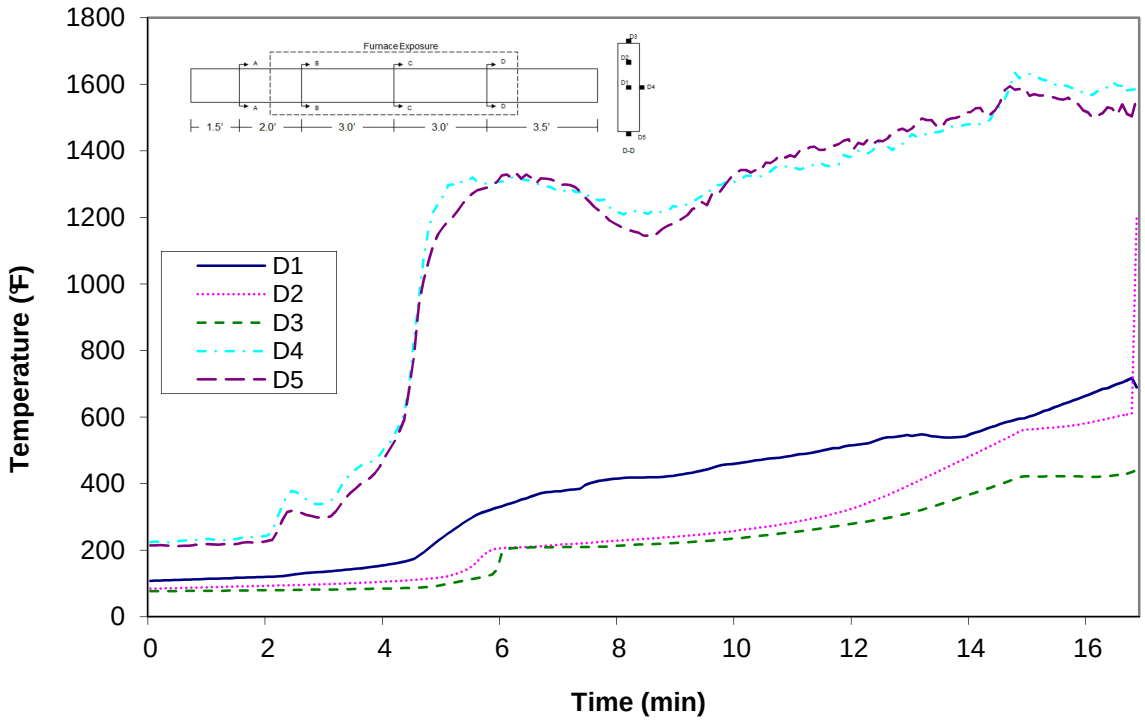

Figure A-46: Temperature distribution in wood joist T5 at cross-section D

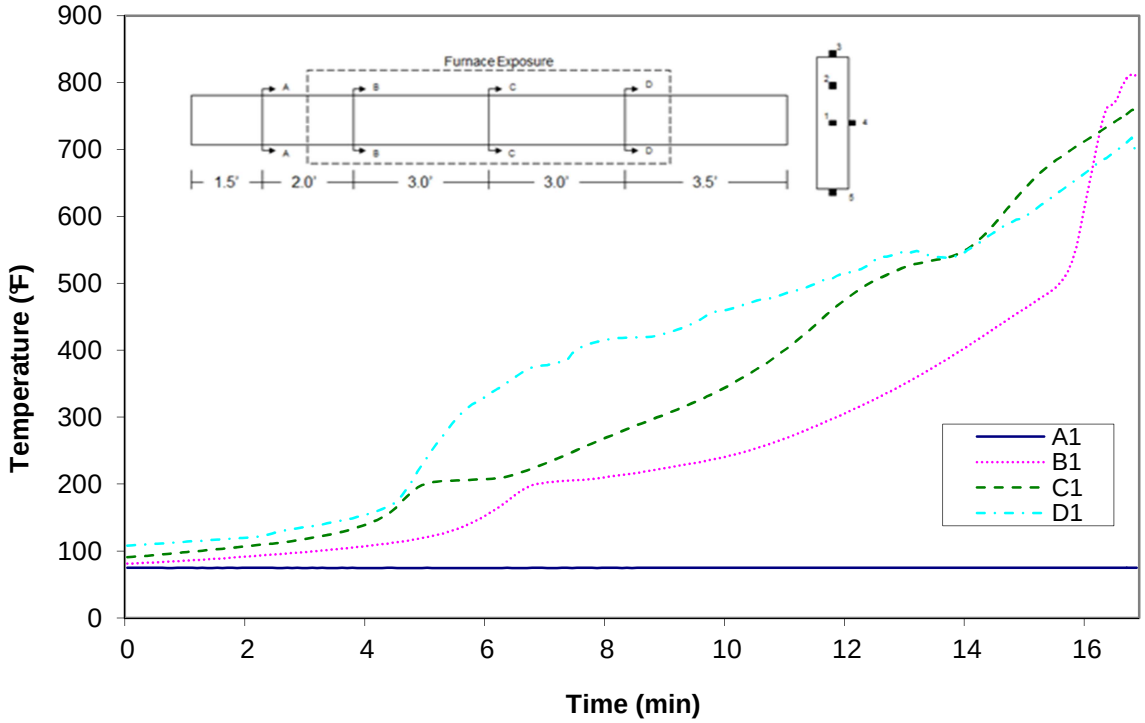

Figure A-47: Temperature distribution in wood joist T5 at thermocouple location 1

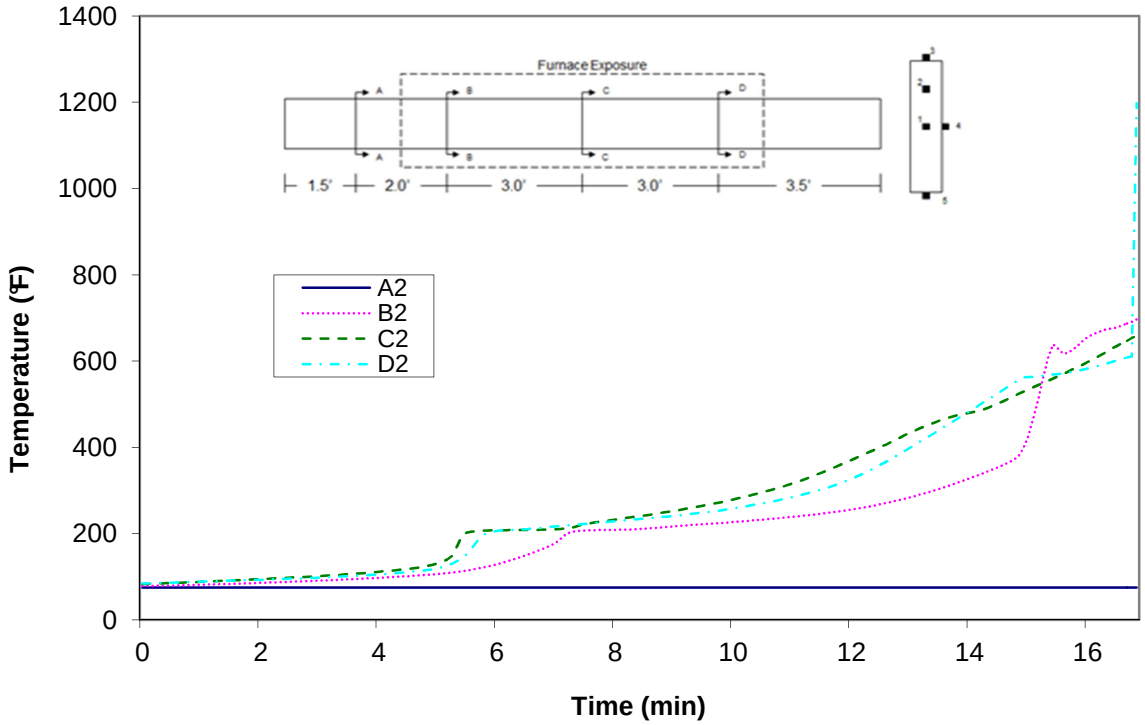

Figure A-48: Temperature distribution in wood joist T5 at thermocouple location 2

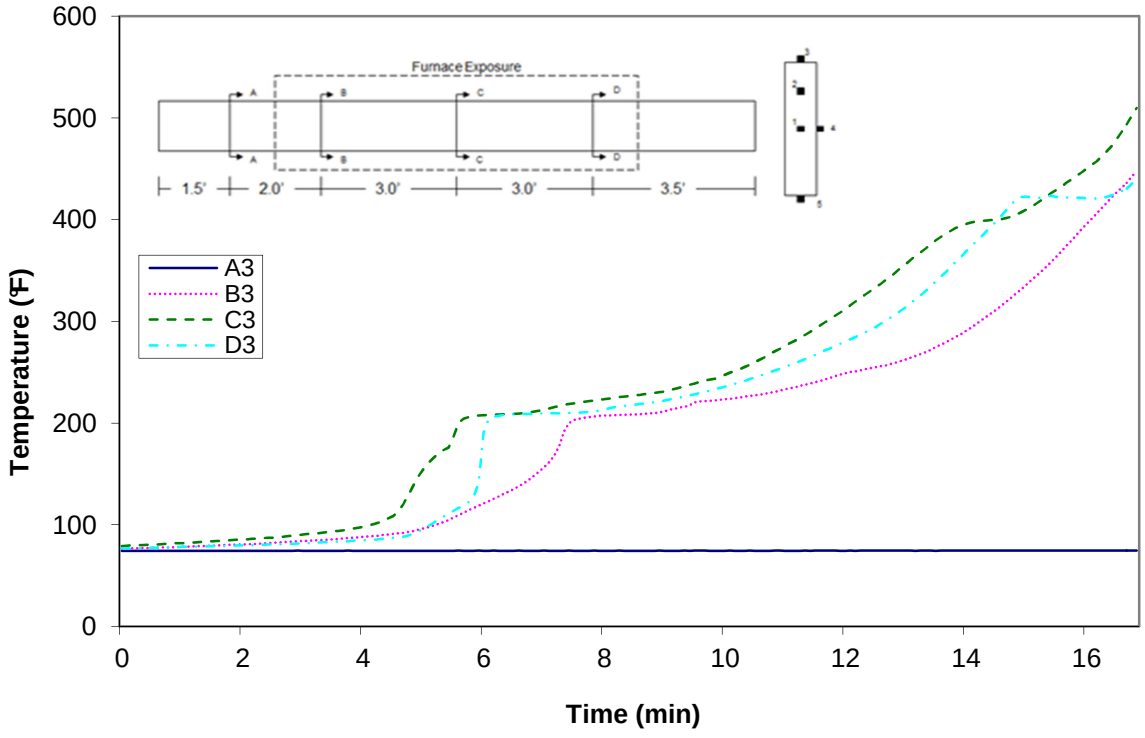

Figure A-49: Temperature distribution in wood joist T5 at thermocouple location 3

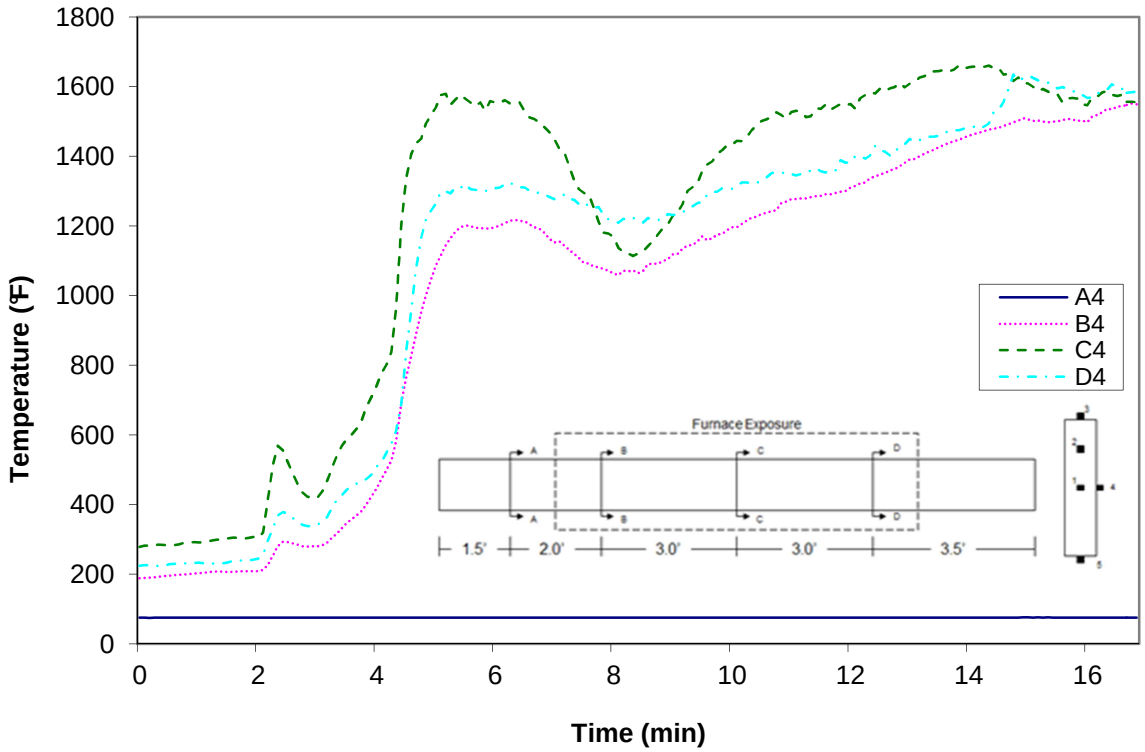

Figure A-50: Temperature distribution in wood joist T5 at thermocouple location 4

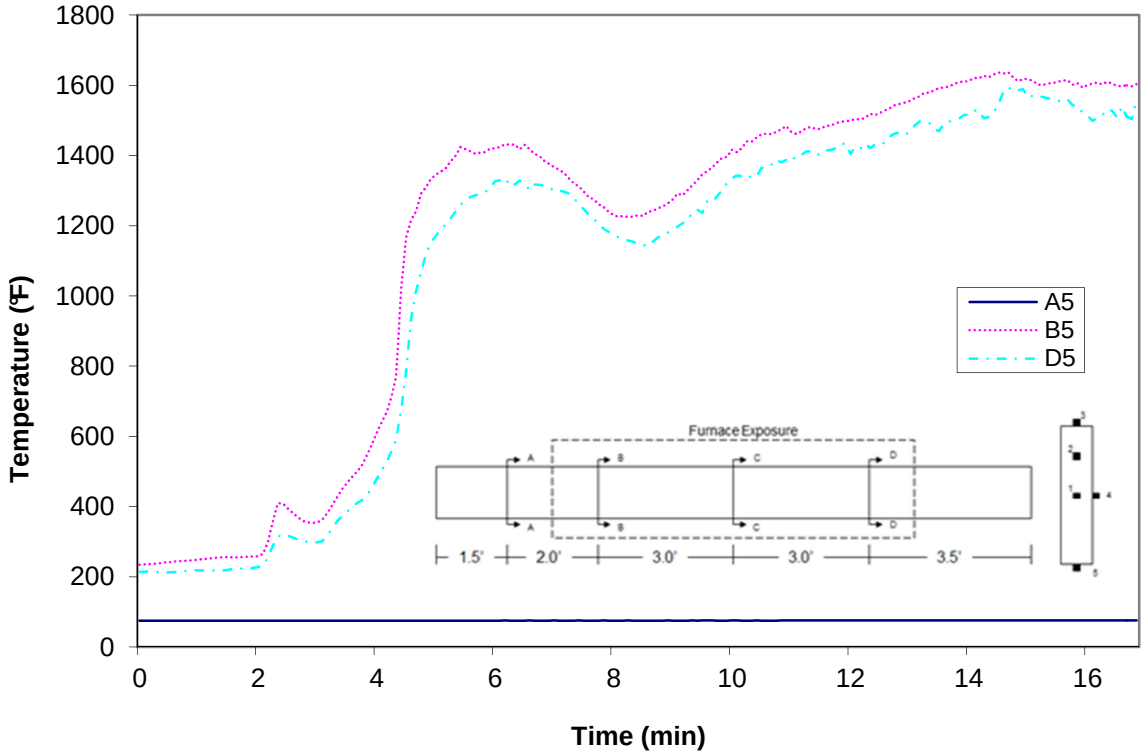

Figure A-51: Temperature distribution in wood joist T5 at thermocouple location 5

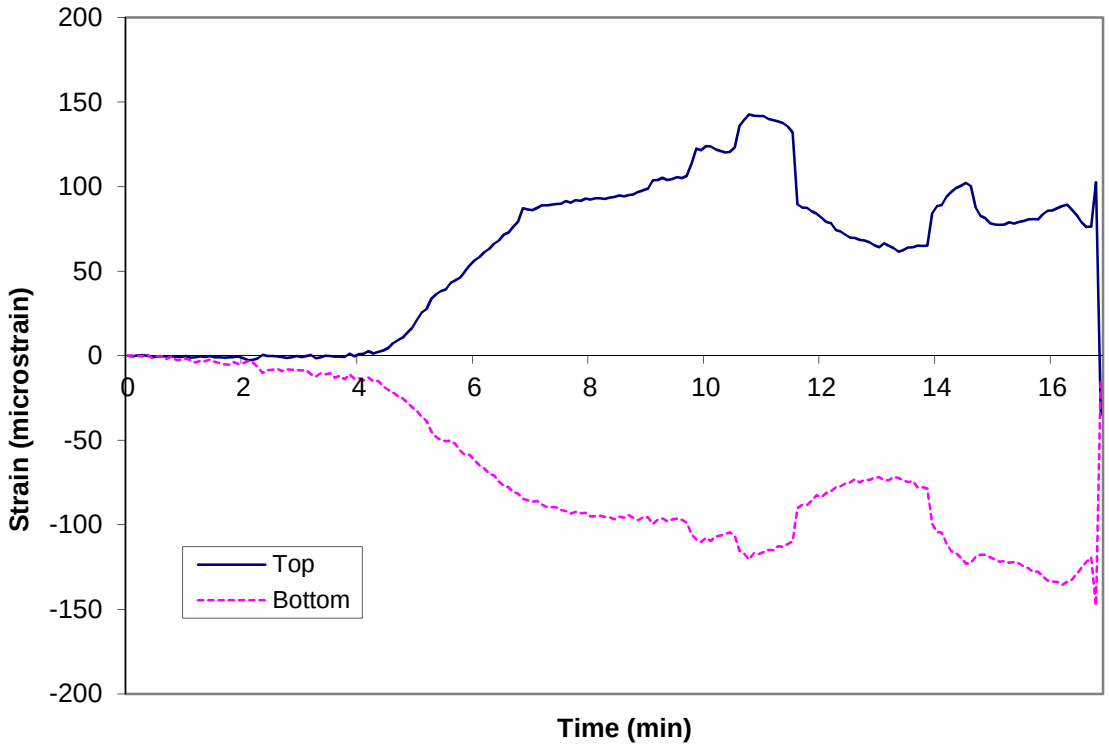

Figure A-52: Measured strains recorded during fire resistance tests of wood joist T5

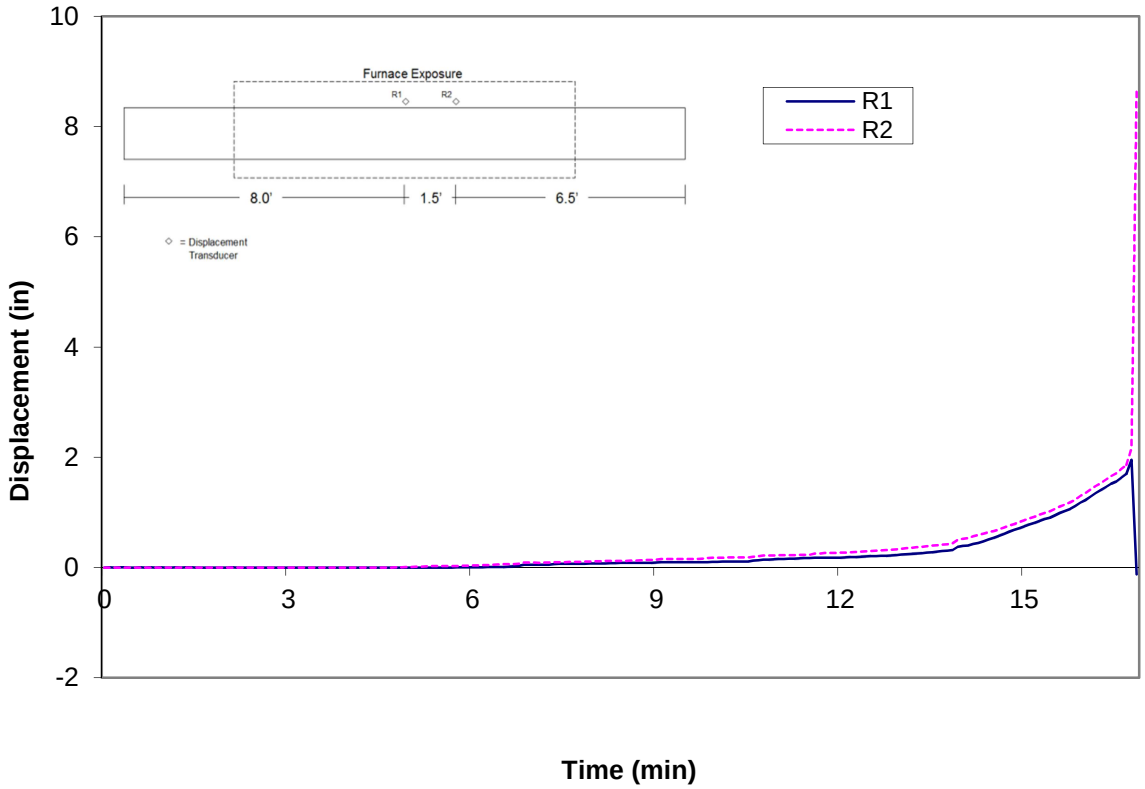

Figure A-53: Measured displacements recorded during fire resistance tests of wood joist T5

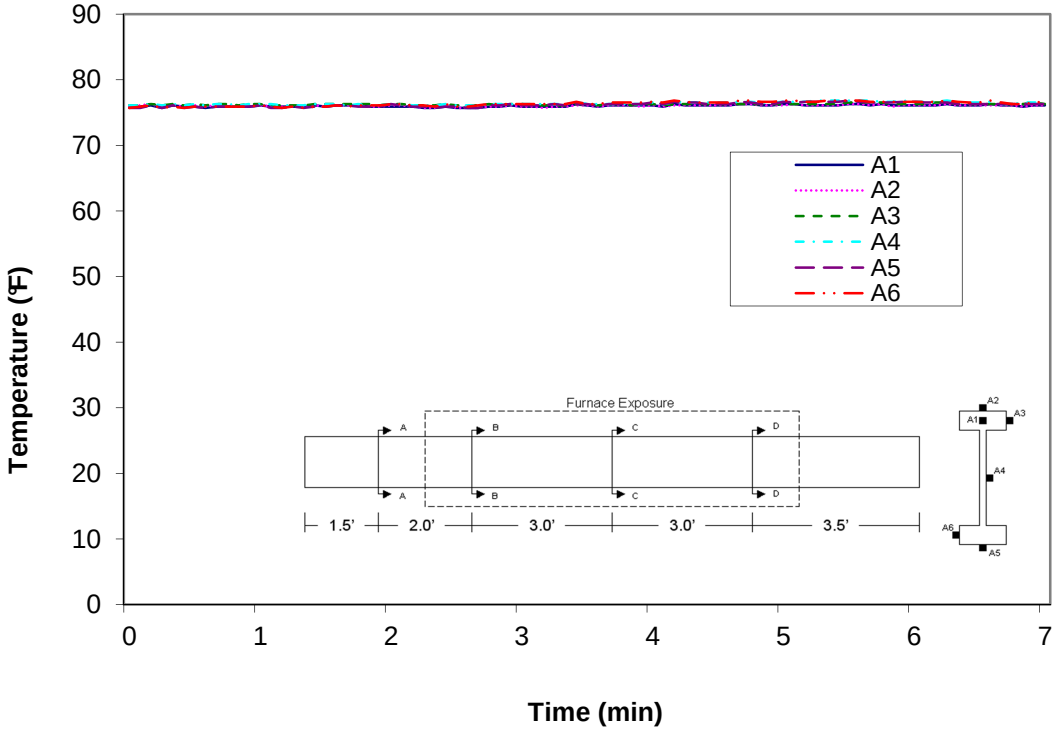

Figure A-54: Temperature distribution in wood joist E1 at cross-section A

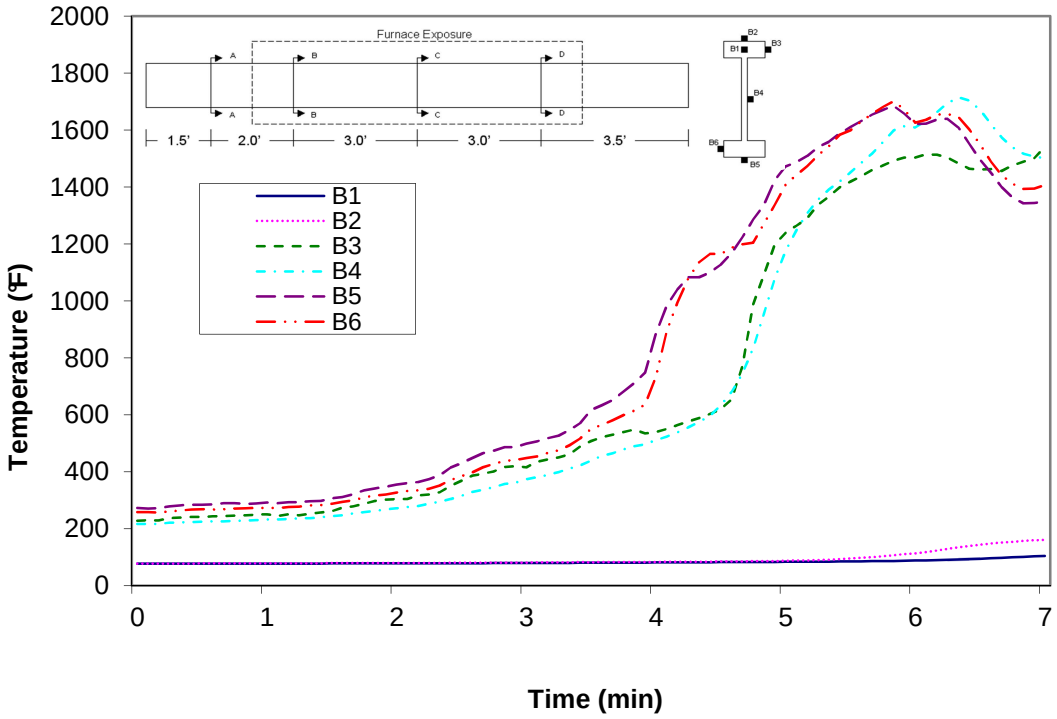

Figure A-55: Temperature distribution in wood joist E1 at cross-section B

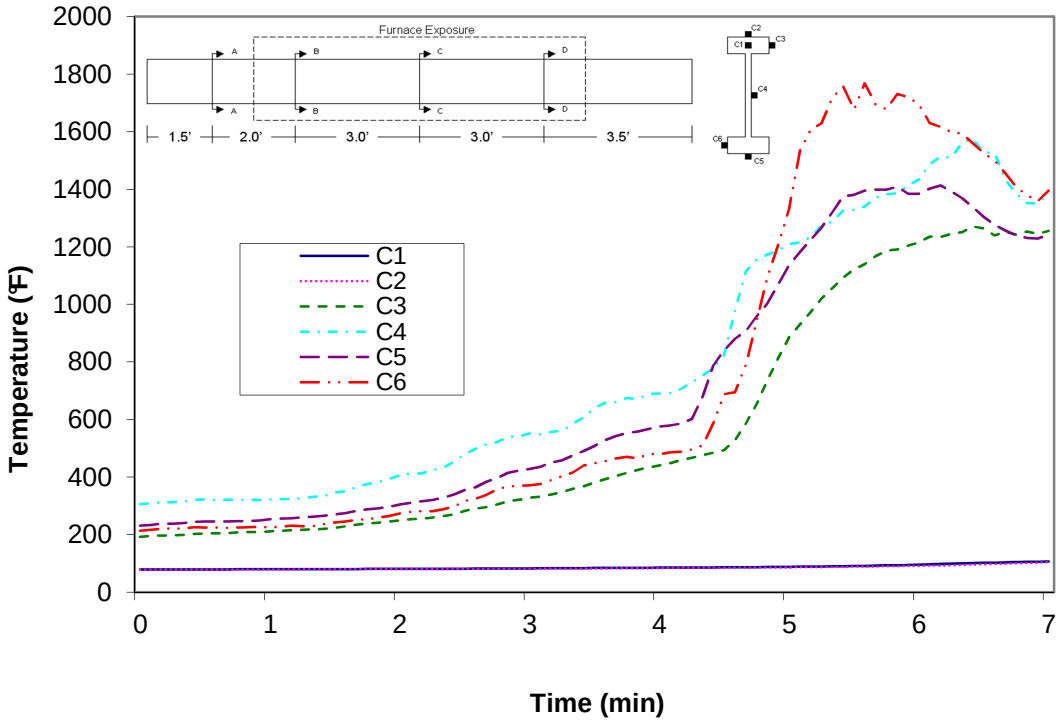

Figure A-56: Temperature distribution in wood joist E1 at cross-section C

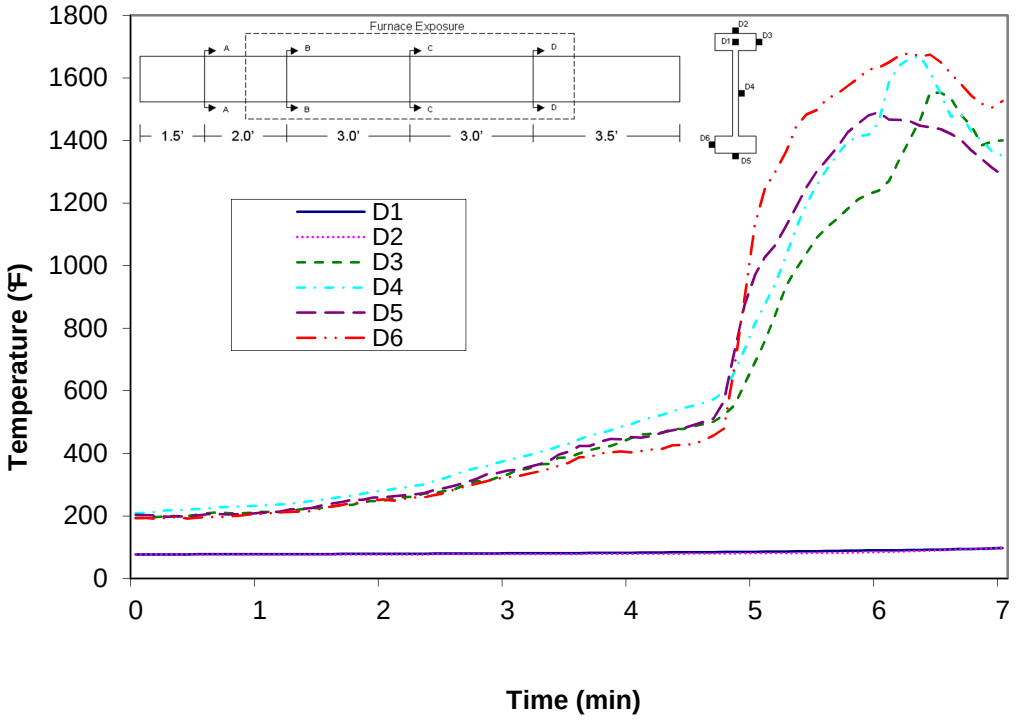

Figure A-57: Temperature distribution in wood joist E1 at cross-section D

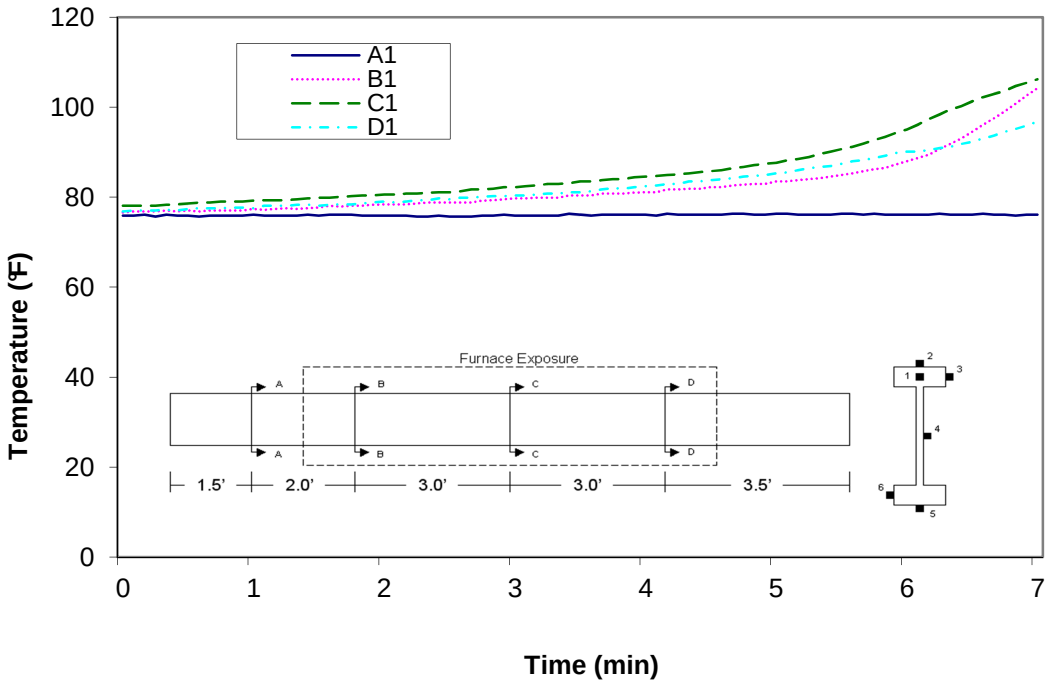

Figure A-58: Temperature distribution in wood joist E1 at thermocouple location 1

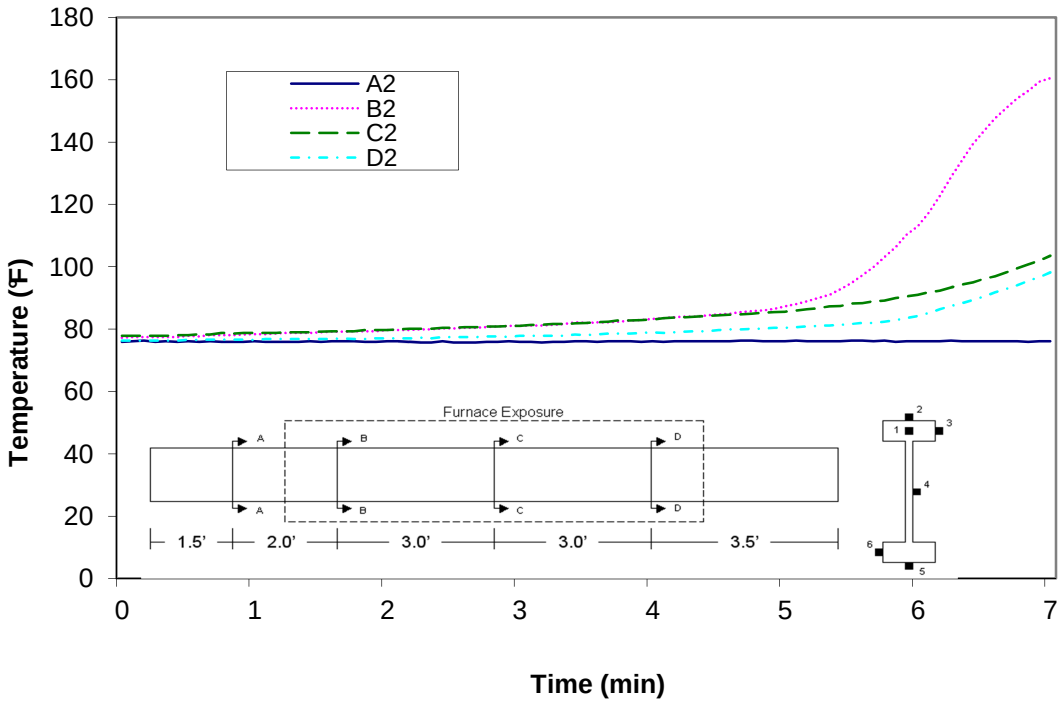

Figure A-59: Temperature distribution in wood joist E1 at thermocouple location 2

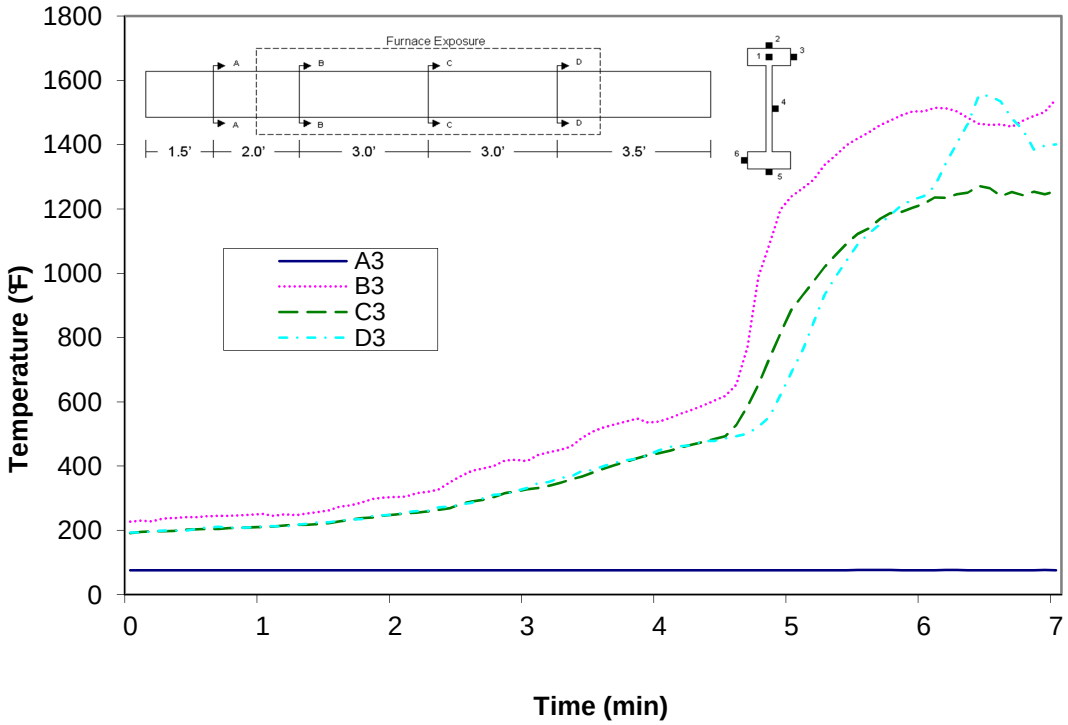

Figure A-60: Temperature distribution in wood joist E1 at thermocouple location 3

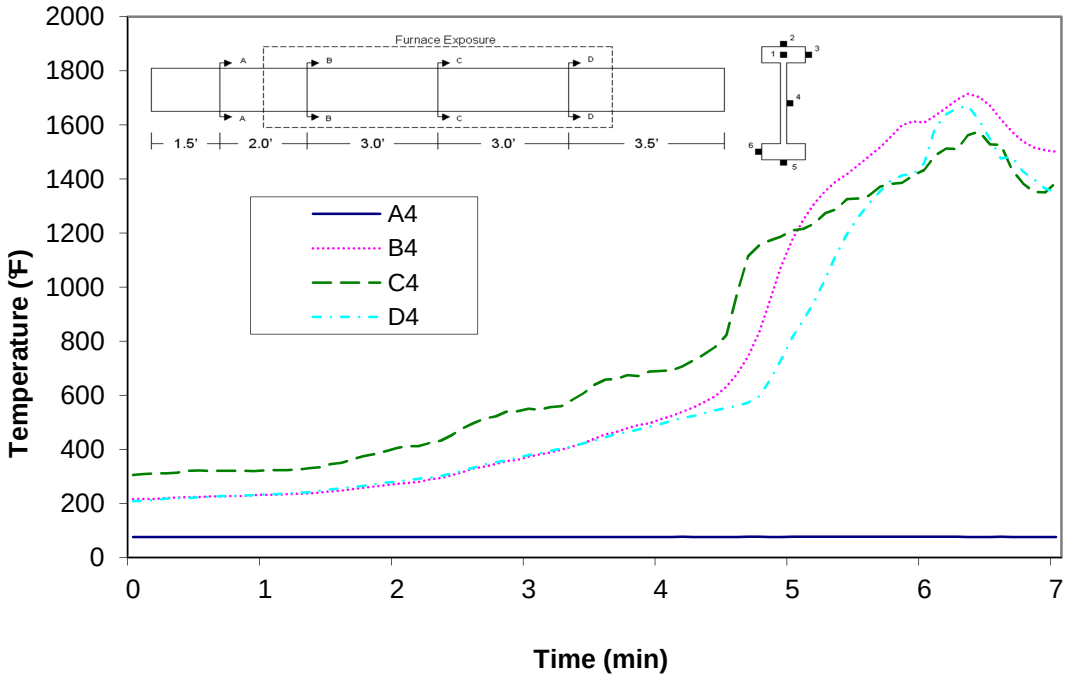

Figure A-61: Temperature distribution in wood joist E1 at thermocouple location 4

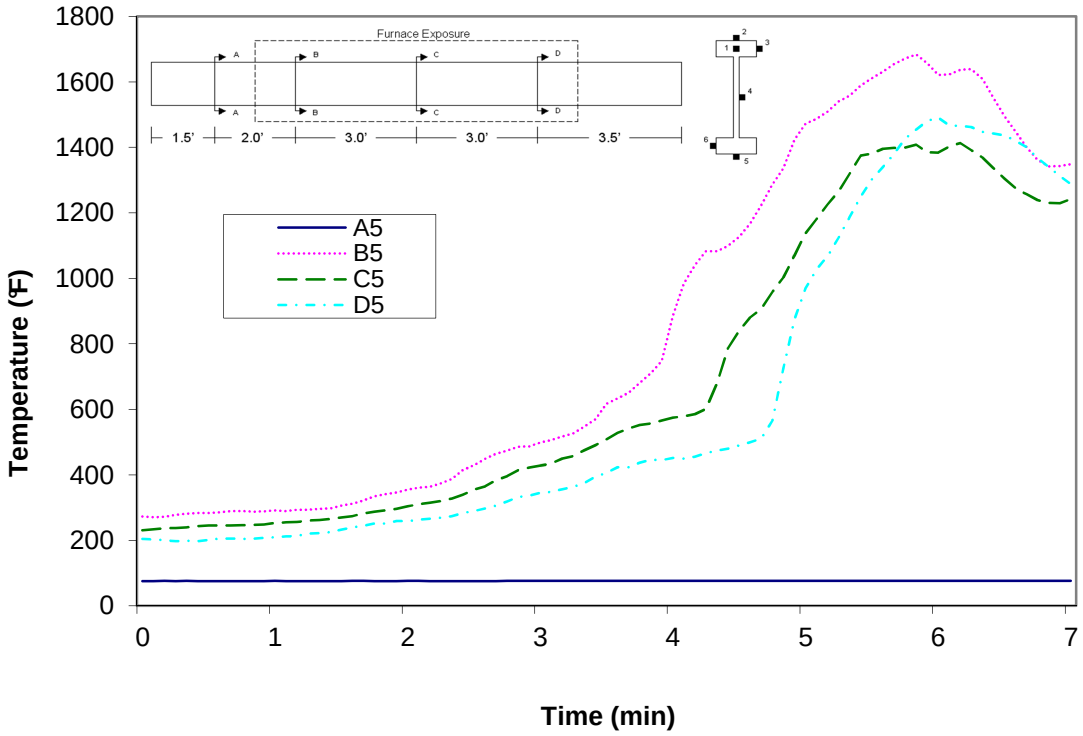

Figure A-62: Temperature distribution in wood joist E1 at thermocouple location 5

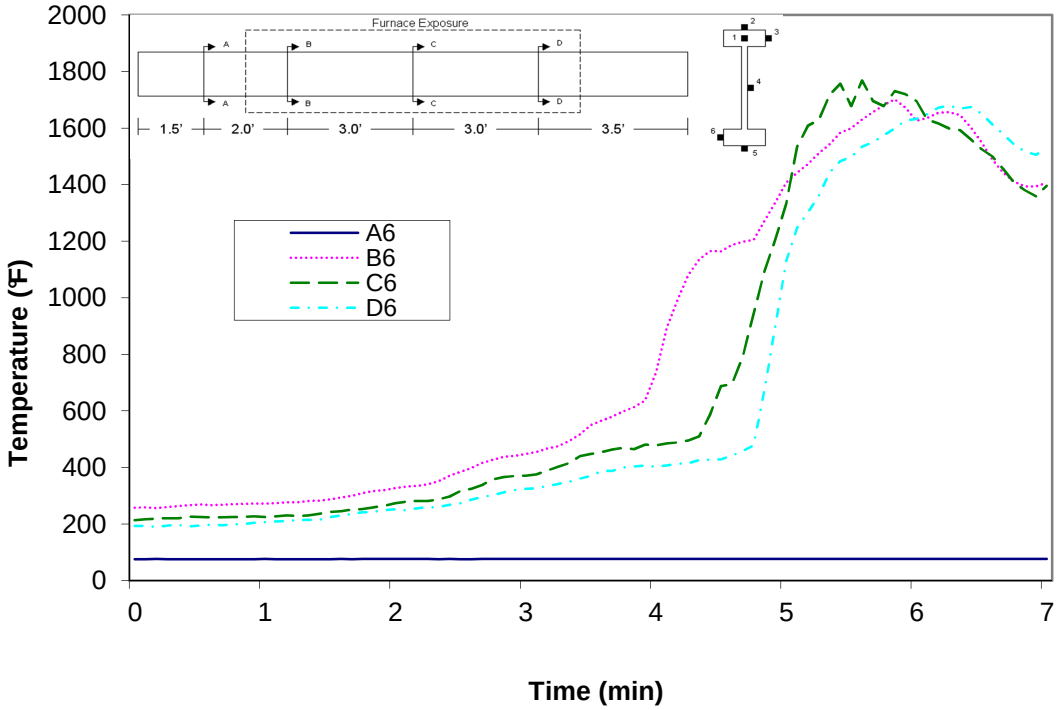

Figure A-63: Temperature distribution in wood joist E1 at thermocouple location 6

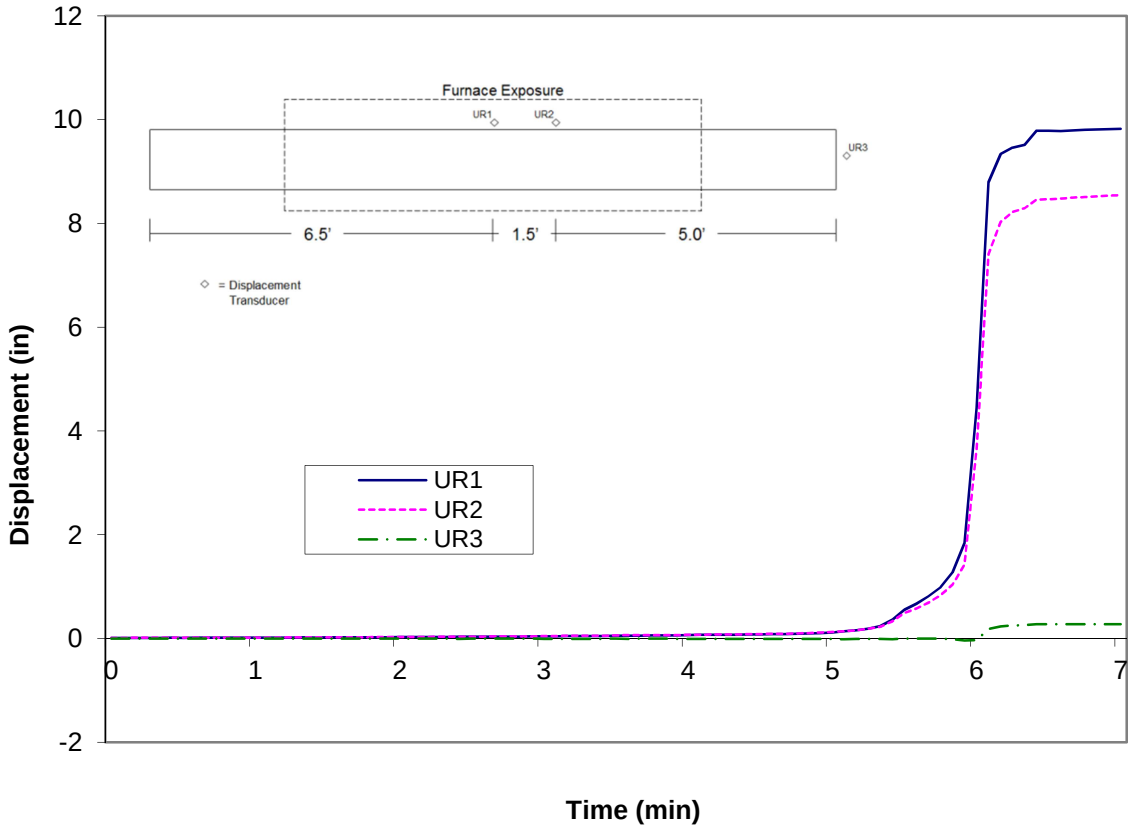

Figure A-64: Measured displacements recorded during fire resistance tests of wood joist E1

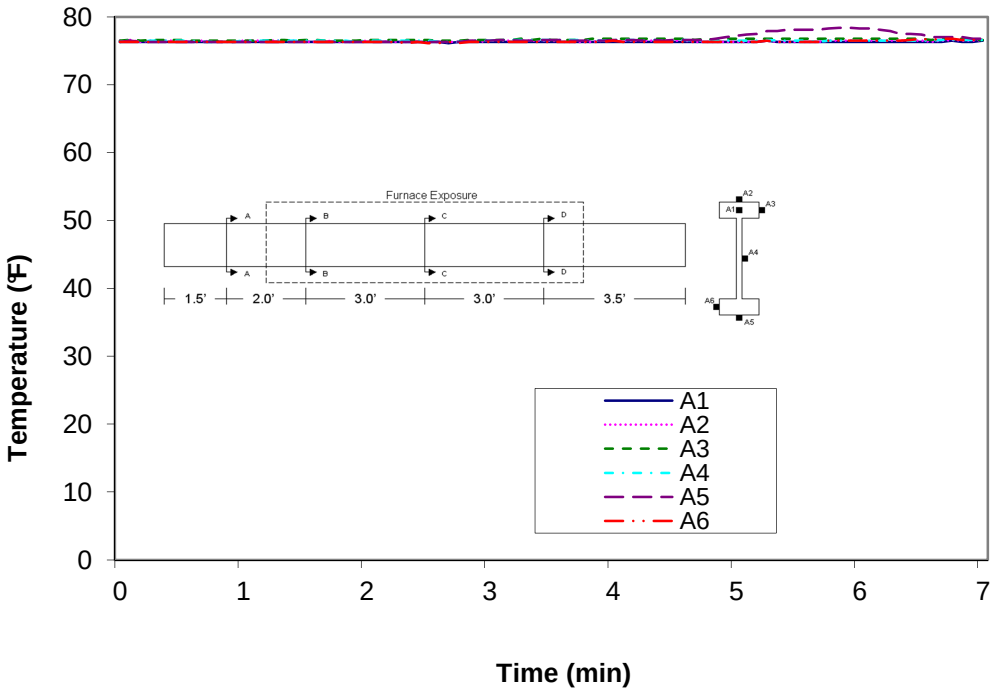

Figure A-65: Temperature distribution in wood joist E2 at cross-section A

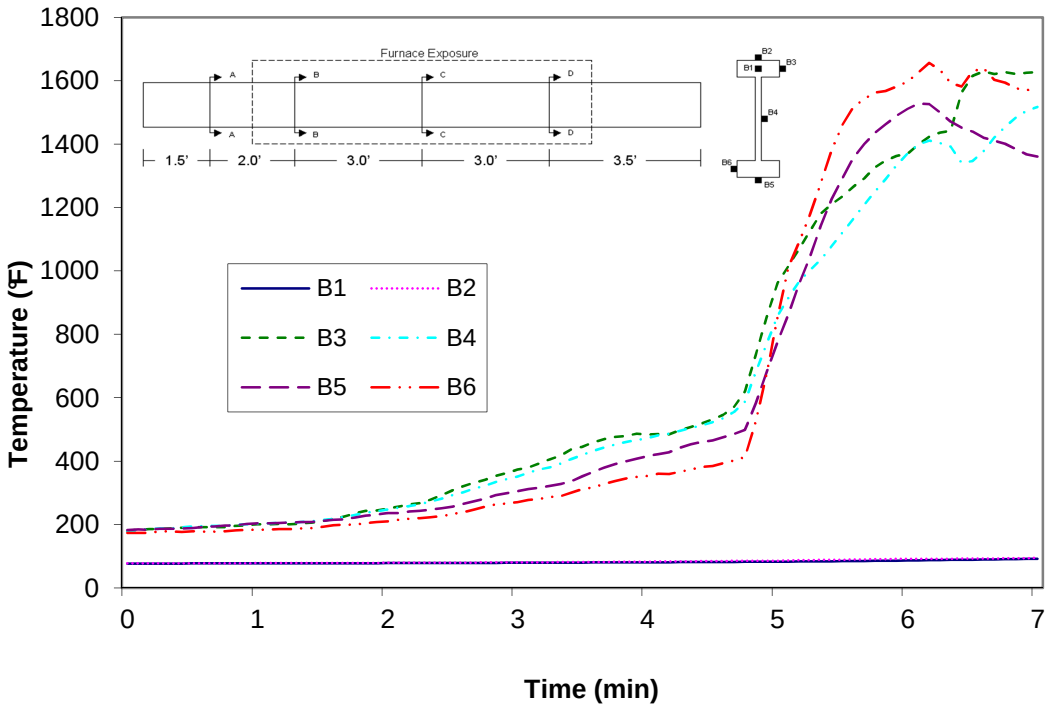

Figure A-66: Temperature distribution in wood joist E2 at cross-section B

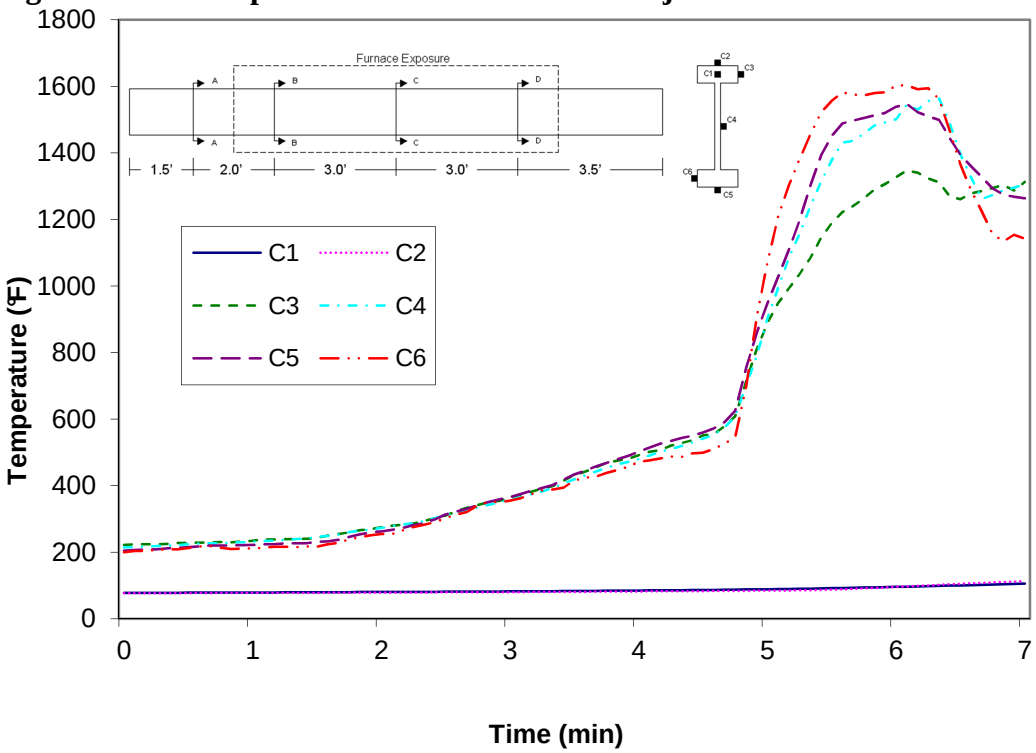

Figure A-67: Temperature distribution in wood joist E2 at cross-section C

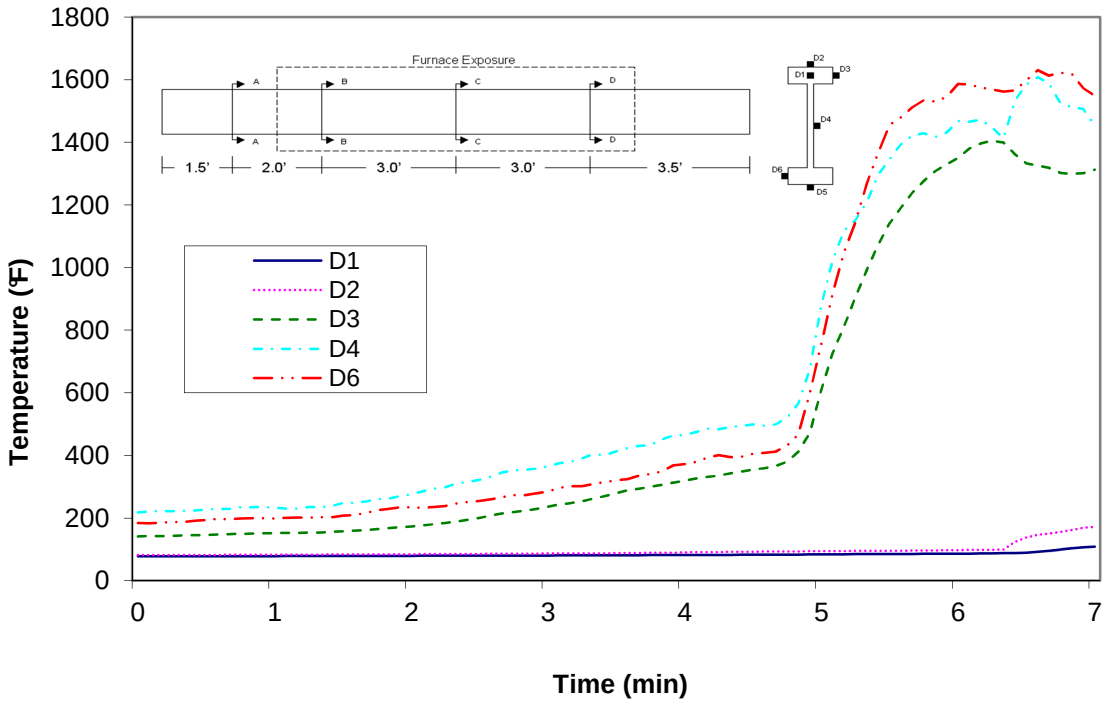

Figure A-68: Temperature distribution in wood joist E2 at cross-section D

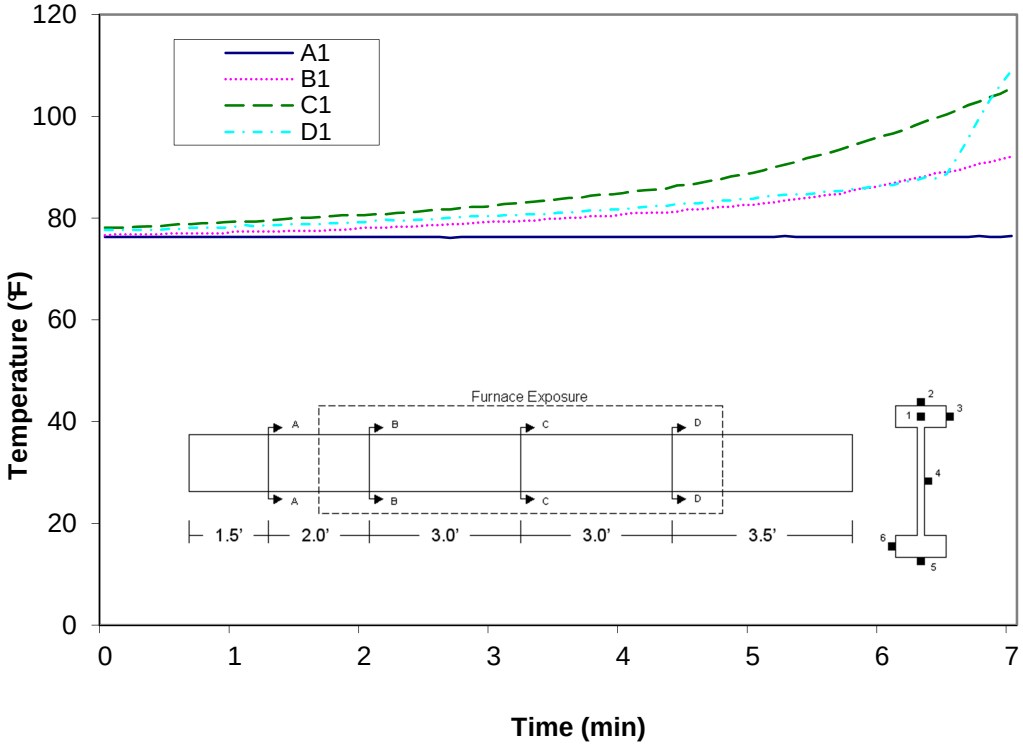

Figure A-69: Temperature distribution in wood joist E2 at thermocouple location 1

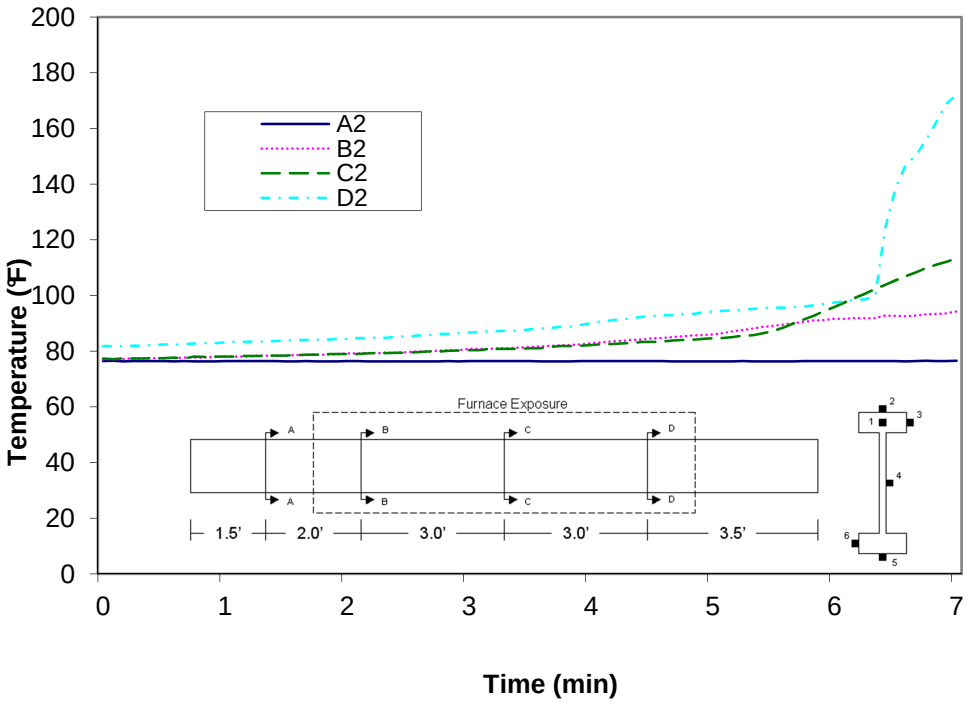

Figure A-70: Temperature distribution in wood joist E2 at thermocouple location 2

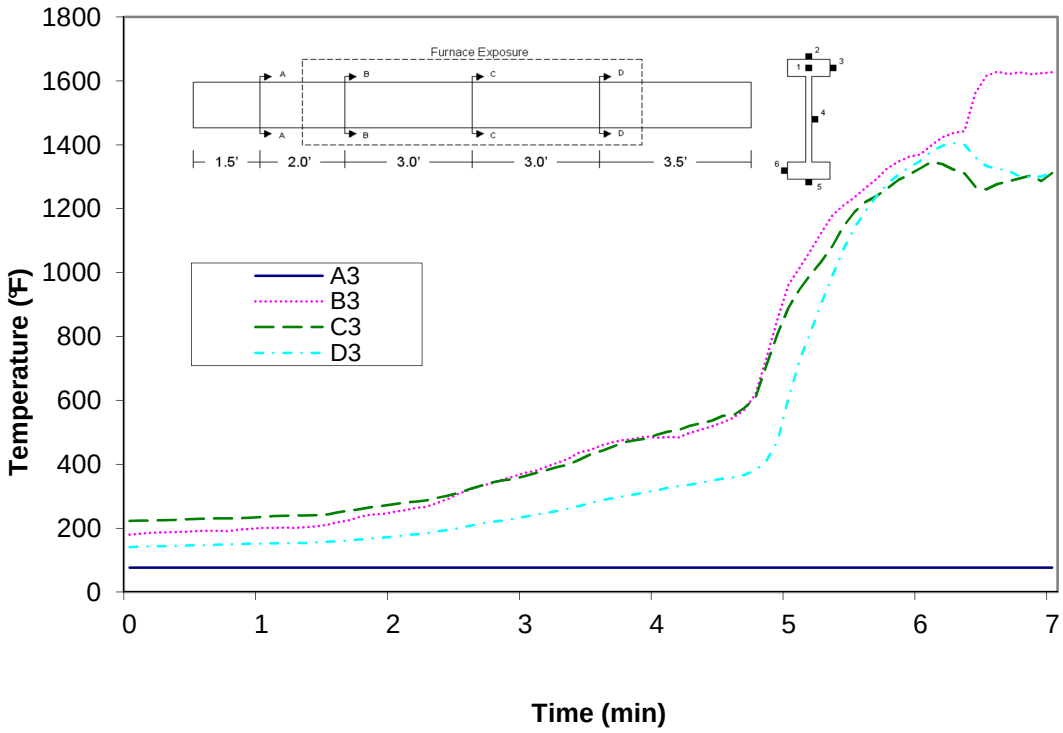

Figure A-71: Temperature distribution in wood joist E2 at thermocouple location 3

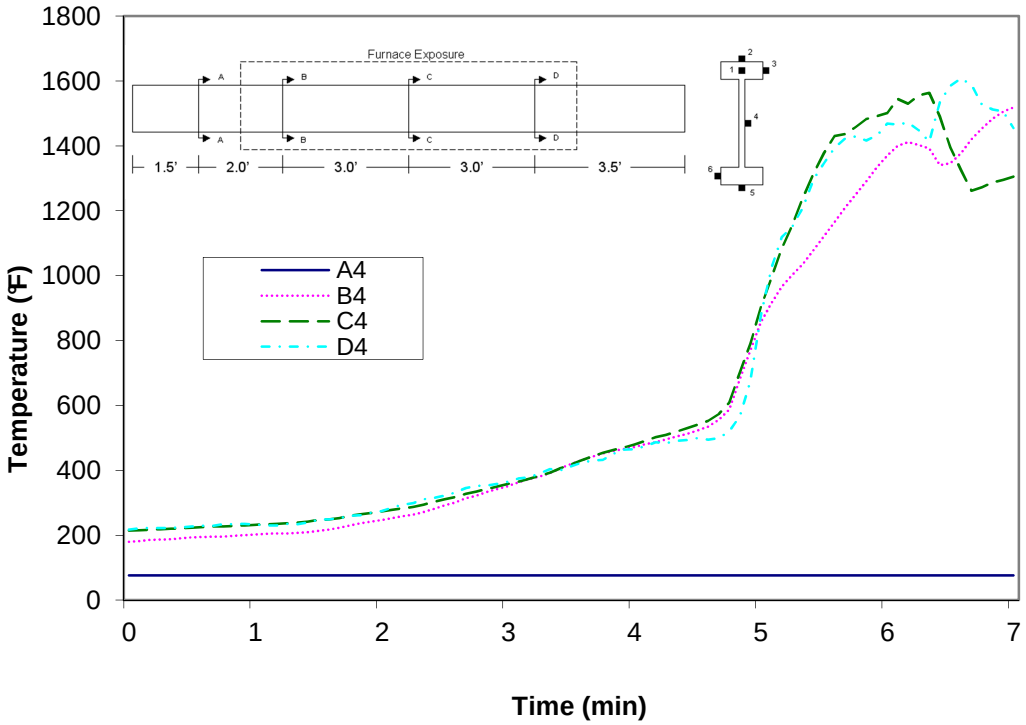

Figure A-72: Temperature distribution in wood joist E2 at thermocouple location 4

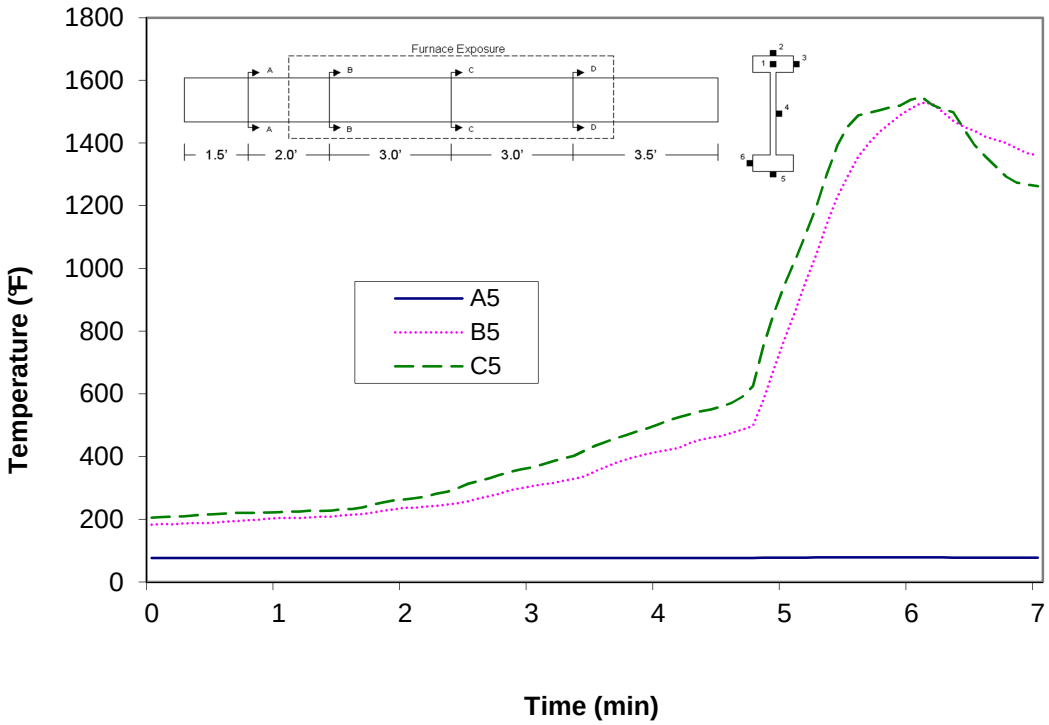

Figure A-73: Temperature distribution in wood joist E2 at thermocouple location 5

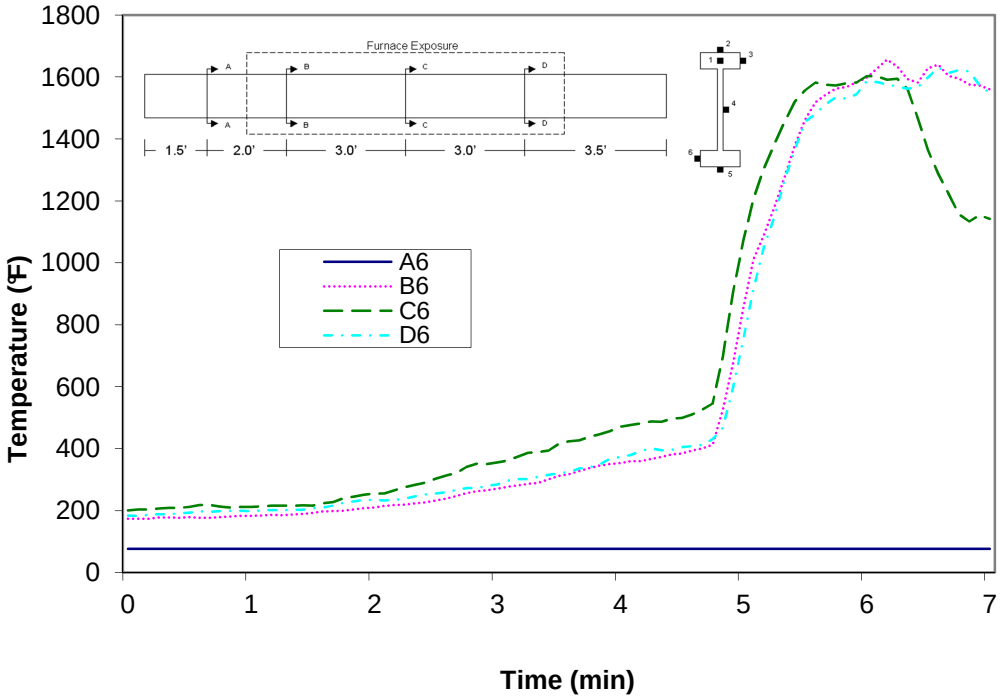

Figure A-74: Temperature distribution in wood joist E2 at thermocouple location 6

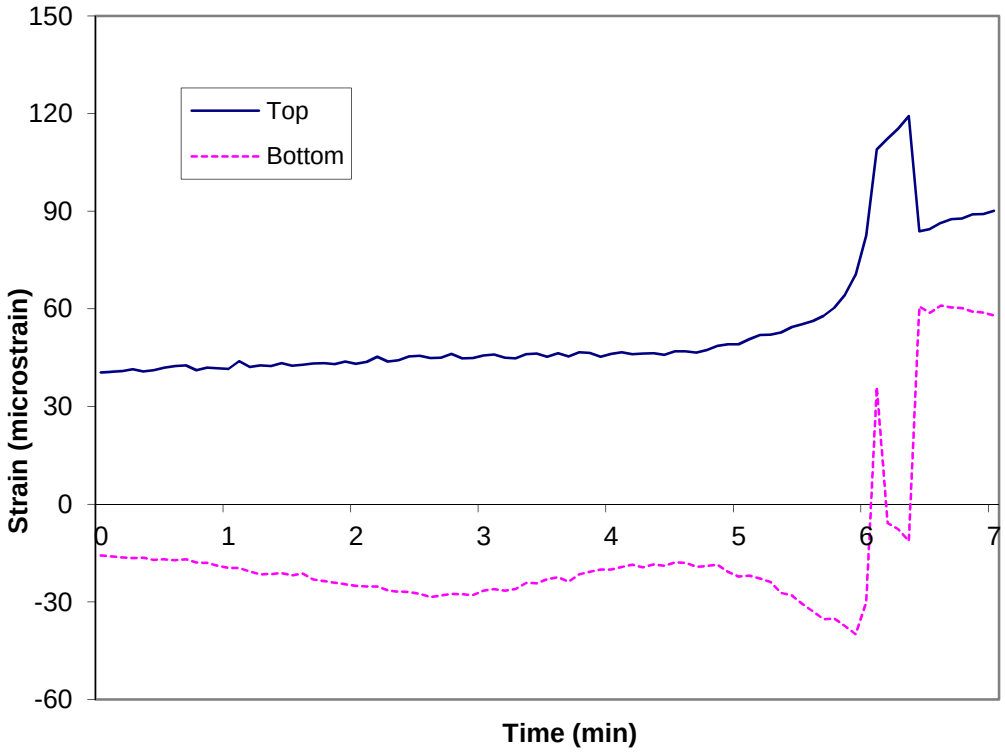

Figure A-75: Measured strains recorded during fire resistance tests of wood joist E2

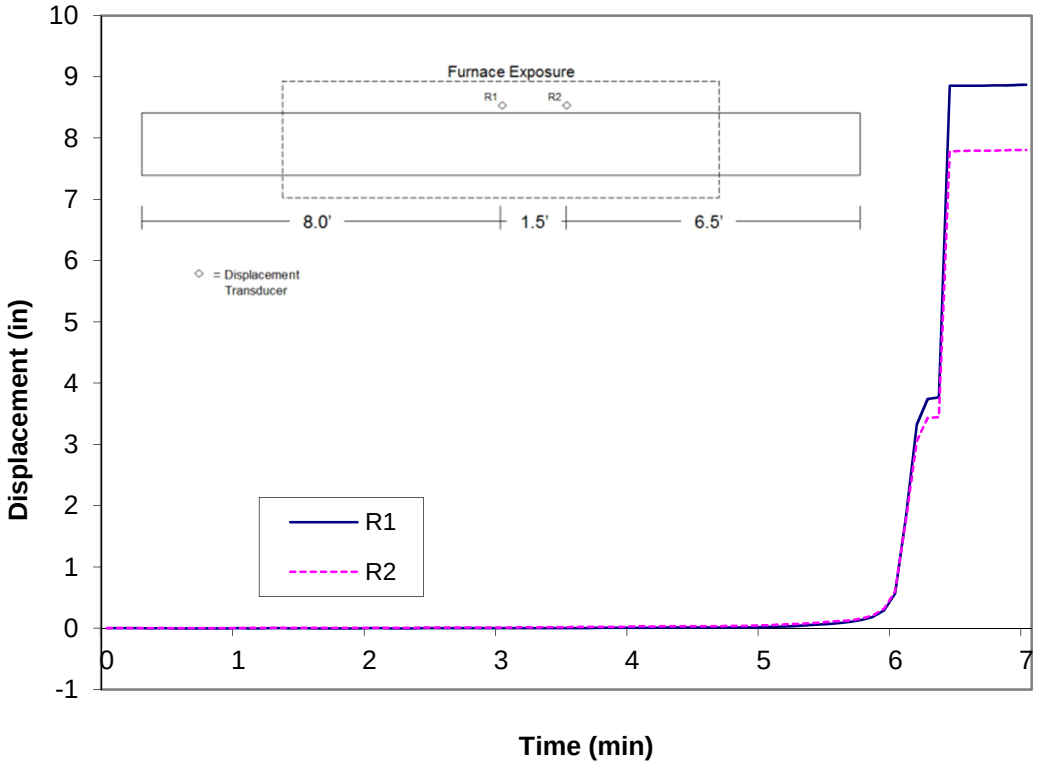

Figure A-76: Measured displacements recorded during fire resistance tests of wood joist E2

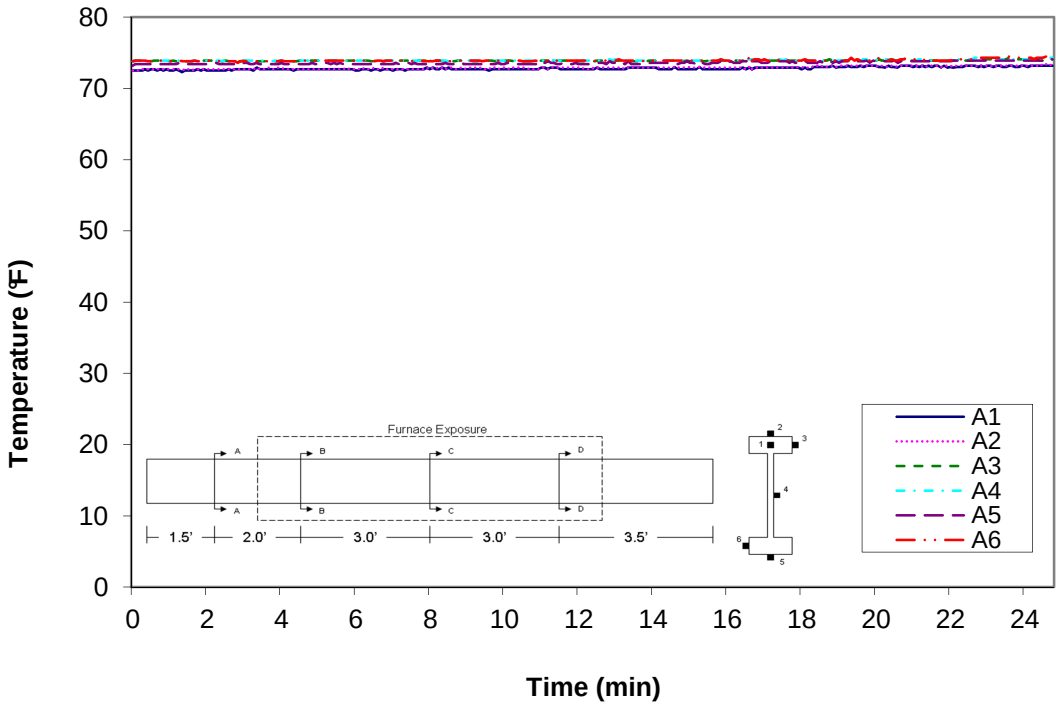

Figure A-77: Temperature distribution in wood joist E3 at cross-section A

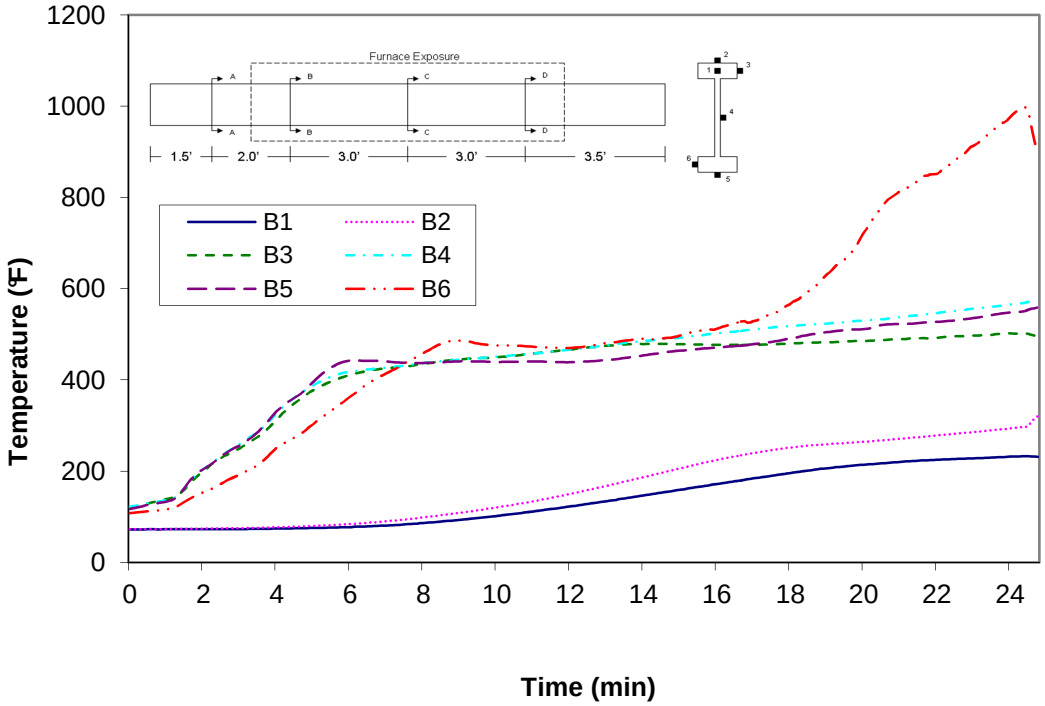

Figure A-78: Temperature distribution in wood joist E3 at cross-section B

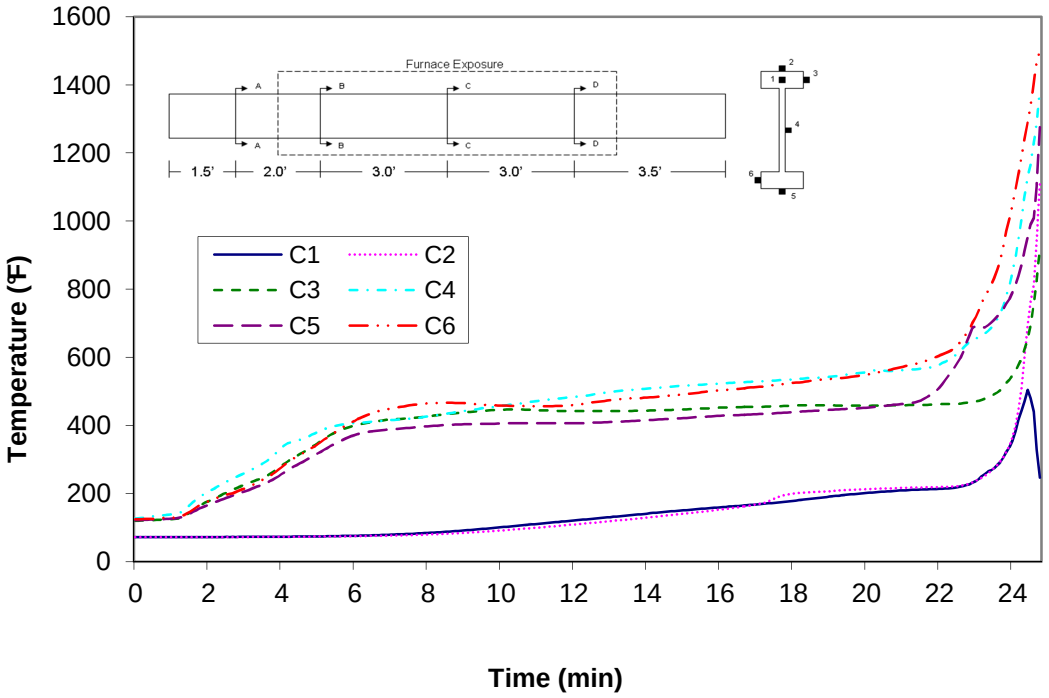

Figure A-79: Temperature distribution in wood joist E3 at cross-section C

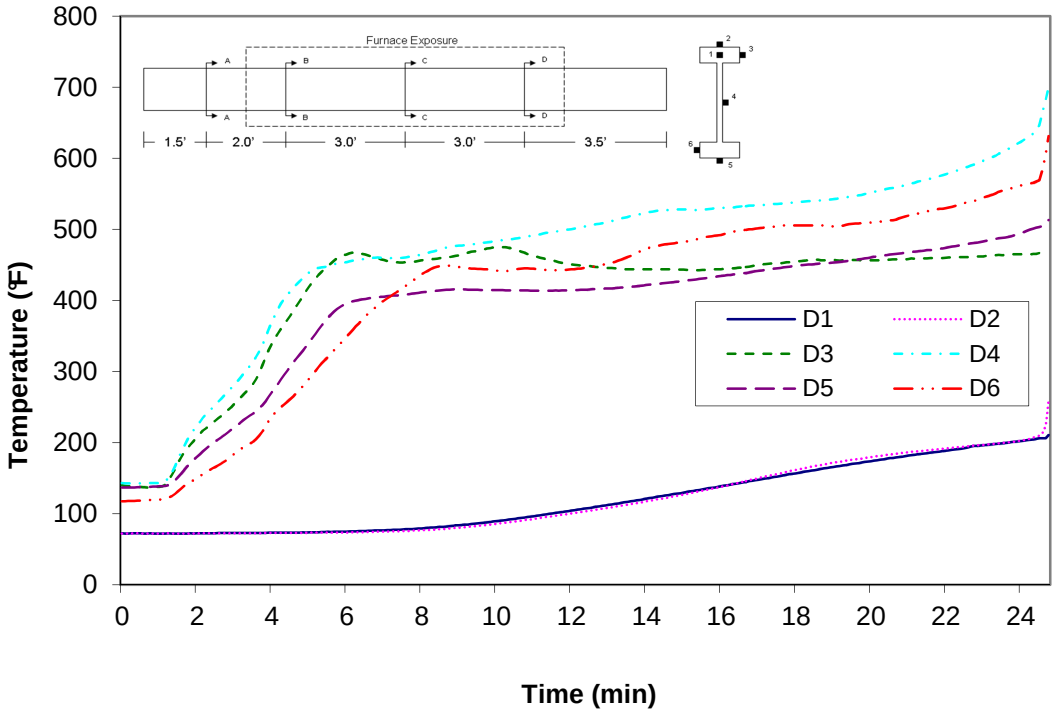

Figure A-80: Temperature distribution in wood joist E3 at cross-section D

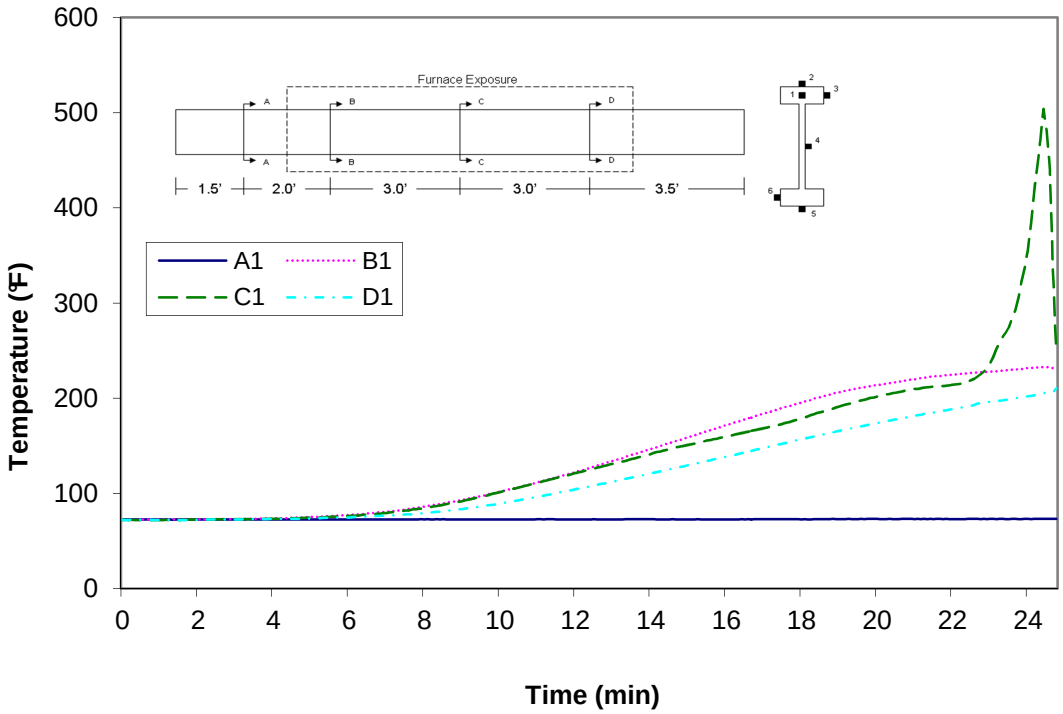

Figure A-81: Temperature distribution in wood joist E3 at thermocouple location 1

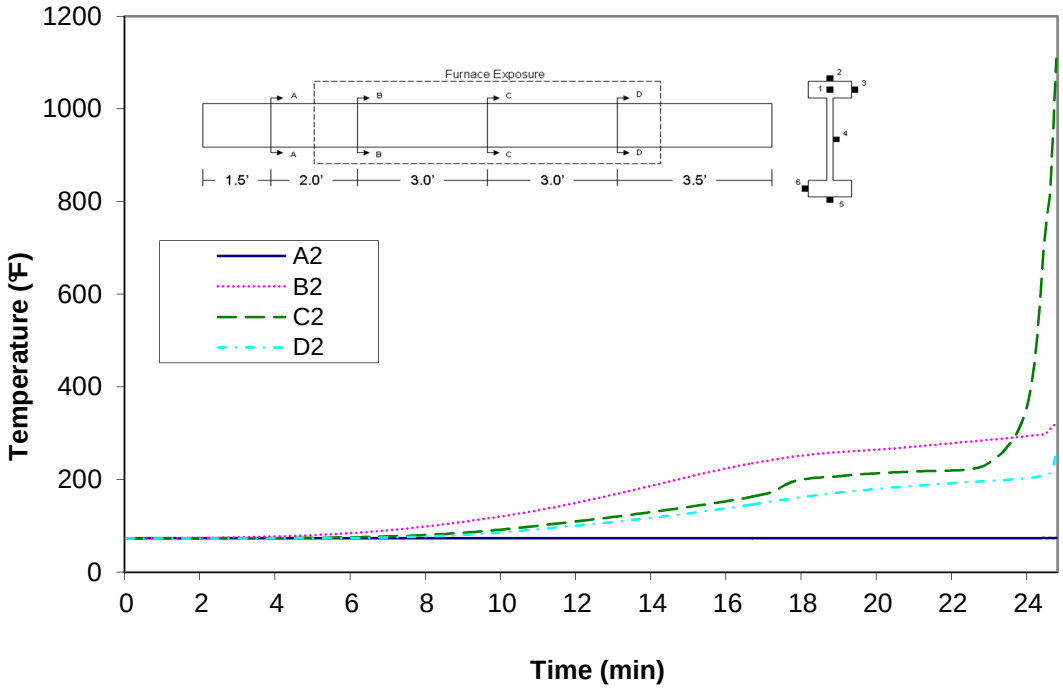

Figure A-82: Temperature distribution in wood joist E3 at thermocouple location 2

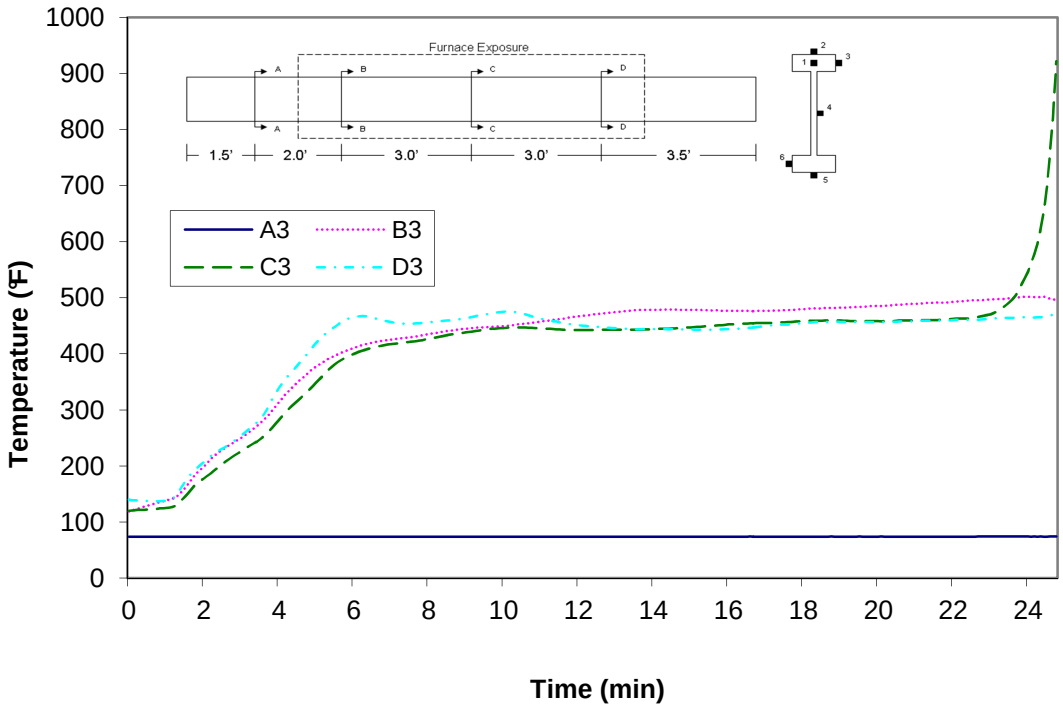

Figure A-83: Temperature distribution in wood joist E3 at thermocouple location 3

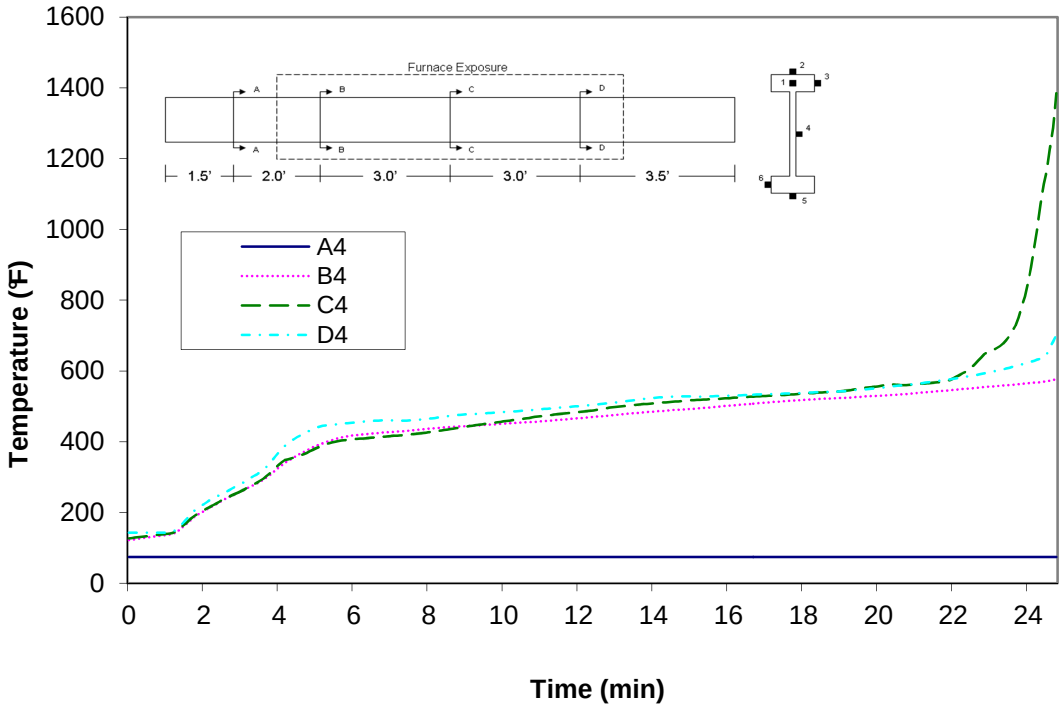

Figure A-84: Temperature distribution in wood joist E3 at thermocouple location 4

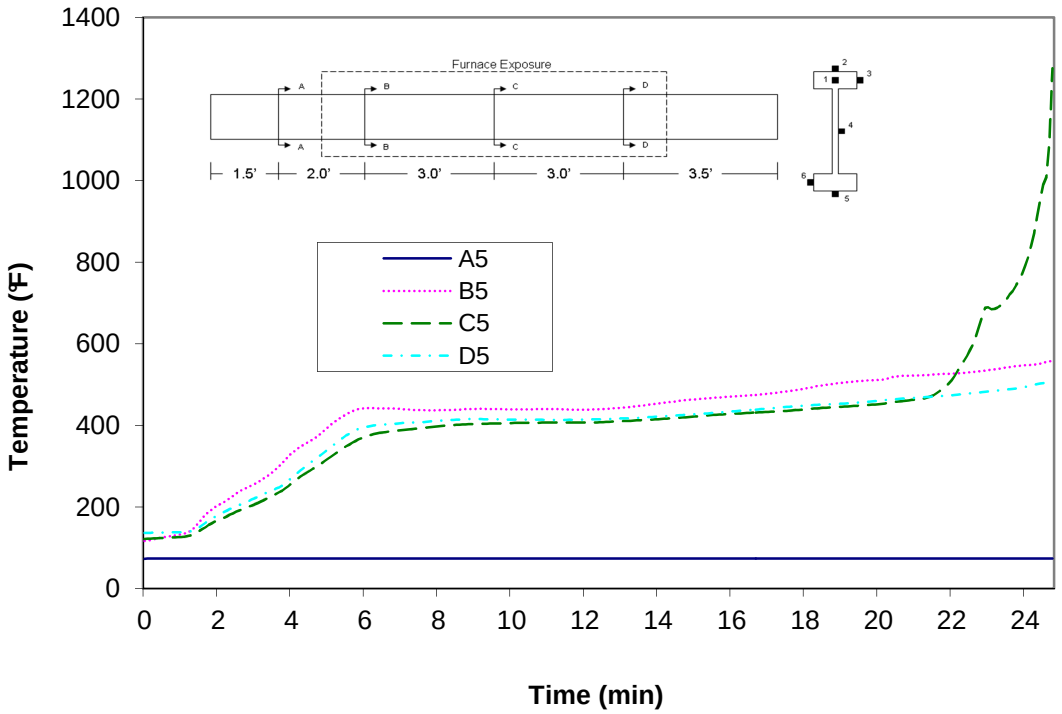

Figure A-85: Temperature distribution in wood joist E3 at thermocouple location 5

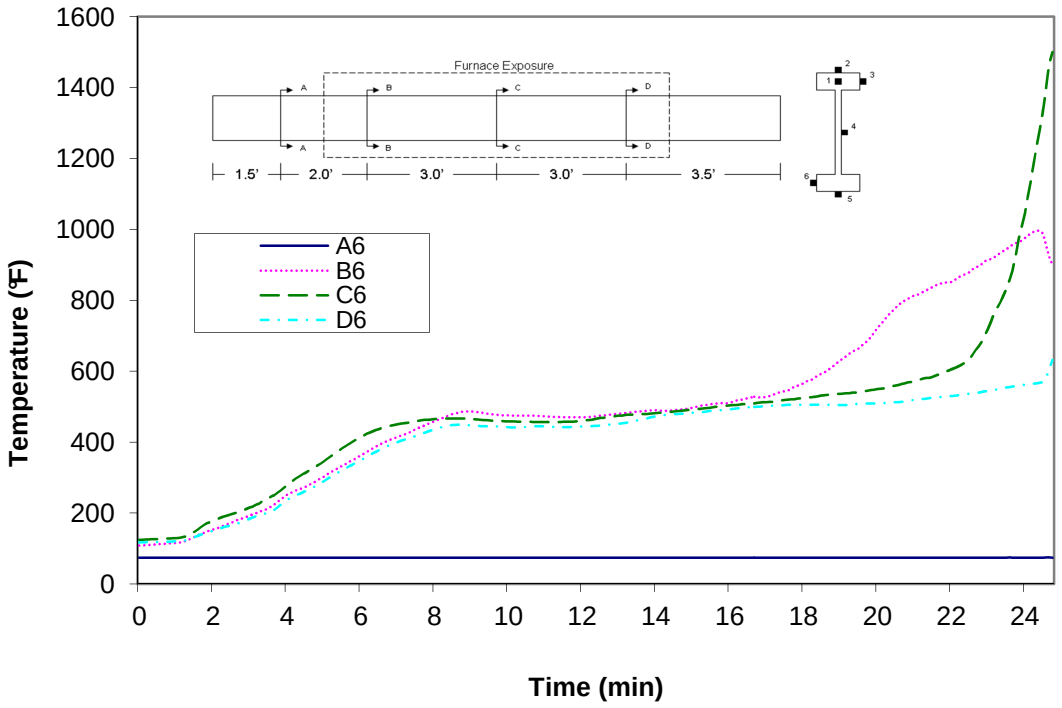

Figure A-86: Temperature distribution in wood joist E3 at thermocouple location 6

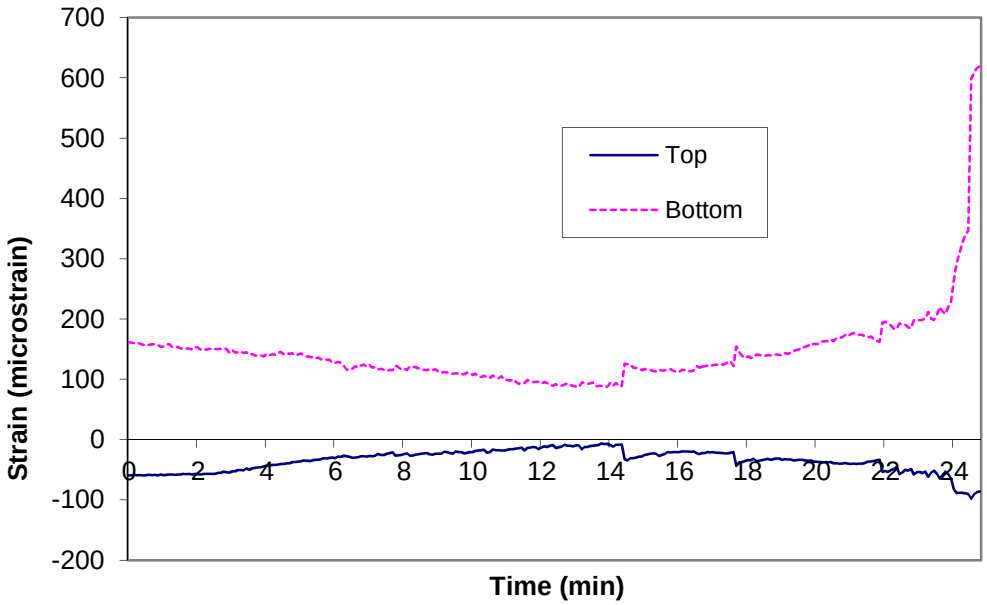

Figure A-87: Measured strains recorded during fire resistance tests of wood joist E3

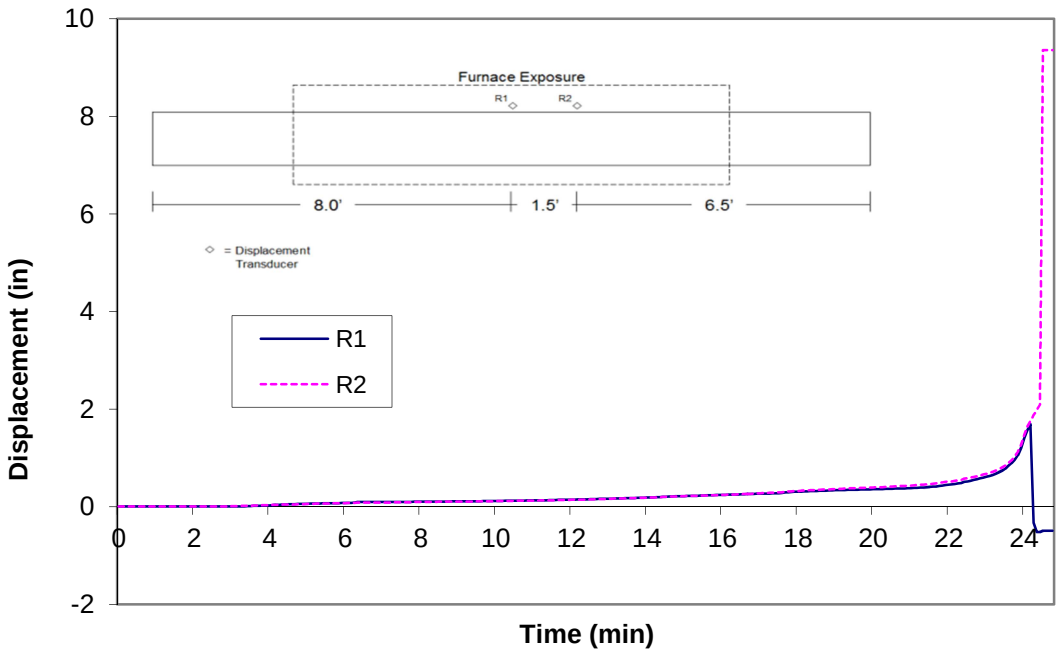

Figure A-88: Measured displacements recorded during fire resistance tests of wood joist E3

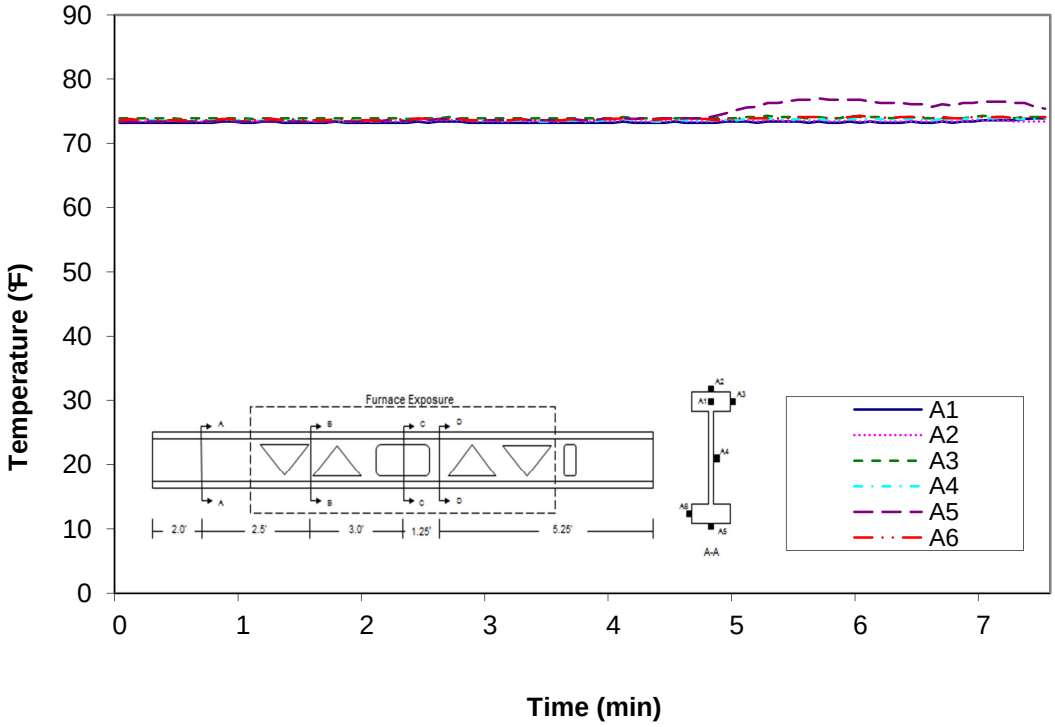

Figure A-89: Temperature distribution in wood joist C1 at cross-section A

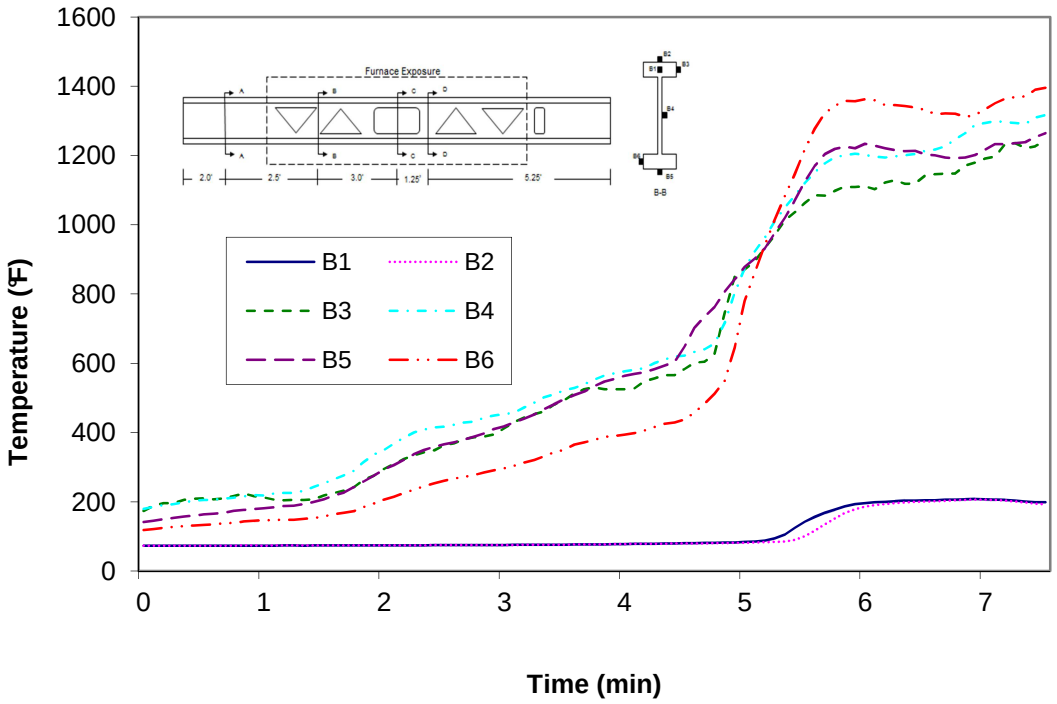

Figure A-90: Temperature distribution in wood joist C1 at cross-section B

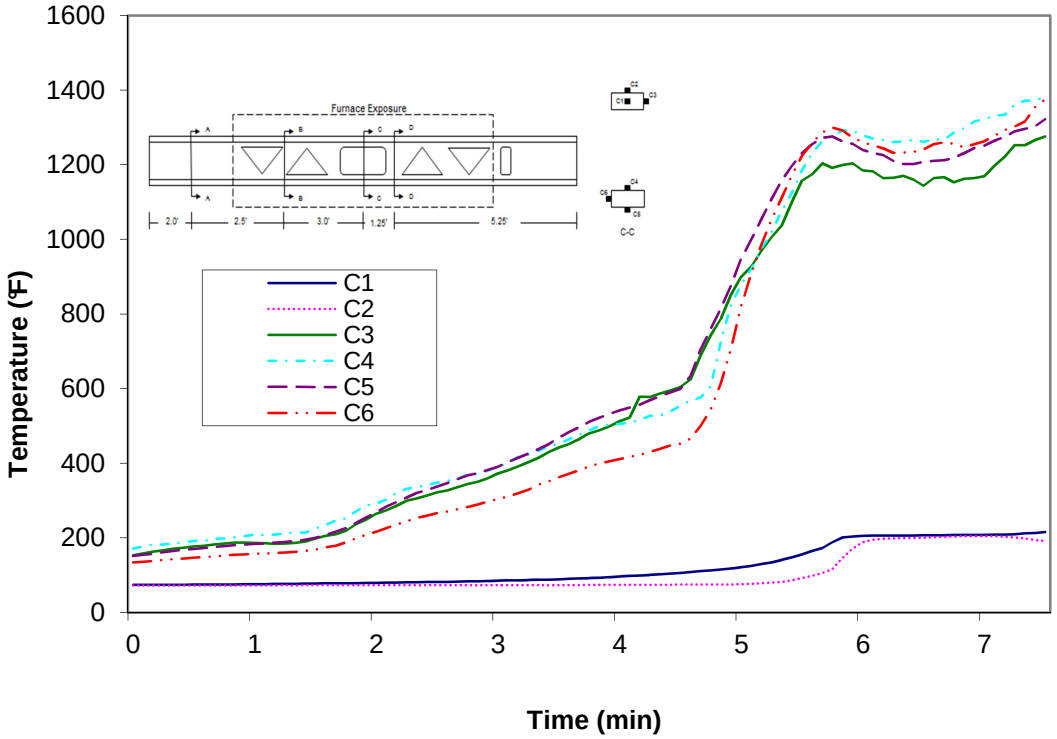

Figure A-91: Temperature distribution in wood joist C1 at cross-section C

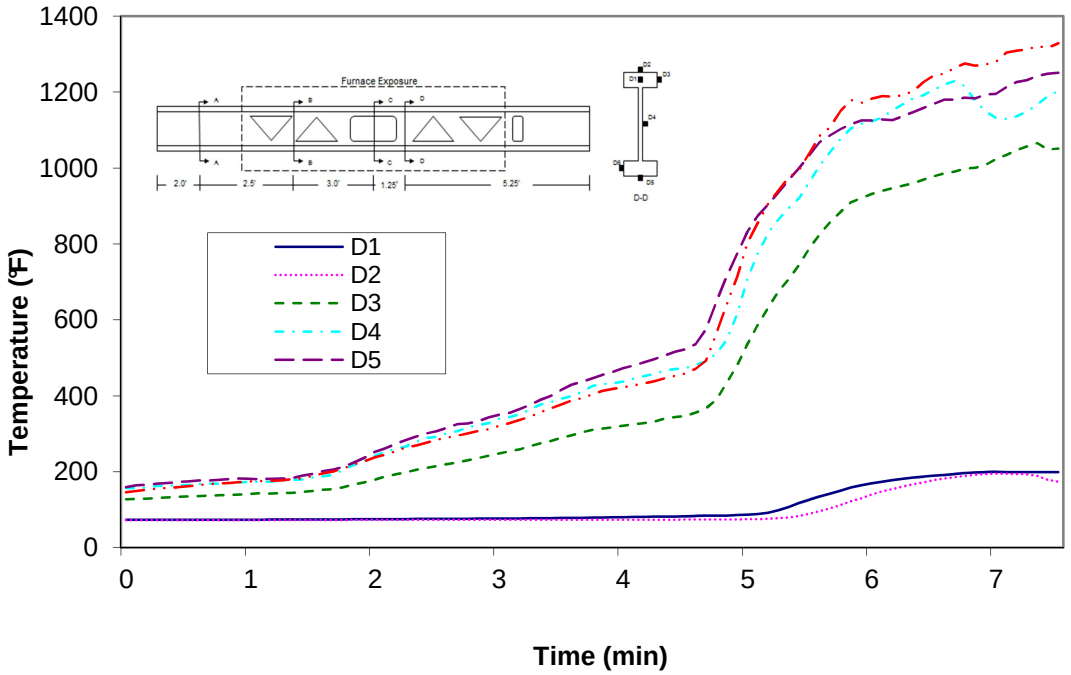

Figure A-92: Temperature distribution in wood joist C1 at cross-section D

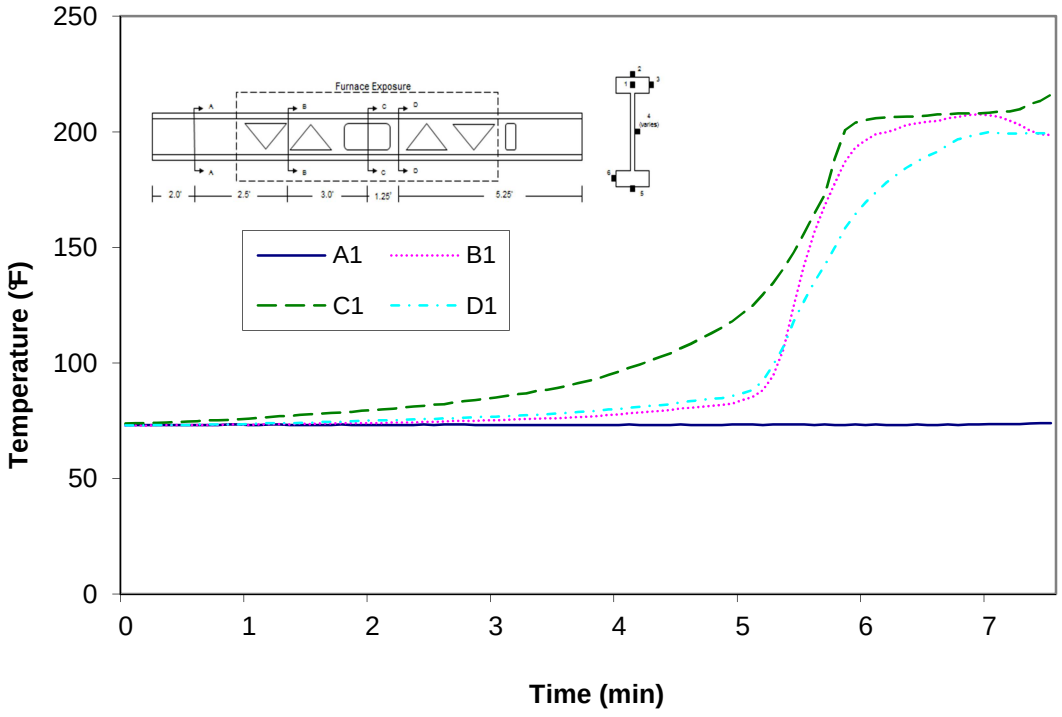

Figure A-93: Temperature distribution in wood joist C1 at thermocouple location 1

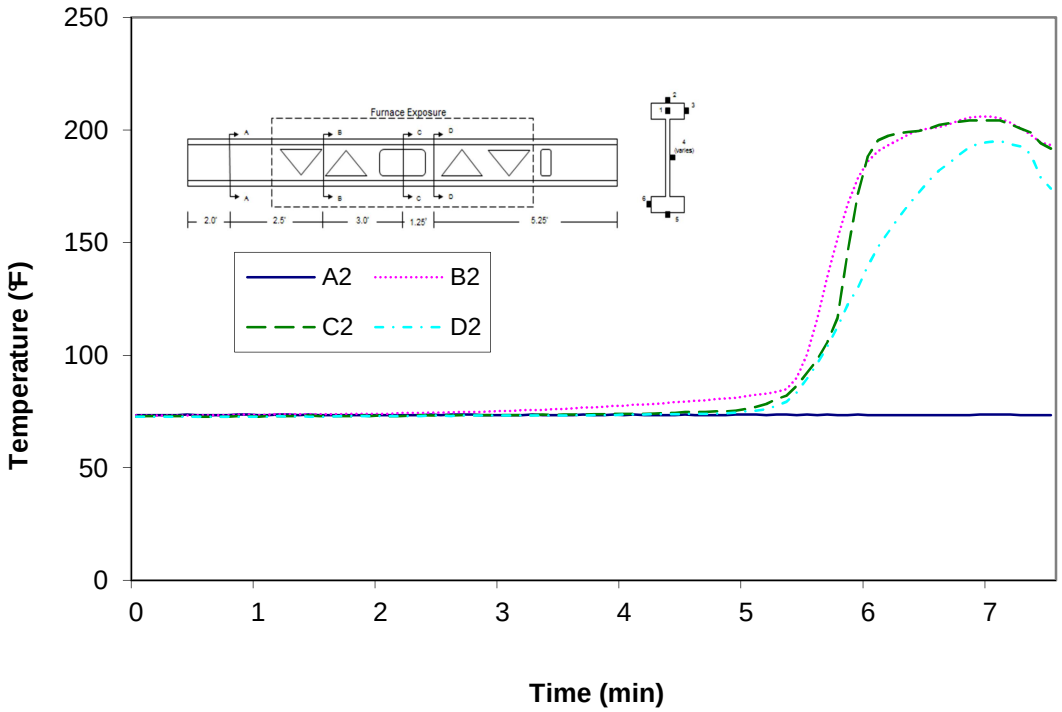

Figure A-94: Temperature distribution in wood joist C1 at thermocouple location 2

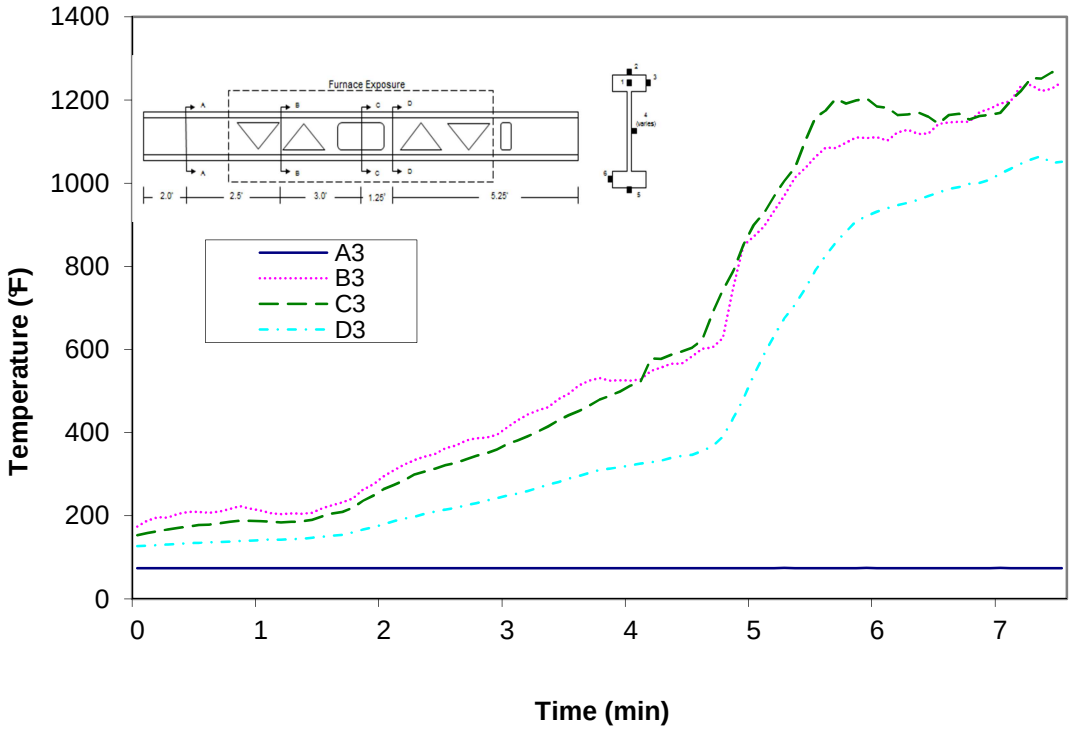

Figure A-95: Temperature distribution in wood joist C1 at thermocouple location 3

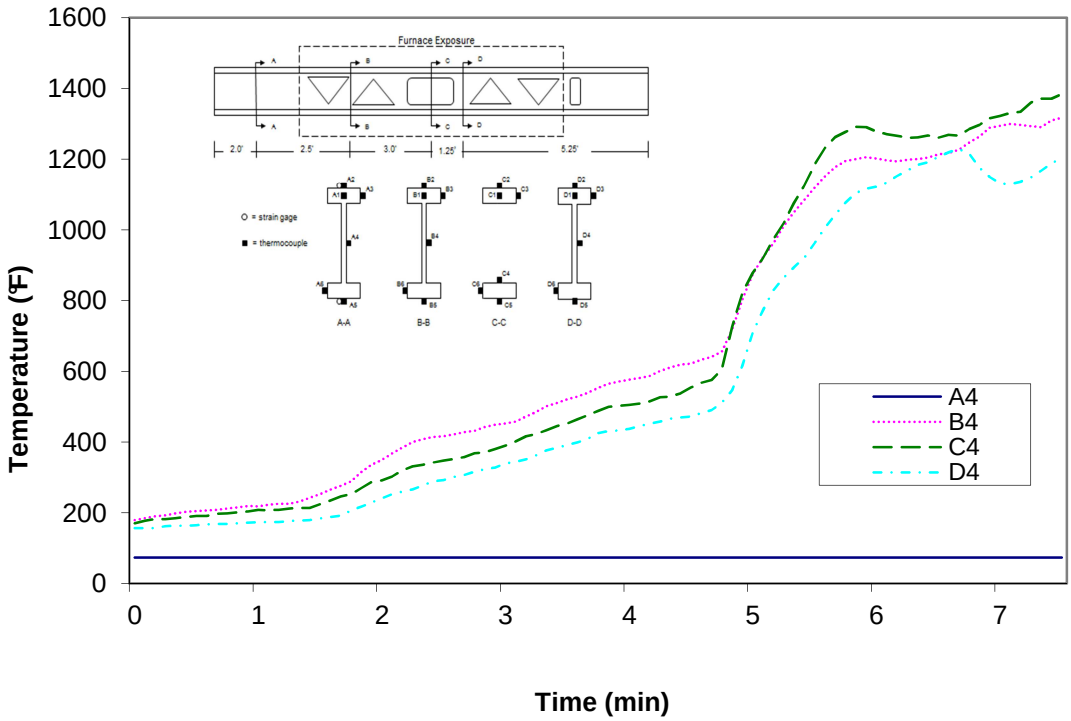

Figure A-96: Temperature distribution in wood joist C1 at thermocouple location 4

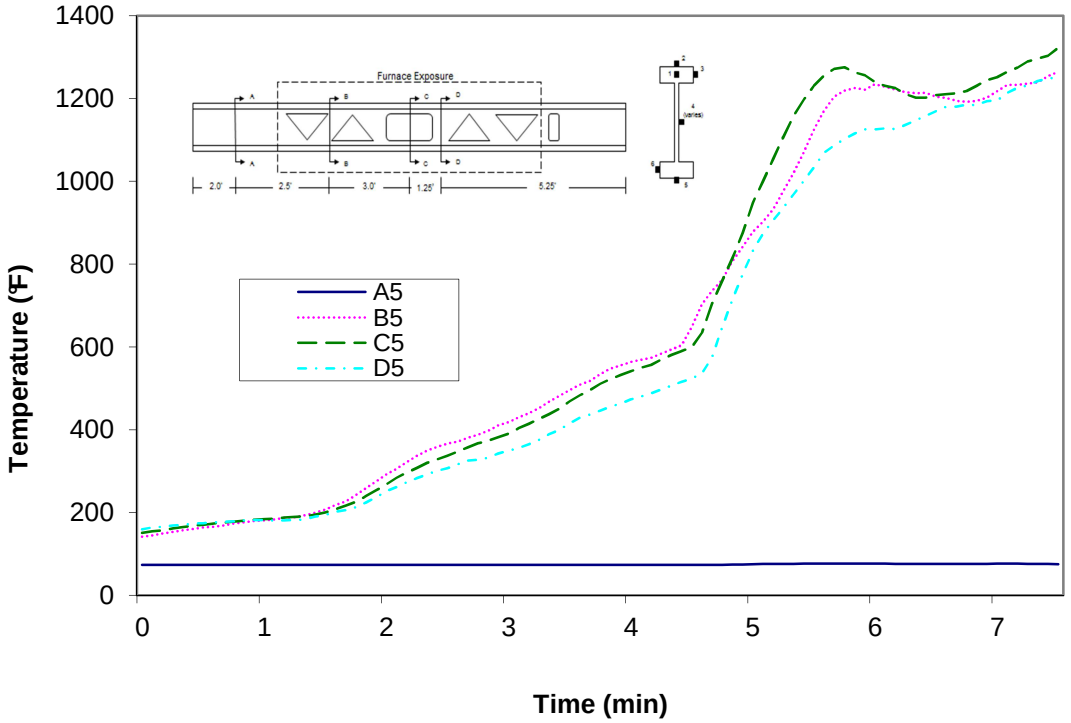

Figure A-97: Temperature distribution in wood joist C1 at thermocouple location 5

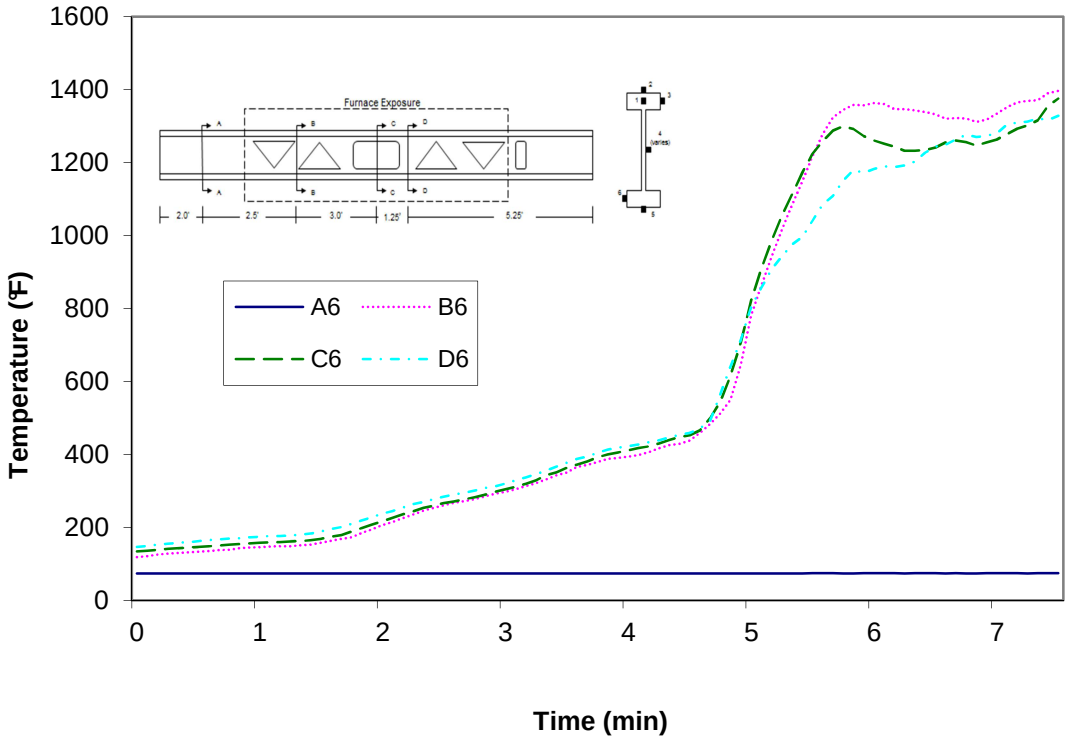

Figure A-98: Temperature distribution in wood joist C1 at thermocouple location 6

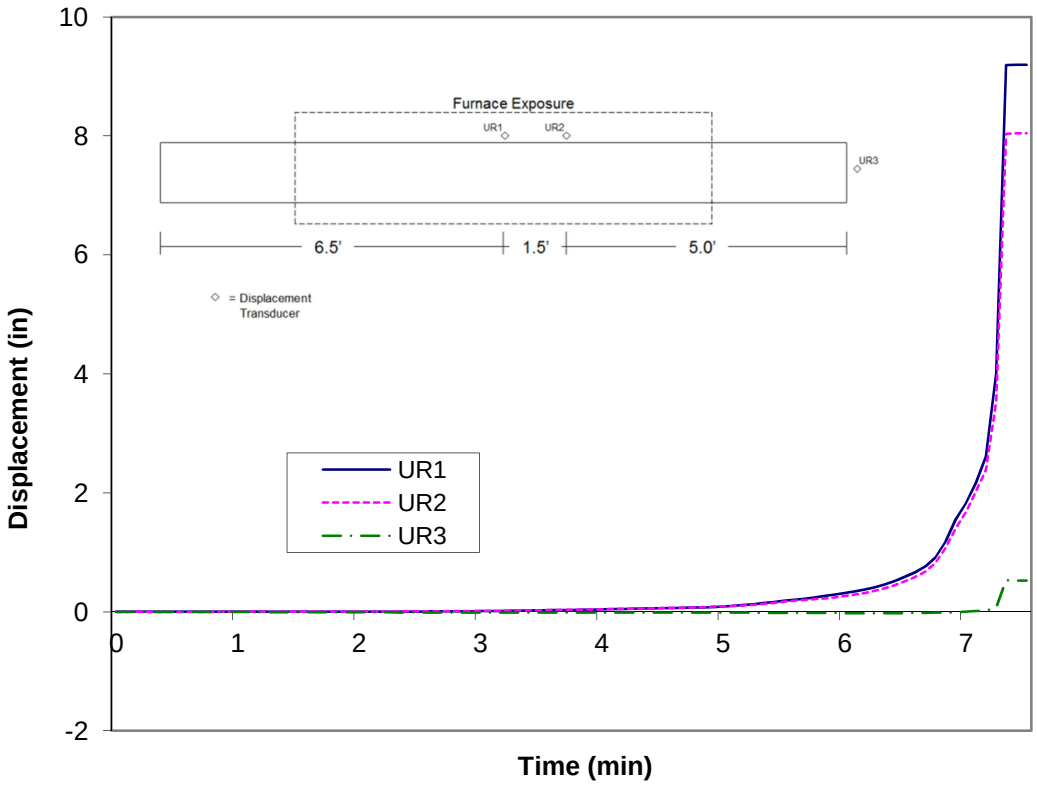

Figure A-99: Measured displacements recorded during fire resistance tests of wood joist C1

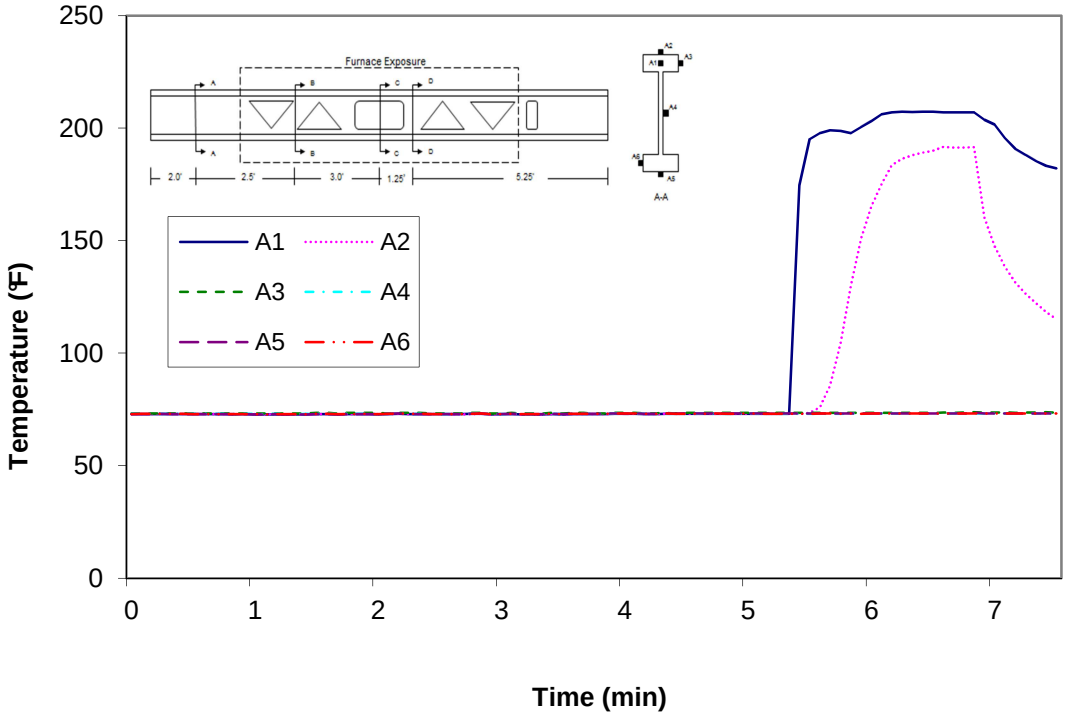

Figure A-100: Temperature distribution in wood joist C2 at cross-section A

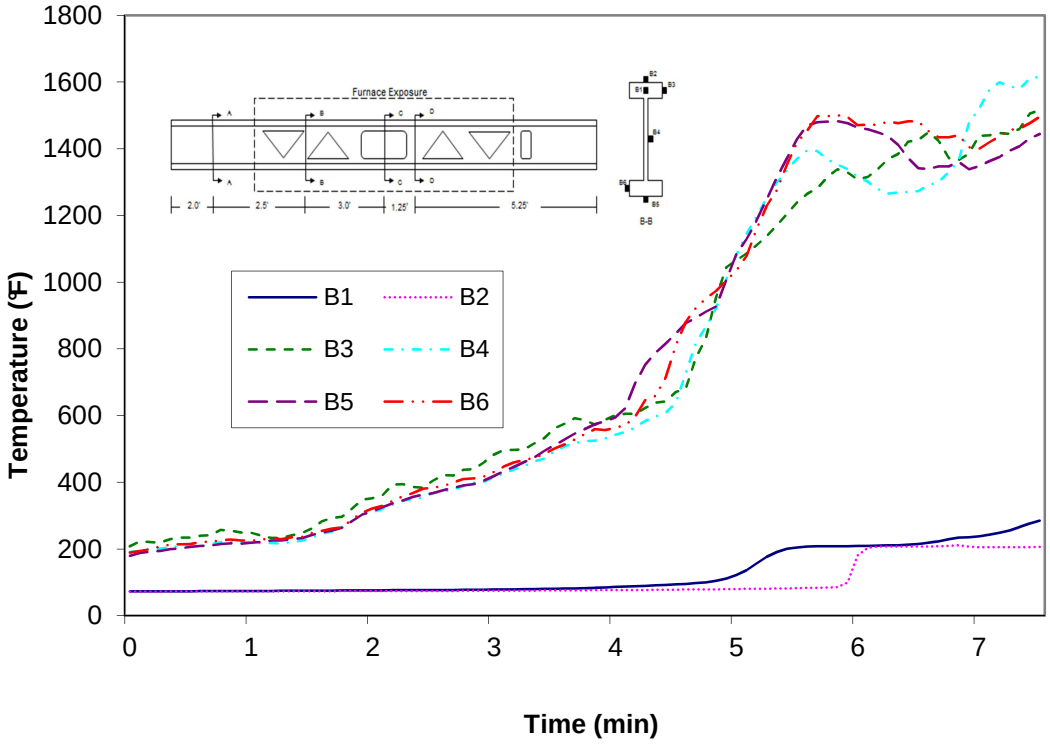

Figure A-101: Temperature distribution in wood joist C2 at cross-section B

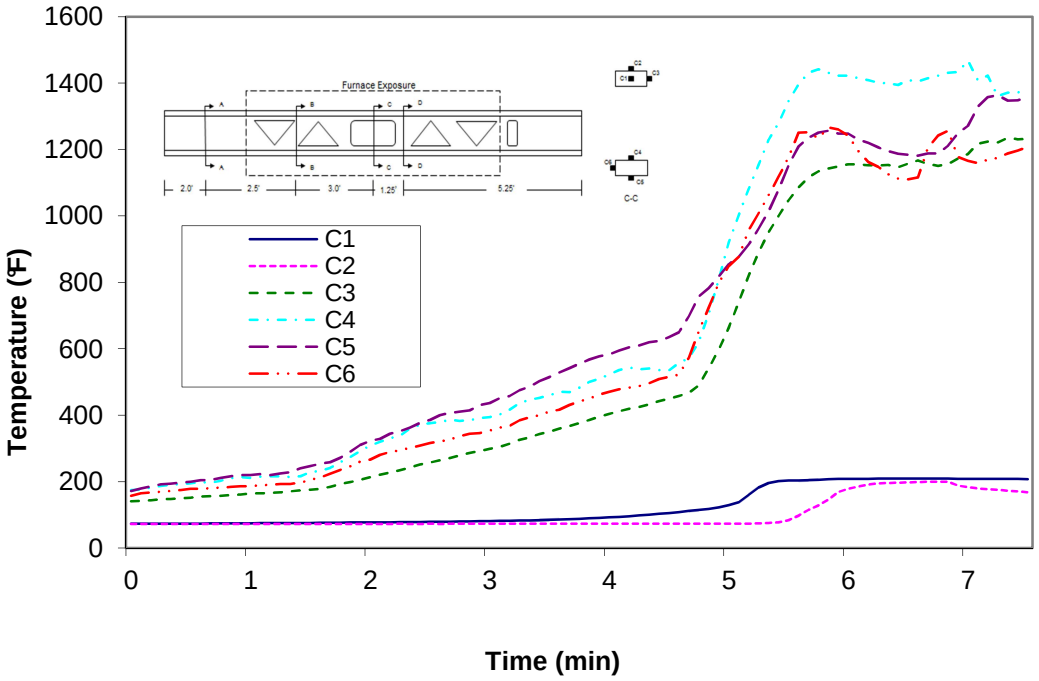

Figure A-102: Temperature distribution in wood joist C2 at cross-section C

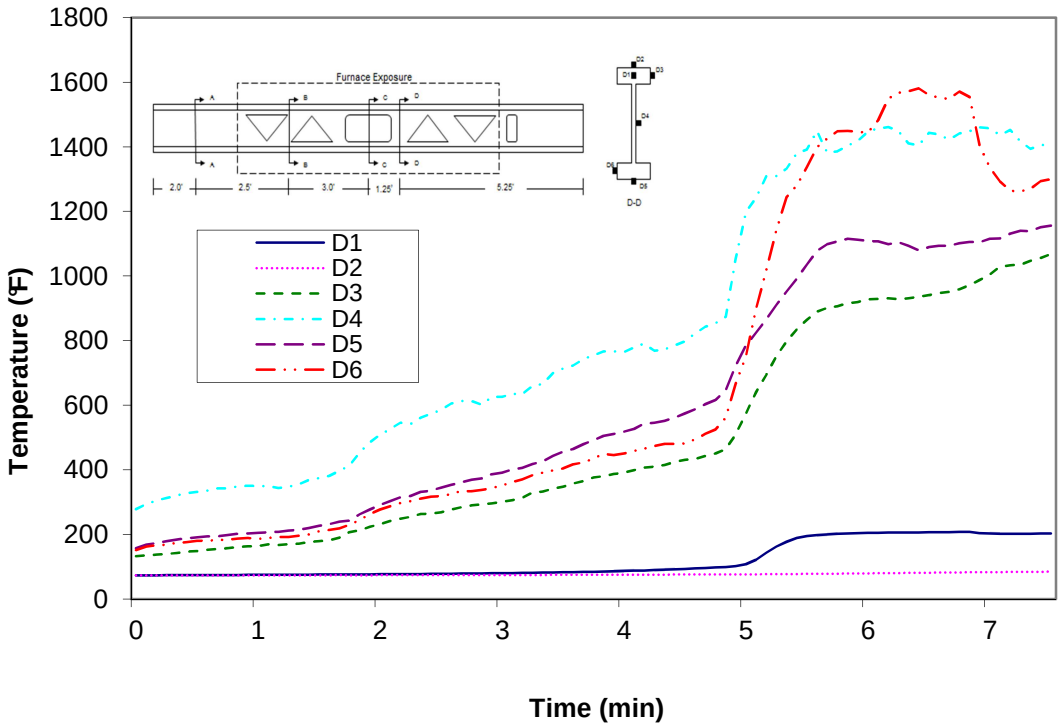

Figure A-103: Temperature distribution in wood joist C2 at cross-section D

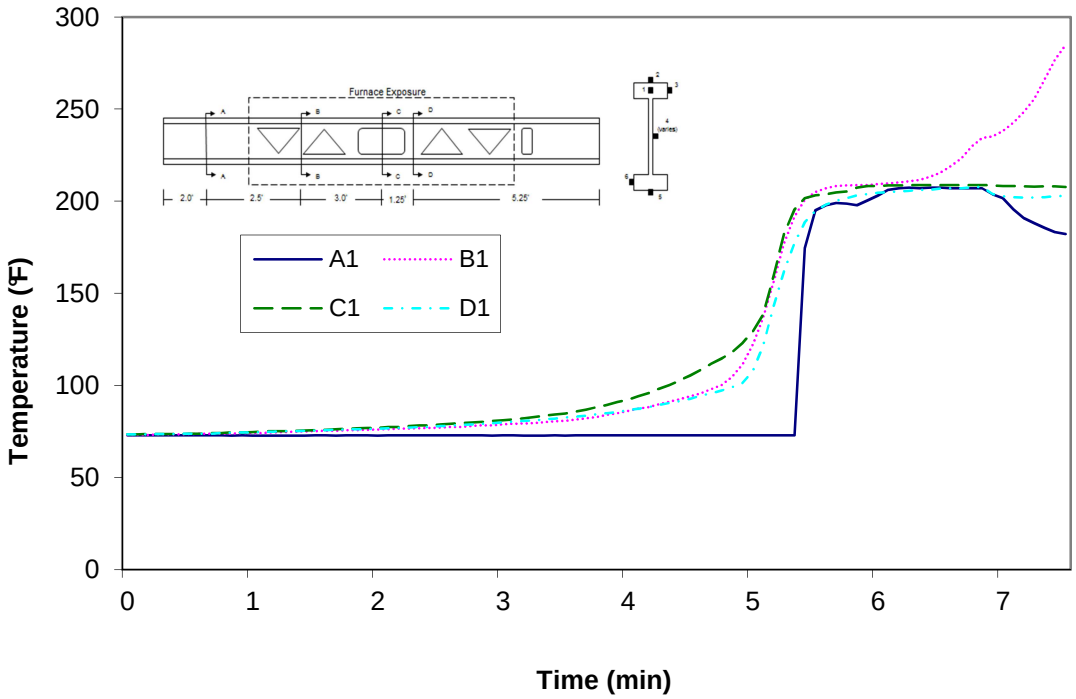

Figure A-104: Temperature distribution in wood joist C2 at thermocouple location 1

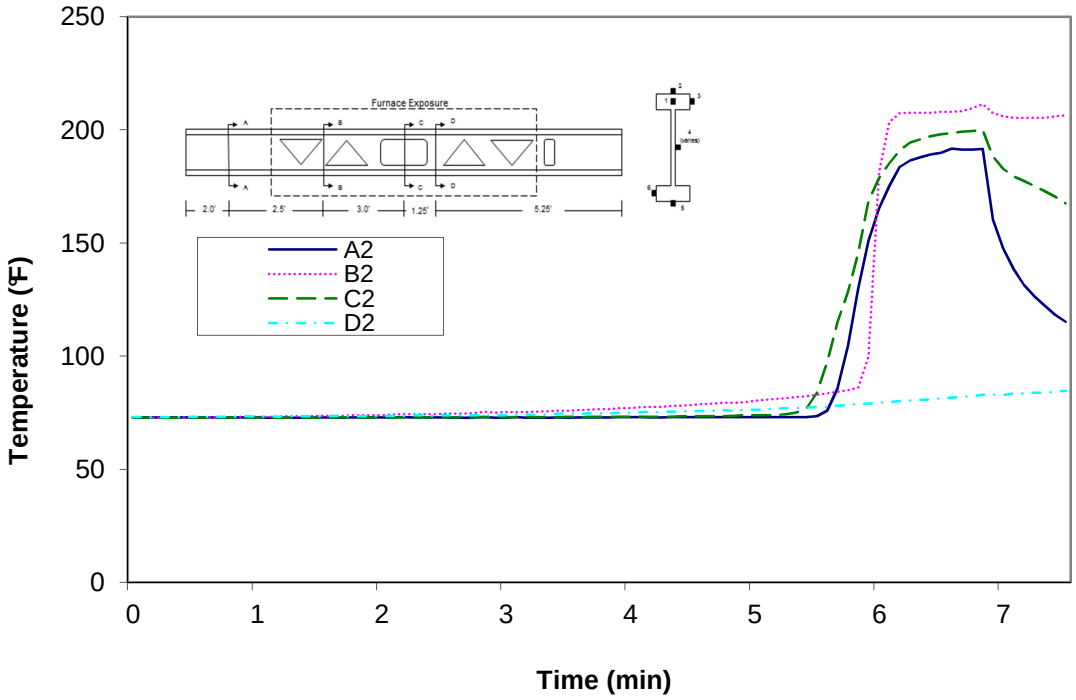

Figure A-105: Temperature distribution in wood joist C2 at thermocouple location 2

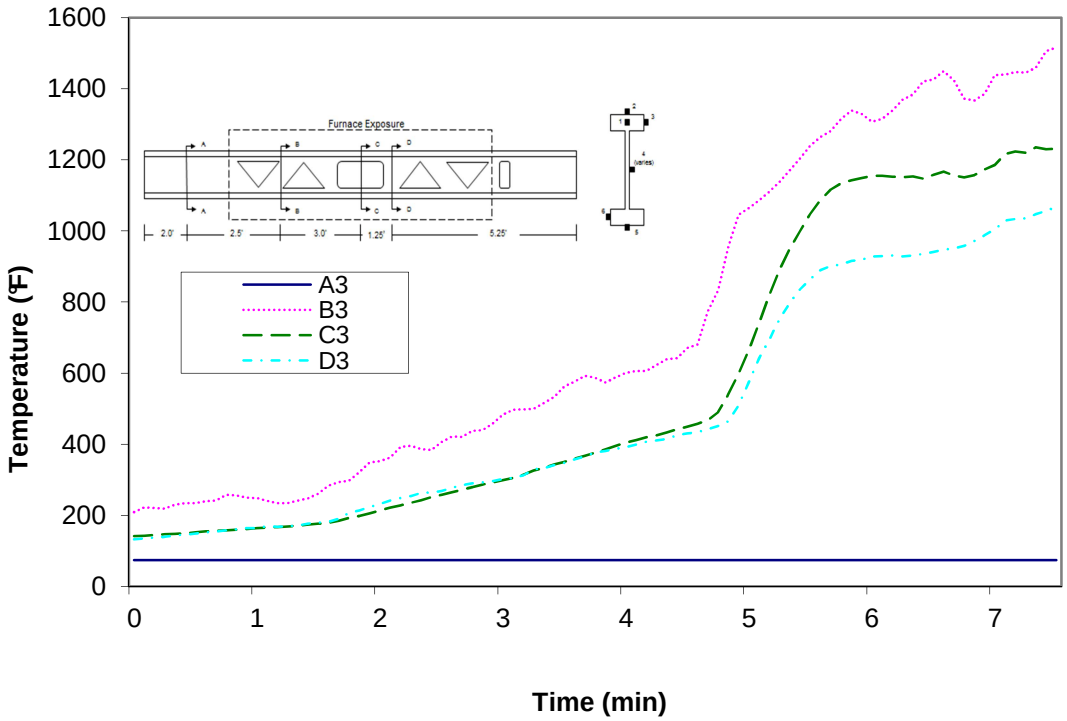

Figure A-106: Temperature distribution in wood joist C2 at thermocouple location 3

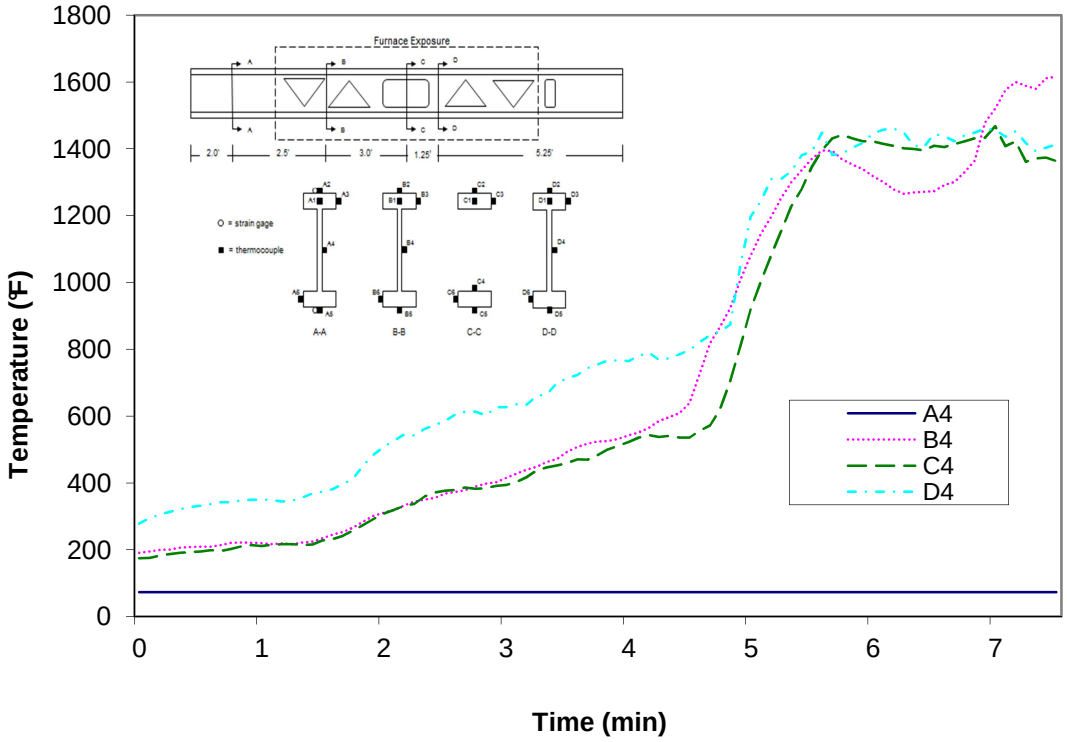

Figure A-107: Temperature distribution in wood joist C2 at thermocouple location 4

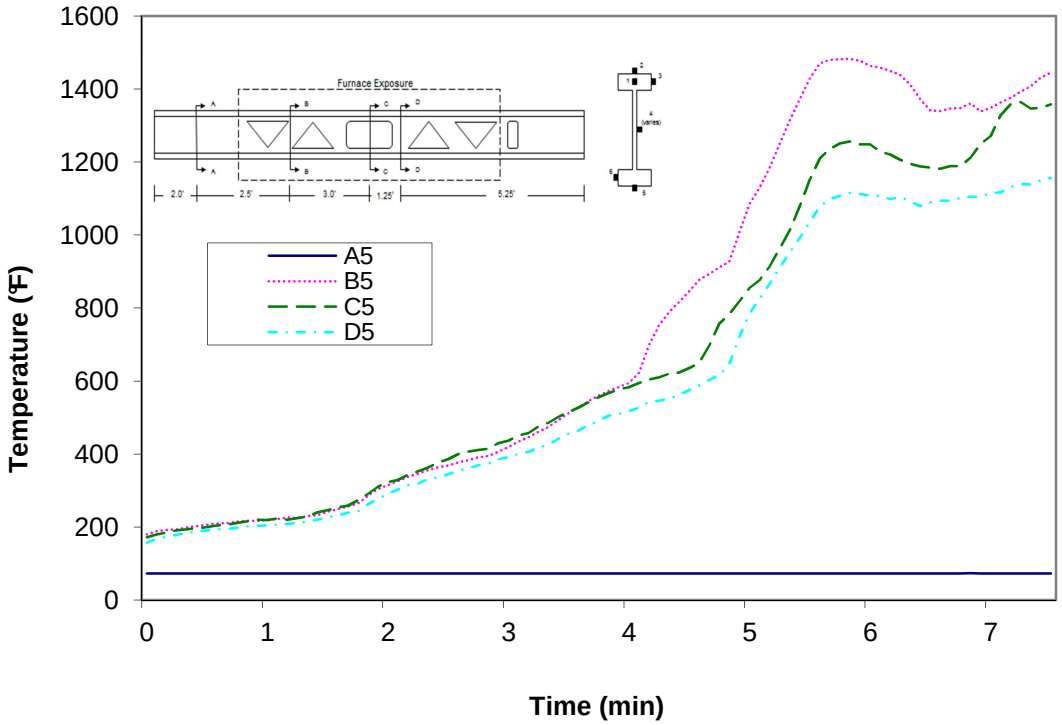

Figure A-108: Temperature distribution in wood joist C2 at thermocouple location 5

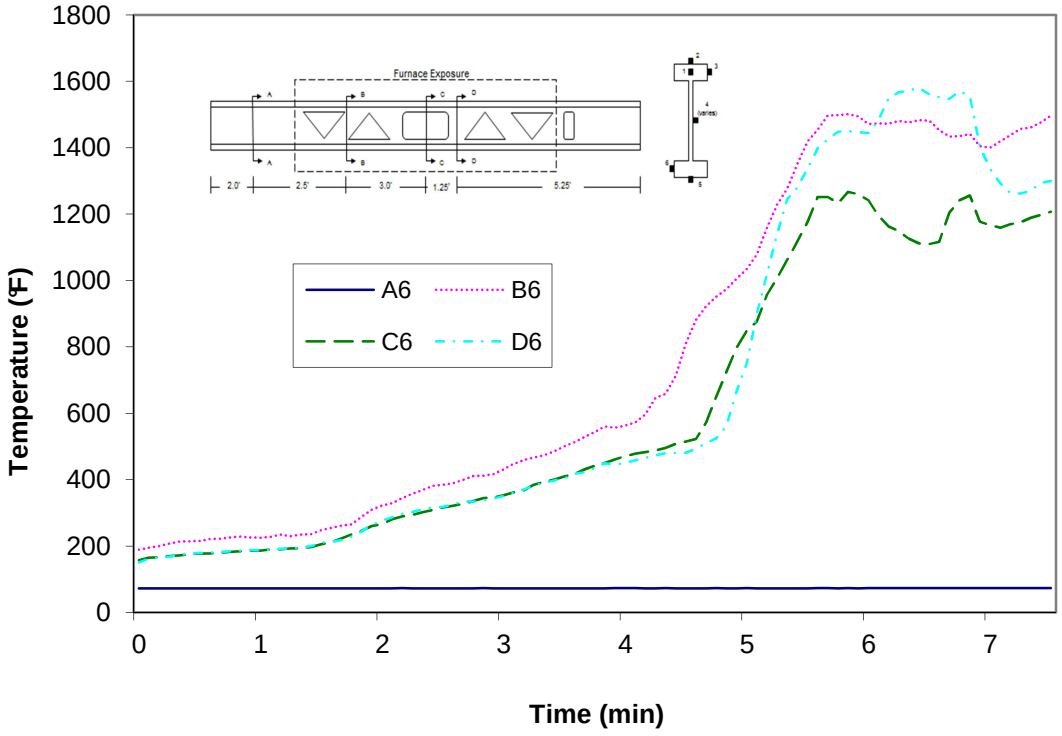

Figure A-109: Temperature distribution in wood joist C2 at thermocouple location 6

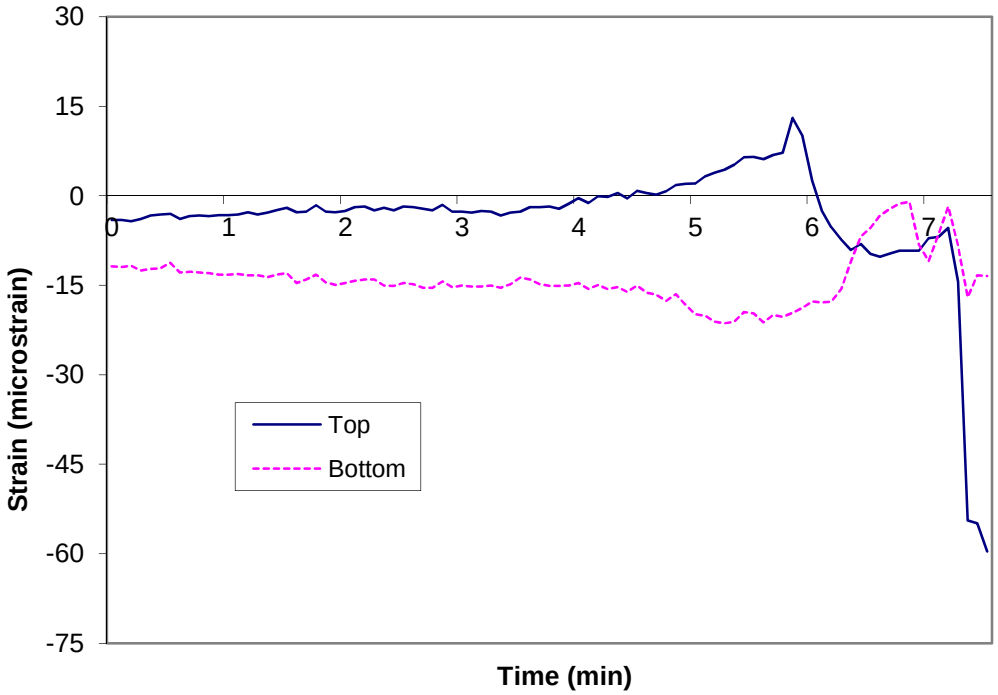

Figure A-110: Measured strains recorded during fire resistance tests of wood joist C2

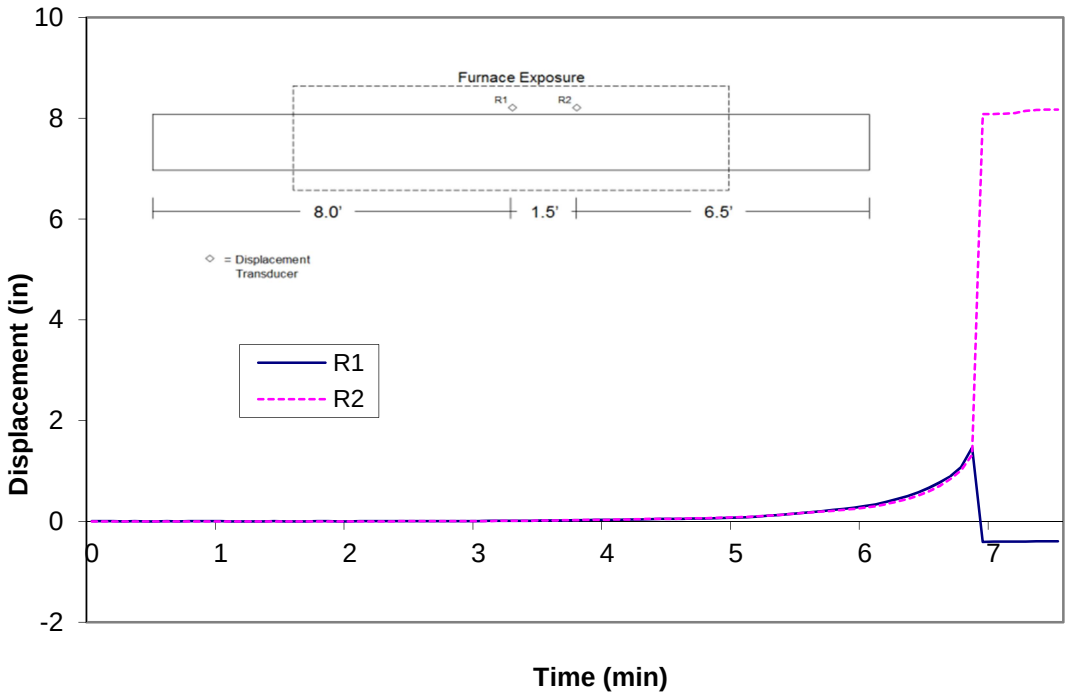

Figure A-111: Measured displacements recorded during fire resistance tests of wood joist C2

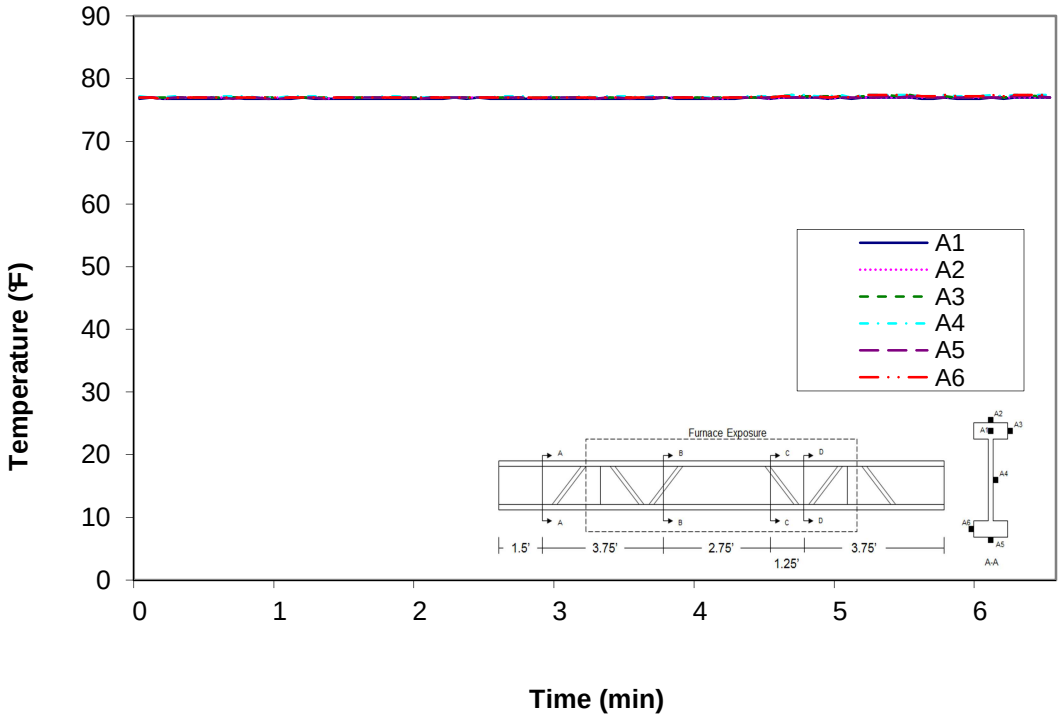

Figure A-112: Temperature distribution in wood joist H1 at cross-section A

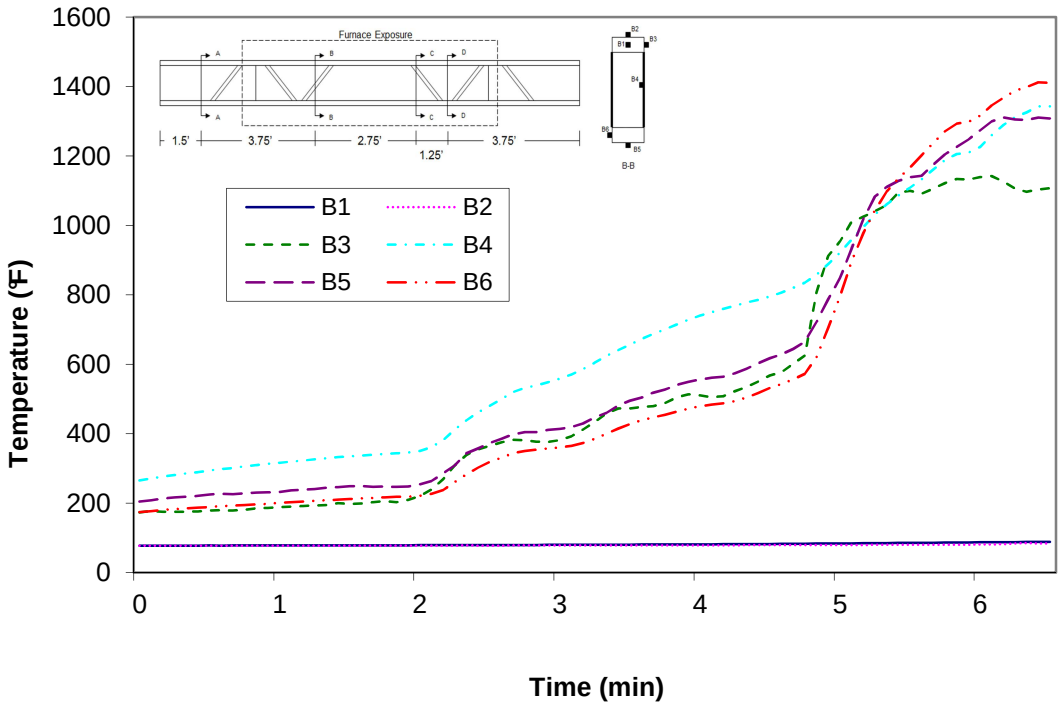

Figure A-113: Temperature distribution in wood joist H1 at cross-section B

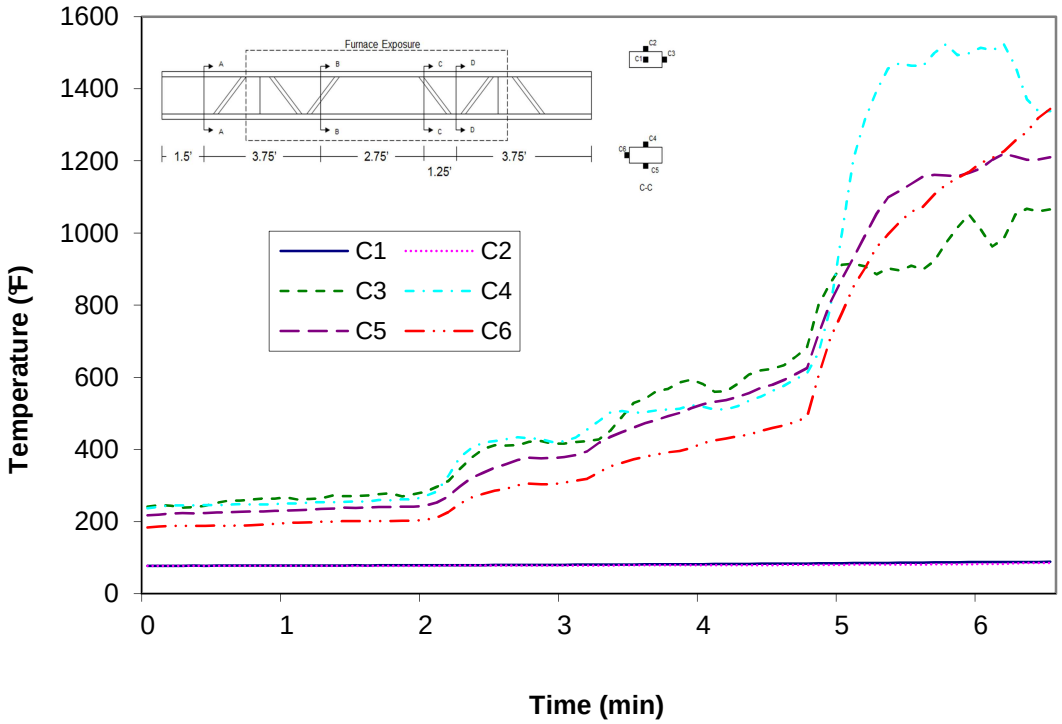

Figure A-114: Temperature distribution in wood joist H1 at cross-section C

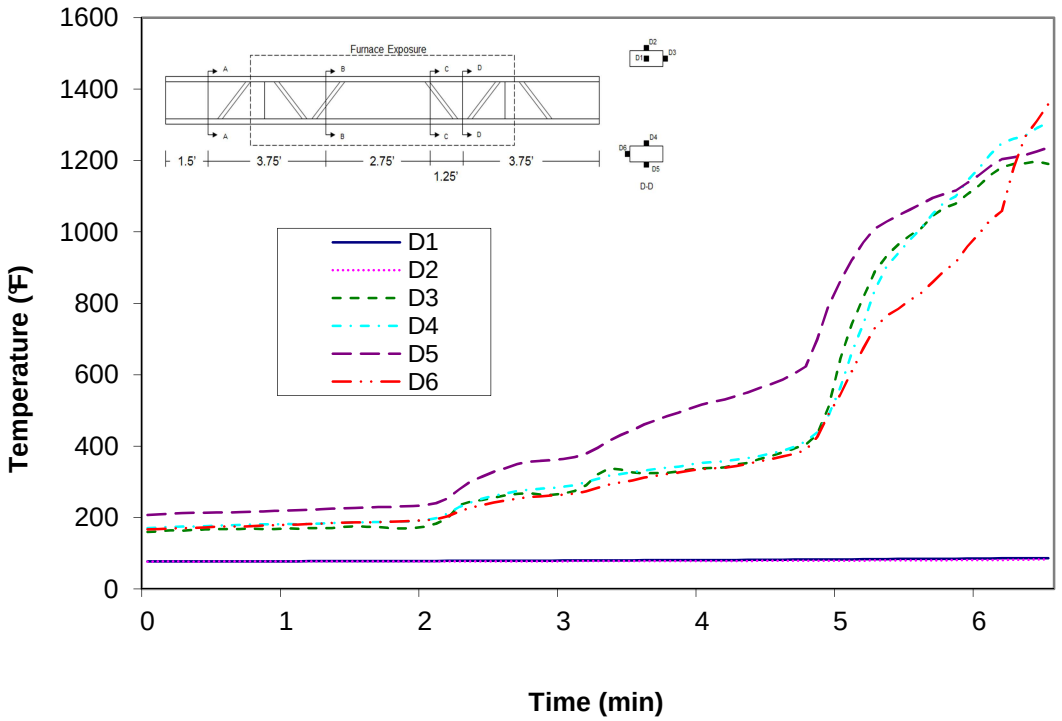

Figure A-115: Temperature distribution in wood joist H1 at cross-section D

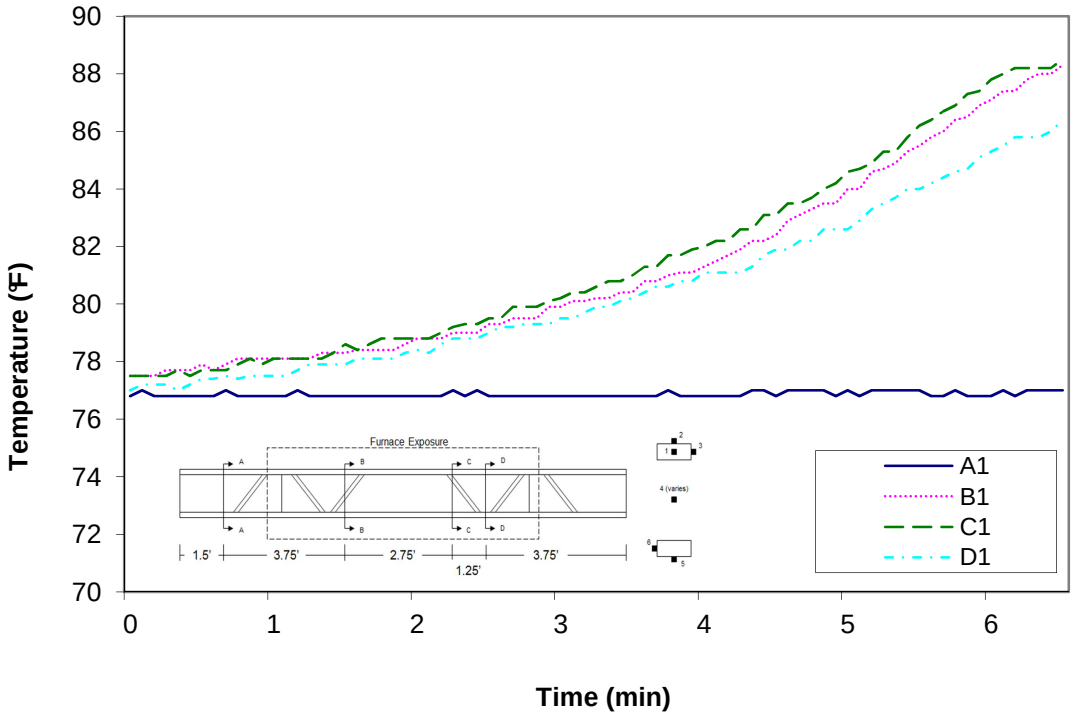

Figure A-116: Temperature distribution in wood joist H1 at thermocouple location 1

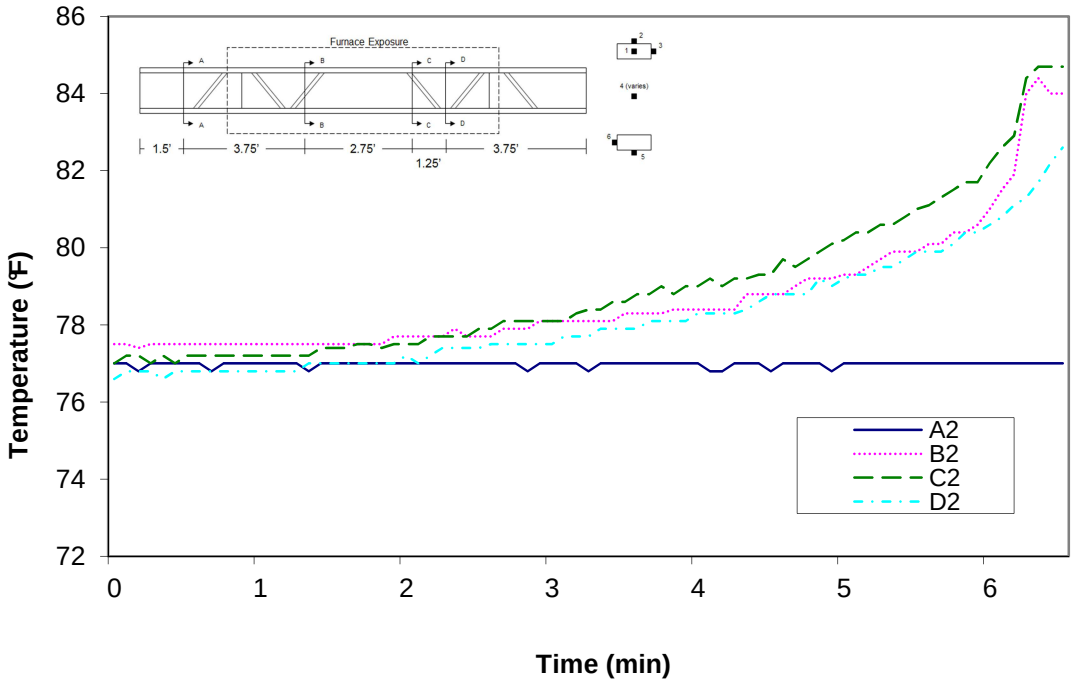

Figure A-117: Temperature distribution in wood joist H1 at thermocouple location 2

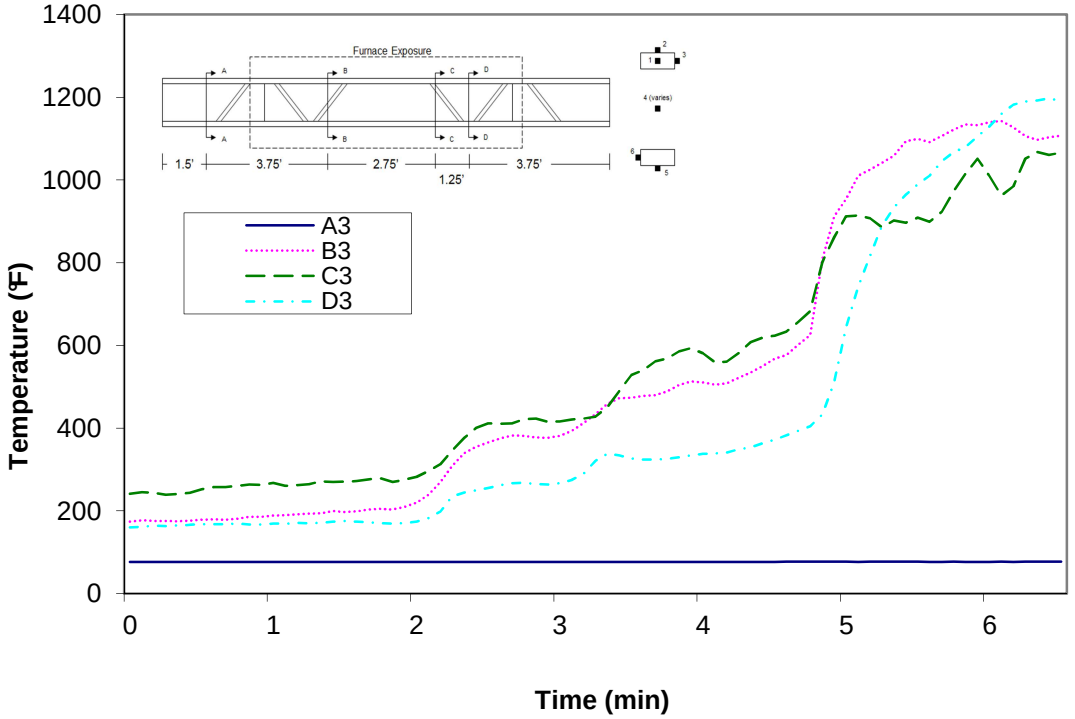

Figure A-118: Temperature distribution in wood joist H1 at thermocouple location 3

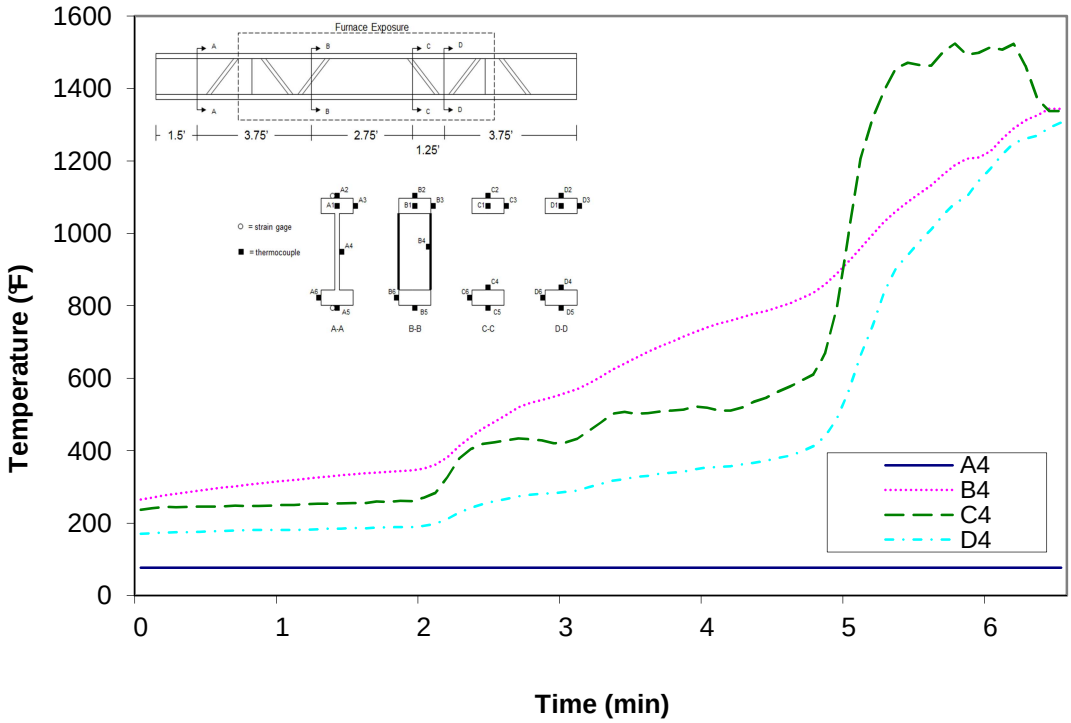

Figure A-119: Temperature distribution in wood joist H1 at thermocouple location 4

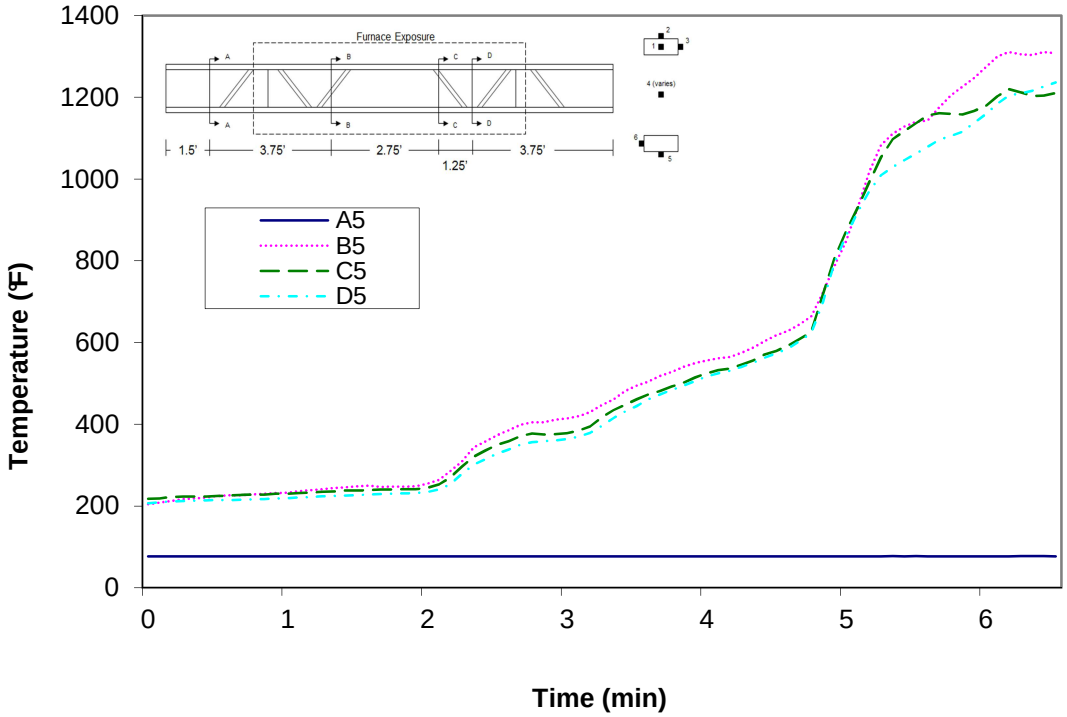

Figure A-120: Temperature distribution in wood joist H1 at thermocouple location 5

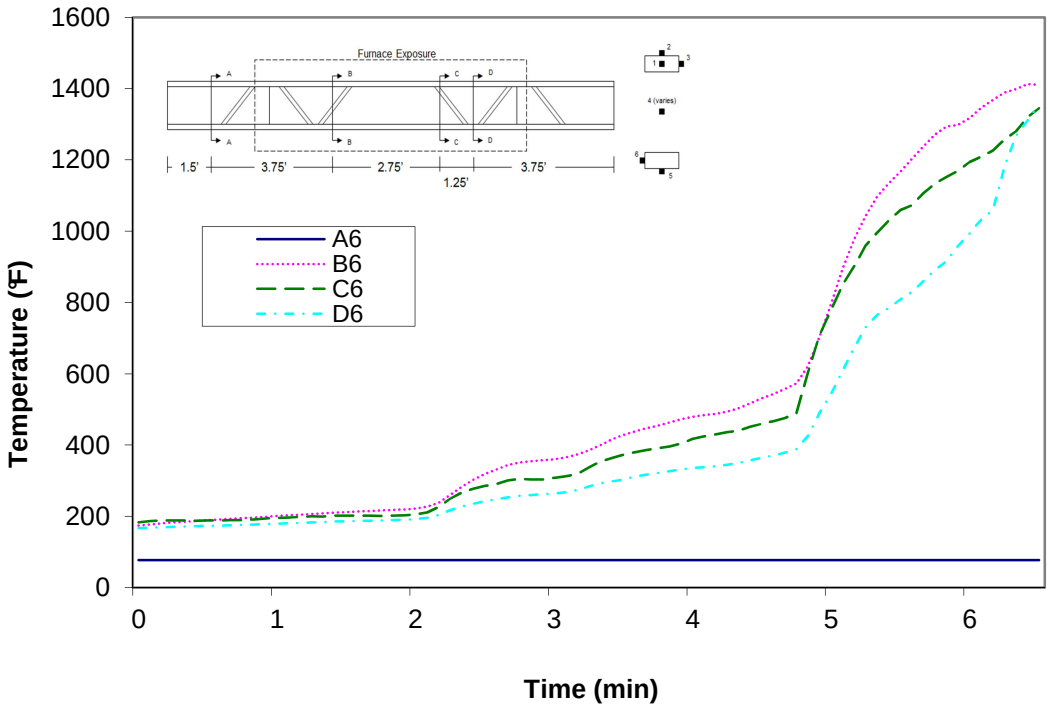

Figure A-121: Temperature distribution in wood joist H1 at thermocouple location 6

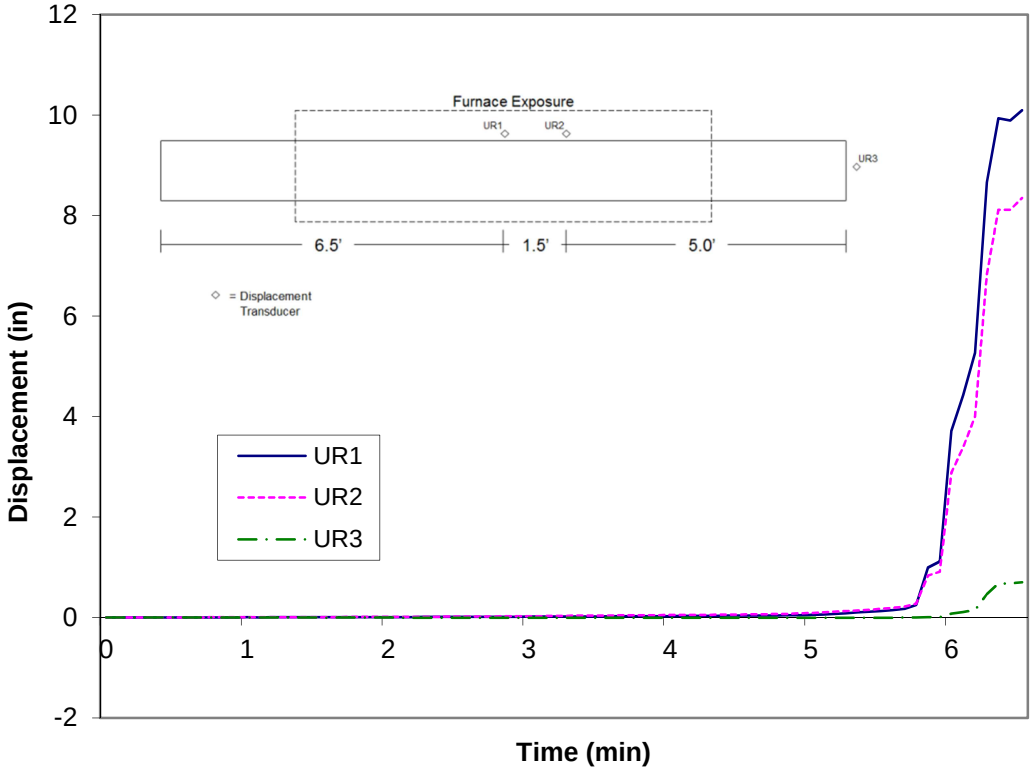

Figure A-122: Measured displacements recorded during fire resistance tests of wood joist H1

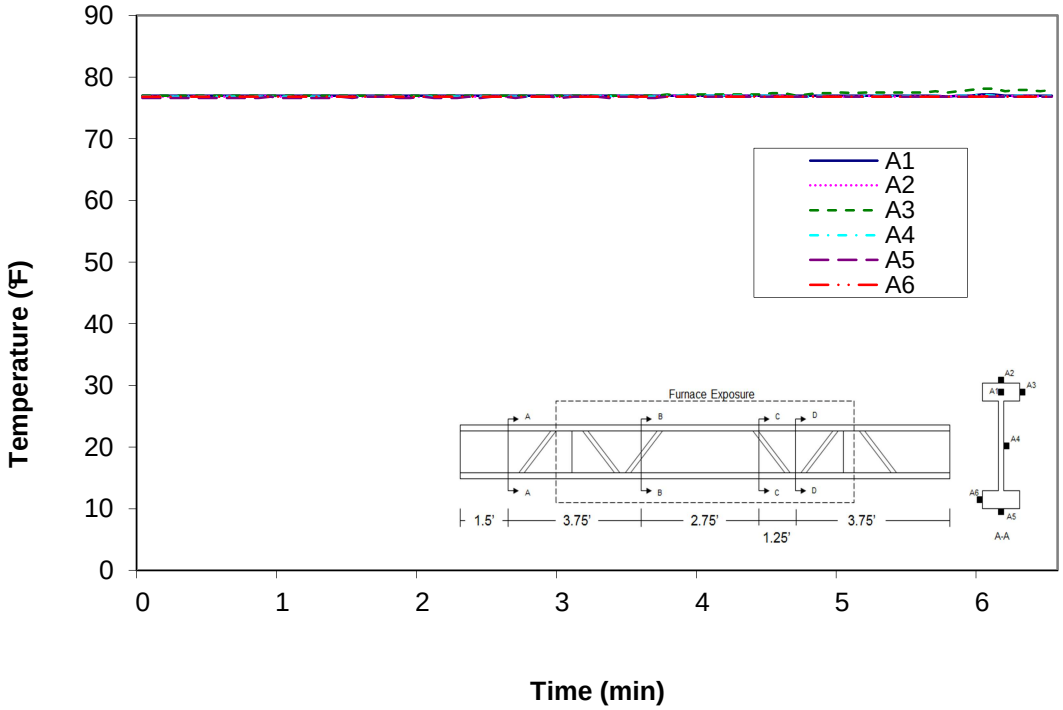

Figure A-123: Temperature distribution in wood joist H2 at cross-section A

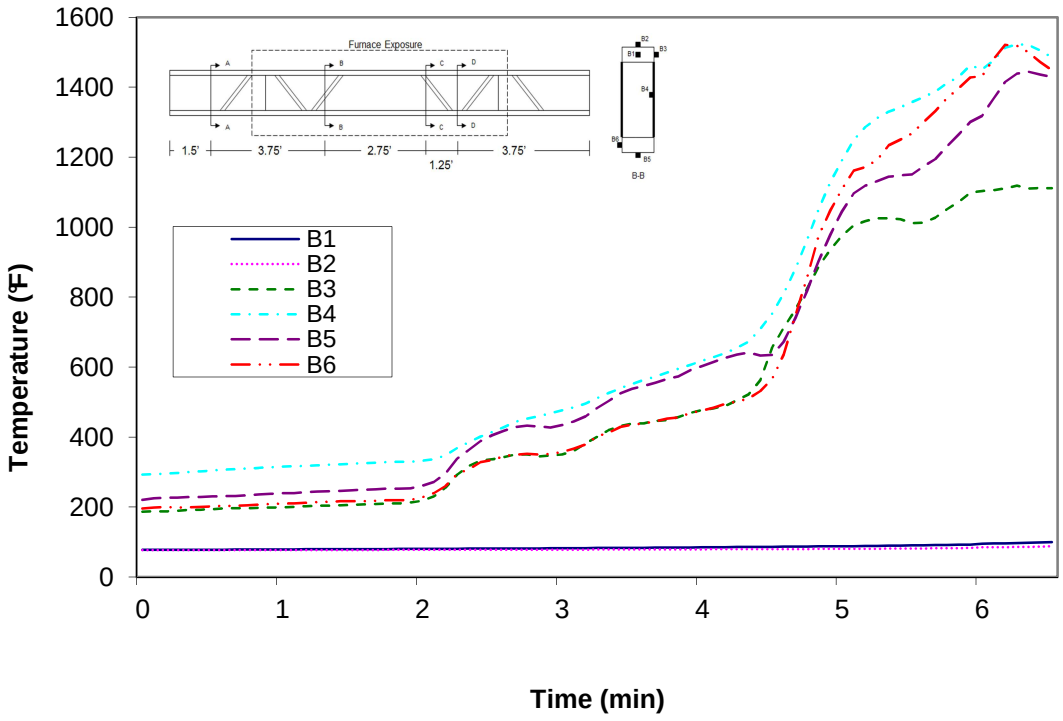

Figure A-124: Temperature distribution in wood joist H2 at cross-section B

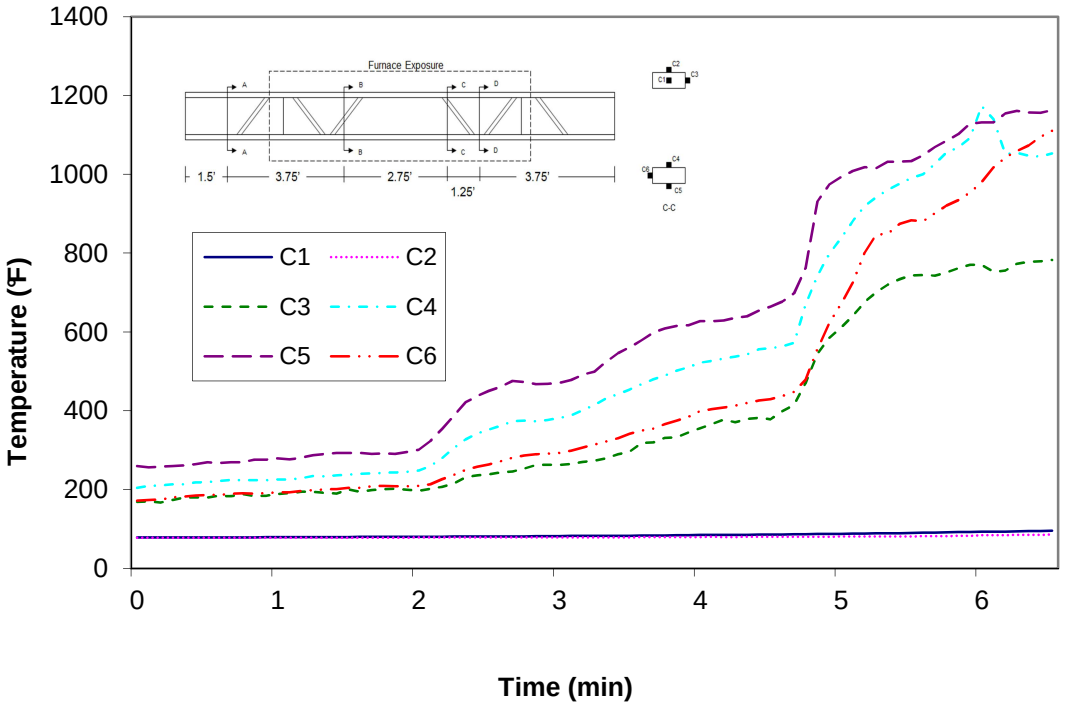

Figure A-125: Temperature distribution in wood joist H2 at cross-section C

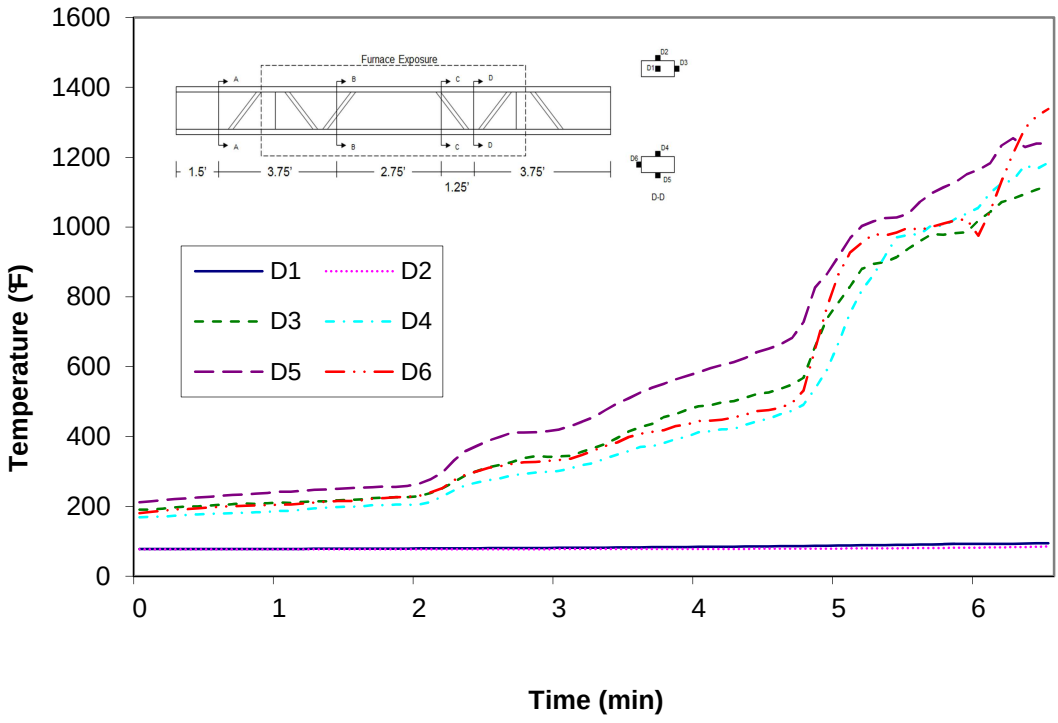

Figure A-126: Temperature distribution in wood joist H2 at cross-section D

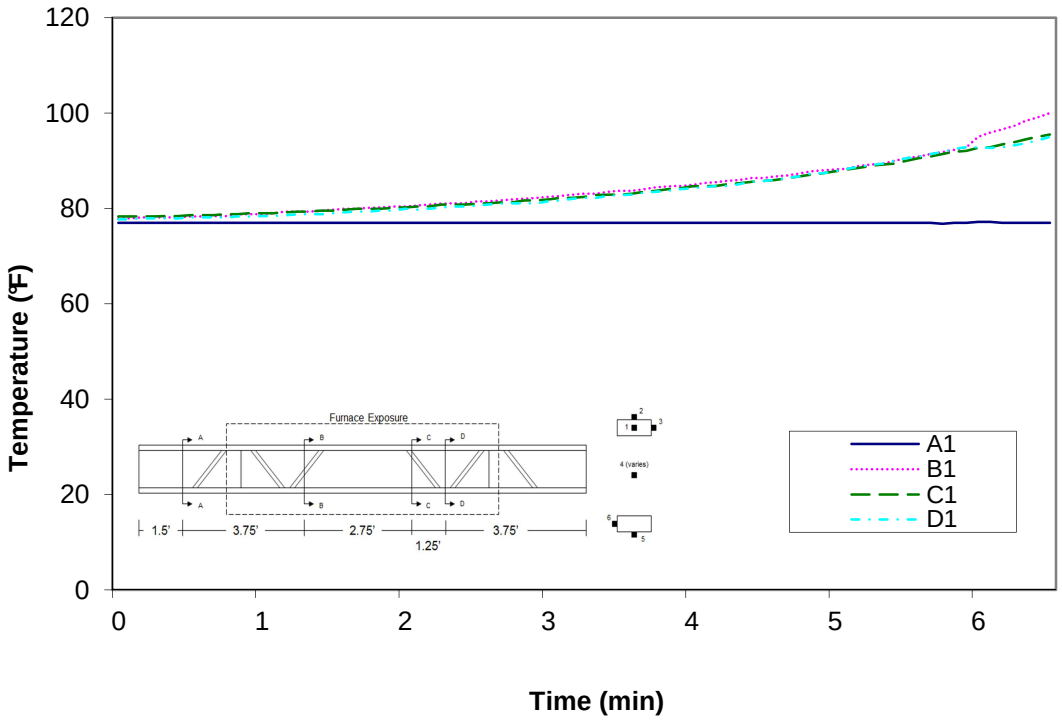

Figure A-127: Temperature distribution in wood joist H2 at thermocouple location 1

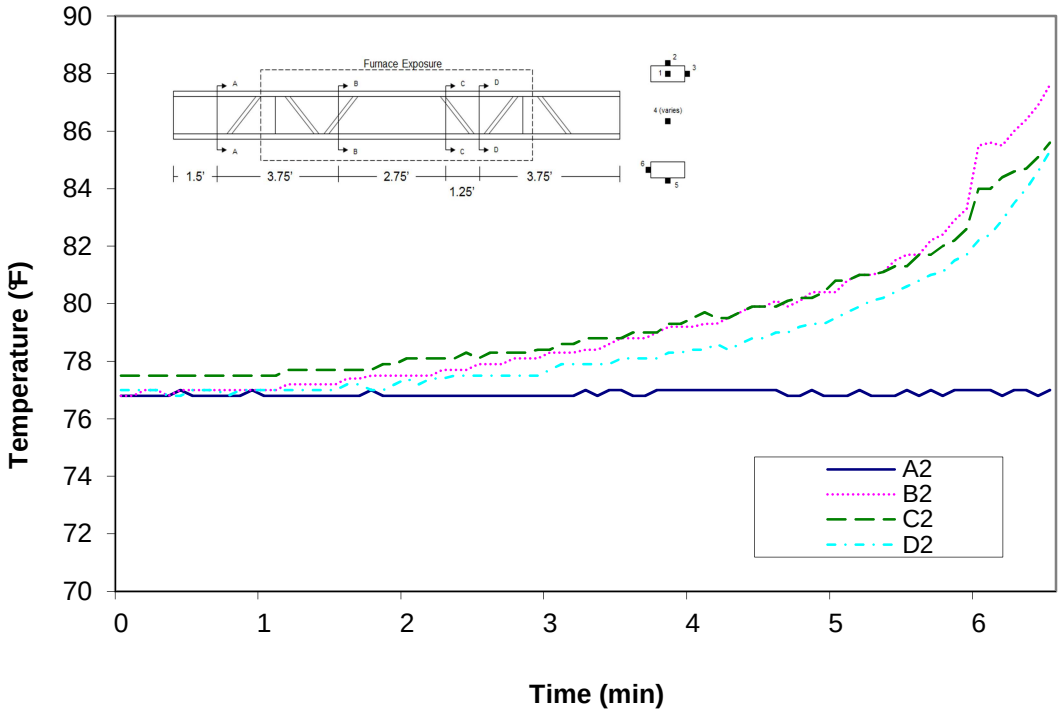

Figure A-128: Temperature distribution in wood joist H2 at thermocouple location 2

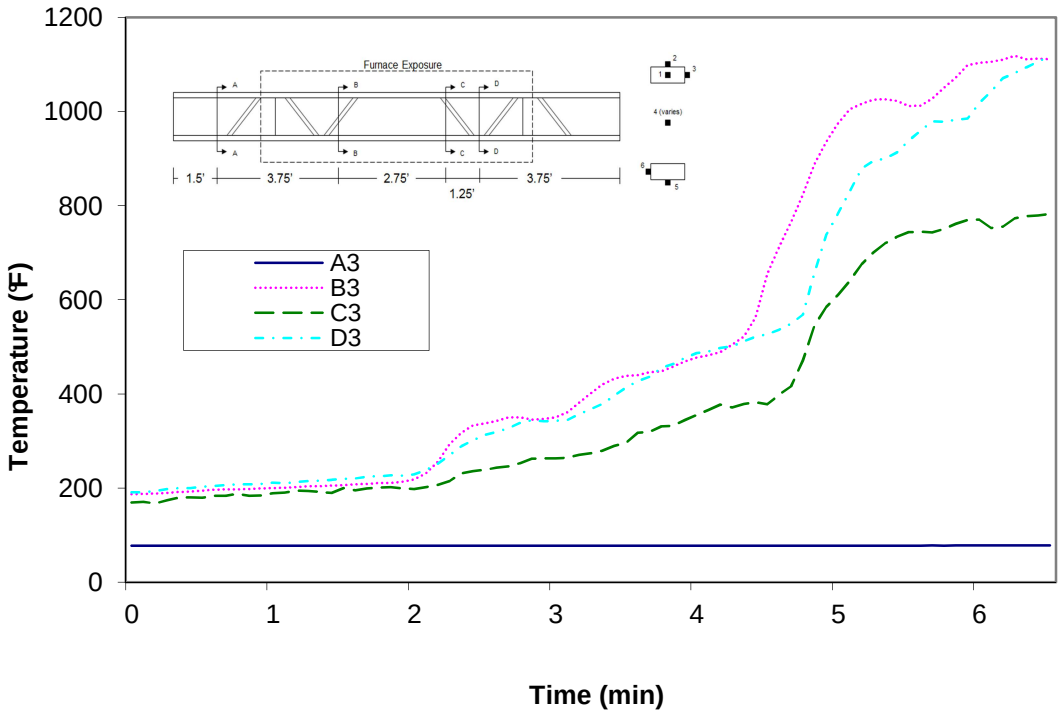

Figure A-129: Temperature distribution in wood joist H2 at thermocouple location 3

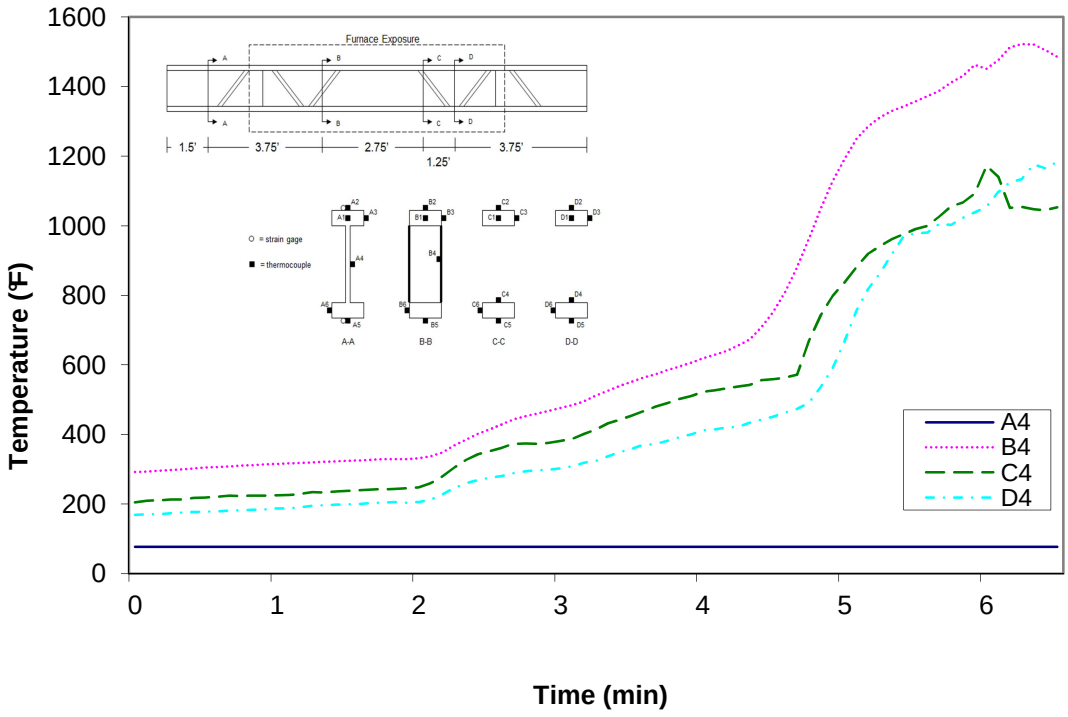

Figure A-130: Temperature distribution in wood joist H2 at thermocouple location 4

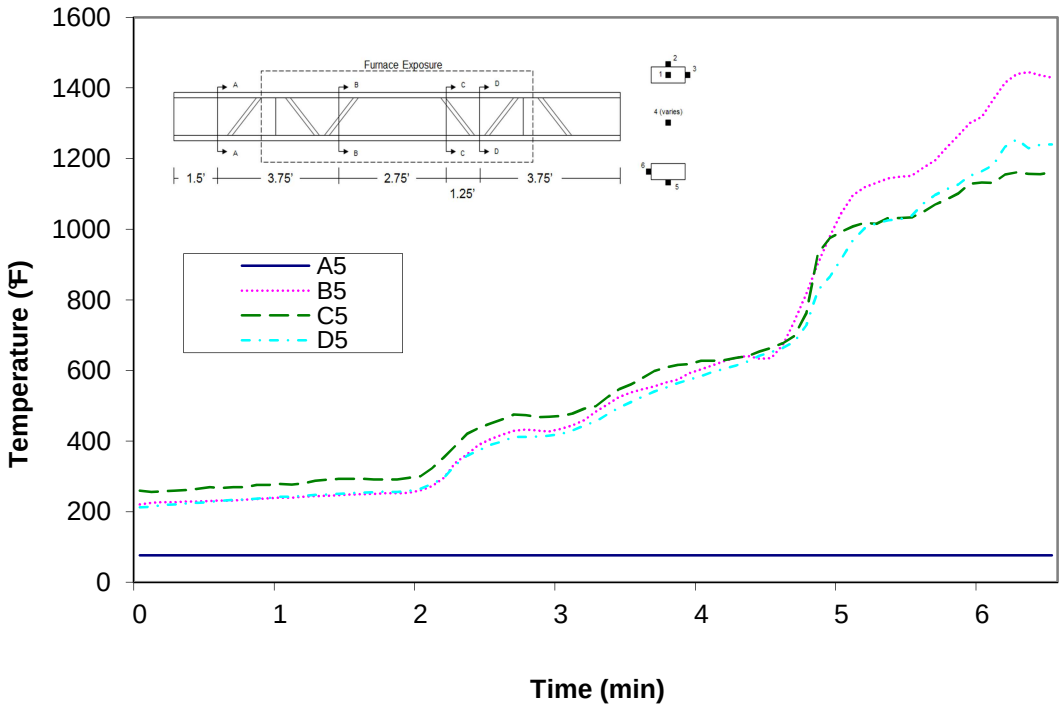

Figure A-131: Temperature distribution in wood joist H2 at thermocouple location 5

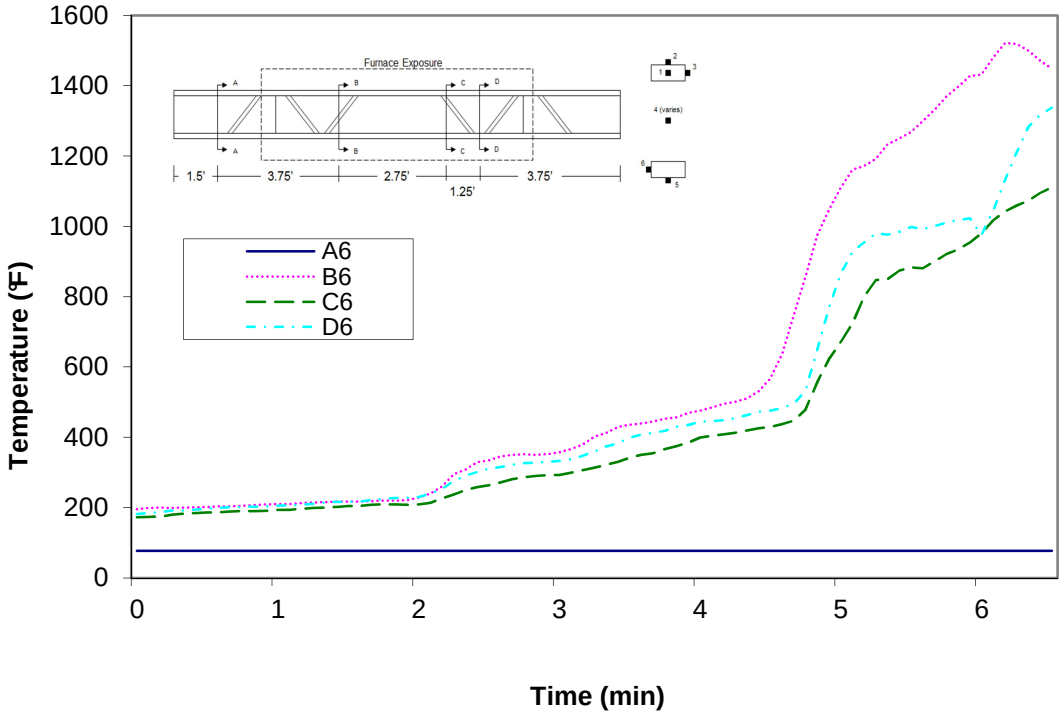

Figure A-132: Temperature distribution in wood joist H2 at thermocouple location 6

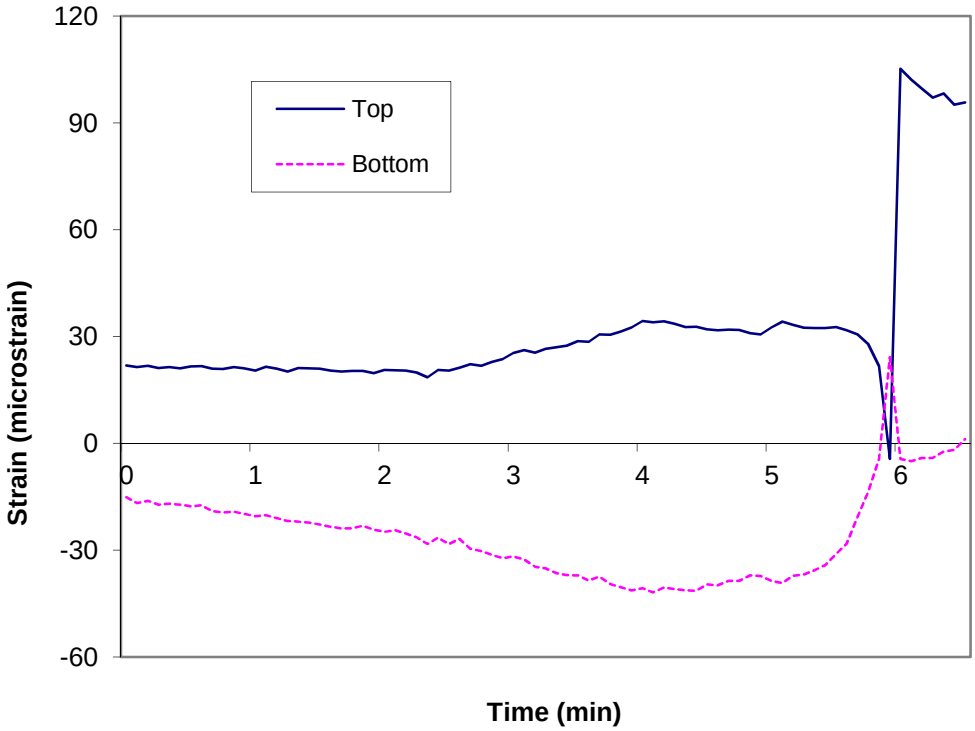

Figure A-133: Measured strains recorded during fire resistance tests of wood joist H2

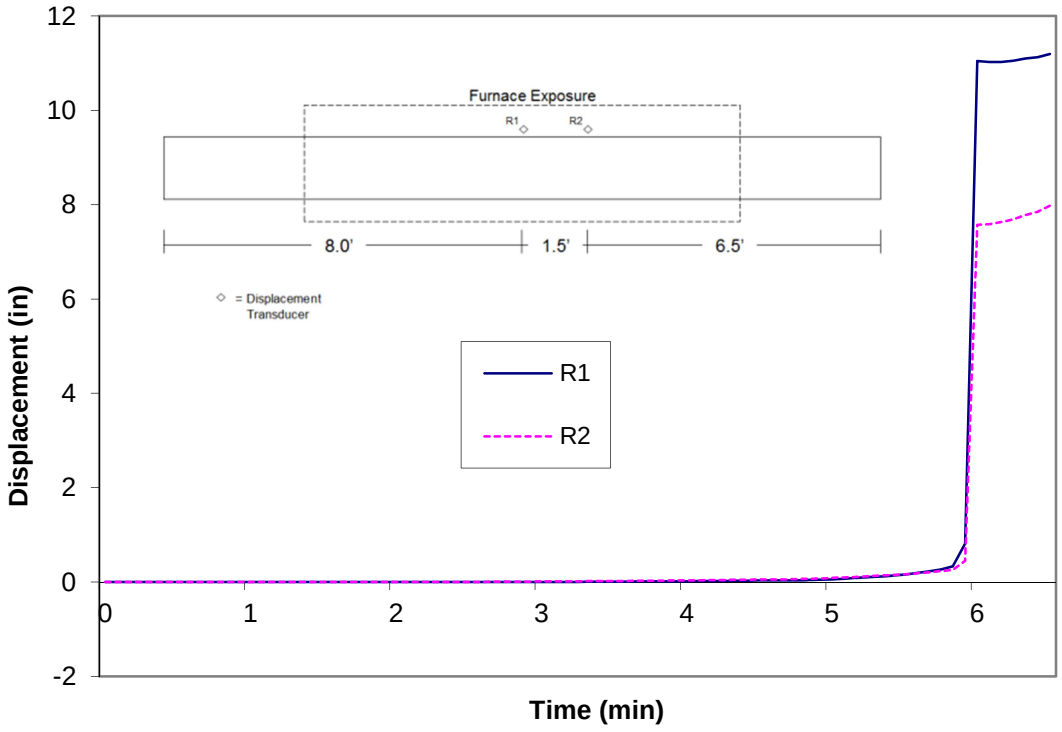

Figure A-134: Measured displacements recorded during fire resistance tests of wood joist H2

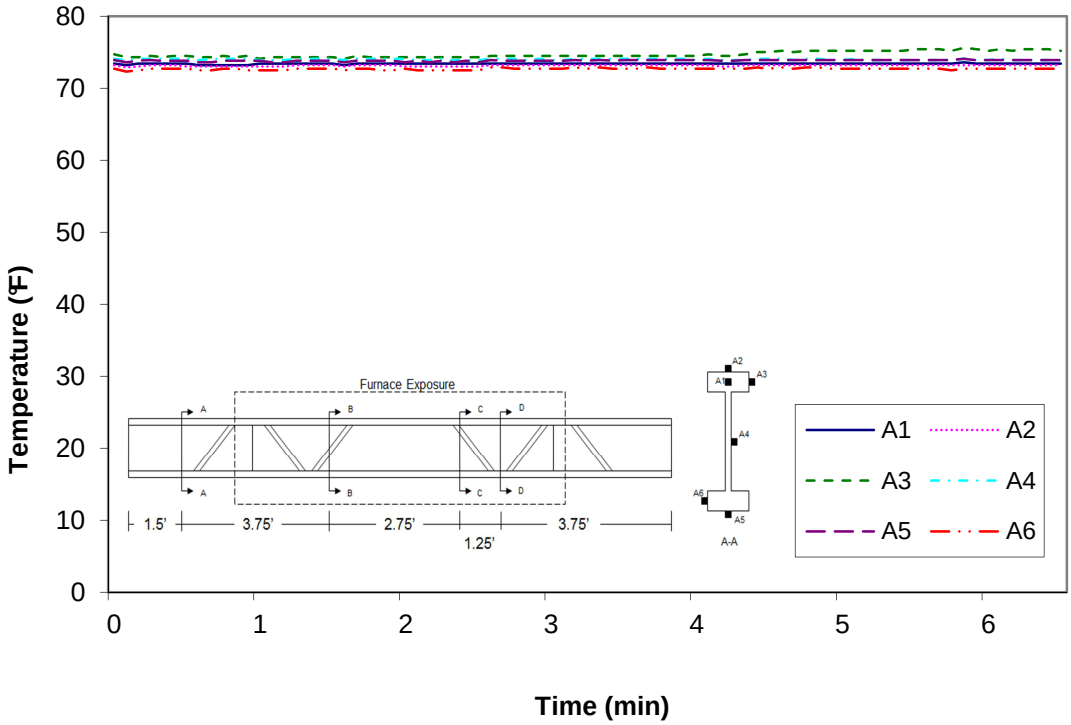

Figure A-135: Temperature distribution in wood joist H3 at cross-section A

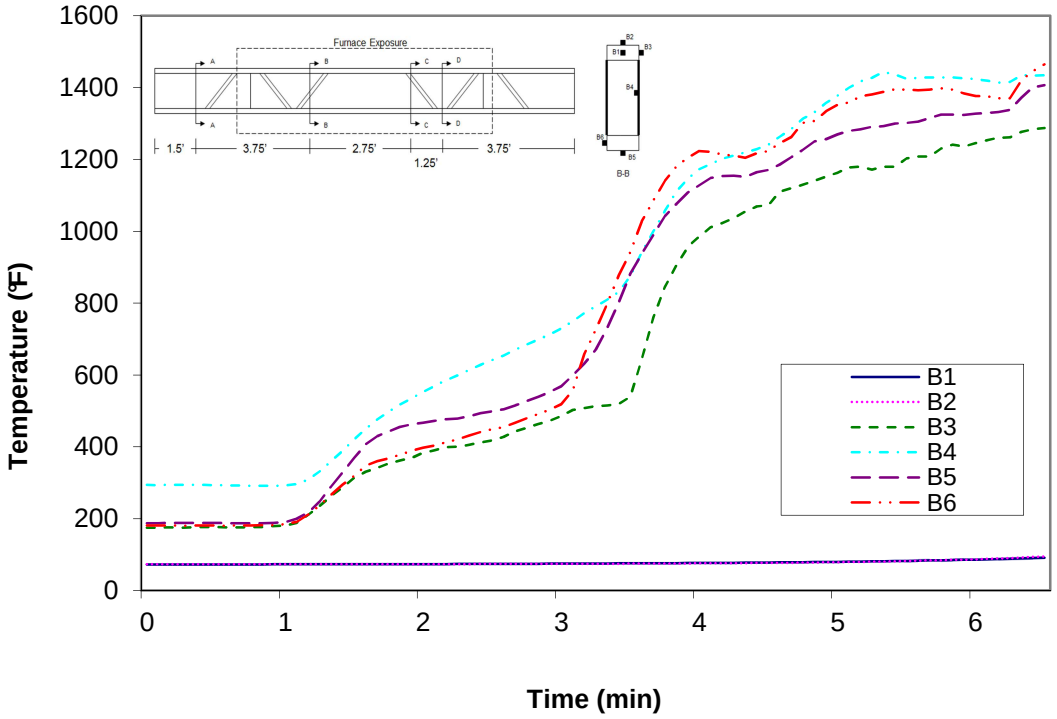

Figure A-136: Temperature distribution in wood joist H3 at cross-section B

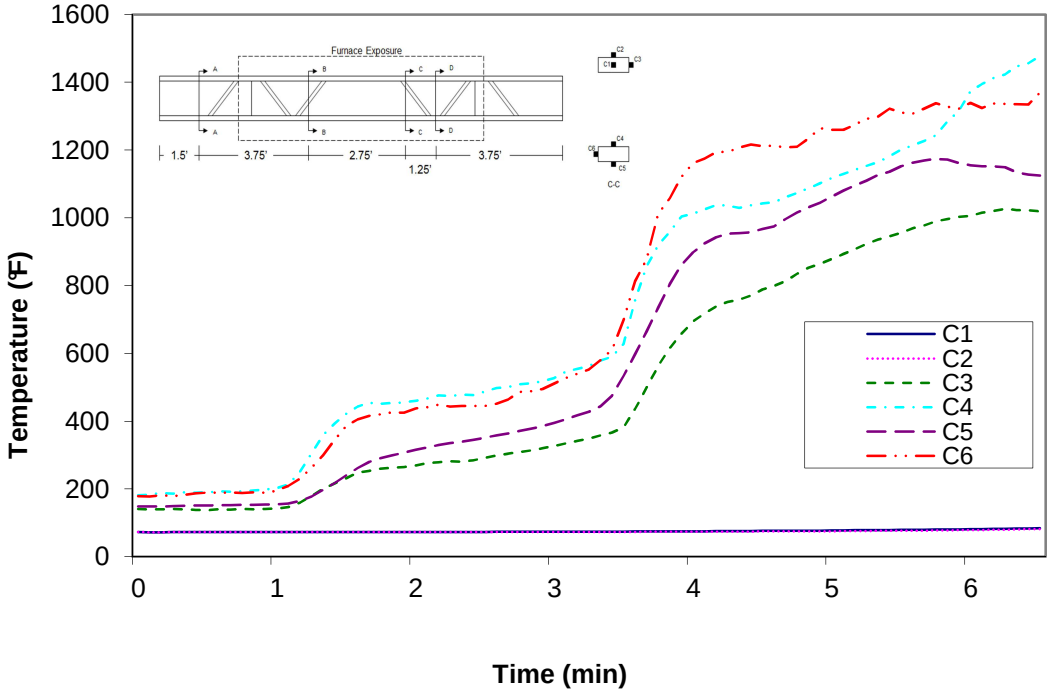

Figure A-137: Temperature distribution in wood joist H3 at cross-section C

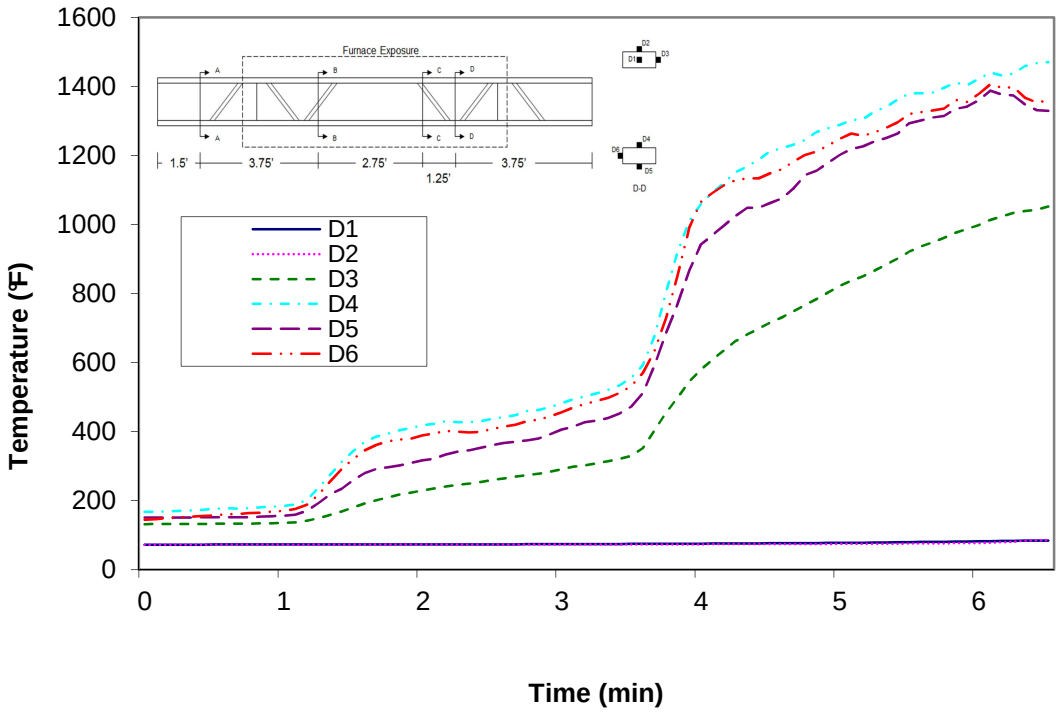

Figure A-138: Temperature distribution in wood joist H3 at cross-section D

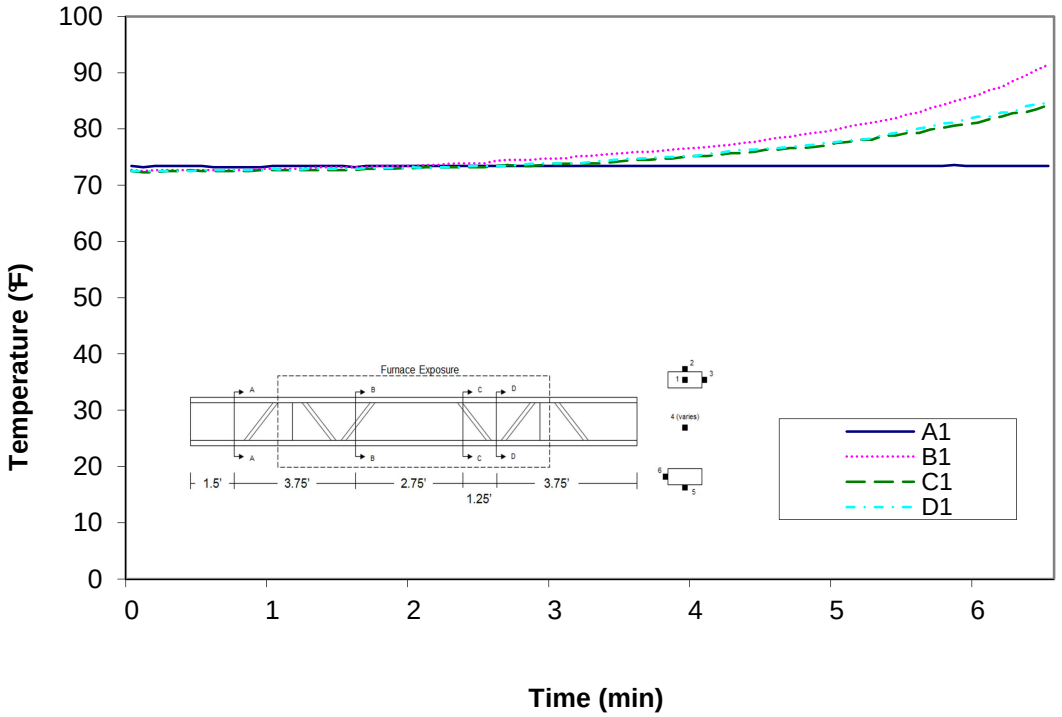

Figure A-139: Temperature distribution in wood joist H3 at thermocouple location 1

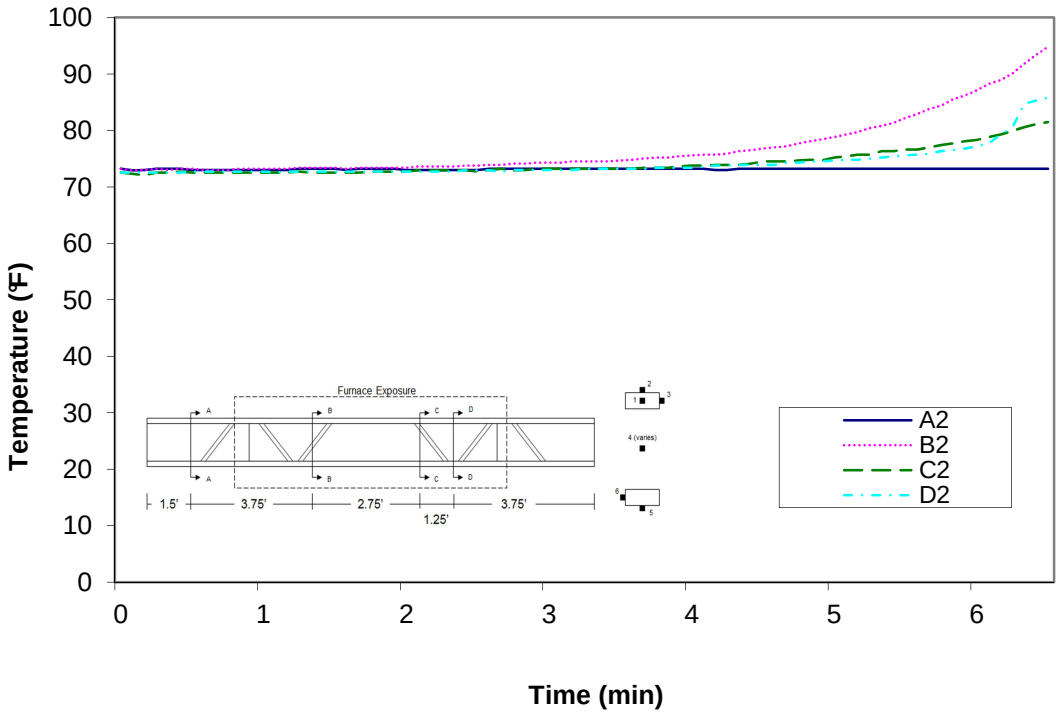

Figure A-140: Temperature distribution in wood joist H3 at thermocouple location 2

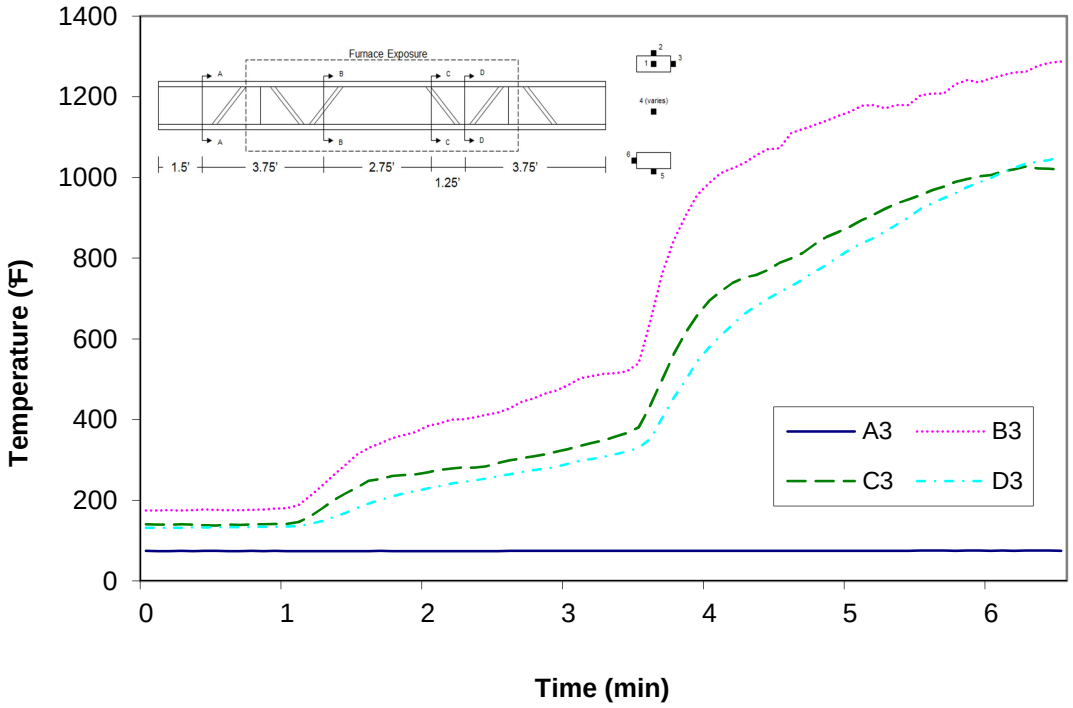

Figure A-141: Temperature distribution in wood joist H3 at thermocouple location 3

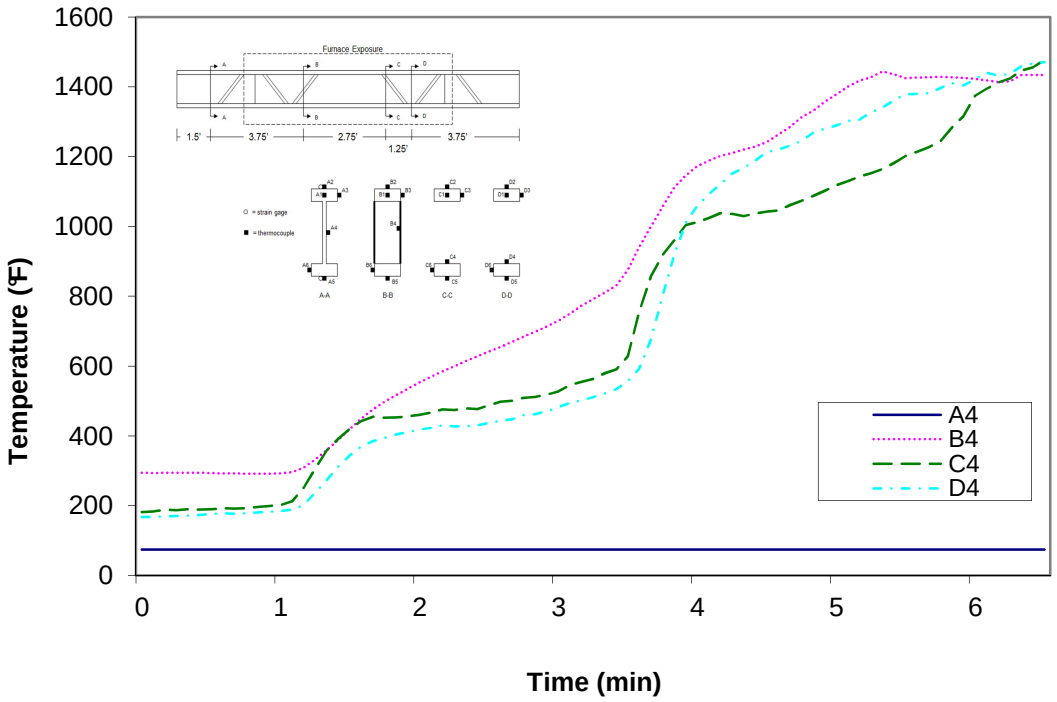

Figure A-142: Temperature distribution in wood joist H3 at thermocouple location 4

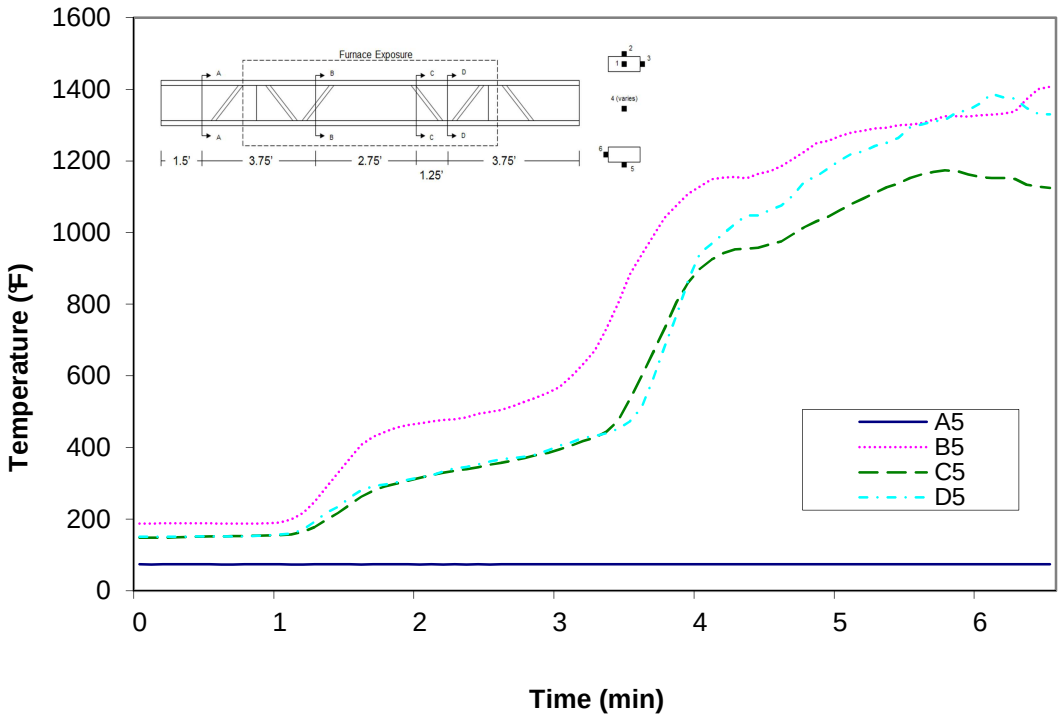

Figure A-143: Temperature distribution in wood joist H3 at thermocouple location 5

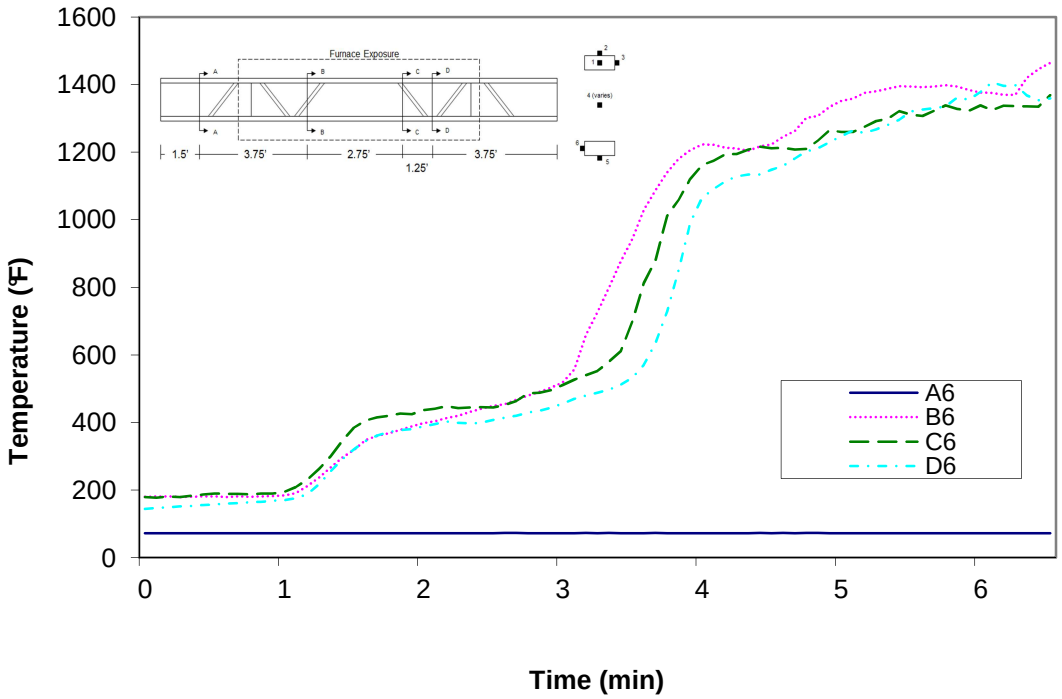

Figure A-144: Temperature distribution in wood joist H3 at thermocouple location 6

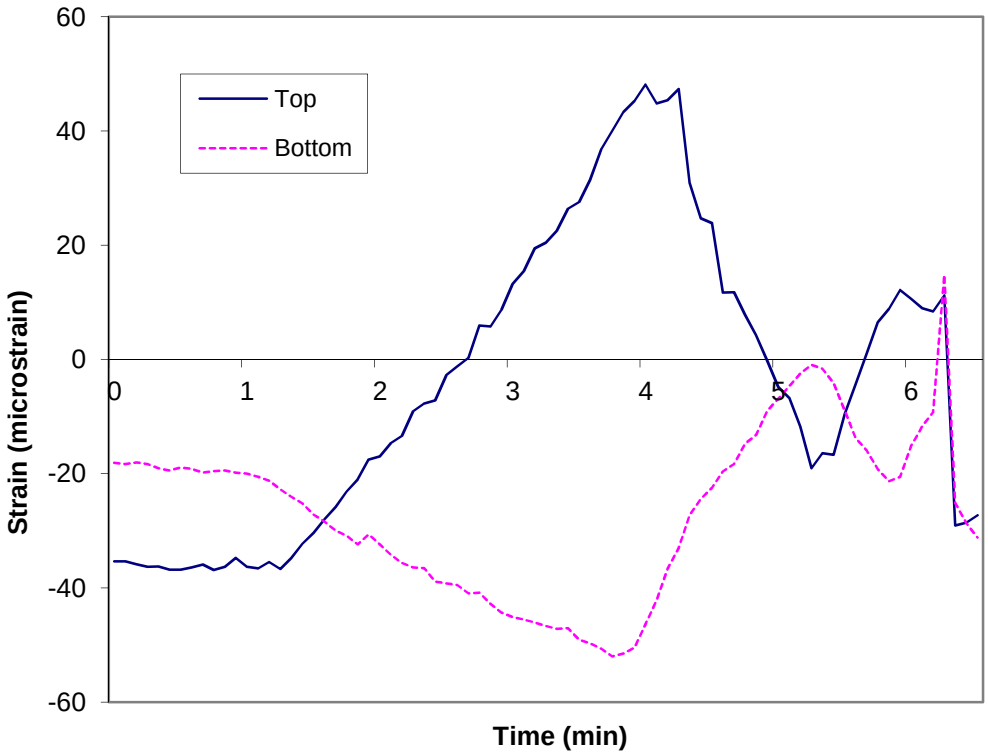

Figure A-145: Measured strains recorded during fire resistance tests of wood joist H3

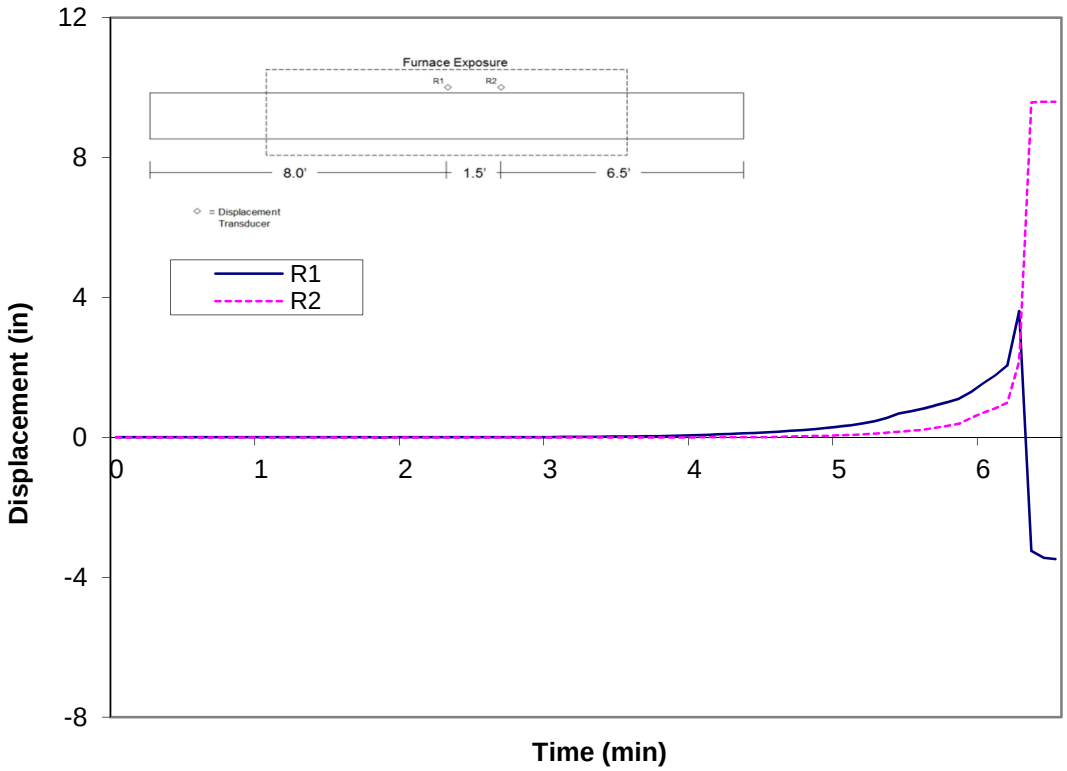

Figure A-146: Measured displacements recorded during fire resistance tests of wood joist H3

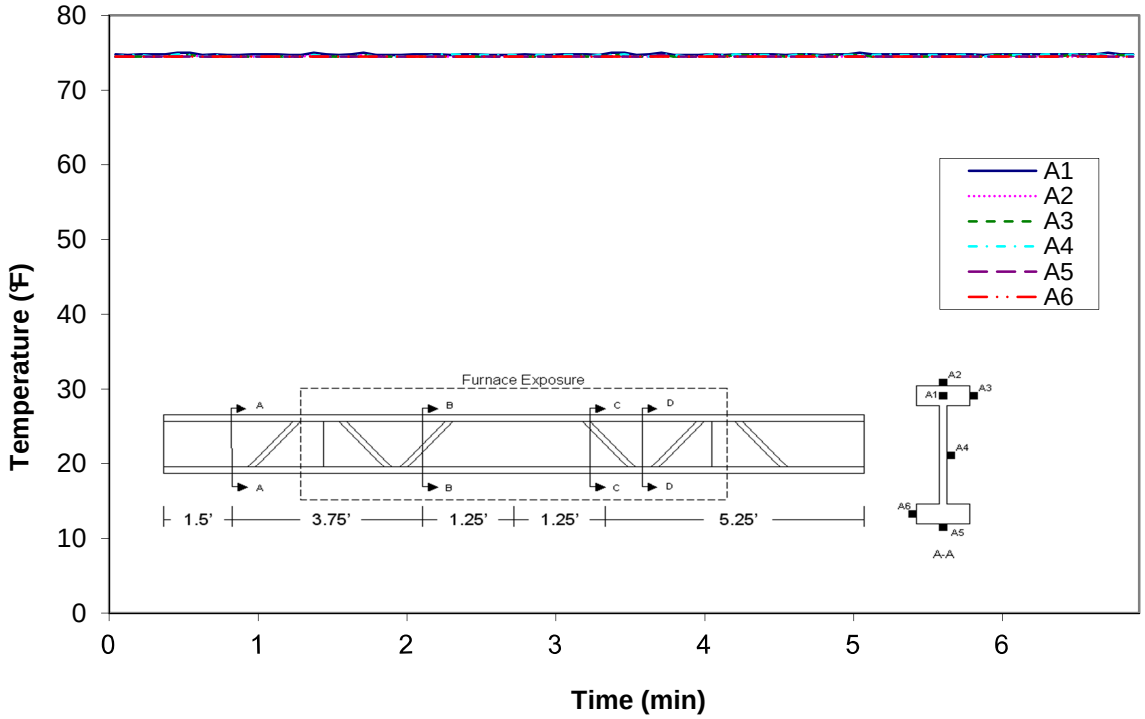

Figure A-147: Temperature distribution in wood joist H4 at cross-section A

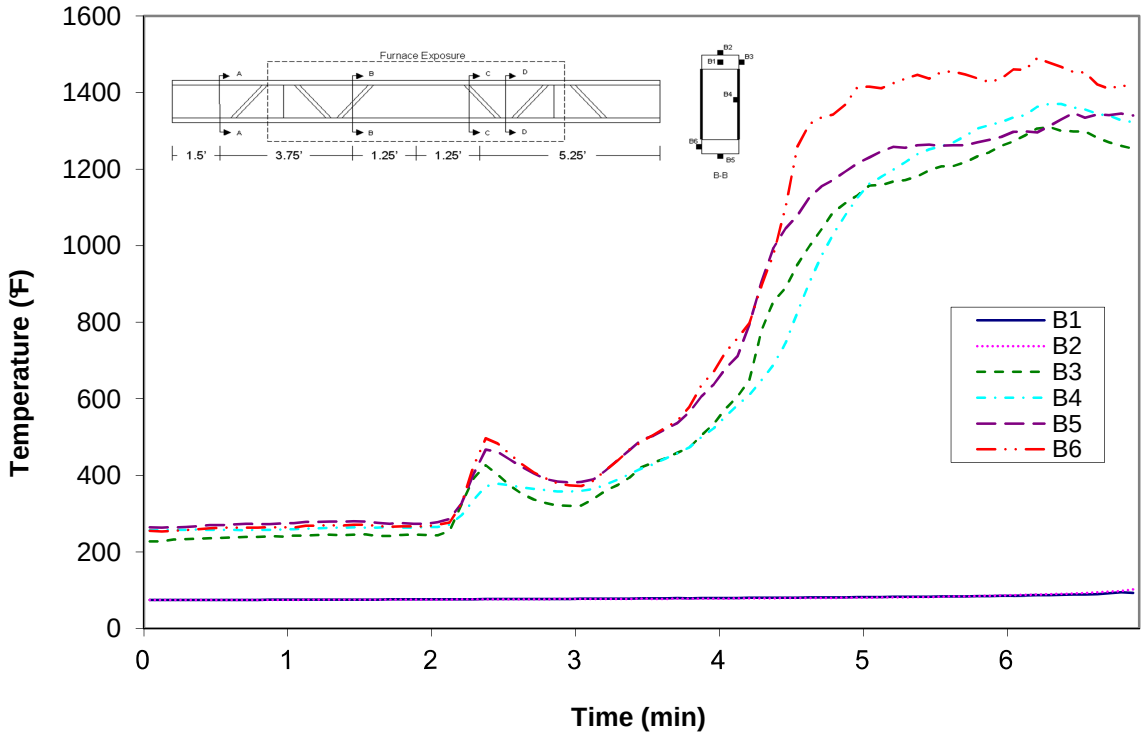

Figure A-148: Temperature distribution in wood joist H4 at cross-section B

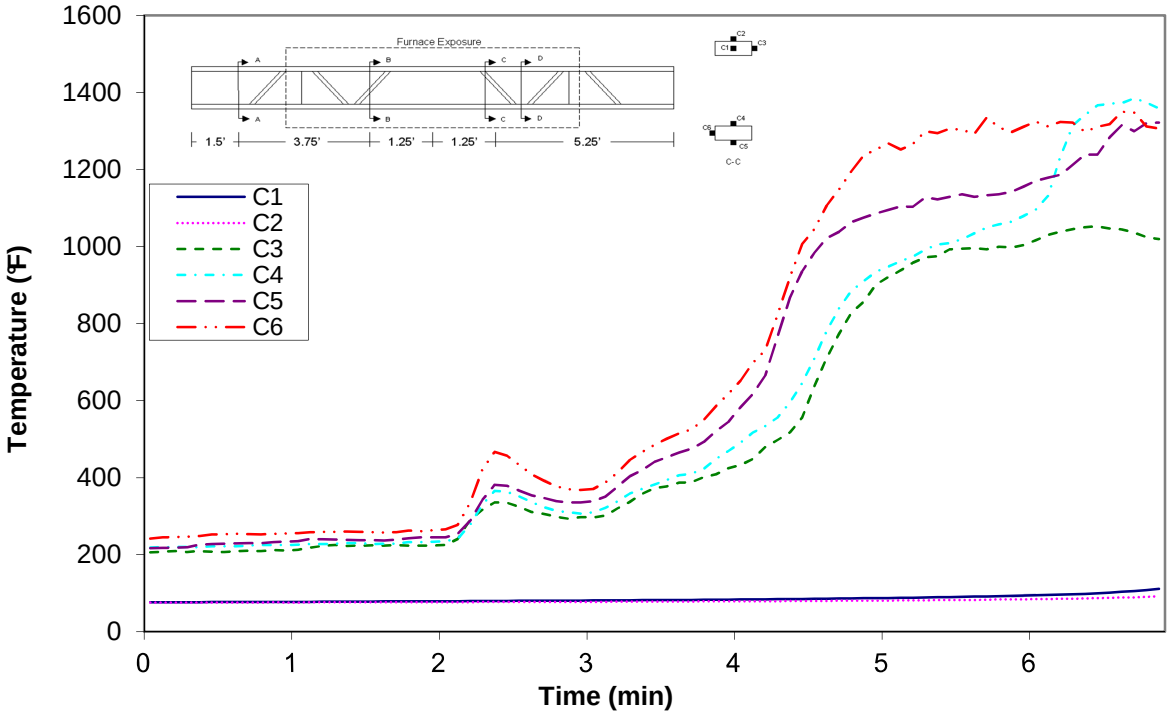

Figure A-149: Temperature distribution in wood joist H4 at cross-section C

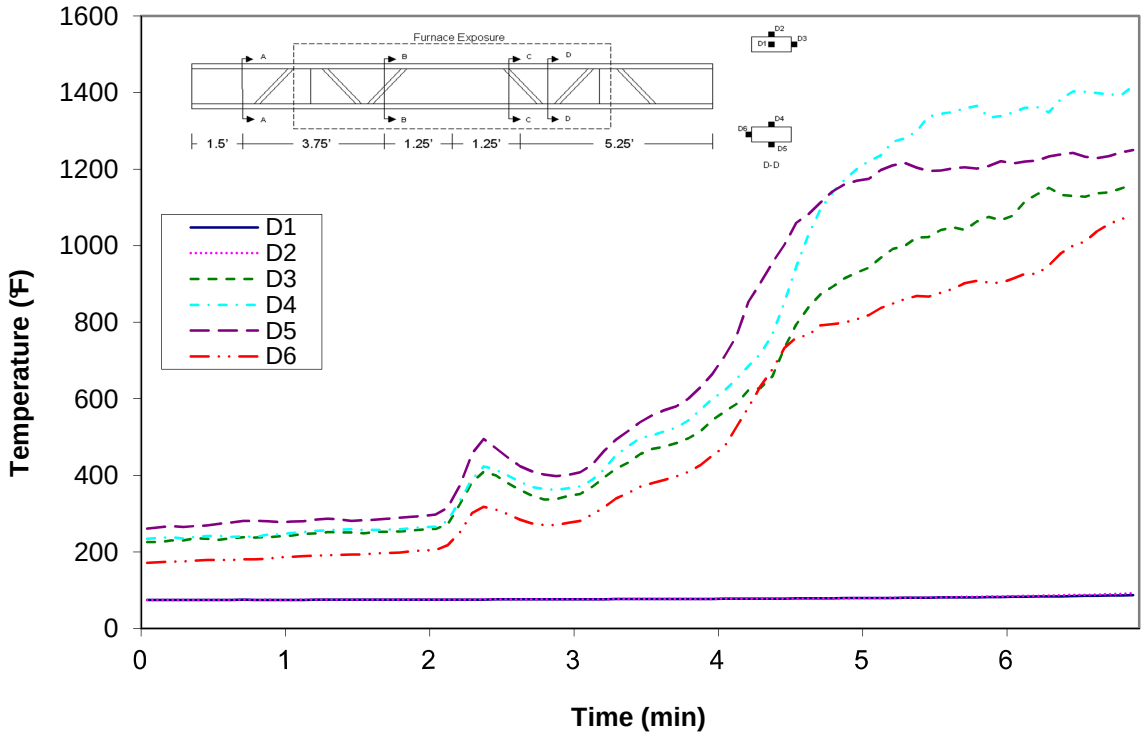

Figure A-150: Temperature distribution in wood joist H4 at cross-section D

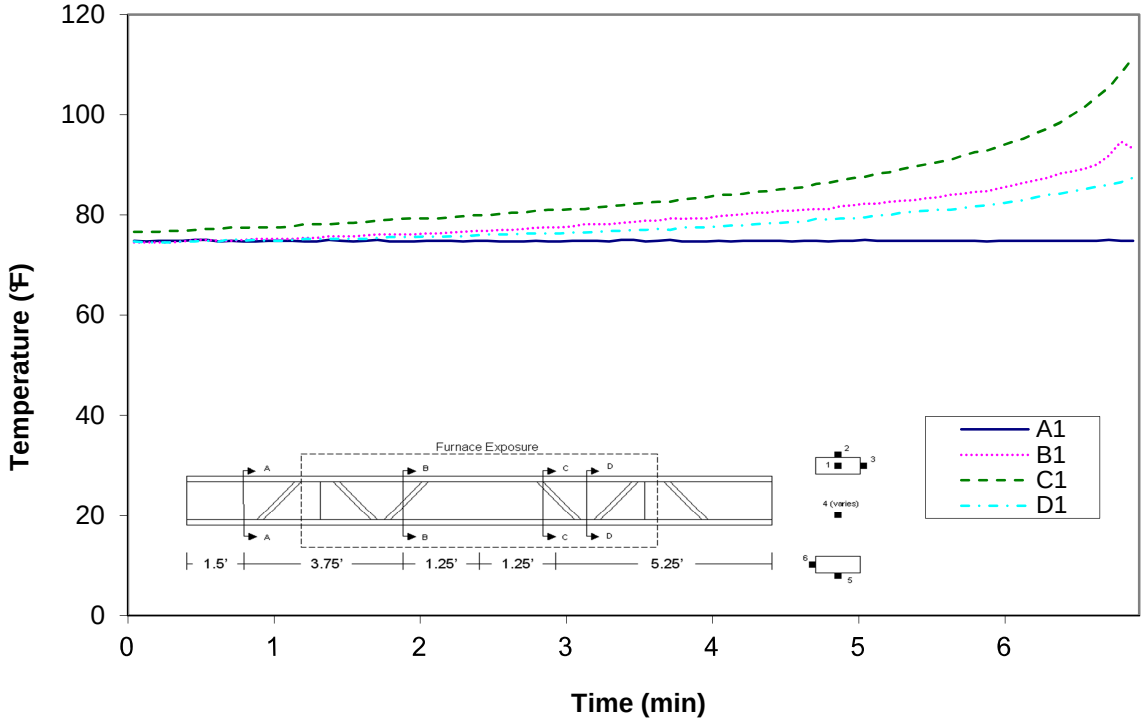

Figure A-151: Temperature distribution in wood joist H4 at thermocouple location 1

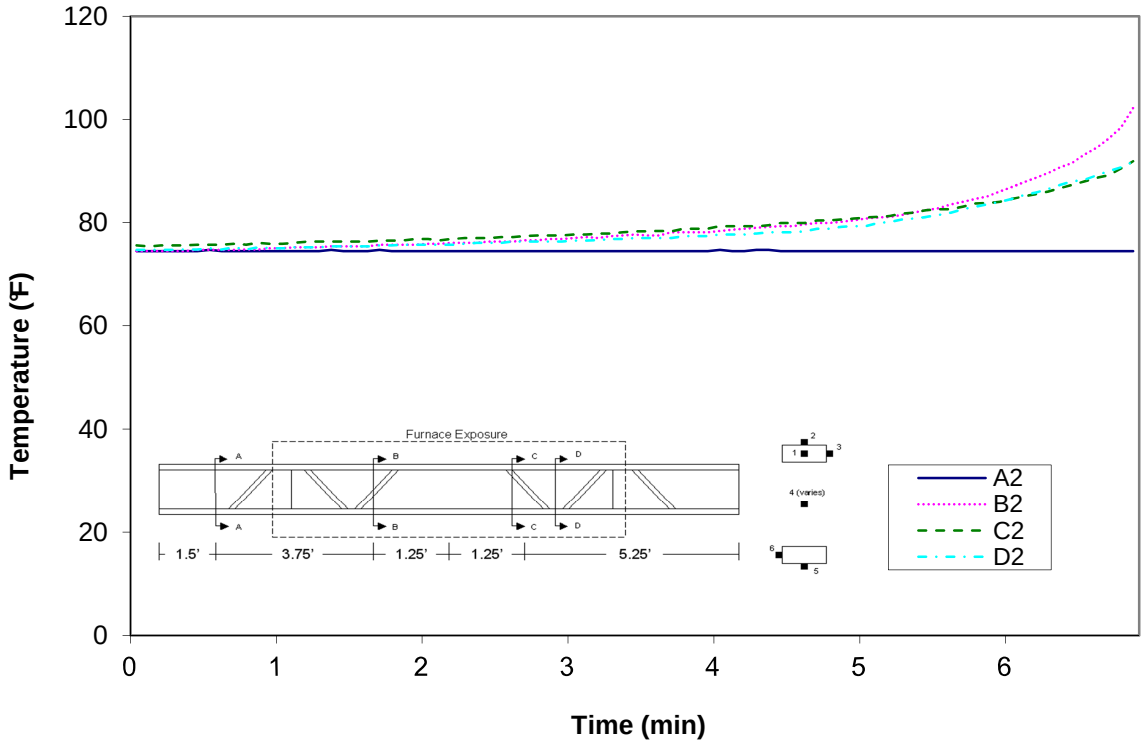

Figure A-152: Temperature distribution in wood joist H4 at thermocouple location 2

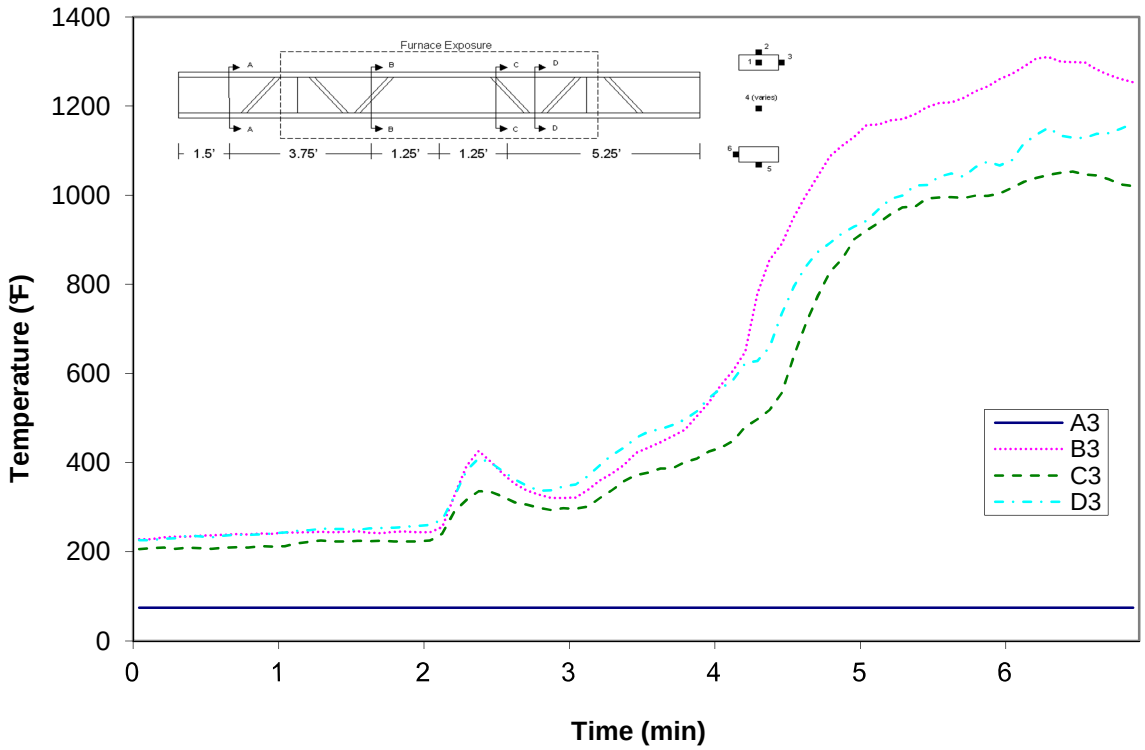

Figure A-153: Temperature distribution in wood joist H4 at thermocouple location 3

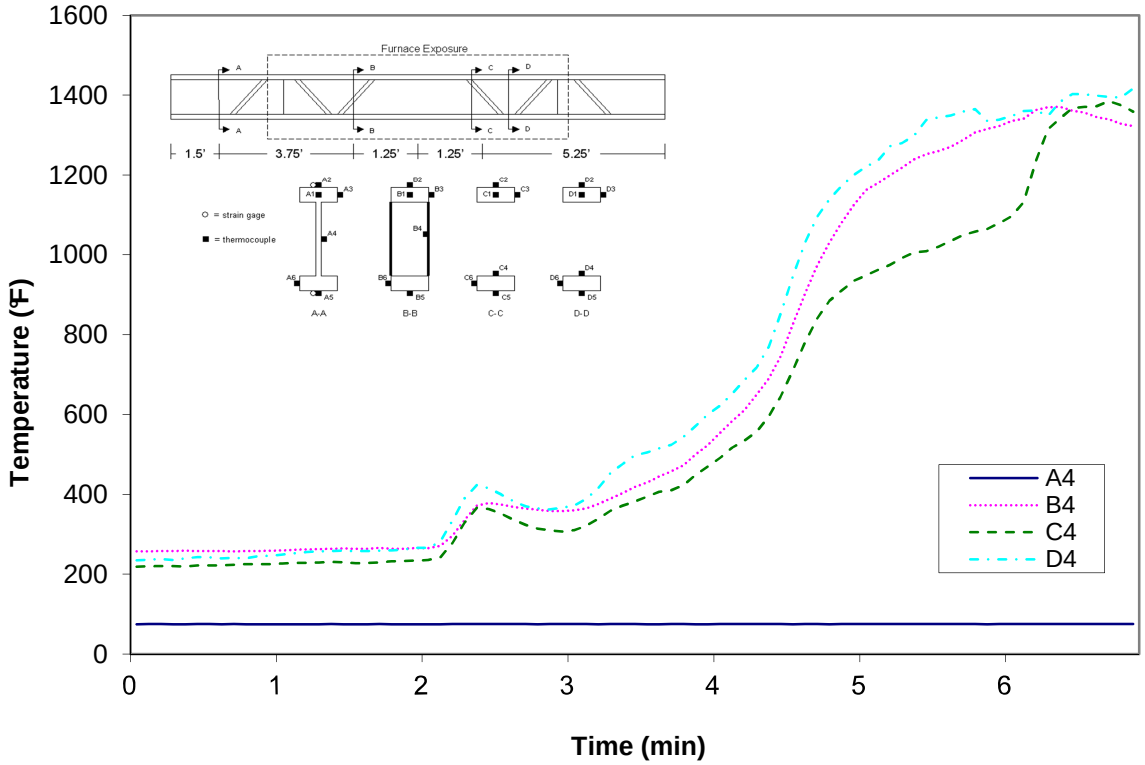

Figure A-154: Temperature distribution in wood joist H4 at thermocouple location 4

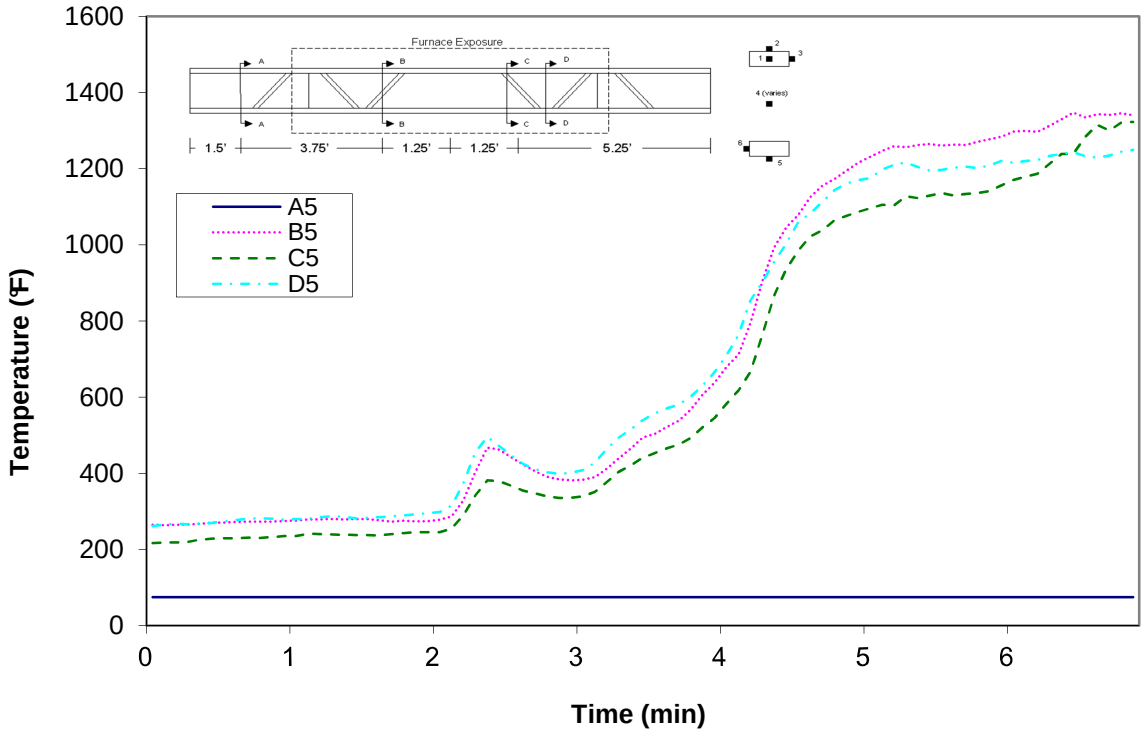

Figure A-155: Temperature distribution in wood joist H4 at thermocouple location 5

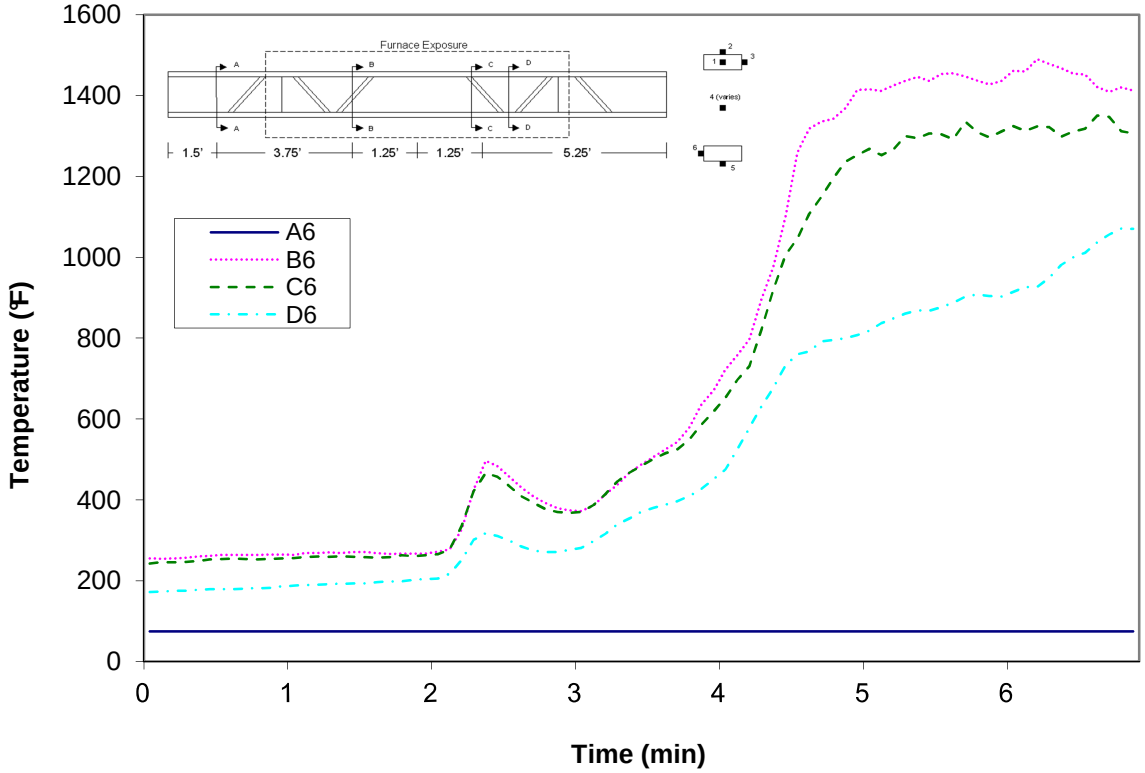

Figure A-156: Temperature distribution in wood joist H4 at thermocouple location 6

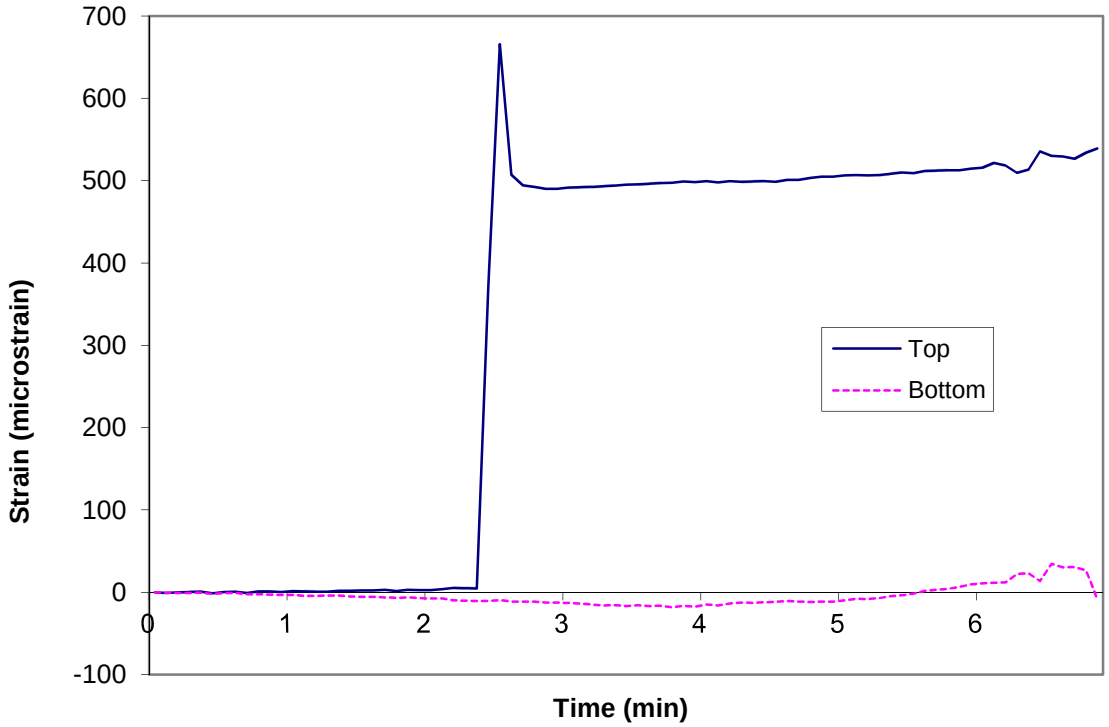

Figure A-157: Measured strains recorded during fire resistance tests of wood joist H4

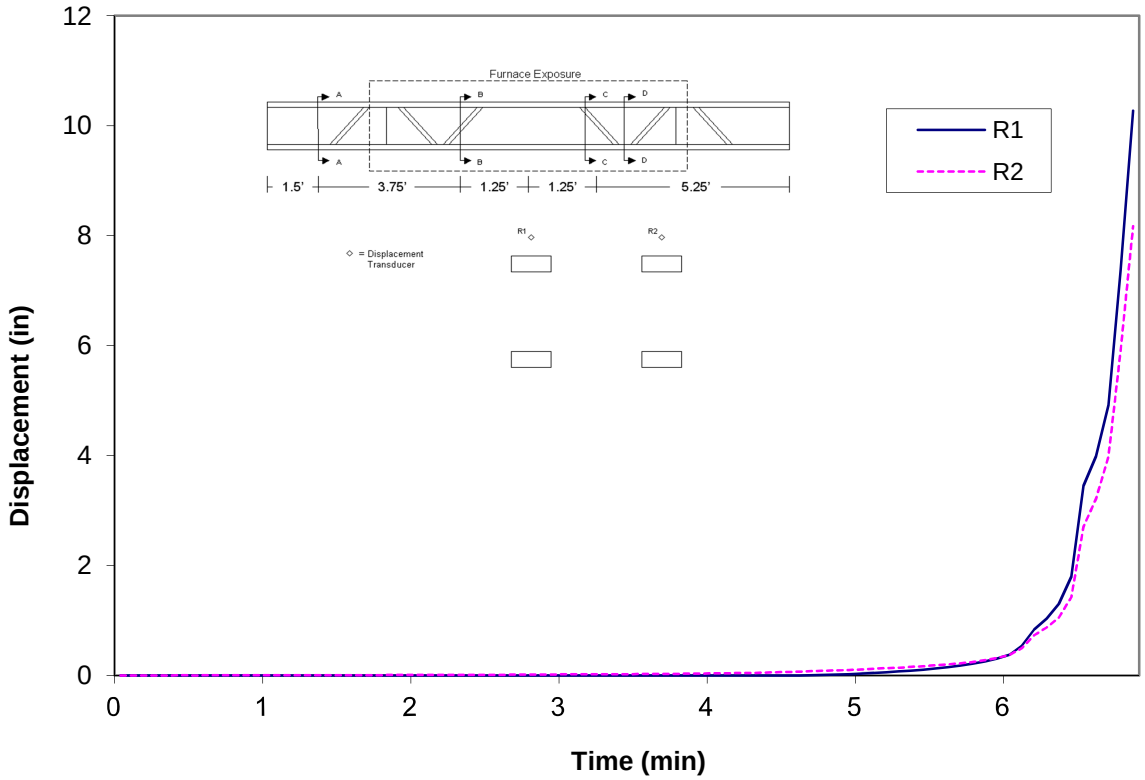

Figure A-158: Measured displacements recorded during fire resistance tests of wood

joist H4

APPENDIX B

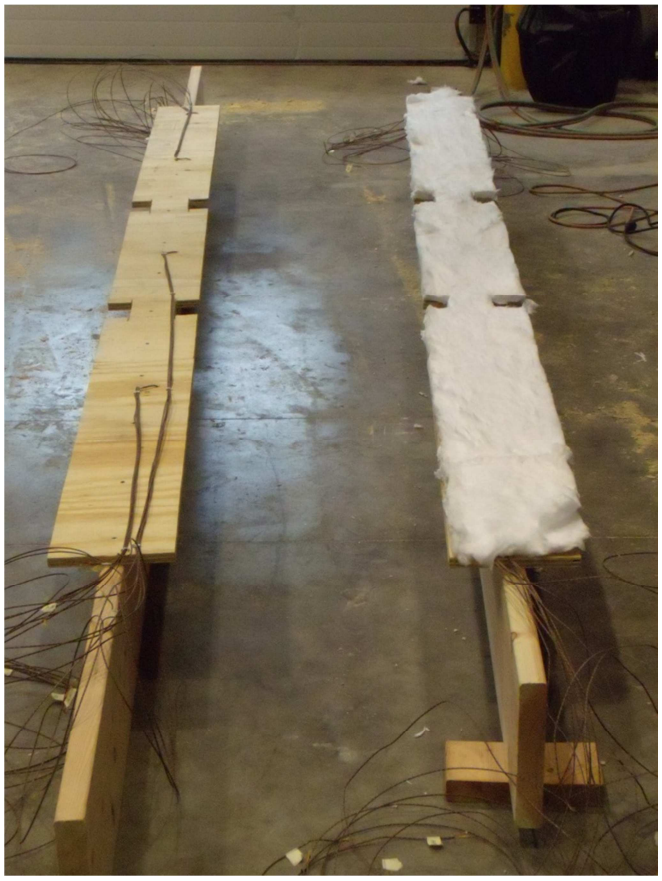

Figure B-1: Joists T3 (right) and T4 (left) with sheathing attached

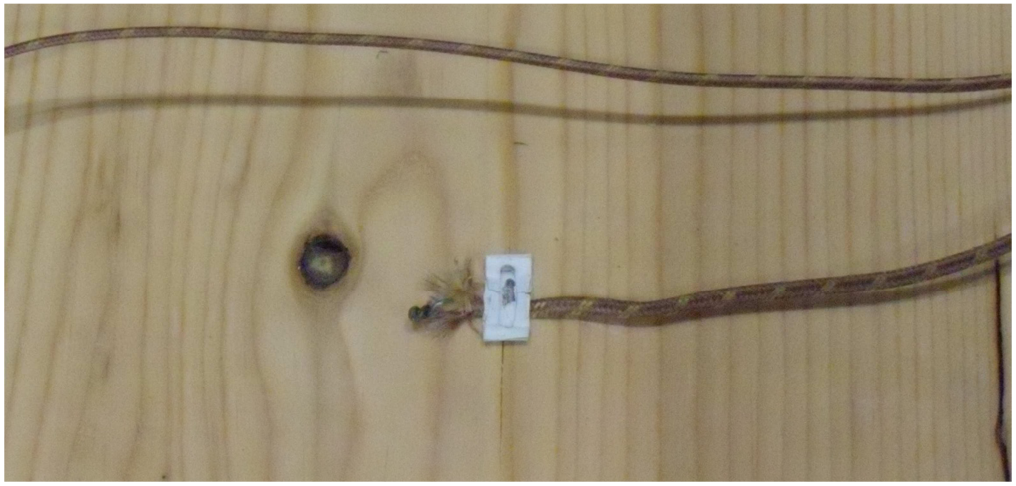

Figure B-2: Thermocouple mounted to side of traditional joist T2

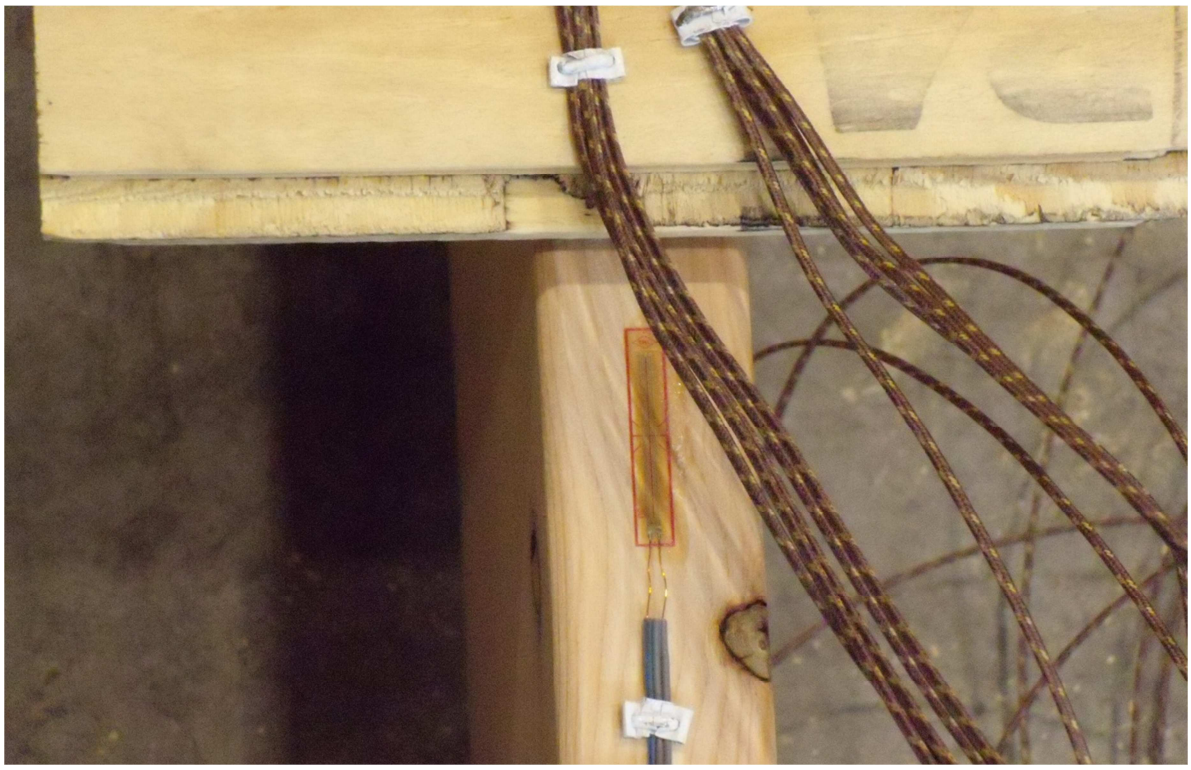

Figure B-3: Strain gauge mounted to top surface of joist T4

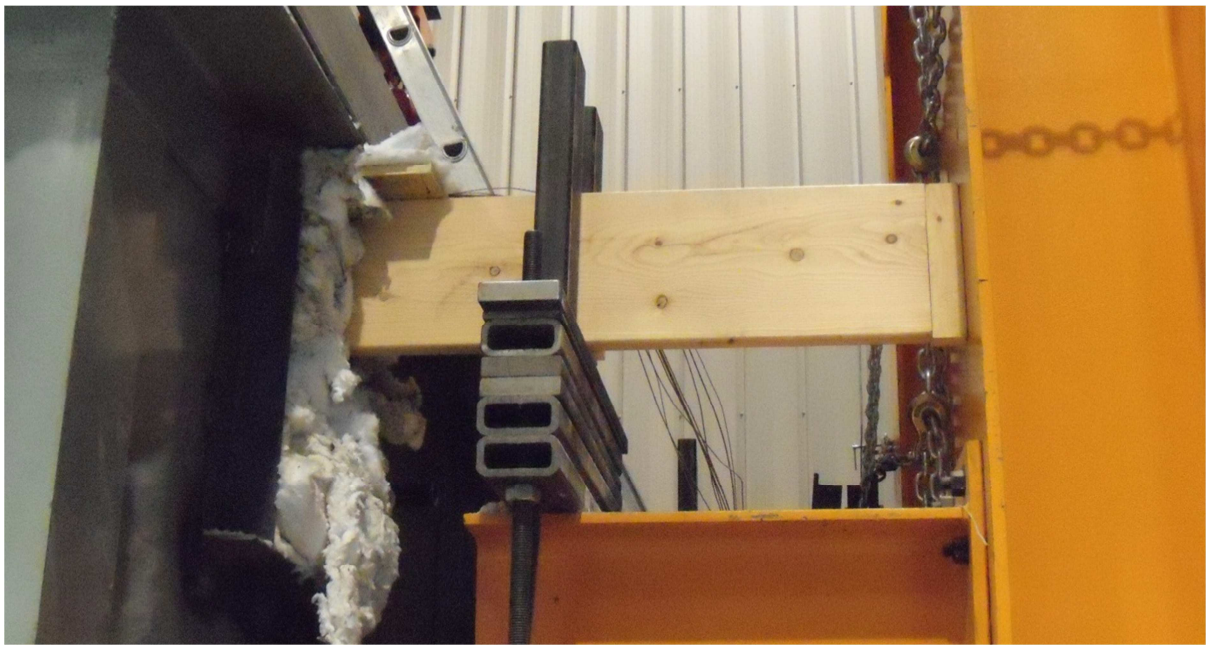

Figure B-4: Joist T4 axially restrained against test frame and laterally restrained at support

Figure B-5: Vertical displacement transducer connected to joist at midspan

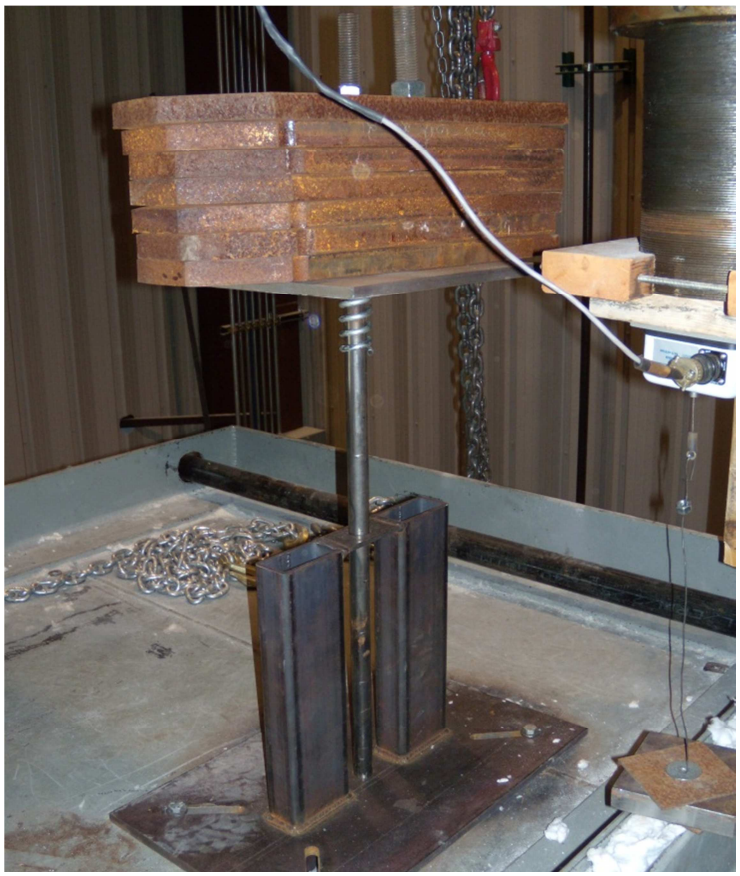

Figure B-6: Loading and lateral restraining system for joist E1

Figure B-7: Traditional joist (T4) immediately after failure

Figure B-8: Engineered joist (E1) after failure

Figure B-9: Castellated joist (C2) after failure

Figure B-10: Hybrid joist (H2) after failure

Figure B-11: Joist E3 with intumescent coating

Figure B-12: Joist E3 immediately after failure

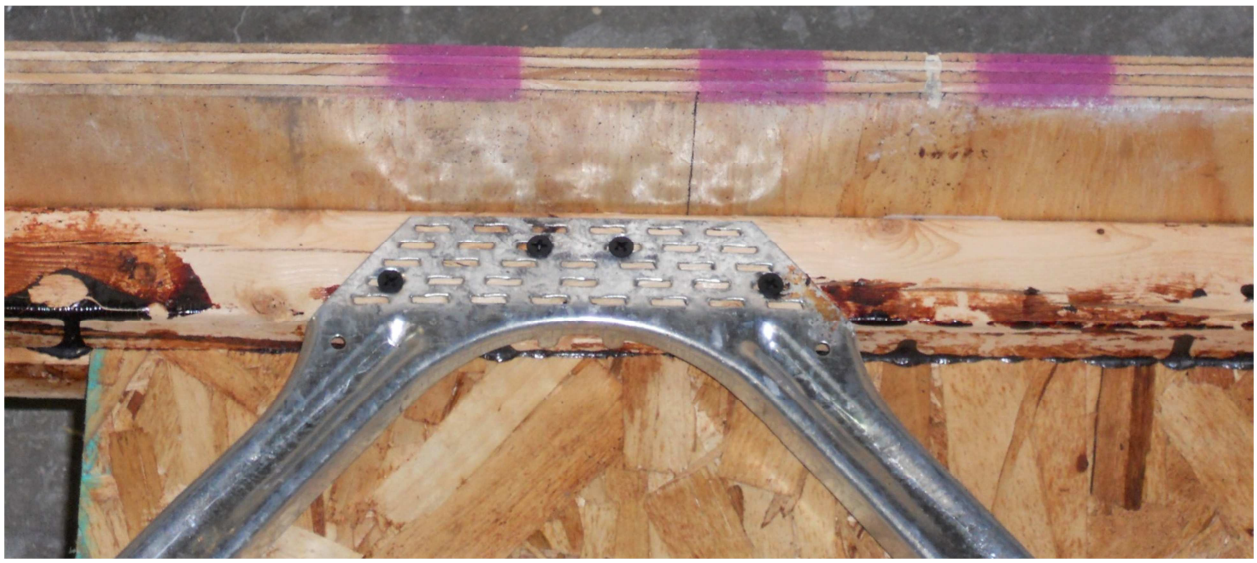

Figure B-13: Steel/wood connection in hybrid joist (H3) reinforced with screws

Figure B-14: Hybrid joist (H3) after failure

Figure B-15: Flame progression of joist E1 at time 04:00 (ignition of bottom cord)

Figure B-16: Flame progression of joist E1 at time 04:14 (embers form on bottom cord at midspan)

Figure B-17: Flame progression of joist E1 at time 04:16 (flame appears at the location of embers)

Figure B-18: Flame progression of joist E1 at time 04:29 (embers form on top cord)

Figure B-19: Flame progression of joist E1 at time 04:33 (flame appears at the location of embers)

Figure B-20: Flame progression of joist E1 at time 04:48 (joist engulfed in flame)

APPENDIX C

Capacity of Traditional Joists Using Allowable Stress Design (ASD)

The traditional 2x10 lumber used in the fire tests is of Douglas Fir-Larch wood species, it is graded as No. 2 dimensional lumber, and that it was kiln dried assuring that the moisture content of the lumber is less than 19%.

The load carrying capacity of these beams is evaluated by applying National Design Specification for Wood Construction (NDS) and the NDS Supplement (NDS-S). The value of interest is the adjusted bending design stress defined by the following equation from Table 4.3.1 on page 27 of the NDS:

$$F_b^{'} = F_b C_D C_M C_t C_L C_F C_{fu} C_i C_r$$

Because the lumber's nominal dimensions are 2x10 it can be determined by Table 1B on page 14 of the NDS-S that the actual dimensions of the lumber are 1.5"x9.25". The section modulus is found as well:

$$b = 1.5"$$
$$d = 9.25"$$
$$S_{xx} = 21.39 in^3$$

Using the species and grade of the lumber, the following values can be determined from Table 4A on page 32 of the NDS-S:

$$F_b = 900\, psi$$
$$F_v = 180\, psi$$
$$E_{\min} = 580{,}000\, psi$$

From the Adjustment Factors for Table 4A on page 30 of the NDS-S the following factors were determined:

$$C_M = 1.0$$
$$C_F = 1.1$$
$$C_{fu} = 1.0$$
$$C_r = 1.0$$

By 4.3.8 on page 27 of the NDS:

$$C_i = 1.0$$

Assuming normal load duration, from Table 2.3.2 on page 9 of the NDS the following duration factor is determined:

$$C_D = 1.0$$

Another factor that must be considered is the temperature factor. This factor is 1.0 for members exposed to temperatures less than 100°F and is less than 1.0 for members with prolonged exposure to temperatures between 100 and 150°F. Temperatures exceeding 150°F are not recognized. Therefore, because the beams will be exposed to temperatures less than 100°F until testing and there are no design considerations for over 150°F, this factor is assumed to be 1.0:

$$C_t = 1.0$$

By 4.4.2 on page 29 of the NDS:

$$C_T = 1.0$$

By Table 4.3.1 on page 27 of the NDS:

$$E'_{\min} = E_{\min} C_M C_t C_i C_T = 580000(1.0)(1.0)(1.0)(1.0) = 580{,}000\,psi$$

This leaves only the beam stability factor, C_L. In order to determine this value, many other values must be found as defined by 3.3.3 on pages 13-15 of the NDS. (l_u is the longest span without lateral support.)

$$F_b^* = F_b C_D C_M C_t C_F C_i C_r = 900(1.0)(1.0)(1.0)(1.1)(1.0)(1.0) = 990\,psi$$

$$l_u = 4.5' = 54''$$

$$l_u / d = 54 / 9.25 = 5.8 < 7$$

$$\therefore l_e = 2.06 l_u = 2.06(54) = 111.24''$$

$$R_B = \sqrt{\frac{l_e d}{b^2}} = \sqrt{\frac{111.24(9.25)}{1.5^2}} = 21.385 < 50$$

$$F_{bE} = \frac{1.20 E'_{\min}}{R_B^2} = \frac{1.20(580000)}{(21.385)^2} = 1522\,psi$$

$$C_L = \frac{1 + (F_{bE}/F_b^*)}{1.9} - \sqrt{\left[\frac{1 + (F_{bE}/F_b^*)}{1.9}\right]^2 - \frac{F_{bE}/F_b^*}{0.95}}$$

$$C_L = \frac{1 + (1522/990)}{1.9} - \sqrt{\left[\frac{1 + (1522/990)}{1.9}\right]^2 - \frac{1522/990}{0.95}} = 0.93$$

Now the adjusted bending design stress can be calculated as:

$$F'_b = F_b C_D C_M C_t C_L C_F C_{fu} C_i C_r = 900(1.0)(1.0)(1.0)(0.93)(1.1)(1.0)(1.0)(1.0) = 920.7\,psi$$

By applying equation 3.3-1, the actual bending stress in the member is determined as:

$$f_b = \frac{M}{S_{xx}}$$

The section modulus is already determined. Setting the actual bending stress, f_b, equal to the adjusted bending design stress, $F_b^{'}$, will provide the maximum allowable bending moment that the beam can be subjected to:

$$f_b = \frac{M}{S_{xx}} \longrightarrow M = f_b S_{xx} = 920.7(21.39) = 19693.8lb - in = 1641.15lb - ft$$

By equating the maximum moment to the beam capacity, the following equation is obtained and can be used to determine the magnitude of one point load (P):

$$P = \frac{M}{4.5} = \frac{1641.15}{4.5} = 364.7lb$$

The above equation states that the maximum design load that the beams can sustain under normal conditions is 365 lb at each point. Because it is desired to load the beams to only 50% of the design load, each point load should be only about 180 lb. To load the beams to 70% of the design load, each point load should be about 250 lb.

Figure 1-C below illustrates the elevation and cross-section of the test beam.

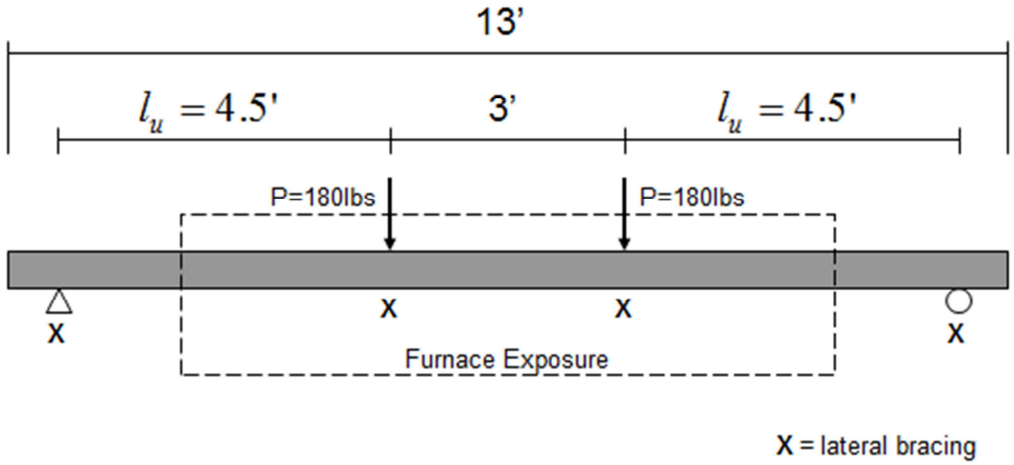

(a) Elevation

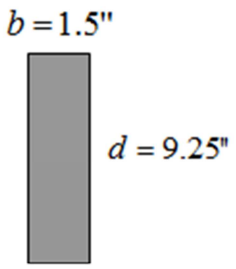

(b) Cross-section

Figure C-1: Layout of typical wood joist

Capacity of Engineered I-joist

From the user specifications, for a span of 12 feet, the specified design linear distributed load was 165 plf. The corresponding maximum internal moment (at midspan) can be found.

$$R_1 = 165plf(6') = 990lb$$
$$\sum M_{cut} = 0$$
$$M + 165plf(6')(3') - 990lb(6') = 0$$
$$M = 2970lbft$$

With the maximum midspan internal moment found, the maximum design point load values can be found for the tests.

$$R_2 = P$$
$$\sum M_{cut} = 0$$
$$M = 2970lbft$$
$$2970lbft - R_2(4.5') = 0$$
$$R_2 = 660lb = P$$

The maximum design load is 660 pounds (for each point load). The load to be used for the fire resistance tests is 50% of the maximum design load; therefore the applied load is 330 pounds.

Capacity of Castellated I-joist and Hybrid joist

The manufacturer's specifications for the castellated and hybrid joists did not pertain to the loading configuration used in testing. Therefore, the axially unrestrained (base) joist was loaded until an immediate vertical deflection of L/480 at midspan was recorded based on the manufacturer's recommendation. For the castellated joist, each point load was 480 pounds, while for the hybrid joist, each point load was 400 pounds. These load levels were used for all castellated and hybrid joists.

Deflection-Based Failure Criteria

Using Underwriters Laboratories' *Report on Structural Stability of Engineered Lumber in Fire Conditions*, deflection-based failure criteria from ISO 834 was consulted [4]. With these criteria, failure is defined as the point when:

1. Deflection exceeds: $\frac{L^2}{400d}$; or
2. When deflection exceeds $\frac{L}{30}$, the Rate of Deflection exceeds: $\frac{L^2}{9000d}$

where L is the clear span in millimeters and d is the depth of the joist in millimeters (extreme tensile fiber to extreme compressive fiber) [4]. Table C-1 summarizes the application of these criteria to the fire resistance tests.

Table C-1: Summary of deflection-based failure criteria

Joist type	Clear span, L (mm)	Joist depth, d (mm)	$L^2/400d$ (mm)	$L^2/400d$ (in)	$L/30$ (mm)	$L/30$ (in)
Taditional (T)	3657.6	235.0	142.3	5.6	121.9	4.8
Engineered (E)	3657.6	301.6	110.9	4.4	121.9	4.8
Hybrid (H)	3657.6	355.6	94.1	3.7	121.9	4.8
Castellated (C)	3657.6	406.4	82.3	3.2	121.9	4.8

Comparing the results from Table C-1 (the values in inches) with the deflection plots in Appendix A (Figures A-10, A-21, A-31, A-42, A-53, A-65, A-77, A-88, A-100, A-111, A-123, and A-135), one can see that the deflection-based failure criteria is not applicable to the specimens tested. For the case considering $L^2/400d$, the joists failed prior to experiencing the calculated deflections displayed in Table C-1. For the case considering $L/30$ and rate of deflection, once again the joists failed prior to experiencing the calculated deflections displayed in Table C-1. Therefore, the deflection rate criteria could not be applied. Because the joists experienced structural failure prior to experiencing the deflections defined by ISO 834, the deflection-based failure criteria discussed is not applicable to the fire resistance tests conducted.